

***DE NOVO* DESIGNED FOLDAMERS BASED ON BIOTIC
AND ABIOTIC BUILDING BLOCKS**

THESIS SUBMITTED TO
THE UNIVERSITY OF PUNE
FOR THE DEGREE OF
DOCTOR OF PHILOSOPHY

IN
CHEMISTRY

BY
DEEKONDA SRINIVAS

Research Guide
Dr. G. J. Sanjayan

**DIVISION OF ORGANIC CHEMISTRY
NATIONAL CHEMICAL LABORATORY
PUNE 411008**

April, 2008



Dr. G. J. Sanjayan

Division of Organic Chemistry

Tel: +91-20-25902082

Fax: +91-20-25902624

Email: gj.sanjayan@ncl.res.in

National Chemical Laboratory

Dr. Homibhabha Road

Pune-411 008, India.

CERTIFICATE

Certified that the work incorporated in the thesis entitled “***De Novo Designed Foldamers Based on Biotic and Abiotic Building Blocks***” submitted by **Mr. Deekonda Srinivas** for the degree of **Doctor of Philosophy**, was carried out by the candidate under my supervision at the National Chemical Laboratory, Pune, India. Materials obtained from other sources have been duly acknowledged in the thesis.

Date:

Place: Pune

Dr. G. J. Sanjayan

(Research Guide)

DECLARATION

I here by declare that the thesis entitled “***De Novo Designed Foldamers Based on Biotic and Abiotic Building Blocks***” submitted for the degree of *Doctor of Philosophy* in *Chemistry* to the University of Pune has not been submitted by me to any other university or institution. This work was carried out at the National Chemical Laboratory, Pune, under the supervision of Dr. G. J. Sanjayan (Research Guide)

Date:

Division of Organic Chemistry

National Chemical Laboratory

Pune-411 008.

Deekonda Srinivas

(Research student)

ACKNOWLEDGEMENT

It gives me an immense pleasure to express my deep sense of gratitude towards my research guide Dr. G. J. Sanjayan for all the advice, guidance, support and encouragement during every stage of this work. He made me realize the importance of doing quality research, in a better way at crucial stage of my career.

The kind support from NMR group is greatly acknowledged and thanks to Dr. P. R. Rajamohanam, Dr. Usha phalgune, and Dr. Ravindranathan, Mrs. Kavitha. . I am also thankful to Dr. Rajesh Gonnade for his help in getting the single crystal X-ray structures. My thanks to Mrs. Shantakumari and Dr. Mahesh kulkarni for mass analysis.

I thank my lab mates Panchami, Amol, Pranjal, Ramesh, Gowri, Roshna, Arup, Sangram, Pinak, Kale, Nilesh, Vijaydas Das, for maintaining a cheerful atmosphere in the lab. I also thank Prakash, Satyanarayana Reddy, Marivel, Kapil, Sunil, Amit, Seeta for friendly atmosphere in my previous lab.

My sincere thank to Dr. N Selvakumar, Dr. V. B. Lowhray, Dr. B.B. Lowhray, Dr. G. Prasuna, Dr. Takhi and Prof. Javed Iqbal for their training and inspiration for to do the Doctorate degree of Philosophy in chemistry.

I am very much thankful to my great friends, *Raman* Vyasa Bhattar, Swaroop, Sridahr, Rajender, Srinivas Burgula, Srikanth, Satyanarayana Reddy, Suresh, Prakash Reddy, Raghupathy, Bhargava, Kiran, Murali, Abhijeet, Nageshwar Reddy, Chinna Srinu Shiva, Srinivas Naidu, Ramesh, Indu, Vilas, Santosh, who made cheerful and pleasant atmosphere in and around NCL.

I thank to my friends at NCL, Dr. Gnaneshwar, Dr. Sunil, Dr. Uma Shankar Dr. Vasudeva Naidu, Dr. Maheshwar, who made cheerful and pleasant atmosphere.

The single largest contribution in shaping my present comes from the faith, hope, encouragement and affection of my parents, and I am grateful to them. My heartfelt thanks to my wife Pallavi, She not only endured, but encouraged and assisted. I am lucky to have son Adhi whose attachment cherished every day. My special thanks to my brother (Anna), and sisters, (Swaroopa, Kalvathi) brother-in-laws (Ram narsaiah, Yadaiah) and all family members for their support and encouragement throughout my studies. My special thanks to my in-laws (Venkulu, Gunavati) and their family members.

It is great pleasure for me to thank of my friends, Dr. K. Srinivas Rao, D. Nageshwar, Paka Srinivas, Dr. Saibaba, Dr. Rajmohan Reddy, Dr. T. V. R. S. Sastry, Dr. Mallikarjun Goud, Dr. Uma Devi, Dr. K. Anantha Reddy, Dr. Mallesh, Vijay, Dr. Prabhakara Chary, Sarangam, whose wishes which were always with me.

I thank director NCL, for allowing me to work in this premier institute, providing the infrastructure. It is my sincere thanks to CSIR, New Delhi, for the financial support.

Deekonda Srinivas

CONTENTS

	Abbreviations	iv
	Thesis Abstract	v
	List of publications	ix
Chapter 1	<i>Design, Synthesis of α-Amino Acid and Aromatic Amino Acid Conjugated Foldamer</i>	
1.1	Foldamers: Definition and Significance	1
1.1.1	Structural characterization	4
1.1.2	Backbone rigidified foldamers	5
1.1.3	Anthranilamides	5
1.1.4	Oligo (<i>m</i> -phenylene ethynylenes)	6
1.1.5	Crescent Oligoarylamides	7
1.1.6	β -peptide foldamers	8
1.2	Conformationally constrained amino acid Aib (α -amino isobutyric acid) rich foldamers	9
1.3	Classification and importance of turns	11
1.3.1	γ -turn	12
1.3.2	β -turn	13
1.3.3	Significance of β -turns	14
1.3.4	α -turn	15
1.4.	Turn inducing foldamers	15
1.5	Objective of the present work	18
1.5.1	Design Principles	19
1.5.2	Synthesis	20
1.5.3	Results and Discussion	21
1.6	Spirobiindane-derived hybrid foldamer	26
1.6.1	Results and Discussion	28
1.7	Foldamers with Aib-Pro-Adb motif	31

1.7.1	Synthesis	32
1.7.2	Results and Discussion	33
1.7.3	Conclusion	37
1.8	Experimental procedures	38
1.9	References and notes	59
Chapter 2 <i>Concurrent display of both α-and β-turns in a semi synthetic peptide</i>		
2.1	Introduction and significance of reverse turns	67
2.2	Importance of three-centered/bifurcated H-bonding	68
2.3	Turn induced small peptides and depsipeptides	70
2.4	Objective of the present work	73
2.4.1	Design principle	73
2.4.2	Synthesis	74
2.4.3	Results and Discussion	76
2.4.4	Conformational analysis of peptide 5a	78
2.4.5	Conformational analysis of peptide 9	80
2.4.6	Conclusions	84
2.5	Experimental procedures	85
2.6	References and notes	107
Chapter 3 <i>Efficient synthesis and structural investigations of BINOL-m-phenylenediamine derived macrocycles</i>		
3.1	Aromatic oligoamide foldamers: Overview and significance	112
3.2	Synthesis and characterization of the oligomers	116
3.3	Macrocycles: An overview	117
3.3.1	Macrocycles- A Short History	119

3.4	Present work	121
3.4.1	Synthesis	122
3.4.2	Results and discussions	126
3.4.3	NMR studies of the Macrocycles	129
3.4.4	Attempted synthesis of large hybrid oligomers (R) –17	133
3.4.5	Synthesis	134
3.4.6	Conclusion	135
3.5	Experimental procedures	136
3.6	References and notes	169

ABBREVIATIONS

Ac	Acetyl
Ac₂O	Acetic anhydride
CDCl₃	Deuterated chloroform
EtOAc	Ethyl acetate
TEA/Et₃N	Triethylamine
m. p	Melting point
TMEDA	Tetramethylethylenediamine
THF	Tetrahydrofuran
CHCl₃	Chloroform
CH₂Cl₂	Methylene chloride
MeOH	Methanol
TFA	Trifluoro acetic acid
IBCF	Isobutyl chloroformate
DMS	Dimethyl sulphate
DIPEA	Diisopropylethylamine
DMF	N,N-Dimethylformamide
Aib	α -aminoisobutyric acid
EDCI	1-ethyl-3-(3'-dimethylaminopropyl) carbodiimide
<i>t</i>-Boc	<i>tert</i> -butyloxycarbonyl
d-Gly	Delta glycine
Pro	Proline
Gly	Glycine
H-bond	Hydrogen bond
HBTU	<i>O</i> -(1H-Benzotriazol-1-yl) <i>N,N,N</i> i, <i>N</i> i-tetramethyluronium hexafluorophosphate
ESI-MS	Electrospray Ionization Mass Spectroscopy
Hz	Hertz
IR	Infra red
Pd/C	Palladium 10% on activated carbon
SOCl₂	Thionyl chloride
MALDI-TOF	Matrix Assisted Laser Desorption Ionisation-Time Of Flight
mg	Milligram
MHz	Megahertz
M	Molar
μL	Microliter
ml	Milliliter
mmol	Millimoles
Pyr	Pyridine
NMR	Nuclear Magnetic Resonance
HMBC	Hetero multiple bond correlation
COSY	Correlated spectroscopy
NOESY	Nuclear Overhauser Enhancement Spectroscopy

ABSTRACT

Chapter 1 describes the design and synthesis of a novel hybrid foldamer, derived from a conformationally constrained aliphatic–aromatic amino acid conjugate that adopts a well-defined, compact, three-dimensional structure, governed by a combined conformational restriction imposed by the individual amino acids with which the foldamer is made of. Conformational investigations confirmed the prevalence of a unique doubly bent conformation for the foldamer, in both solid and solution states, as evidenced from single crystal X-ray and 2D NOESY studies, respectively.

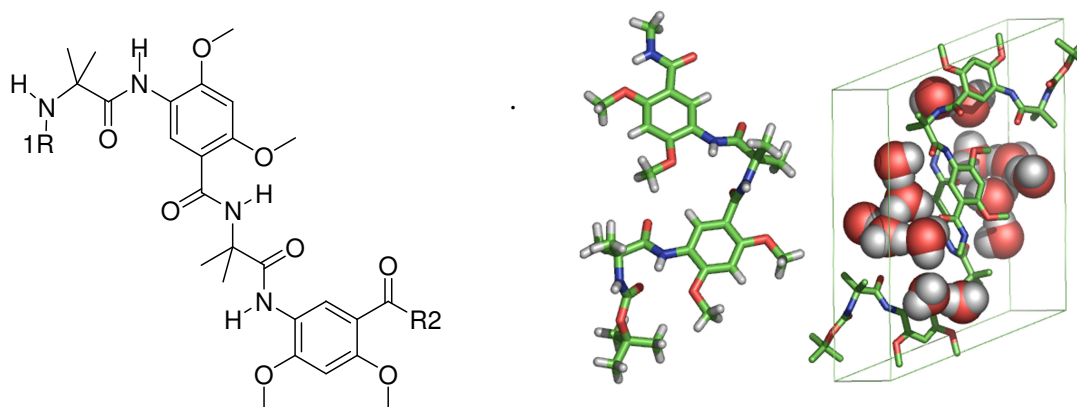


Figure 1: Adb-Aib hybrid foldamer and its single crystal X-ray structure

Chapter 1 also describes the design, synthesis, and structural studies of novel hybrid foldamers derived from Aib-Pro-Adb building blocks that display repeat β -turn motif. The foldamer having a conformationally constrained aliphatic-aromatic amino acid conjugate adopts a well-defined, compact, three-dimensional structure; governed by a combined conformational restriction imposed by the individual amino acids with which it is made of. Conformational investigations by single-crystal X-ray and solution state NMR studies were undertaken to investigate the conformational preference of these foldamers with a hetero backbone.

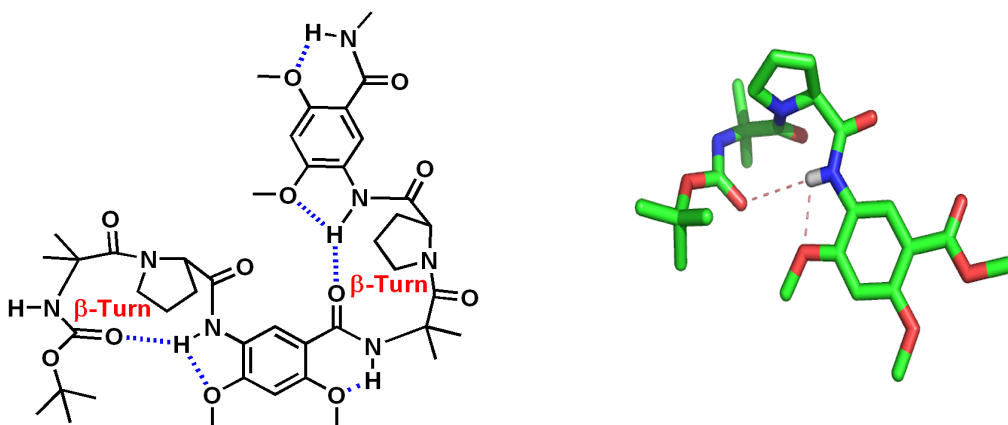


Figure 2: Adb-Pro-Aib tripeptide dimer Single crystal X-ray of Adb-Pro-Aib peptide

Chapter I also describes the full account of synthesis and secondary structural investigations of hybrid foldamers containing Adb-Aib and Spirobisindane building blocks.

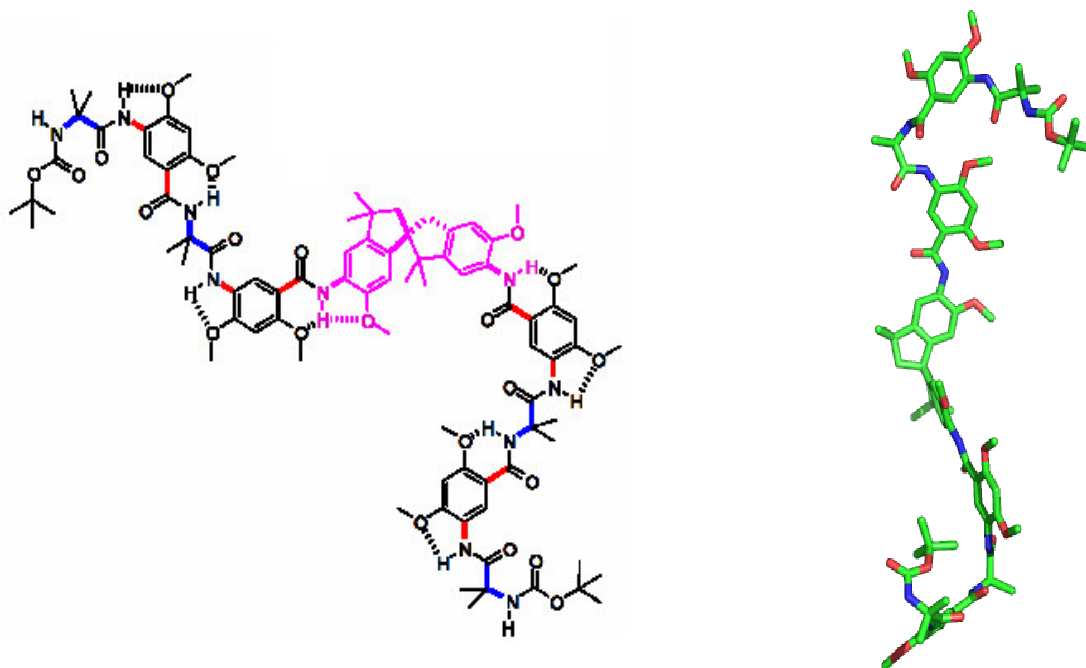


Figure 3: Adb-Aib-spirobisindane hybrid foldamer and its single crystal X-ray structure

Chapter 2 describes a semi synthetic peptide motif that concurrently displays both α - and β -turns, as evidenced from extensive structural investigations by single crystal X-ray crystallography and solution-state NMR studies.

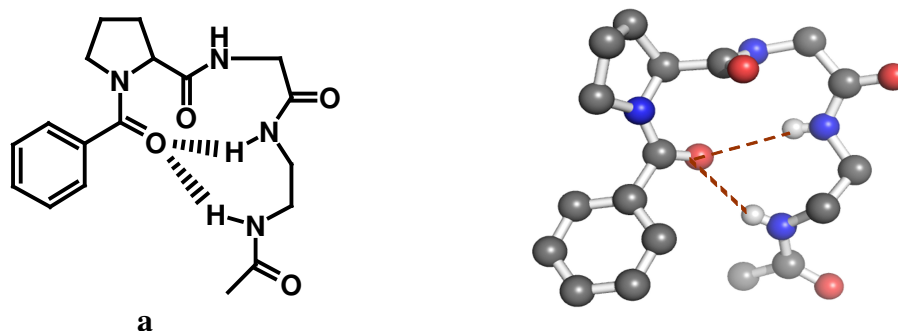


Figure 4: Molecular structure of a semi synthetic peptide motif (left) and its single crystal X-ray structure (right)

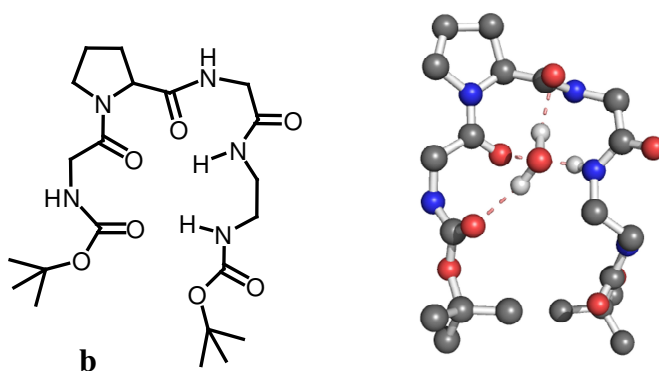


Figure 5: Molecular structure of a semi synthetic peptide motif (left) and its single crystal X-ray structure (right)

Chapter 3 describes the serendipitous discovery of an efficient synthetic route to BINOL-*m*-phenylenediamine-derived macrocycles. These macrocycles are quickly accessible in an one-pot procedure by the direct condensation of (R) and (S) BINOL bis-acids with suitably substituted *m*-phenylenediamine analogs. Structural investigations by single crystal X-ray crystallography and solution-state NMR studies provided convincing evidence of their intramolecular hydrogen bonding arrangement and rigid structural

architecture. The striking feature of these macrocycles is their ready accessibility in optically pure form coupled with their ease of synthesis.

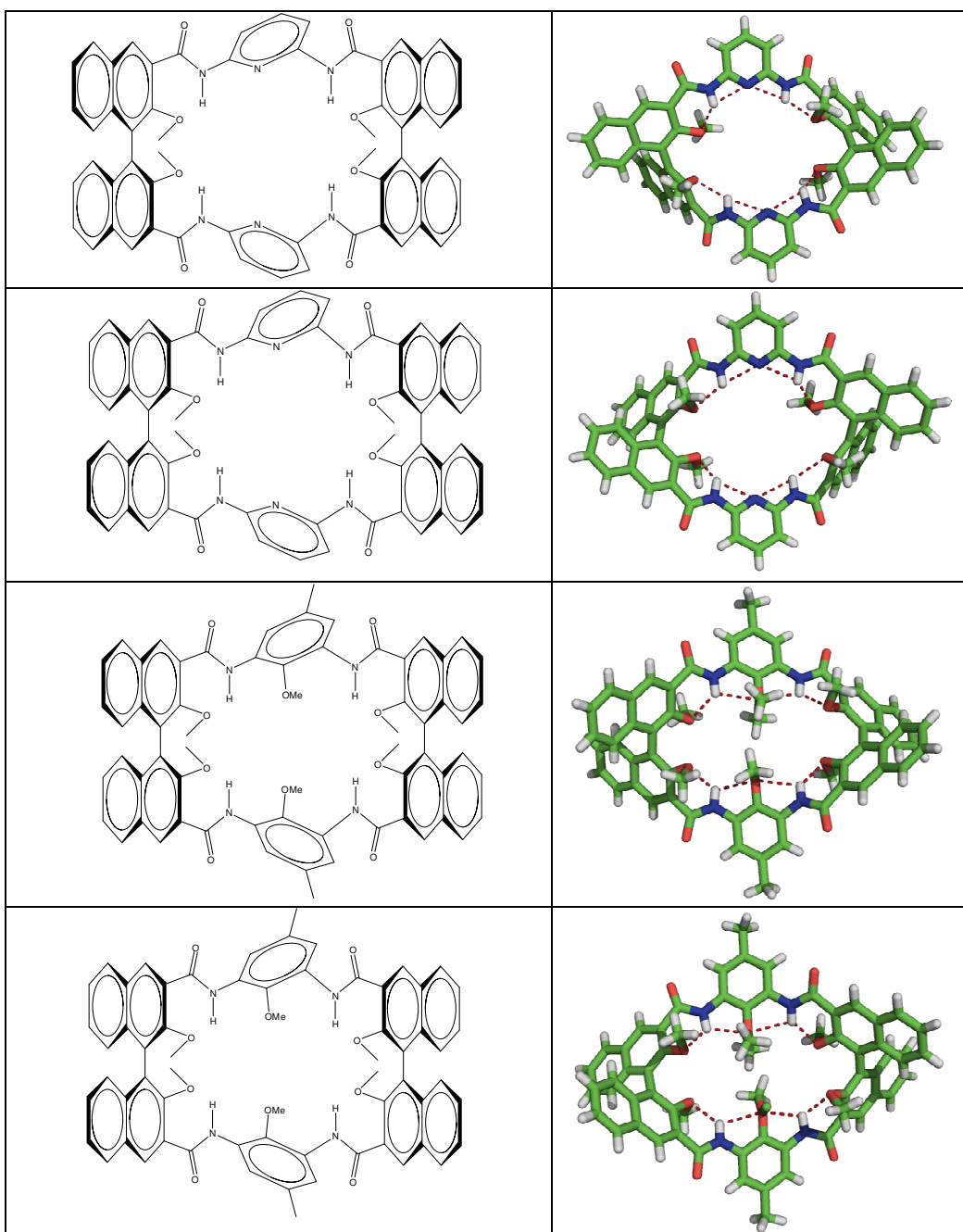


Figure 6: Macrocycles derived from 2, 2'-dimethoxy-1, 1'-binaphthyl-3, 3'-dicarboxylic acid, pyridine 2, 6 diamine, and 2-Methoxy-5-methyl-benzene-1, 3-diamine and their single crystal X-ray structures (right)

LIST OF PUBLICATIONS

1. A hybrid foldamer with unique architecture from conformationally constrained aliphatic-aromatic amino acid conjugate

Srinivas, D.; Gonnade, R; Ravindranathan, S.; Sanjayan, G. J. *Tetrahedron*. **2006**, *62*, 10141-10146.

2. Constrained Aliphatic-Aromatic Amino acid-Conjugated Hybrid Foldamers with Periodic β -Turn Motifs

Srinivas, D.; Gonnade, R; Ravindranathan, S.; Sanjayan, G. J. *J. Org. Chem.* **2007**, *72*, 7022-7025.

3. Pre-organization-mediated macrocyclization: efficient synthesis and structural investigations of BINOL-*m*-phenylene diamine-derived macrocycles

Srinivas, D.; Gonnade, R.; Rajmohan, P.R., Sanjayan, G. J. *Tetrahedron Letters*. **2008**, *49*, 2139–2142.

4. Concurrent Display of Both α - and β -Turns in a Semi Synthetic Peptide

Srinivas, D.; Gonnade, R.; Usha D. Phalgune, U. D.; Rajamohan, P. R.; Sanjayan, G. J. (Manuscript to be submitted)

5. Spirobiindane-Derived Abiotic Hybrid Foldamers with Unique Structural Architecture

Srinivas, D.; Gonnade, R; Ravindranathan, S.; Sanjayan, G. J. (Manuscript under preparation)

CHAPTER 1

Design and Synthesis of α -Amino Acid and
Aromatic Amino Acid Conjugated Foldamer

1.1 Foldamers: Definition and Significance

Nature performs its chemical tasks such as catalysis, molecular recognition, or light energy conversion, by using large polymeric structures, mostly proteins. The tertiary structure of proteins is determined by conformationally well-defined secondary structures such as α -helices, β -sheets coiled-coils, etc. These locally structured units give order to the overall system by positioning functional groups precisely in three dimensional space, thus creating an active site where catalysis occurs or recognition takes place. Although amino acid based superstructures are almost the rule in the biological world, the number of synthetic super molecules based on oligopeptides is relatively small. The main obstacles are the difficulty to predict and control the conformation of amino acid sequences and, in the meantime, introduce (un)natural functional groups in appropriate positions where they can perform recognition or catalytic tasks. Early examples in this field were extensively reviewed by Voyer a few years ago.¹

The relationship between biopolymer function and conformation has inspired many chemists to seek unnatural oligomers with strong folding propensities. Over the past three decades, chemists have started focusing on the development of new foldamers by introducing new structural elements in an artificial sequence that impose a conformational restriction on the oligopeptide. In this context, a foldamer² as defined by Moore, is any '*oligomer* that folds into a conformationally ordered state in solution, the structures of which are stabilized by a collection of noncovalent interactions between non-adjacent monomer units.^{2c} Although, more simply, a foldamer can be expressed as an unnatural system that adopts a well defined secondary structure.³ Later Prof.Gellman gave a generalized definition for the foldamer "any oligomer with a strong tendency to

adopt a specific compact conformation”. Among proteins, the term “compact” is associated with tertiary structure.

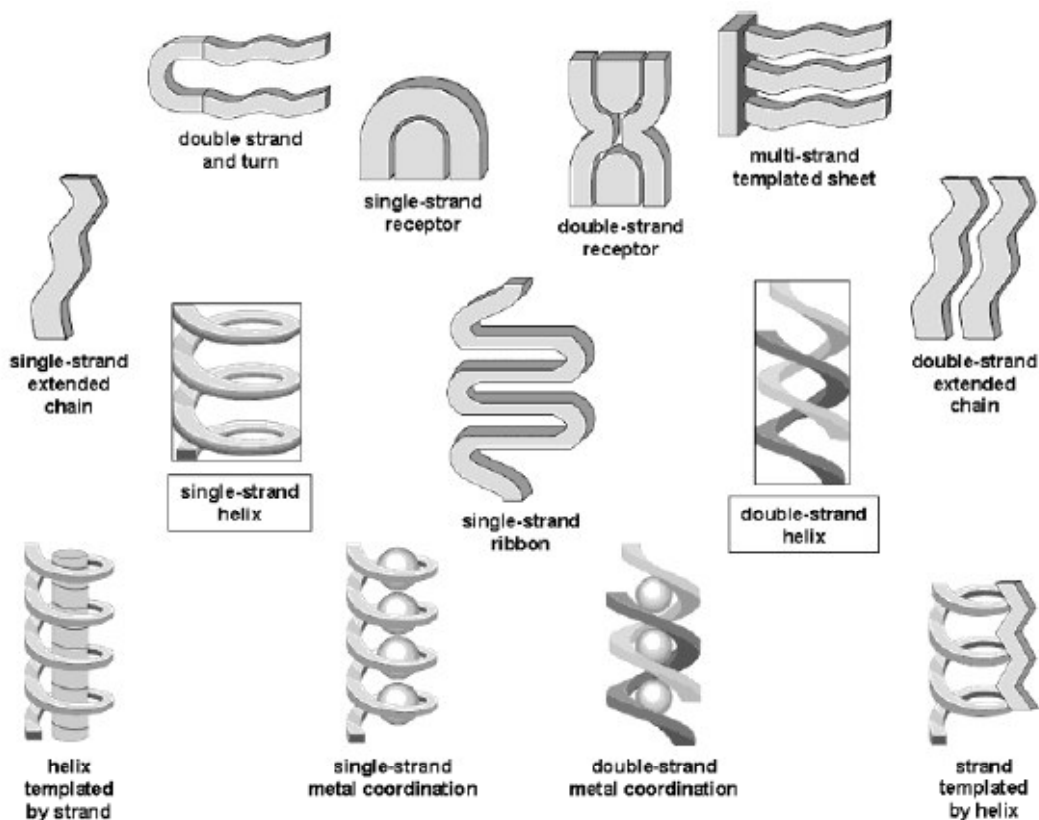


Figure 1: Illustrations depicting different types of foldamer secondary structures^{2c}

Numerous unnatural oligomers that fold into these well-defined secondary structures (foldamers) have been reported since the pioneering work of Gellman and Seebach on peptides. Considerable progress has been made in designing pseudo-biological polymers (oligomers) which fold predictably. Peptidic foldamers studied to date include: β -peptides,^{4,5} γ -peptides,^{6,7} δ -peptides,^{8,9} peptoids,^{10,11} oligoureas,¹² oligopyrrolidinones,¹³ α -aminoxy acid oligomers,¹⁴ sulfonamide oligomers,¹⁵ and vinyllogous peptides.¹⁶ nucleic acid mimetics including nucleic acid analogues,¹⁷ peptide nucleic acids,¹⁸ and β -peptide nucleic acids¹⁹ can also be considered as foldamers. Other

foldamers include anthranilic acid oligomers,²⁰ guanidine oligomers²¹ and pyridine/pyrimidine oligomers,²² aedamers,²³ and *m*-phenyl acetylene oligomers.²⁴

The development of foldamers encompasses three goals: design of novel oligomeric backbones that fold into a predictable shape, efficient synthesis of monomers and oligomers, and application to interesting problems in physical or biological chemistry.²⁵

Among reported systems, foldamers adopting various helical conformations represent the overwhelming majority.

The first step in the foldamer design must therefore be to identify new backbones with well-defined secondary structural preferences. The field of unnatural foldamers was pioneered by the research groups Gellman, and Sebach from the studies of secondary structural properties of β -peptides.²⁶

Foldamers as a class of conformationally ordered synthetic oligomers have ushered into prominence primarily due to their enormous potential for the creation of unnatural oligomers that adopt discrete tertiary structures; just as biopolymers. Synthetic oligomers can exist in a variety of different conformations. It ranges from randomly coiled chains to more spatially ordered structures. Oligomers with specific shape and conformation are attractive candidates for future technologies. For example foldamers can be designed based on helical oligomers for systematic arrangement of chromophores or functional groups in space that can be used for molecular recognition, catalysis and optical data storage. Oligomers of multifunctional monomeric building blocks have been extensively studied in recent years to mimic the structures and functions of

biopolymers.²⁷ They are also expected to be more stable toward proteolytic cleavage in physiological system than their natural counter parts.

Extensive investigations by several groups have resulted in the generation of a myriad of such synthetic oligomers with diverse backbone structures, conformations²⁸ and functions.²⁹ Of late, increasing attention is being devoted to the design and development of hybrid foldamers with a view to expanding the conformational space available for foldamer design.³⁰⁻³² The most synthetic foldamers examined to date and the biofoldamers, α -peptides and RNA, have homogeneous backbones; they are built from a single type of monomer. Oligomers with heterogeneous backbones are also important subjects of conformational design and analysis. Heterogeneous backbones, composed of two or more residues type, can also display well-defined folding behavior, and this strategy for foldamer design is rapidly growing till to the date. The exploration of heterogeneous backbones is important because different monomers will have different functional and structural features, and therefore, hybrid foldamers may have unique structural functional features.³⁰⁻³² Of particular interest are α,β -hybrid peptides, reported by Gellman's group,³⁰ composed of alternately changing α -and β -amino acid constituents. NMR studies provided convincing hints for the formation of special helix types in this novel foldamer class.

1.1.1 Structural characterization

Each folding system is unique, and as such requires special attention to the methods used to characterize the folded superstructure. There are general techniques explored by foldamer researchers which are worthy of note.

The folding of non-natural oligomer backbones can be detected by a variety of spectroscopic techniques. Low resolution techniques include circular dichroism (CD) and infrared (IR) spectroscopy. Each secondary structure generates a characteristic CD signature, but interpretation requires that these signatures be correlated to high resolution structural data. IR spectroscopy can detect hydrogen bonds, but does not provide any spatial resolution. High resolution techniques, such as two dimensional NMR and X-ray crystallography, provide details about the precise orientation of functional groups in the oligomer. X-ray diffraction generates solid-state structures, while NMR analysis can be used in combination with molecular modeling to generate solution-phase structures.

1.1.2 Backbone rigidified foldamers

1.1.3 Anthranilamides

In 1997, Hamilton *et al*³³ reported that Anthranilamide derivatives can be used as the basis for a series of novel oligomers that fold into helical secondary structures in the solid state (figure 2). When combined with pyridine-2,6-dicarboxylic acid and 4,6-dimethoxy-1,3-diaminobenzene subunits, oligoanthranilamides can be induced to take up a coiled conformation corresponding to two turns of a helix. X-ray crystallography shows that intramolecular hydrogen bonding and π - π stacking interactions are important in stabilizing the extended helical structures.

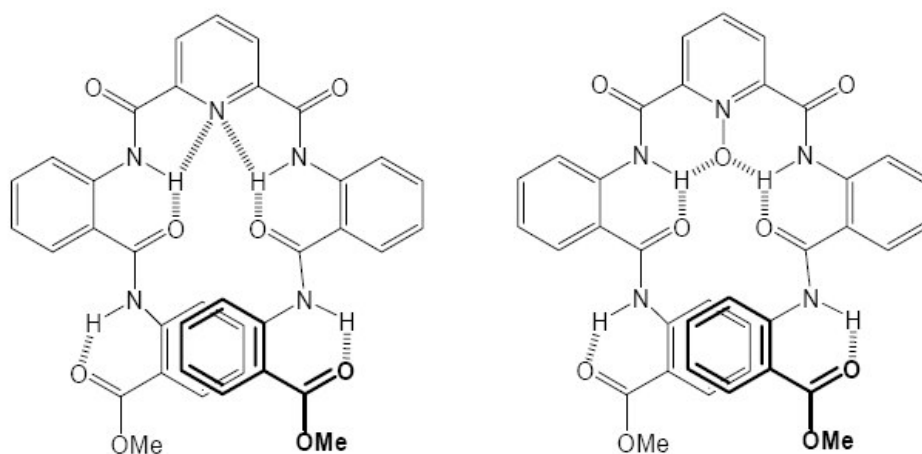
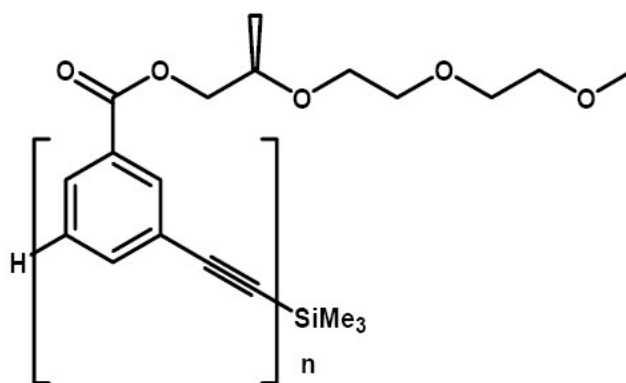


Figure 2: Folding anthranilamides³³

1.1.4 Oligo(*m*-phenylene ethynylenes)

Moore *et al*³⁴ have shown that solvent can play a key role in the adoption of secondary structures. Moore *et al* developed a non-biological system of acetylene linked benzene rings with polar side chains and demonstrated that in the presence of the appropriate polar solvents, such foldamers can adopt helical conformation.



$$n = 2, 4, 6, 8, 10, 12, 14, 16, 18$$

Figure 3: Oligo-phenylacetylenes³⁴

1.1.5 Crescent Oligoarylamides

Bing gong *et al*³⁵ have reported new class of oligoamides with backbones that adopt well-defined, crescent conformation. The monomeric unit of these oligoamides is 3-amino-4, 6-dimethoxy benzoic acid (Adb). The S (5) and S (6) type intramolecularly hydrogen bonding interactions reinforces the backbone structural architecture (figure 4).

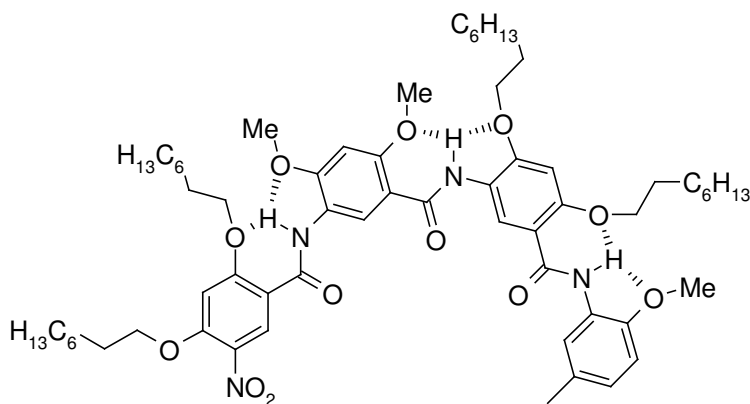


Figure 4: Crescent folding structures of oligoarylamides³⁵

Bing gong *et al*³⁶ also reported a new class of shape-persistent, cyclic hexa (aramides) from the one-step macrocyclization of monomeric building blocks (figure 5). Macrocycles were prepared from the monomeric building blocks 4, 6-dimethoxy-1, 3-phenylenediamine and 4, 6-dimethoxy-1, 3-diacid chloride. The one-pot macrocyclization described here has provided a highly efficient method for preparing multigram quantities of a new class of shape-persistent macrocycles. Because of the three-center intramolecular hydrogen bond consisting of the S (5) and S (6) type interaction, the corresponding oligoamides adopt a robust conformation.

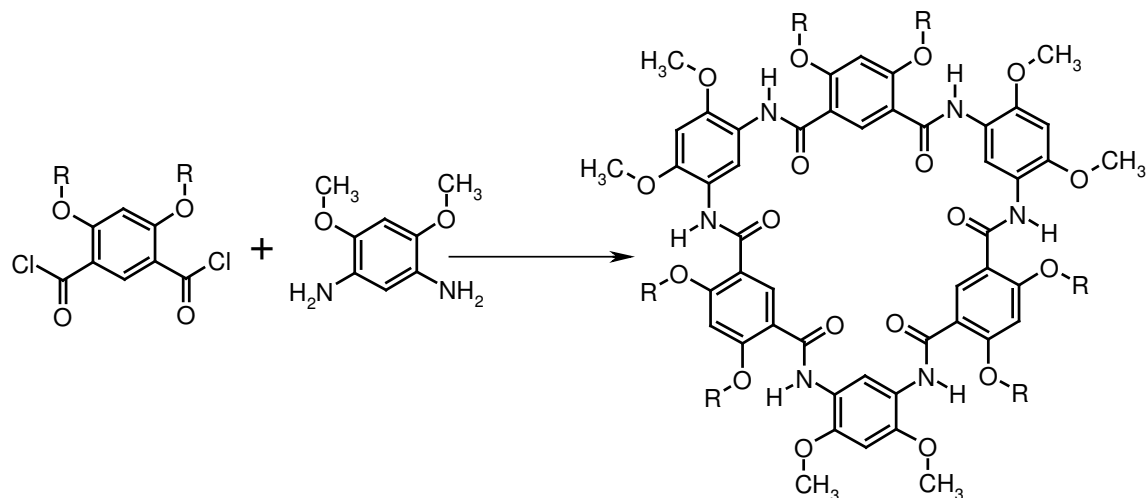


Figure 5: Gong's cyclic oligoarylamides³⁶

1.1.6 β -peptide foldamers

Over the past three decades, the folding properties of several synthetic oligomers with unnatural backbones have been explored. Seebach's group at the ETH in Zurich, and Gellman group in Wisconsin University have been the most active in the exploration of β -peptides (figure 6).²⁶ They focused on conformationally rigidified residues in constructing helical β -peptides, because of their long-term interest in generating stable tertiary folding patterns with a minimum number of residues. β -amino acids, and other extended amino acids, are intriguing in this regard, because it is possible to incorporate the amino acid backbones into small rings, which greatly restricts flexibility without blocking H-bonding sites.

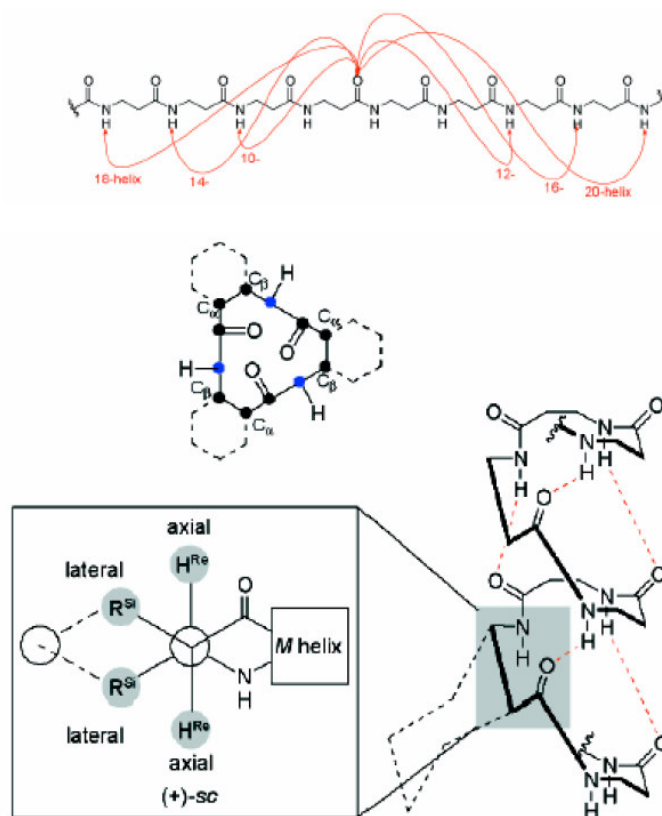


Figure 6: Side and top views (bottom) from crystal data of Gellman's ACHC 14-helix (top)²⁶

Helical secondary structures for both the *trans*-aminocyclopentane carboxylic acid (ACPC) and *trans*-aminocyclohexane carboxylic acid (ACHC) based backbones were confirmed by X-ray crystallographic data and NMR experiments.²⁶

1.2 Conformationally constrained amino acid Aib (α -aminoisobutyric acid) rich foldamers

Aib is the simplest achiral amino acid of this family. Aib (α -aminoisobutyric acid) should function as an extremely conformationally restricted residue, with allows regions restricted largely to the right- and left-handed helical regions of conformational space. The first crystal structures of Aib-containing peptides reveal the pronounced

tendency of this residue to nucleate β -turn and 3_{10} helical structures even in small oligopeptides.³⁷

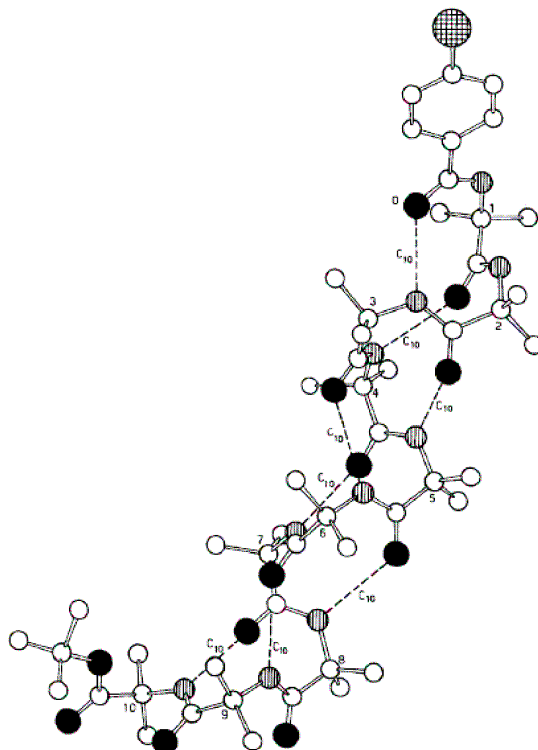


Figure 7: The 3_{10} -helical structure of *p* BrBz- (Aib)₁₀-OtBu³⁷

The extraordinary ability of Aib-containing peptides to adopt conformationally defined structures resulted in a very large number of crystal structure determinations of synthetic sequences by laboratories across the world.³⁸

Toniolo *et al*³⁹ reported the synthesis and conformational studies of homooligomer of α -aminoisobutyric acid. All the Aib homopeptides investigated assume (a regular right-left handed) 3_{10} -helical structure³⁹ (a series of type III/III' β -bends.) The peptide adopts a regular 3_{10} -helical structure stabilized by eight NH----O=C intramolecular 1 \leftarrow 4 (C₁₀) H bonds.³⁹

Toniolo *et al*⁴⁰ reported the molecular and crystal structures of terminally blocked (L-Pro-Aib)_n (n=3, 4) sequential peptides.⁴⁰ The solid state conformational studies reveal that it adopted a novel helical structure called right handed β -bend ribbon spiral, stabilized by maximum possible number of intramolecular N-H-O=C H-bonds. This structure may be considered as a subtype 3₁₀- helix having approximately the same helical fold of the peptide chain and being stabilized by 1 \leftarrow 4(C₁₀) intramolecular N-H--O=C H-bonds.

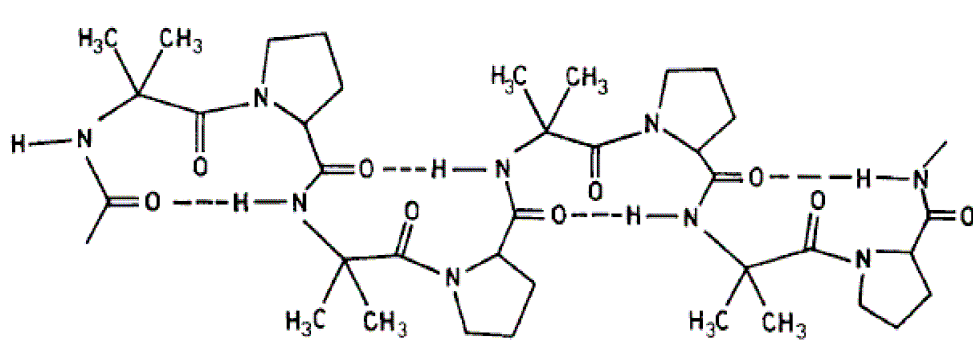


Figure 8: Representation of the β -bend ribbon spiral generated by the repeating –L-Pro-Aib- dipeptide unit.⁴⁰

1.3 Classification and importance of turns

From last three decades chemist have synthesized a large variety of oligomeric compounds with an aim to mimic the structures and functions of biopolymers. Rationally designed monomeric units were threaded together in specific sequences by iterative synthetic methods leading to many novel homo and hetero polymers exhibiting helical and other secondary structures.²⁷ Among the regular structures found in proteins, reverse turns are known to account for nearly one third of the residues in protein known structure.

Modification of peptides by introducing conformational constraints in the backbone is an area of current interest. In recent years, particular interest has been shown in the design of peptidomimetics that may adopt a bioactive β -turn-type conformation. Turns, defined as sites where a peptide chain reverses its overall direction, are common motifs in protein structures; these are aperiodic or non repetitive motif elements of the secondary structures of proteins. Among them, γ -turns and β -turns have been studied in details. Turns (or bends) are elements of primary importance both in the structure and function of peptides and proteins. First, they mediate folding of the polypeptide chain in to a compact globular or other tertiary structure. Second, turns usually occur on the environment exposed surface region of proteins, and therefore, they are likely to be involved in cellular and molecular recognition processes and in interactions between peptide and nonpeptide substrates and receptors. However, the recognition event is not necessarily a consequence of the turn conformation. It may simply be the result of a favorable side-chain clustering which facilitates intermolecular interaction. Many naturally occurring oligopeptides have been proposed to adopt turns in their bioactive conformation.⁴¹ Turns may also serve as templates for designing new molecules such as drugs, pesticides, and antigens.

Different types turns have been recognized according to the number and spatial arrangement of the residues involved.

1.3.1 γ -turn

The well-established subtype of tight folded structures is the γ -turns, comprising only three amino acid residues connected by two peptide groups (figure 9). The 1 \leftarrow 3 (C7) H-bond for a γ -turn is formed between the backbone CO (i) and NH ($i + 2$) groups.

Two types of γ -turns have been characterized, the classical and inverse ones, which are defined by the torsion angles of central amino acid residue. Whereas inverse γ -turns are more frequently observed in proteins, classical γ -turns are rather rare. γ -turns consisting of three amino acid residues have been implicated in several biological events.

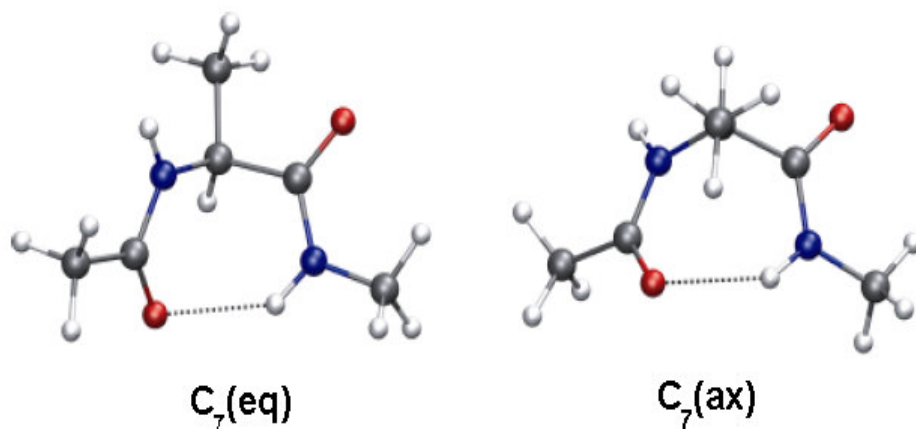


Figure 9: Classical and inverse γ -turns with a $1\leftarrow 3$ (C_7^{ax} or C_7^{eq}) intramolecular H-bond

1.3.2 β -turn

The most common is the β -turn, which involves four consecutive amino acids (i to $i+3$) and is generally stabilized by an intramolecular hydrogen bond between the CO group at position i and the NH group at $i+3$. Several subclasses of β -turns⁴² are further distinguished on the basis of the backbone dihedral angles (ϕ , ψ) associated with the central ($i+1$) and ($i+2$) positions (Table 1).

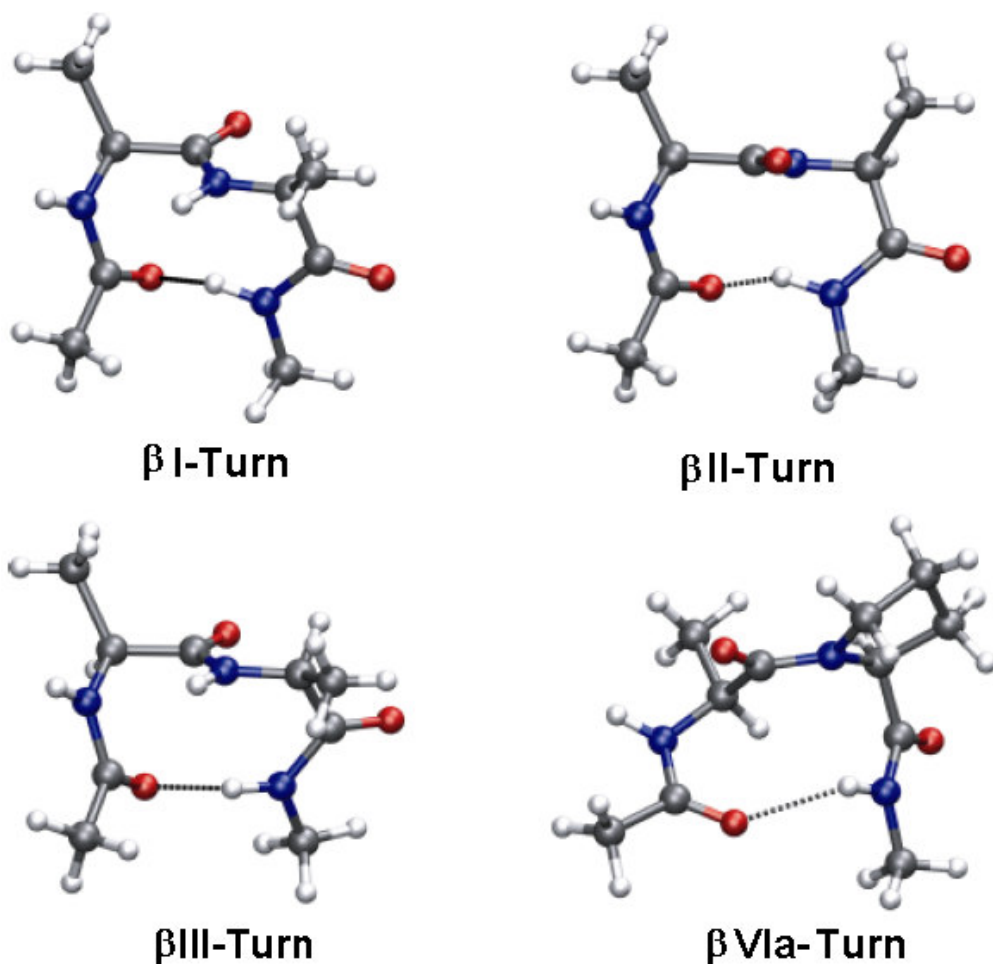


Figure 10: Typical β -Turns featuring a 1 \leftarrow 4 (C_{10}) intramolecular H-bond

1.3.3 Significance of β -turns

β -turns are often located at the surface of proteins where they can undergo post translational modification and serve as sites of recognition in interactions with receptors and antibodies.⁴³ Structural studies have also revealed that small peptides functioning as hormones, neurotransmitters, or having other regulatory roles in the organism may contain β -turn structural motifs.

Turn type	Mean Dihedral angles			
	$\Phi(i+1)$	$\Psi(i+1)$	$\Phi(i+2)$	$\Psi(i+2)$
I	-60	-30	-90	0
I'	60	30	90	0
II	-60	120	80	0
II'	60	-120	-80	0
III	-60	-30	-60	-30
III'	60	30	60	-30
IV	-61	10	-53	17
VI a1	-60	120	-90	0
VI a2	-120	120	-60	0
VI b	-135	135	-75	160
VIII	-60	-30	-120	120

Table 1: Mean dihedral angles for the standard β -turns

1.3.4 α -turn

In comparison to β , and γ -turns, α -turns are little investigated due to their lower occurrence in proteins and peptides. The α -turn corresponds to a chain reversal involving five amino acids and may be stabilized by a hydrogen bond between the CO group of the first residue and the NH group of the fifth amino acid.

1.4 Turn inducing foldamers

Chakraborty *et al* reported the homooligomer of furanoid sugar amino acids,^{44,45} and rigid pyrrolidine based peptides⁴⁶ using solution phase peptide synthesis protocols

(figure 11). Conformational analysis of these motifs by NMR and constrained molecular dynamics studies revealed that these oligomers adopt a well-defined structure in CDCl_3 with repeating β -turns, each involving a 10-membered ring structure with intramolecular hydrogen bonds between $\text{NH } i \rightarrow \text{C=O } i-2$. Here they demonstrated the abilities of sugar amino acids to introduce interesting secondary structures in peptides that can have many potential applications in designing novel peptidomimetics. These efforts would permit the design of compounds that will successfully mimic the structure and functions of biopolymers.

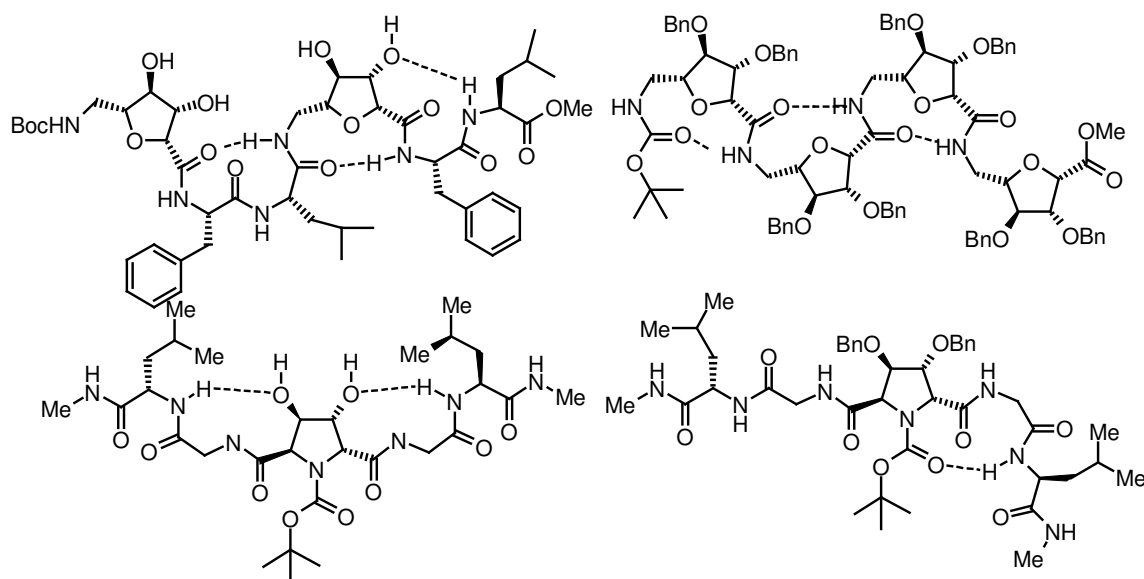


Figure 11: Various sugar amino acid adopting oligomers repeated β -turn structural architecture⁴⁴⁻⁴⁶

Fleet *et al*⁴⁷ have shown that short oligomeric furanose sugar amino acid chains can adopt well defined novel secondary structures stabilized by intramolecular hydrogen bonds (figure 12). The ease of synthesis of a wide range of structures such as the

tetrahydrofuran is likely to give flexibility and control in the design and applications of peptidomimetics with well-defined secondary structure.

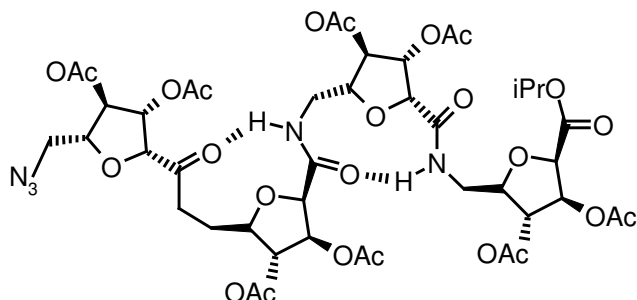


Figure 12: Homooligomer of furanose sugar amino acid adopting repeated β -turn structure⁴⁷

Sanjayan *et al*⁴⁸ have designed and synthesized a novel hybrid foldamer that adopts a well-defined compact, three-dimensional architecture, which is governed by a combined conformational restriction imposed by the individual amino acids of which it is composed (figure 13).

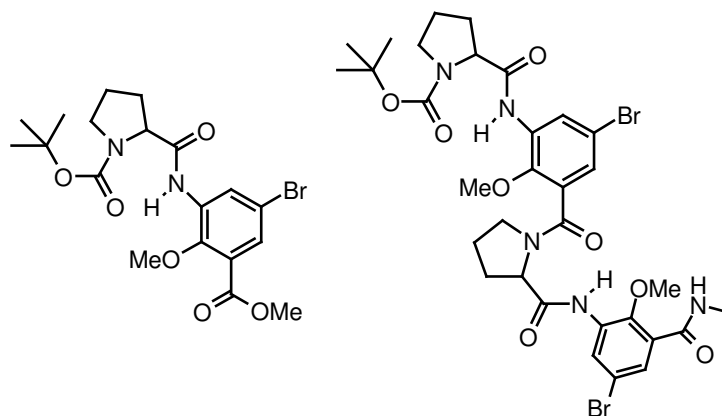


Figure 13: A Hybrid foldamer that adopt repeated γ -turn structure⁴⁸

Conformational investigations by single-crystal X-ray studies, solution state NMR, and ab initio MO theory strongly suggest the prevalence of γ -turn motifs in both the di-and

tetra peptide foldamers, which are presumably stabilized by strong bifurcated hydrogen bonds in the solid and solution states.

Dan yang *et al*⁴⁹ designed and synthesized $\beta^{2,3}$ -cyclic aminoxy acids in which the α - and β -carbon atoms are part of an aliphatic ring (cyclopentane and cyclohexane unit). The conformational analysis revealed that these $\beta^{2,3}$ -cyclic aminoxy acids adopt rigid β N-O turns and 1.8₉-helix structures. These secondary structures exist independently of the ring size of the aliphatic side chains (either five or six atoms), unlike the case of the β -peptides having cyclically constrained backbones. The strong local conformational control exerted by the $\beta^{2,3}$ -cyclic aminoxy acids provides a powerful tool that allows the preparation of short peptides having rigid and predictable conformations.

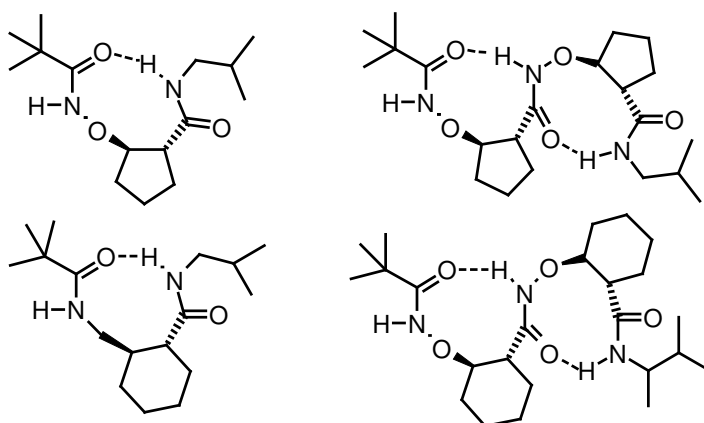


Figure 14: Cyclic aminoxy acids adopt repeat β -turn structure⁴⁹

1.5 Objective of the present work

The main objective of the work described in this chapter is to design and synthesize hybrid foldamers derived from natural and constrained synthetic amino acid residues and to study their folding patterns both in solution and solid state.

1.5.1 Design Principles

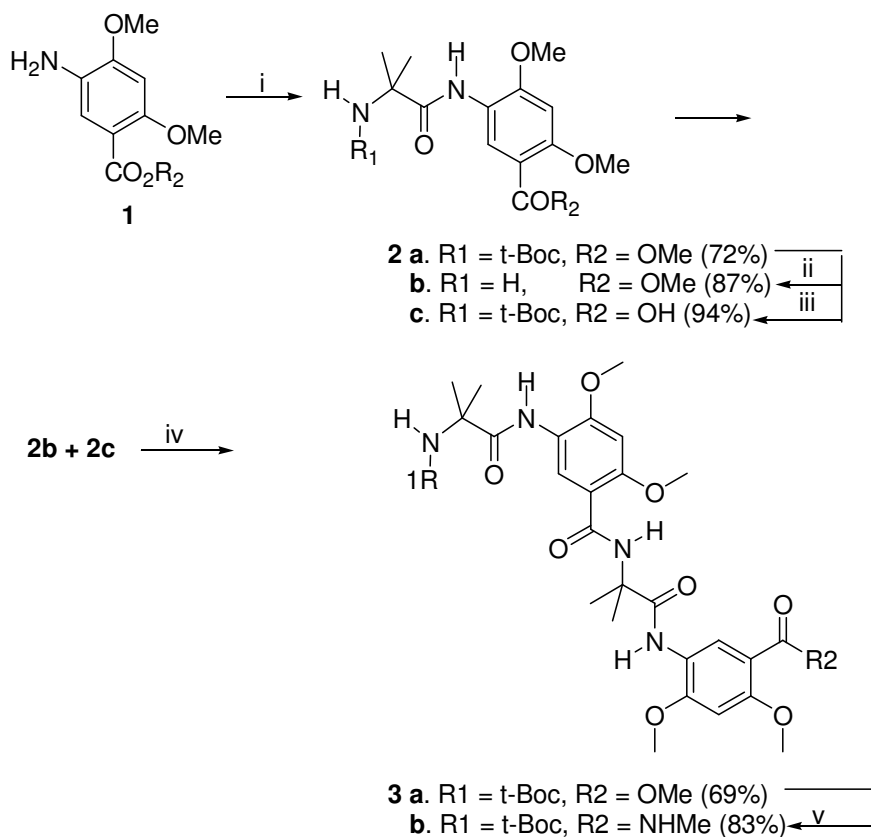
In an effort to augment the repertoire of conformational space available for foldamer design, we set out to generate novel foldamers, which contain conformationally constrained α -amino acid-aromatic amino acid-conjugated building blocks as subunits. We designed the Aib-Adb motif-based foldamer **3b** anticipating that the corresponding oligomers would adopt a well-defined, compact, and three dimensional structures, governed by a combined conformational restriction imposed by both Aib and Adb residues. The achiral Aib residue is known to play a key role^{39,50} in the conformational restriction of polypeptides due to its overwhelmingly constrained phi ($\phi \pm 60^\circ$) and psi ($\psi \pm 30^\circ$), while the backbone-rigidified aromatic amino acid residue Adb³⁵ is known to induce a crescent conformation in its oligomers via localized five- and six-membered ring hydrogen bonding interactions. Thus, we reasoned that hetero-oligomers made of Aib-Adb repeat motif should also display conformational rigidity. Structural studies (*vide infra*) indeed showed that the Aib-Adb dimer **3b** folds into a well-defined, compact, three-dimensional structure, as evidenced from single crystal X-ray and 2D NOESY studies. Interestingly the crystal structure analysis revealed a fascinating arrangement of water clusters, in the crystal lattice, held by the backbone amide groups of the foldamer with a peculiar architecture. It is noteworthy that the understanding of three-dimensional structures of water clusters has profound implications in several areas ranging from water-mediated molecular self-assembly⁵¹ to protein structure and function.⁵² Furthermore, exploration of conformationally ordered synthetic oligomers that interact with water molecules may enable better understanding of the much debated issue of

water interaction with Anti Freeze Proteins (AFPs), and Anti Freeze Glyco Proteins (AFGPs).⁵³

1.5.2 Synthesis

The Aib-Adb motif-based foldamer **3b** was assembled from Boc-Aib-Adb-OMe building block **2a**, which in turn was synthesized by coupling the protected amino acids Aib and Adb using TBTU as a coupling agent (scheme 1). However, attempts to synthesize higher oligomers using this “segment doubling strategy” were unsuccessful, due to the formation of intractable mixture of products under various conditions.

Scheme 1



Reagents and conditions: (i) Boc-Aib-OH, DIPEA, TBTU, MeCN, RT, 6 h; (ii) dry HCl (gas), dioxane, RT, 5 min; (iii) 2N LiOH, MeOH, RT, 12h; (iv) DIPEA, TBTU, MeCN, RT, 8h; (v) methanolic MeNH₂, 48h, RT.

1.5.3 Results and Discussion

The foldamer **3b** crystallized from acetonitrile: water (90:10), in triclinic space group *P*-1. The unit cell contained two foldamers and fourteen water molecules (figure 15). Investigation of the crystal structure revealed that the intrinsically constrained Aib residues imposed a significant twist on the foldamer backbone, as expected, with ϕ and ψ torsion angles close to 60° and 30° , respectively, forcing the foldamer backbone to adopt a doubly bent conformation. It is interesting to compare the conformational propensities of the homo-oligomers made of the individual amino acids (Aib and Adb) and their hybrid oligomer **3b**.

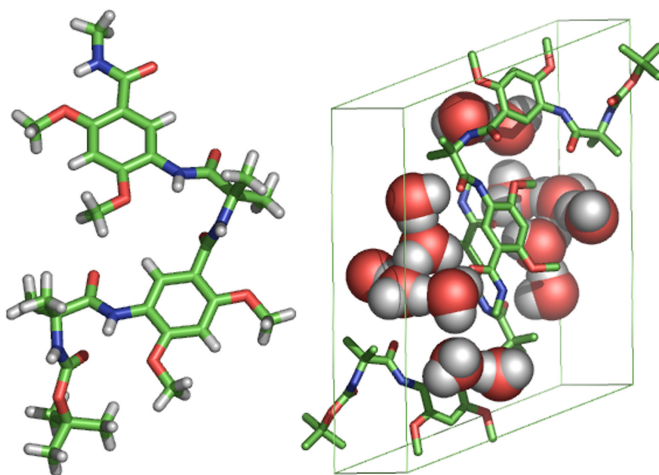


Figure 15: Crystal structure of the Aib-Adb motif-based foldamer **3b**. Water molecules in the unit cell are represented in spheres, for aiding quick identification. Color coding: C green, H gray, N blue, O red.

Whereas the homo-oligomers of Aib and Adb have been reported to adopt 3_{10} -helical^{39,50} and crescent architectures,³⁵ respectively, the hybrid foldamer **3b**, containing alternately changing Aib and Adb residues, shows an entirely different structural architecture, a fact that clearly attests to the importance of hybrid foldamer strategy³⁰ for augmenting the conformational space available for novel foldamer design.

Investigation of the crystal structure of **3b** revealed the presence of water molecules embedded in the crystal lattice. A detailed analysis of the arrangement of water molecules revealed highly interesting features (figure 16).

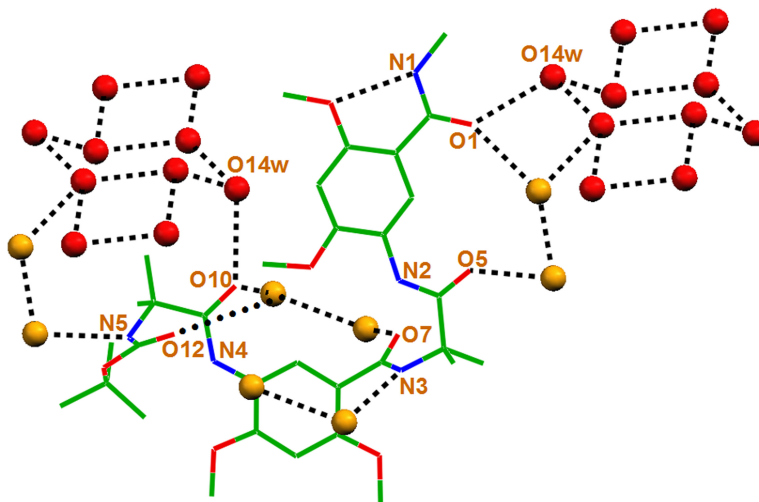


Figure 16: Crystal structure of Aib-Adb motif-based foldamer **3b** showing interaction of the foldamer backbone with water molecules.

There are mainly two types of water molecules discernible in the crystal lattice; the first type (colored red) forms a polymeric chain of water clusters, and the second type (colored orange), bridges adjacent foldamer molecules as well as connects the foldamer to the water clusters, eventually forming a complex three-dimensional hydrogen bonded network. All the backbone carbonyl oxygens of the foldamer are involved in strong hydrogen bonding interactions with water molecules ($O\cdots O = < 3.0 \text{ \AA}$).⁵⁴ However, only the Aib amide NHs ($N3H$ and $N5H$) partake in interactions with water molecules, leaving the Adb amide NHs ($N2H$ and $N4H$) and the methyl amide NH ($N1H$) to be satisfied with S(5) and S(6)-type⁵⁵ hydrogen bonding interactions, respectively. The water molecules, in pairs (colored orange), that bridge the backbone carbonyls of the adjacent residues, donate two hydrogen bonds to the backbone carbonyl oxygens of the foldamer forming

12-membered ring hydrogen bonded network. Further, these *water pairs* accept hydrogen bonds (one each) from the Aib NHs of the adjacent foldamers. The backbone carbonyls O1 and O10 keep the parallel running water chains in place by hydrogen bonding with the water molecule (O14_w) that is part of the Centrosymmetric six-membered water cluster. Interestingly, the same water molecule (O14_w) helps in building the hydrogen bonded three-dimensional network by donating a hydrogen bond to the carbonyl oxygens (O1 and O10) of another foldamer.

The infinite chain of water clusters has alternate 4- and 6-membered rings (oxygen atoms) sharing one edge. The oxygen atoms of the water molecules in 4-membered rings assume square planar structure and the 6-membered rings display a centrosymmetric chair conformation. The infinite chains of water clusters are held together by strong O_w–H···O_w hydrogen bonding interactions (O_w···O_w = 2.73 – 2.85 Å).⁵⁴ The supramolecular chains of water clusters are aligned parallel to each other (figure 17).

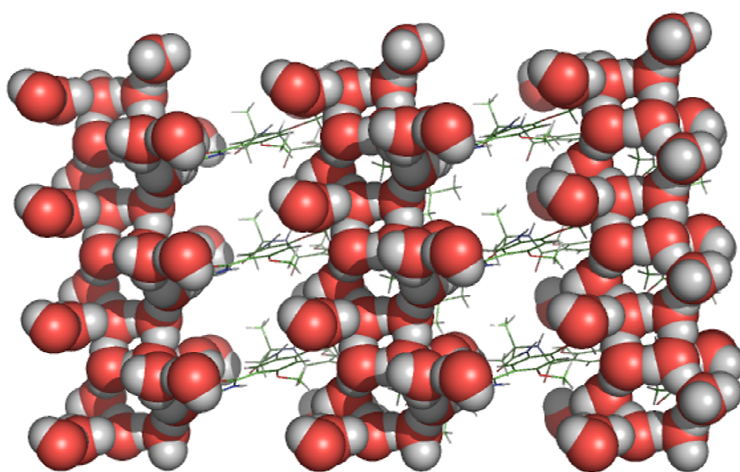


Figure 17: A view of the arrangement of polymeric chain of water clusters in the crystal lattice of **3b**. For clarity, the polymeric chains of water clusters are represented in spheres and the foldamers in lines. Color-coding: C green, H gray, N blue, O red.

The folded structure is organized by the backbone H-bonds in solution state, as evidenced from the FT-IR spectroscopy, a sensitive tool that is easily applicable for the detection of vibrational modes influenced by the presence of the H-bonds. In the N-H stretch region of **3b**, the free N-H vibration, presumably due to the N-terminal Boc amide NH, appear as a weak signal at 3419 cm^{-1} , while intramolecular H-bonded N-H stretches give rise to a broad band in the region 3388 cm^{-1} . Another important source of information in IR spectra is the amide carbonyl region ($1600\text{-}1700\text{ cm}^{-1}$). The band at 1647 cm^{-1} can be ascribed to the H-bonded carbonyl in the backbone. Weaker H-bonds result in a slightly increased frequency. The band at 1683 cm^{-1} could be assigned to the N-terminal Boc carbonyl that is not taking part in intramolecular H-bonding.

Solution state NMR studies (500 MHz) of the foldamer **3b** in CDCl_3 strongly suggested the prevalence of a doubly bent conformation in solution state, similar to the one observed in the solid state, although the existence of water clusters in solution-state could not be verified. One of the most characteristic nOe interactions that can be anticipated for a doubly bent conformation for **3b**, as observed in the solid-state, would be the NH vs NH dipolar couplings of the amide NHs of the adjacent Aib-Adb residues. Analysis of the 2D NOESY data (500 MHz, CDCl_3) indeed revealed the existence of NH vs NH dipolar couplings of the adjacent Aib-Adb residues (NH1/NH2 and NH3/NH4), as anticipated (figure 18). Furthermore, the characteristic NOE interactions between amide-NH and the adjacent *O*-aryloxymethyls in **3b** (NH2/OMe1, NH3/OMe2, NH4/OMe3, and NH5/OMe4) also strongly suggest their *syn* orientation, thereby making space for the S(5) and S(6)⁵⁵ type hydrogen bonded arrangement, a common feature in *O*-alkoxy arylamides.³⁵

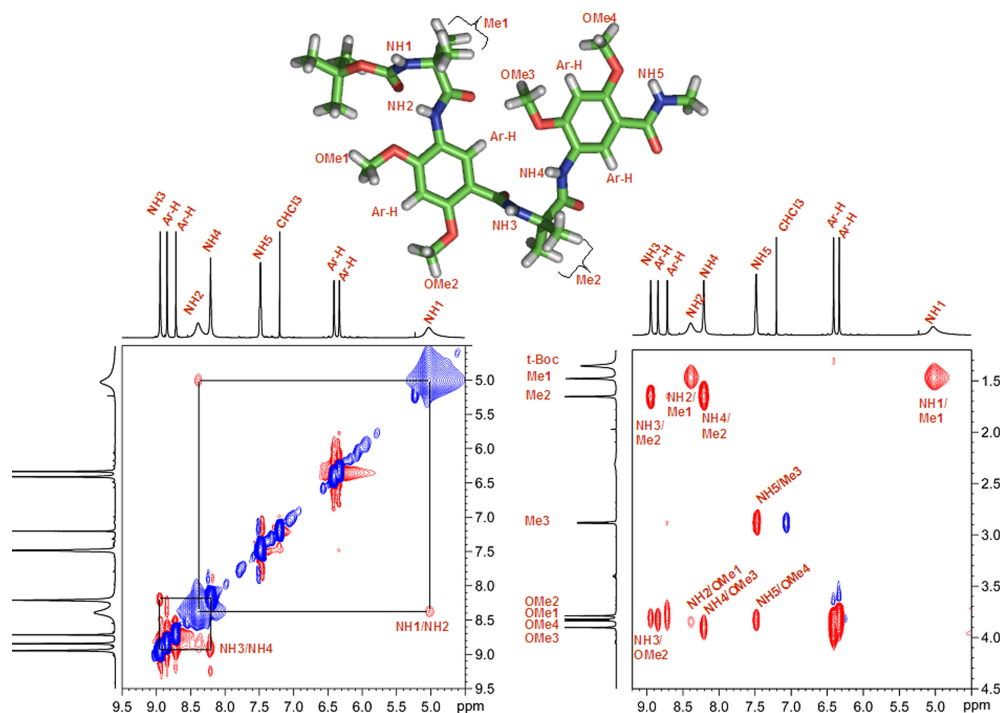


Figure 18: Partial 2D NOESY spectra of **3b** (500 MHz, CDCl_3) showing characteristic NH1/NH2 and NH3/NH4 interactions. For aiding interpretation of the 2D data, crystal structure of **3** with selected labeled atoms is also shown.

To confirm that intramolecular hydrogen bonds are clearly prevalent in solution, we also performed $[\text{D}_6]$ DMSO titration studies of foldamer **3b**. The chemical shift changes of all the amide protons are presented in (figure 19). Except the N-terminal Aib-NH, all other NHs appear at downfield region and show little shift when solutions of foldamer **3b** are titrated gradually with $[\text{D}_6]$ DMSO ($\Delta\delta < 0.28$ ppm), suggesting their strong involvement in intramolecular hydrogen bonding interaction. In contrast, the chemical shift of N-terminal Aib amide NH1 proton undergoes significant chemical shift changes on incremental addition of $[\text{D}_6]$ DMSO suggesting their involvement in intermolecular hydrogen bonding.

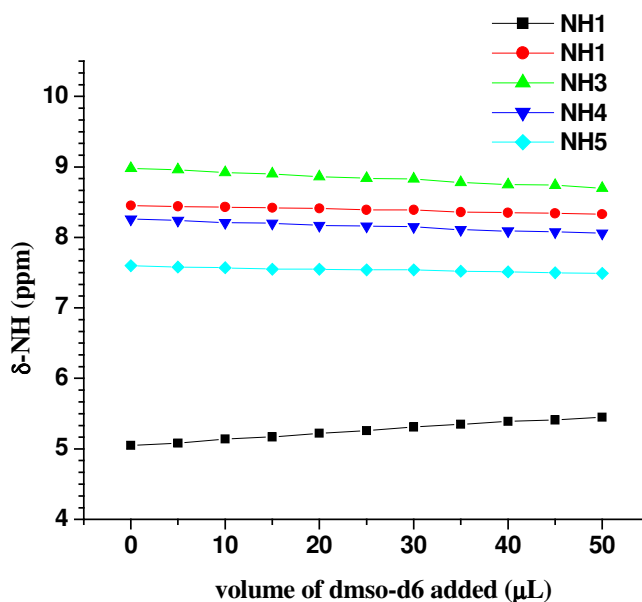


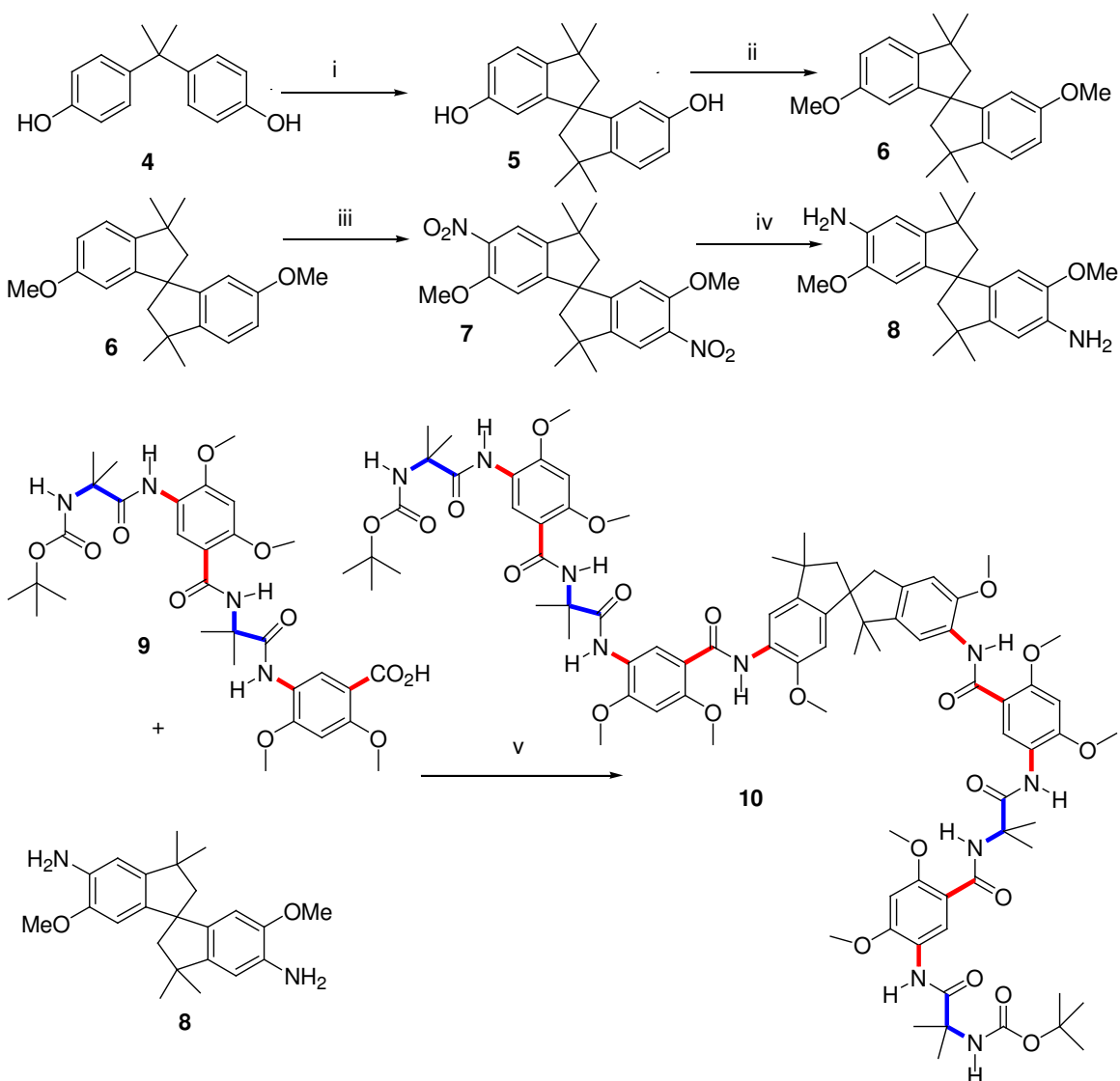
Figure 19: ^1H NMR DMSO- d_6 Titration Experiments of the foldamer **3b** Amide proton chemical shifts as a function of the amount of DMSO- d_6 added in a 16.0 mM solution of the foldamer **3b** (0.6 mL in CDCl_3).

1.6 Spirobiindane-derived hybrid foldamer

The fundamental importance of water in many biological, chemical physical processes has prompted intensive research efforts in the area of interaction of water with organic molecules.⁵³ To investigate the possibility of water cluster stabilization in higher oligomers of Adb-Aib, spirobiindane system was used to connect the water stabilizing of Adb-Aib motif.

The Spirobiindane derived hybrid foldamer **10** was assembled from (Boc-Aib-Adb-Aib-Adb-OH) building block **9** and spirobiindane diamine **8** (scheme 2). The building block **9** was prepared by using segment doubling strategy method, as mentioned earlier.⁵⁶ The spirobiindane diamine was prepared in four steps.⁵⁷ The synthesis started

with dihydroxy spirobiindane **5** which was prepared from bisphenol, in the presence of methanesulfonic acid. The compound **6** was made by treatment of dihydroxy spirobiindane **8** with dimethyl sulfate and potassium carbonate in acetone. Compound **6** upon careful nitration furnished the dinitro compound **7**. Hydrogenation of the dinitro compound **7** in the presence of palladium carbon, and ammonium formate afforded the spirobiindane diamine **8** in good yield.



Reagents and conditions: (i) bisphenol, methanesulfonic acid, 135⁰C, 3h; (ii) dimethyl sulfate, K₂CO₃, acetone, rt, 8h; (iii) nitric acid, sulphuric acid, acetic acid, rt, 1h; (iv) ammonium formate, 10% Pd/C, methanol, rt, 12h; (v) HBTU, DIPEA, dry acetonitrile, rt, 24h.

1.6.1 Results and Discussion

The foldamer **10** could be crystallized readily from acetonitrile-chloroform (70:30) solvent mixture (figure 20). Contrary to our expectations, investigation of single crystal–X-ray data of the foldamer **10** revealed that foldamer aided water cluster formation could not be realized. A closer inspection of single crystal X-ray data revealed the presence of extensive bifurcated hydrogen bonding interactions.

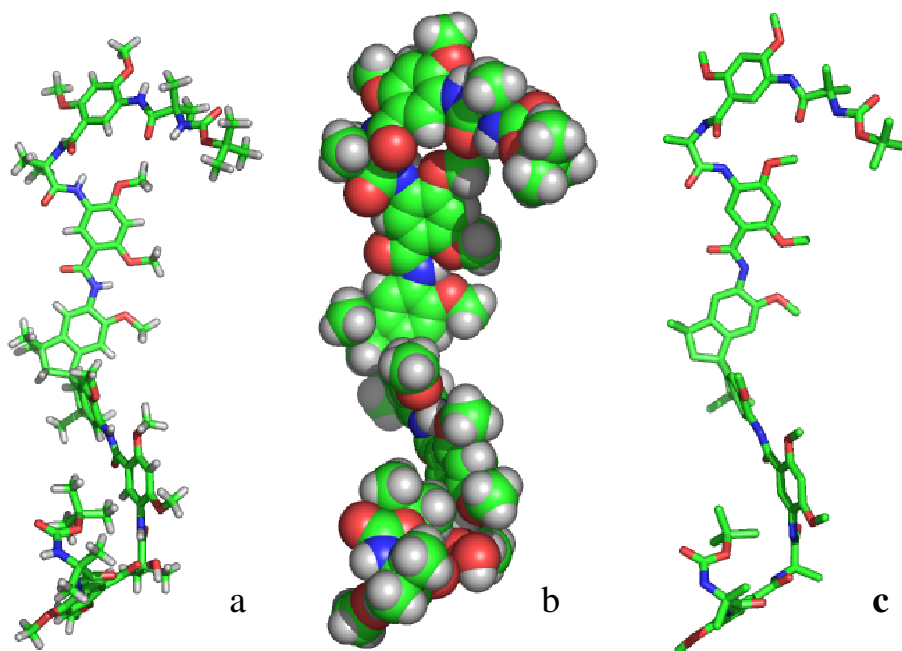


Figure 20: (a) PyMOL- rendered single crystal X-ray of foldamer **10** (b) sphere representation (c) stick representation.

The conformationally constrained Aib residues imposed significant twist on the foldamer backbone, as expected, forcing along the foldamer backbone, rendering a robust structural architecture to the foldamer, backbone to adopt a repeat bent conformation.

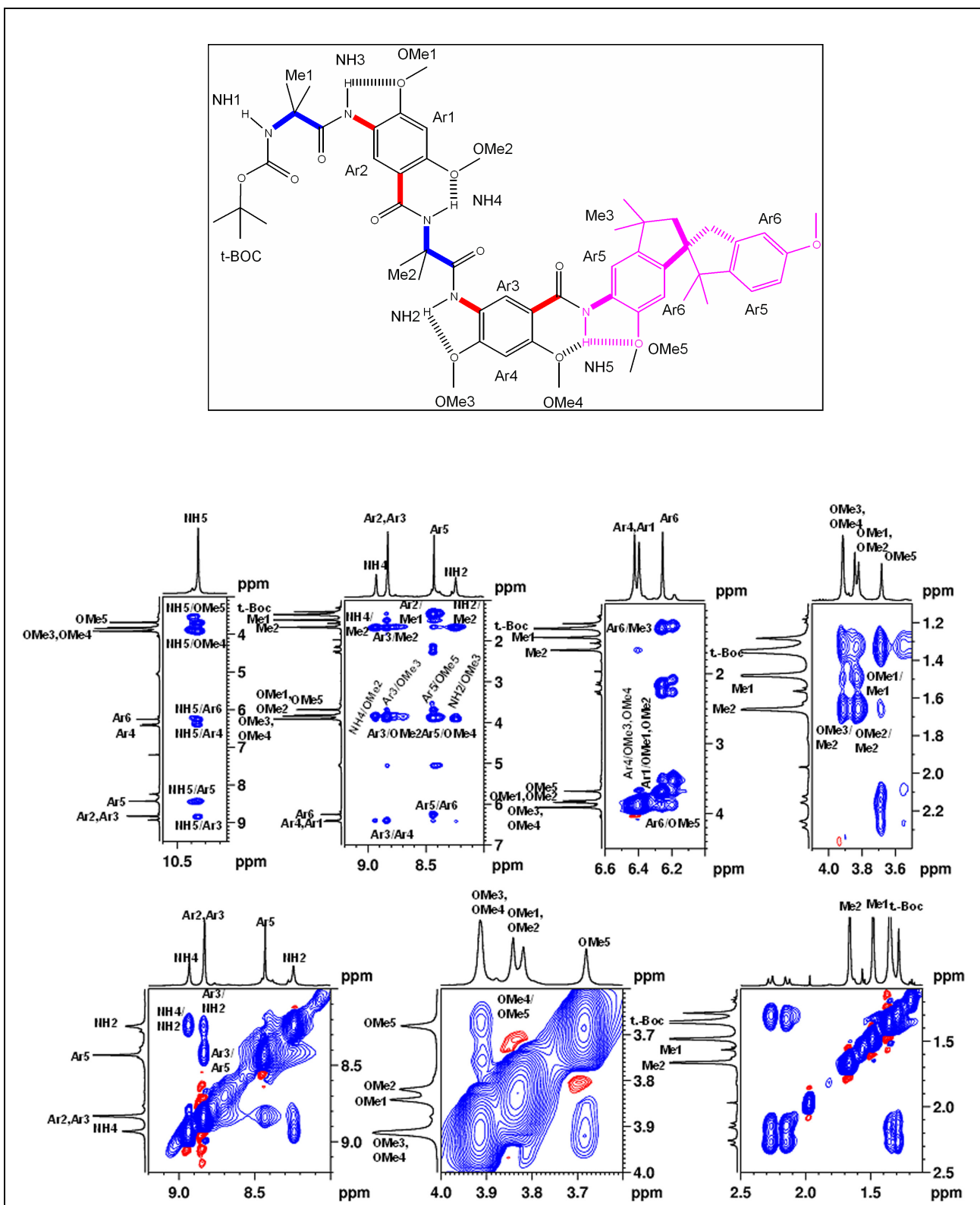


Figure 21: Molecular structure of **10** with selectively numbered protons and partial 2D NOESY spectra of **10** (500 MHz, CDCl₃) showing characteristic nOes.

Inspection of the ^1H NMR spectrum of **10** revealed that all the signals of the amide protons except terminal Aib NH (NH1) appeared in the downfield region (8.2-10.4 ppm) suggestive of their involvement in H-bonding interaction. The signal assignments were carried out with the help of nuclear Overhauser effect spectroscopy (NOESY) (figure 21). Analysis of the 2D NOESY data (500 MHz, CDCl_3) revealed the characteristic NOE interactions between amide-NH and the adjacent *O*-aryloxymethyls in **10** (NH2/OMe3, NH4/OMe2, NH5/OMe4, and NH5/OMe5) also strongly suggesting their *syn* orientation, thereby making space for the S(5) and S(6)⁵⁵ type hydrogen bonded arrangement, a common feature in *O*-alkoxy arylamides.³⁵ Further analysis of the 2D NOESY data revealed the existence of NH vs NH dipolar couplings of the adjacent Aib-Adb residues (NH2/NH4), as anticipated.

To confirm that intramolecular hydrogen bonds are clearly prevalent in solution, we also performed $[\text{D}_6]$ DMSO titration studies of foldamer **10**. The chemical shift changes of all the amide protons are presented in (figure 22). Except the N-terminal Aib-NHs, all other NHs appear at downfield region and show little shift when solutions of foldamer **10** are titrated gradually with $[\text{D}_6]$ DMSO ($\Delta\delta < 0.24$ ppm), suggesting their strong involvement in intramolecular hydrogen bonding interaction. In contrast, the chemical shift of both N-terminal Aib amide NH protons undergoes significant chemical shift changes ($\Delta\delta = 1.60$ ppm), on incremental addition of $[\text{D}_6]$ DMSO suggesting their involvement in intermolecular hydrogen bonding.

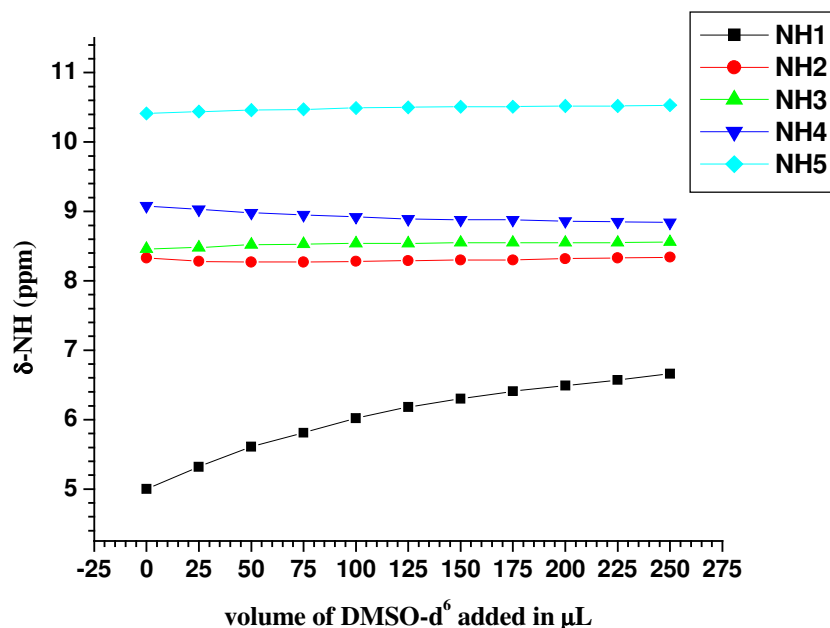


Figure 22: [D₆]DMSO titration graph of the foldamer **10**. The initial concentration of the sample in CDCl₃ was 10.2 mM, and the total amount of [D₆] DMSO used was 29.3% of the total volume.

1.7 Foldamers with Aib-Pro-Adb motif

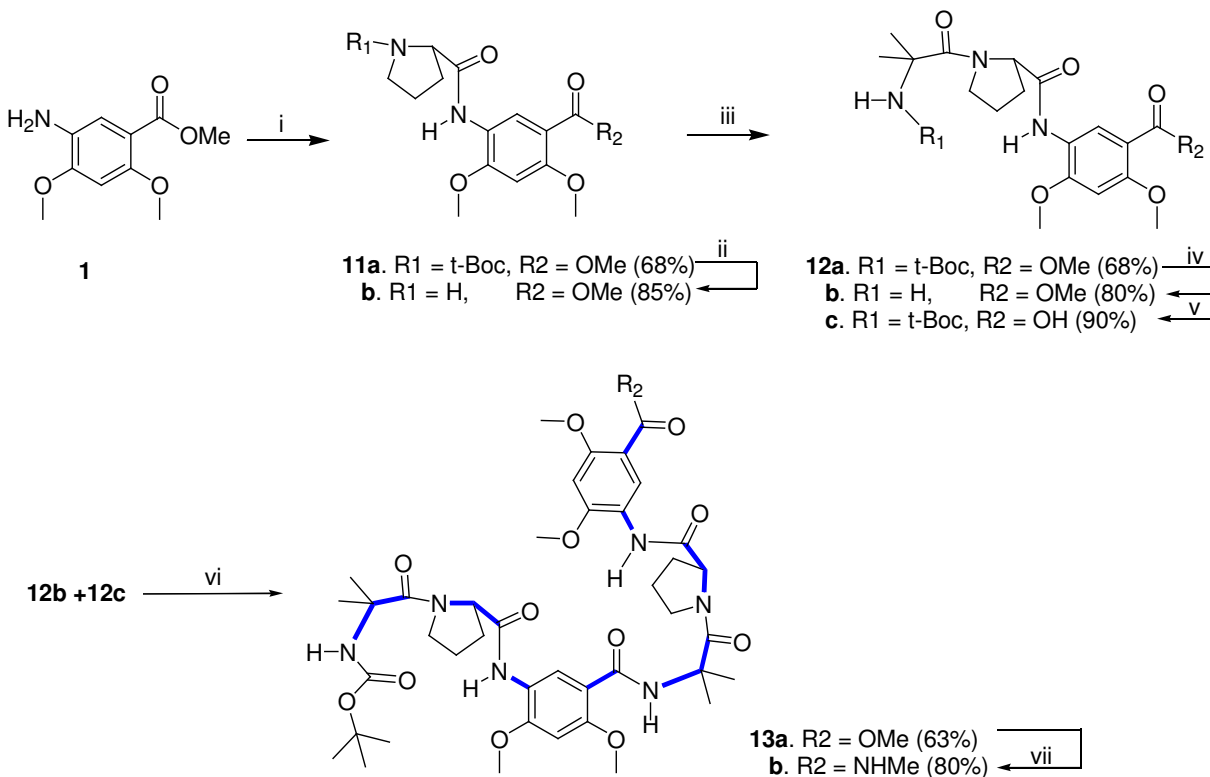
Continuing the previous work we designed the Aib-Pro-Adb motif-based foldamer building block **13b** (scheme 3) anticipating that the corresponding oligomers would adopt a well-defined, compact, three dimensional structure, governed by a combined conformational restriction imposed by the conformationally constrained individual amino acid residues: Aib, Pro, and Adb (the conformationally restricted *Sp3* backbone bonds in **13b** are highlighted in bold bonds). Central to the design strategy is stabilizing and restoring the 10-membered cyclic hydrogen bond between residue *i* and *i*+3 defining a β-bend ribbon spiral motif; a characteristic feature found in peptides with -(Aib-Pro)- sequence.⁵⁸

In a sequential peptide, the alternation of a Pro (proline) residue that disrupts the conventional H-bonding schemes found in helices and a helix-forming residue such as Aib (α -aminoisobutyric acid) may give rise to a novel helical structure, called the β -bend ribbon spiral.⁵⁸ This structure may be viewed as a subtype of the 3_{10} -helix, having somewhat the same helical fold of the peptide chain with intramolecular N-H...O=C H-bonds of the β -bend type,⁵⁹ and is characterized by two sets of (ϕ, ψ) angles: $\phi_i = -54^\circ$, $\psi_i = -40^\circ$; $\phi_{i+1} = -78^\circ$, $\psi_{i+1} = -10^\circ$ associated with the Aib-Pro motif. The complete structural characterization of this peptide conformation, which may be of relevance in the development of model systems for peptaibol antibiotics (e.g., zervamicin)⁵⁸ and for the numerous (Pro-X)_n (with X \neq Pro) segments found in globular and fibrous proteins, was achieved by x-ray diffraction studies of terminally blocked (L-Pro-Aib)_n sequential peptides.⁵⁹

1.7.1 Synthesis

The Aib-Pro-Adb motif-based foldamer **13b** was assembled from Boc-Aib-Pro-Adb-OMe building block **12a** (scheme 3). The easily crystallizing building block **12a**, readily available by the TBTU-mediated coupling of the dipeptide H-Pro-Adb-OMe **11b** with BOC-Aib-OH, was subjected to segment doubling strategy to afford **13a**, which could be easily amidated to afford the amide analog **13b**.

Scheme 3



Reagents and conditions: (i) BOC-Pro-OH, IBCF (isobutyl chloroformate), Et₃N, dry DCM, rt, 6 h; (ii) dry HCl (gas), dioxane, rt, 5 min; (iii) **11b**, BOC-Aib-OH, DIPEA, TBTU, dry MeCN, rt, 8h; (iv) dry HCl (gas), dioxane, rt, 5 min; (v) 2N LiOH, MeOH, rt, 12 h; (vi) DIPEA, TBTU, dry MeCN, rt, 12 h; (vii) methanolic MeNH₂, 50^oC, 70 h, rt. *Note:* To facilitate identification, the conformationally restricted *Sp*³ backbone bonds in **13b** are highlighted in bold bonds.

1.7.2 Results and Discussion

The shorter foldamer **12a** could be crystallized readily from ethyl acetate-pet-ether (1:1) solvent mixture. Investigation of its crystal structure revealed the existence of the anticipated folded conformation having Aib- and Pro residues taking the *i+1* and *i+2* positions, respectively, of a β -bend ribbon spiral motif (figure 23), characteristic of (L-Pro-Aib)*n* sequential peptides.^{58,59} The D-H...A angle is 173.57^o, and the D-H...A distance is 3.04 Å, which is on the higher side of the limit. The phi (ϕ^o) and psi (ψ^o)

dihedral angles from the crystal structure of **12a** were: $\phi_1 = -55$, $\psi_1 = -36$; $\phi_2 = -75$, $\psi_2 = -11$; which are in excellent agreement with the observed ϕ and ψ dihedral angles observed in (L-Pro–Aib) $_n$ sequential peptides ($\phi_1 = -54$, $\psi_1 = -40^\circ$; $\phi_2 = -78^\circ$, $\psi_2 = -10^\circ$) characterized by the β -bend ribbon spiral motif.^{58,59} This also means that incorporation of Adb residue (itself a constrained amino acid) close to the L-Pro–Aib site does not disrupt the β -bend ribbon spiral motif. It is noteworthy that incorporation of constrained amino acids into peptide sequences often causes dramatic conformational flipping.³⁹

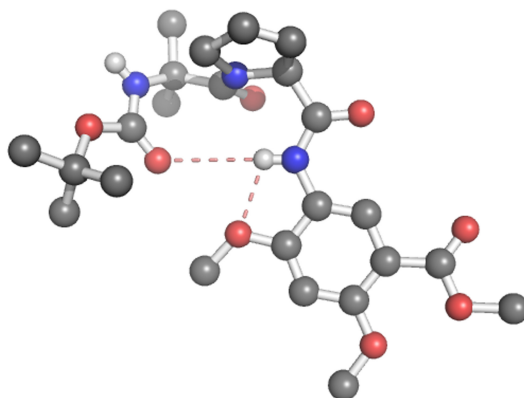


Figure 23: Single crystal X-ray structure (ball and stick representation) of the Boc-Aib-Pro-Adb-OMe foldamer **12a**. H-bonding interactions are highlighted in salmon colored dashes. In addition to the N-H...O=C β -turn interaction, S (5) type interaction³⁹ is also visible. Hydrogens, other than at the hydrogen bonding sites, have been deleted for clarity.

Investigation of the crystal structure further revealed that the amide NH of Aib that does not participate in intramolecular hydrogen bonding interaction participates in intermolecular interaction with the proline C=O of another molecule forming a self-assembled extended chain structure (Experimental procedures).

All efforts to crystallize the Aib-Pro-Adb motif-based hexapeptide foldamer **13b** did not succeed. However, it was possible to investigate the essential structural features

by solution-state NMR studies (figure 24). Due to solubility reasons, the solution-state conformational studies were carried out in CDCl₃, in which the foldamer was readily soluble. It is noteworthy that the occurrence of periodic β -turn motifs in **13b** is strongly supported by 2D NOESY NMR studies in solution (500 MHz, CDCl₃). One of the most characteristic nOe interactions that can be anticipated for a repeat turn conformation, as observed in the solid-state structure of the shorter analog **12a**, would be the requirement of repeat dipolar couplings between the aryl-NH and δ -CH of adjacent proline in **13b**, since they are in spatial proximity. Analysis of the 2D NOESY data indeed revealed the existence of sequential dipolar couplings between proline δ -CH and aryl-NH of the adjacent residues in **13b** (NH2/ δ 1 and NH4/ δ 2).

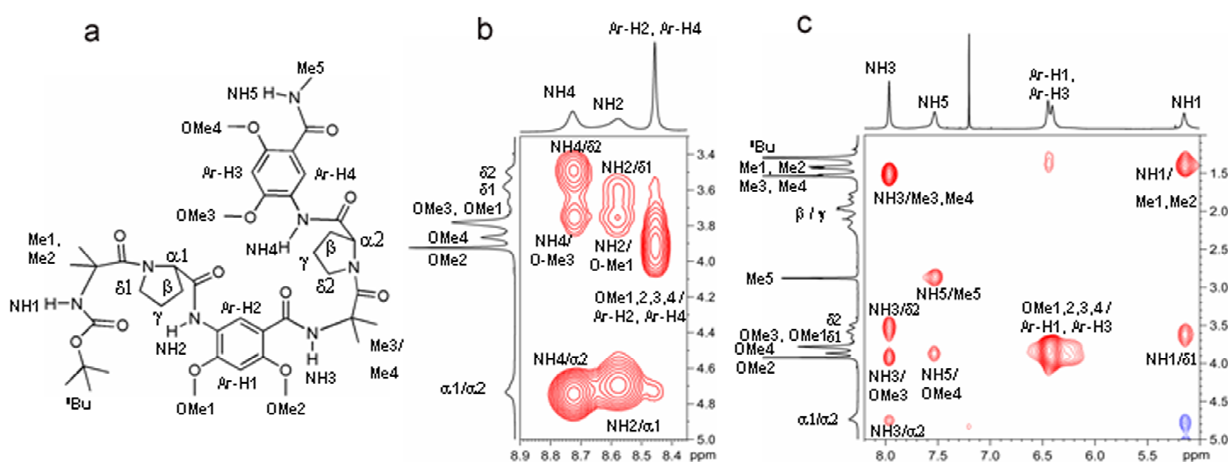


Figure 24: (a) Molecular structure of **13b** with selectively numbered protons; (b, c) partial 2D NOESY spectra of **13b** (500 MHz, CDCl₃) showing characteristic nOes.

Furthermore, the turn conformation also would require the spatial proximity of aryl-NH and α -CH of adjacent proline, which is also readily borne out in the 2D NOESY data (NH2/ α 1 and NH4/ α 2). The characteristic NOE interactions between aryl-NH and the adjacent *O*-aryloxymethyls in **13b** (OMe1/NH2; OMe2/NH3; and OMe3/NH4) strongly

suggest their *syn* orientation, thereby making space for the S(5) type hydrogen bonded arrangement,⁵⁵ a prerequisite for the bifurcated hydrogen bonding in such systems.^{2e,f} Nevertheless, the present study does not rule out the possibility of rotamer formation / local dynamics under the conditions of this NMR study, since some the signals are seemingly broadened.

To confirm that intramolecular hydrogen bonds are clearly prevalent in solution, we also performed [D₆]DMSO titration studies of **13b**. The chemical shift changes of all the amide protons are presented in figure 25. Except the N-terminal Aib-NH, all other NHs appear at downfield region and show little shift when solutions of **13b** are titrated gradually with [D₆]DMSO ($\Delta\delta < 0.15$ ppm), suggesting their strong involvement in intramolecular hydrogen bonding interaction. In contrast, the chemical shift of N-terminal Aib amide NH proton undergoes significant chemical shift changes ($\Delta\delta = 1.26$ ppm), on incremental addition of [D₆]DMSO suggesting its involvement in intermolecular hydrogen bonding.

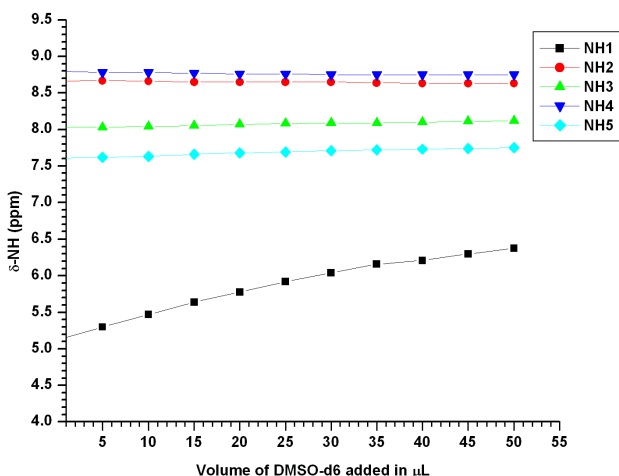


Figure 25: [D₆]DMSO titration graph of the hexapeptide foldamer **13b**. The initial concentration of the sample in CDCl₃ was 19.5 mM, and the total amount of [D₆] DMSO used was 7.7% of the total volume.

1.7.3 Conclusion

In conclusion, we have designed and developed novel aliphatic-aromatic conjugated hybrid foldamer that adopts a well-defined, compact, three-dimensional architecture, governed by a combined conformational restriction imposed by the individual amino acids with they are made of. Conformational investigations confirmed the prevalence of single conformation in both solid and solution-state, as evidenced from single crystal X-ray and 2D NOESY studies, respectively. The findings suggest that constrained aliphatic-aromatic amino acid conjugates offer new avenues for the *de novo* design of foldamers with distinctive structural architectures.

1.8 Experimental procedures

General Methods

Unless otherwise stated, starting materials were obtained from commercial suppliers and used without further purification. 3-amino-4, 6-dimethoxy benzoic acid (Adb) were prepared following the literature procedures.³⁵ dry dichloromethane (DCM) was prepared by distillation over P₂O₅. Dry acetonitrile (CH₃CN) were freshly prepared by distillation over CaH₂. Dry acetone was freshly distilled over KMnO₄ followed by K₂CO₃. Dry reactions were performed under argon atmosphere. Purification by column chromatography was performed in 100-200-mesh silica, unless otherwise stated. NMR spectra were recorded in CDCl₃ and d₆-DMSO on AC-200 MHz, DRX-400 MHz, DRX-500 MHz Bruker NMR spectrometers. Electrospray ionization mass spectrometry (ESI-MS) was carried out on a Finnigan MAT-1020 mass spectrometer and MALDI-TOF mass spectra on a Voyager-DE STR mass spectrometer. IR spectra, recorded in CHCl₃ or nujol were obtained from Perkin–Elmer 68515 PC-FTIR spectrophotometer. Combustion data were recorded on Elementar-Vario-EL (Heraeus Company Ltd., Germany). Melting points were measured on Buchi 535 melting point apparatus and are uncorrected. Reactions were monitored by thin layer chromatography (TLC) carried out on 0.25 mm E-Merck silica gel plates.

Crystal data for 3b: C₃₂H₄₅N₅O_{10.7}(H₂O): *M* = 785.84, colorless crystal, approximate size 0.56 x 0.27 x 0.05 mm, multi scan data acquisition, θ range = 2.12 to 25.00°, Triclinic, space group *P*-1, *a* = 6.893 (15), *b* = 15.55 (3), *c* = 20.21 (4) Å, α = 110.27 (5)°, β = 93.77 (5)°, γ = 93.37 (5)°, *V* = 2019 (8) Å³, *Z* = 2, ρ_{calcd} = 1.292 gcm⁻³, *T* = 297 (2), μ (Mo K α) = 0.105 mm⁻¹, 7052 reflections measured, 4044 unique [*I* > 2 σ (*I*)] reflections,

575 refined parameters, R value 0.0551, $wR2 = 0.1244$ (all data $R = 0.0916$, $wR2 = 0.01372$).

Crystal data for 12a: $C_{24}H_{35}N_3O_8$, $M = 493.55$, crystal size, $0.72 \times 0.21 \times 0.12 \text{ mm}^3$, $T = 297(2) \text{ K}$, crystal system, orthorhombic, space group $C222_1$; $a = 16.126(3)$, $b = 21.227(3)$, $c = 16.074(4) \text{ \AA}$, $V = 5502.2(19) \text{ \AA}^3$, $Z = 8$, $F(000) = 2112$, $d \text{ calc} [\text{g cm}^{-3}] = 1.192$, $\mu [\text{mm}^{-1}] = 0.090$, absorption correction, multi-scan, $T_{\min} = 0.9383$; $T_{\max} = 0.9893$; 13748 reflection collected, 4805 unique reflections, 3148 observed reflections, 324 refined parameters, $R_1 [I > 2\sigma(I)] = 0.0695$, $WR_2 = 0.1492$ (all data $R = 0.1093$, $wR2 = 0.1653$), goodness of fit, 1.074, $\Delta\rho_{\max}$, $\Delta\rho_{\min} (\text{e \AA}^{-3}) = 0.182, -0.146$.

5-(2-tert-Butoxycarbonylamino-2-methyl-propionylamino)-2,4dimethoxy-

benzoic acid methyl ester 2a: To an ice-cold stirred solution of the acid Boc-Aib-OH (5.70 g, 28.0 mmol, 1 equiv.) and the aromatic amine **1** (5.33 g, 25.3 mmol, 0.9 equiv.) in dry acetonitrile (30 mL) was added DIPEA (7.53 mL, 42.1 mmol, 1.5 equiv) followed by TBTU (12.61 g, 39.3 mmol, 1.4 equiv.). The resulting mixture was stirred for 6 hrs at room temperature. The solvent was stripped off under reduced pressure and the residue was diluted with dichloromethane and washed sequentially with potassium hydrogen sulphate solution, saturated sodium bicarbonate, and water. Drying and concentration of the dichloromethane extract under reduced pressure gave the crude product which on column chromatography (50% EtOAc/Hexane) afforded the desired pure product **2a** (8 g, 72%); mp $143\text{-}145^{\circ}\text{C}$; IR (Nujol) $\nu \text{ cm}^{-1}$: 3020, 1712, 1531, 1463, 1215, 754; $^1\text{H NMR}$ (500 MHz, CDCl_3): δ 8.81 (s, 1H), 8.58 (bs, 1H), 6.44 (s, 1H), 5.02 (bs, 1H), 3.87 (s, 3H), 3.85 (s, 3H), 3.78 (s, 3H), 1.52 (s, 6H), 1.38 (s, 9H); $^{13}\text{C NMR}$ (125 MHz, CDCl_3): δ

172.4, 165.5, 157.8, 154.5, 152.6, 123.1, 120.4, 111.3, 95.5, 57.6, 56.4, 55.8, 51.5, 28.1, 25.7; ESI Mass: 435.34 (M + K); Anal. Calcd. for C₁₉H₂₈N₂O₇: C, 57.57; H, 7.07; N, 7.07. Found: C, 57.37; H, 7.03; N, 6.99.

5 (2-Amino-2-methyl-propionyl amino)-2,4 dimethoxy-benzoicacid methyl ester hydrochloride. 2b. To an ice cold stirred solution of the compound **2a** (0.5 g, 1.3 mmol) in dry dioxane (10 ml) was bubbled dry HCl gas for five minutes. Then dry ether (15 mL) was added to the reaction mixture, when the amine hydrochloride **2b** precipitated out as a white solid (0.37 g, 87%), The solid was filtered, washed with dry ether, dried and used for the next reaction, without further purification.

5-(2-tert-Butoxycarbonylamino-2-methyl-propionylamino)-2,4-dimethoxy benzoic acid. 2c. To an solution of compound **2a** (2.2 g, 5.6 mmol, 1 equiv.) in methanol (15 mL) was added 2N LiOH solution (11.08 mL, 22.2 mmol, 4 equiv.). The reaction mixture was stirred at room temperature for overnight. The reaction mixture was evaporated to dryness and diluted with distilled water, and acidified with saturated potassium hydrogen sulphate. Then the aqueous layer was extracted with ethyl acetate (2 x 100 mL). The combined organic extracts were washed with brine. Drying and concentration of the organic layer, under reduced pressure, yielded the desired product **2c** (2.0 g, 94 %), which was used for the next reaction, without further purification.

{1-[5-[1-{2,4-Dimethoxy-5-methylcarbamoyl-phenylcarbamoyl}-1-methyl-ethylcarbamoyl]-2,4-dimethoxy-phenylcarbamoyl}-1-methyl-ethyl]-carbamicacid tert-butyl ester 3b: To an ice-cold stirred solution of the acid **2c** (2.0 g, 5.2 mmol, 1 equiv.) and amine **2b** (1.73 g, 5.23 mmol, 1 equiv.) in dry acetonitrile (20 mL) was added

DIPEA (2.3 mL, 13.0 mmol, 2.5 equiv.) followed by TBTU (2.35 g, 7.3 mmol, 1.4 equiv.) The resulting reaction mixture was stirred for overnight at room temperature. The solvent was stripped off under reduced pressure; the residue was dissolved in dichloromethane (100 mL) and washed sequentially with potassium hydrogen sulphate solution, saturated sodium bicarbonate and water. Drying and concentration in vacuo yielded the crude product which on column chromatography (90% EtOAc/Pet-ether, R_f : 0.2) afforded **3a** (2.4 g, 69%), which was directly used for the next amidation reaction, without further purification. The ester **3a** (2.4 g, 3.63 mmol) was taken in saturated methanolic methylamine solution (25 mL) and stirred at room temperature for two days. The solvent was removed under reduced pressure, and the crude product was purified by column chromatography (5% methanol/EtOAc, R_f : 0.4) to yield pure **3b** (2.0 g, 83%) which could be crystallized from acetonitrile: water (90:10); mp 210-212^oC; IR (Nujol) ν cm⁻¹: 3419, 3018, 1647, 1610, 1517, 1215, 758; ¹H NMR (500 MHz, CDCl₃): δ 8.99 (s, 1H), 8.89 (s, 1H), 8.76 (s, 1H), 8.76 (s, 1H), 8.44 (bs, 1H), 8.26 (s, 1H), 7.53 (s, 1H), 6.46 (s, 1H), 6.38 (s, 1H), 5.07 (bs, 1H), 3.95 (s, 3H), 3.88 (s, 3H), 3.87 (s, 3H), 3.84 (s, 3H), 2.93 (d, 3H), 1.70 (s, 6H), 1.52 (s, 6H), 1.40 (s, 9H); ¹³C NMR (125 MHz, CDCl₃): δ 172.5, 172.1, 165.7, 164.7, 154.6, 152.8, 152.4, 124.6, 124, 121.2, 121.1, 114.1, 113.8, 94.9, 94.8, 58.3, 57.5, 56.4, 56.2, 55.9, 28.1, 26.4, 25.5; ESI Mass: 681.95 (M+Na); Anal. Calcd. for C₃₂H₄₅N₅O₁₀: C, 58.27; H, 6.82; N, 10.62. Found: C, 58.15; H, 6.80; N, 10.59.

6,6'-Dimethoxy-3,3,3',3'-tetramethyl-1,1'-spirobiindane-5,5'-bis-1-(5-(1-(2,4-Dimethoxy-5-methylcarbonyl-phenylcarbonyl)-1-methyl-ethylcarbonyl)-2,4-dimethoxy-phenylcarbonyl)-1-methyl-ethyl)-carbamic acid *tert*-butyl ester 10: To

an ice-cold stirred solution of the acid **9** (0.44 g, 0.68 mmol, 2.5 equiv.) and diamine **8** (0.1 g, 0.27 mmol, 1 equiv.) in dry acetonitrile (10 mL) was added DIPEA (0.24 mL, 1.36 mmol, 5 equiv.) followed by HBTU (0.31 g, 0.81 mmol, 3 equiv.). The resulting reaction mixture was stirred for 24 h at room temperature. The solvent was stripped off under reduced pressure; the residue was dissolved in dichloromethane (100 mL) and washed sequentially with potassium hydrogen sulphate solution, saturated sodium bicarbonate and water. Drying and concentration in vacuo yielded the crude product which on column chromatography (5% methanol:ethylacetate, R_f : 0.3) afforded **10** (0.27 g, 62%). mp 239-242^oC; IR (Nujol) ν cm^{-1}): 3018, 2399, 1693, 1612, 1519, 1215, 761; ¹H NMR (400 MHz, CDCl₃): δ 10.51 (s, 2H), 9.17 (s, 2H), 9.03 (s, 4H), 8.60 (s, 2H), 8.55 (bs, 2H), 8.42 (bs, 2H), 6.59 (s, 4H), 6.43 (s, 2H), 5.12 (bs, 2H), 4.09 (s, 12H), 4.01 (s, 12H), 3.88 (s, 6H), 2.50-2.40 (d, 2H), 2.35-2.25 (d, 2H), 1.84 (s, 12H), 1.65 (s, 12H), 1.53 (s, 30H); ¹³C NMR (100 MHz, CDCl₃): δ 172.2, 171.9, 164.5, 162.2, 154.4, 152.9, 152.2, 147.8, 144.2, 127.7, 124.5, 123.6, 121.1, 120.8, 113.9, 113.6, 113.2, 105.1, 94.9, 94.5, 59.2, 58.0, 57.5, 57.2, 56.1, 55.6, 42.9, 31.2, 30.0, 27.8, 25.2; MALDI-TOF Mass: 1646.4(M+Na); Anal. Calcd. for C₈₅H₁₁₀N₁₀O₂₂: C, 62.88; H, 6.78; N, 8.63. Found: C, 62.73; H, 6.65; N, 8.52.

2-{2,4-Dimethoxy-5-methoxycarbonyl-phenylcarbonyl}-pyrrolidine-1-carboxylic

acid tert-butyl ester. 11a: To an ice-cold stirred solution of the acid Boc-Pro-OH (0.85 g, 3.95 mmol, 1 equiv.) in dry dichloromethane (20 mL) was added Et₃N (1.09 mL, 7.9 mmol, 2equiv) followed by isobutyl chloroformate (0.51 mL, 3.95 mmol, 1 equiv.). The resulting mixture was stirred vigorously for 5 min and then the aromatic amine **1** (0.83 g, 3.95 mmol, 1 equiv) was added, then the reaction mixture was stirred for 5 h. The reaction mixture was diluted with dichloromethane and washed sequentially with

potassium hydrogen sulphate solution, saturated sodium bicarbonate, and water. Drying and concentration of the dichloromethane extract under reduced pressure gave the crude product which on column chromatography (50% EtOAc/Hexane) afforded the desired pure product **11a** (1.1 g, 68%); $[\alpha]_D^{26} -56.0$ (chloroform); mp 142-145⁰C; IR (Nujol) ν cm⁻¹: 3018, 2340, 1685, 1533, 1390, 1215, 758; ¹H NMR (200 MHz, CDCl₃): δ 8.81 (s, 1H), 8.58 (bs, 1H), 6.44 (s, 1H), 5.02 (bs, 1H), 3.87 (s, 3H), 3.85 (s, 3H), 3.78 (s, 3H), 1.52 (s, 6H), 1.38 (s, 9H); ¹³C NMR (100MHz, CDCl₃): δ 170.0, 165.5, 157.2, 155.8, 154.5, 152.6, 123.5, 120.7, 120.0, 111.5, 95.5, 80.4, 61.9, 60.5, 56.4, 55.8, 51.5, 47.0, 30.9, 28.2, 24.4, 23.7; ESI Mass: 431.18 (M + Na); Anal. Calcd. for C₂₀H₂₈N₂O₇: C, 58.82; H, 6.86; N, 6.86. Found: C, 58.71; H, 6.80; N, 6.79.

2, 4 Dimethoxy-5-[[pyrrolidine-2-carbonyl]-amino]-benzoic acid methyl ester. 11b.

To an ice cold stirred solution of the compound **11a** (0.5 g, 1.2 mmol) in dry dioxane (10 ml) was bubbled dry HCl gas for five minutes. Then dry ether (15 mL) was added to the reaction mixture, when the amine hydrochloride **11b** precipitated out as a white solid (0.36 g, 85%) The solid was filtered, washed with dry ether, dried and used for the next reaction, without further purification.

5-[[1-(2-tert-Butoxycarbonylamino-2-methyl-propionyl)-pyrrolidine-2-carbonyl]-

2,4-dimethoxy-benzoic acid methyl ester. 12a To an ice-cold stirred solution of the acid Boc-Aib-OH (0.59 g, 2.9 mmol, 1 equiv.) and amine **11b** (1.0 g, 2.90 mmol, 1 equiv.) in dry acetonitrile (15 mL) was added DIPEA (1.29 mL, 7.25 mmol, 2.5 equiv.) followed by TBTU (1.3 g, 4.06 mmol, 1.4 equiv.). The resulting reaction mixture was stirred for 6 h at room temperature. The solvent was stripped off under reduced pressure; the residue was

dissolved in dichloromethane (100 mL) and washed sequentially with potassium hydrogen sulphate solution, saturated sodium bicarbonate and water. Drying and concentration in vacuo yielded the crude product which on column chromatography (100% EtOAc, R_f: 0.6) afforded **12a** (0.95 g, 68%). $[\alpha]_D^{26} -29.2$ (chloroform); mp 165-168^oC; IR (Nujol) ν cm⁻¹: 3020, 2335, 1710, 1531, 1215, 754; ¹H NMR (200 MHz, CDCl₃): δ 8.72 (bs, 1H), 8.46(bs, 1H), 6.42 (s, 1H), 5.03 (bs, 1H), 4.85-4.65 (m, 1H), 3.86 (s, 6H), 3.78 (s, 3H), 3.70-3.5 (m, 2H), 2.60-1.75 (m, 4H), 1.47(s, 6H), 1.35 (s, 9H); ¹³C NMR (100 MHz, CDCl₃): δ 172.9, 170.3, 165.5, 158.0, 154.7, 154.3, 126.2, 119.7, 110.9, 95.6, 79.7, 62.5, 56.2, 55.7, 51.4, 47.9, 28.0, 25.5; MALDI-TOF Mass: 515.1 (M+Na); Anal. Calcd. for C₂₄H₃₅N₃O₈: C, 58.41; H, 7.09; N, 8.51. Found: C, 58.25; H, 6.95; N, 8.45.

5-[[1-{2-Amino-2-methyl-propionyl}-pyrrolidine-2-carbonyl]-amino]-2,4-

dimethoxy-benzoic acid methyl ester. 12b To an ice cold stirred solution of the compound **12a** (0.5 g, 1.01 mmol) in dry dioxane (10 ml) was bubbled dry HCl gas for five minutes. Then dry ether (15 mL) was added to the reaction mixture, when the amine hydrochloride **12b** precipitated out as a white solid (0.35 g, 80%). The solid was filtered, washed with dry ether, dried and used for the next reaction, without further purification.

5-[[1-{2-tert-Butoxycarbonylamino-2-methyl-propionyl}-pyrrolidine-2-carbonyl]-

amino]-2,4-dimethoxy-benzoic acid. 12c. To a solution of compound **12a** (0.75 g, 1.52 mmol, 1 equiv.) in methanol (15 mL) was added 2N LiOH solution (3.04 mL, 6.08 mmol, 4 equiv.). The reaction mixture was stirred at room temperature for overnight. The reaction mixture was evaporated to dryness and diluted with distilled water, and acidified

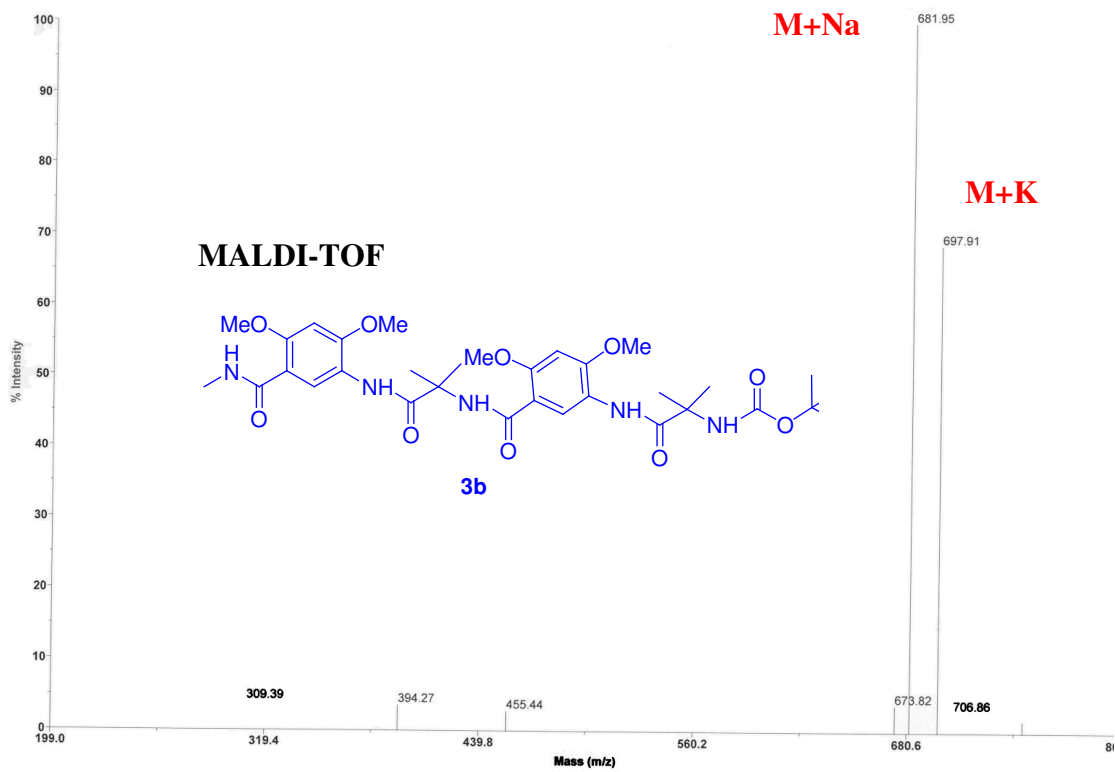
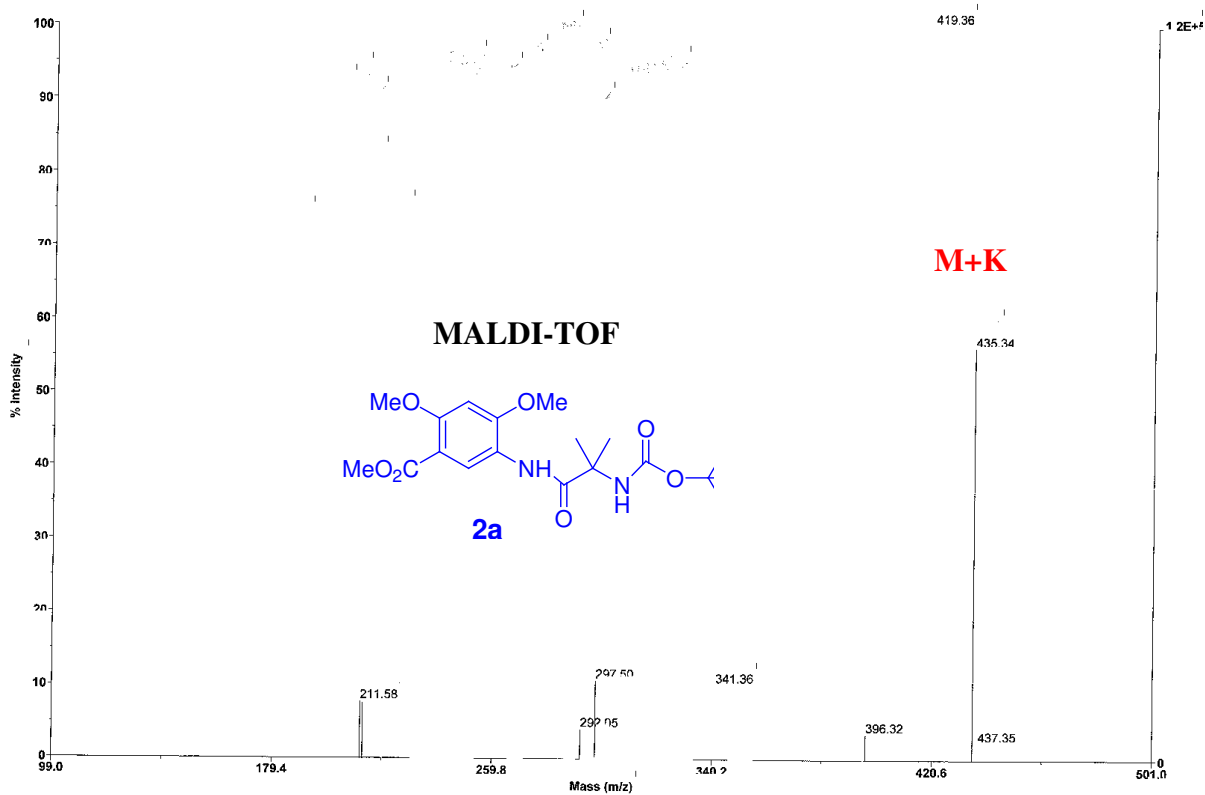
with saturated potassium hydrogen sulphate. Then the aqueous layer was extracted with ethyl acetate (3 x 50 mL). The combined organic extracts were washed with brine. Drying and concentration of the organic layer, under reduced pressure, yielded the desired product **12c** (0.67 g, 90 %), which was used for the next reaction, without further purification.

{2-[2-{5-{2-[2-{2,4-Dimethoxy-5-methylcarbamoyl-phenylcarbamoyl}-pyrrolidin-1-yl]-1,1dimethyl-2-oxo-ethylcarbamoyl}-2,4-dimethoxy-phenylcarbamoyl}-

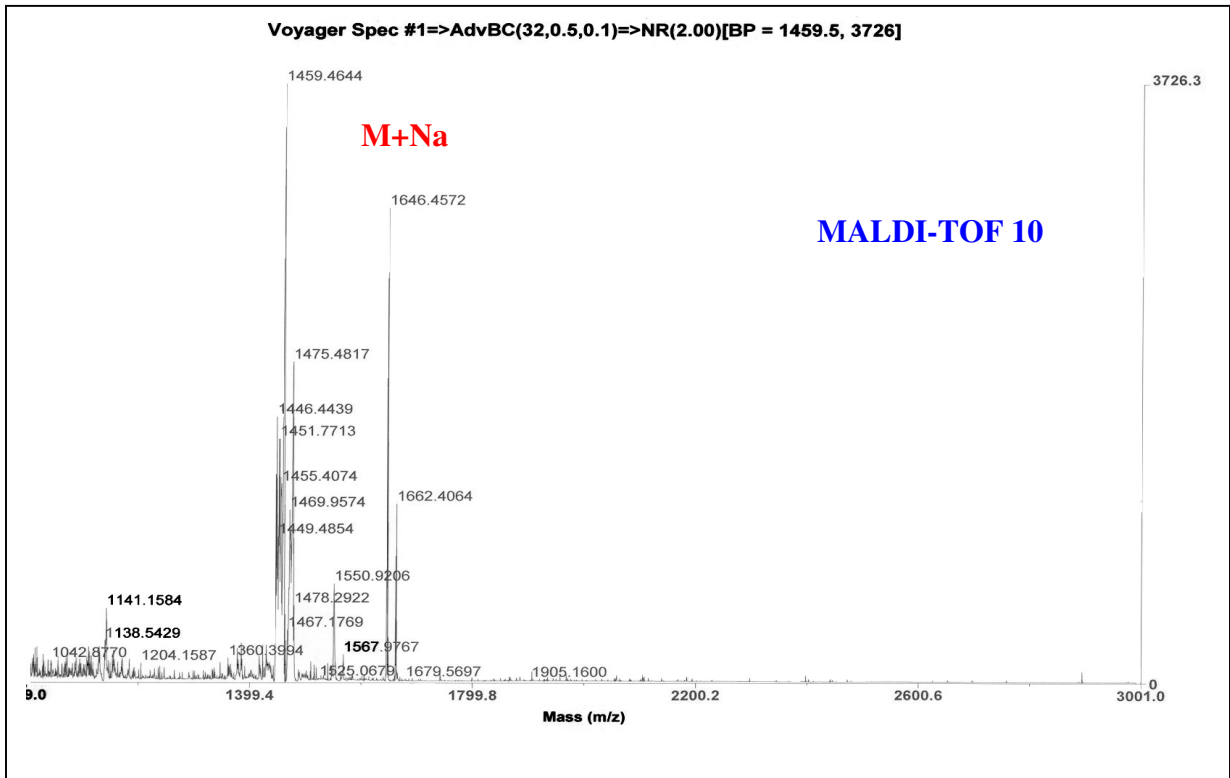
pyrrolidine-1-yl]-1,1-dimethyl-2-oxo-ethyl}-carbamic acid tert-butyl ester **13b**: To an ice-cold stirred solution of the acid **12c** (0.4 g, 0.83 mmol, 1 equiv.) and amine **12b** (0.35 g, 0.83 mmol, 1 equiv.) in dry acetonitrile (10 mL) was added DIPEA (0.37 mL, 2.08 mmol, 2.5 equiv.) followed by TBTU (0.37 g, 1.16 mmol, 1.4 equiv.) The resulting reaction mixture was stirred for overnight at room temperature. The solvent was stripped off under reduced pressure; the residue was dissolved in dichloromethane (100 mL) and washed sequentially with potassium hydrogen sulphate solution, saturated sodium bicarbonate and water. Drying and concentration in vacuo yielded the crude product which on column chromatography (5% methanol/ethyl acetate, R_f :0.2) afforded **13a** (0.45 g, 63%), which was directly used for the next amidation reaction, without further purification. The ester **13a** (0.45 g, 0.52 mmol was taken in saturated methanolic methylamine solution (15 mL) and stirred at room temperature for two days. The solvent was removed under reduced pressure, and the crude product was purified by column chromatography (8% methanol/ethyl acetate, R_f : 0.4) to yield pure **13b** (0.4 g, 80%); $[\alpha]_D^{26} -25.6$ (chloroform); mp 245-248⁰C; IR (Nujol) ν cm^{-1}): 3018, 1645, 1614, 1400, 1215, 758; ¹H NMR (400 MHz, CDCl₃): δ 8.76 (bs, 1H), 8.62 (bs, 1H), 8.49 (s, 1H), 8.32

(s, 1H), 8.02 (s, 1H), 7.60 (s, 1H), 6.50 (bs, 1H), 6.45 (bs, 1H), 5.28 (bs, 1H), 4.90-4.60 (m, 2H), 3.97 (s, 3H), 3.91 (s, 3H), 3.82 (s,6H), 3.75-3.45 (m,4H), 2.92 (d, 3H), 2.25-1.70 (m, 8H), 1.57 (s, 6H), 1.45 (s, 6H), 1.34 (s,9H); ¹³C NMR (100 MHz, CDCl₃): δ 173.1, 170.8, 169.6, 166.2, 164.1, 156.1, 154.9, 128.6, 127.4, 120.8, 113.9, 113.1, 95.8, 80.1, 62.9, 57.0, 48.3, 28.2, 26.7, 26.1, 25.4,; MALDI-TOF Mass: 876.36 (M+Na); Anal. Calcd. for C₄₂H₅₉N₇O₁₂: C, 59.08; H, 6.91; N, 11.48. Found: C, 58.95; H, 6.87; N, 11.39.

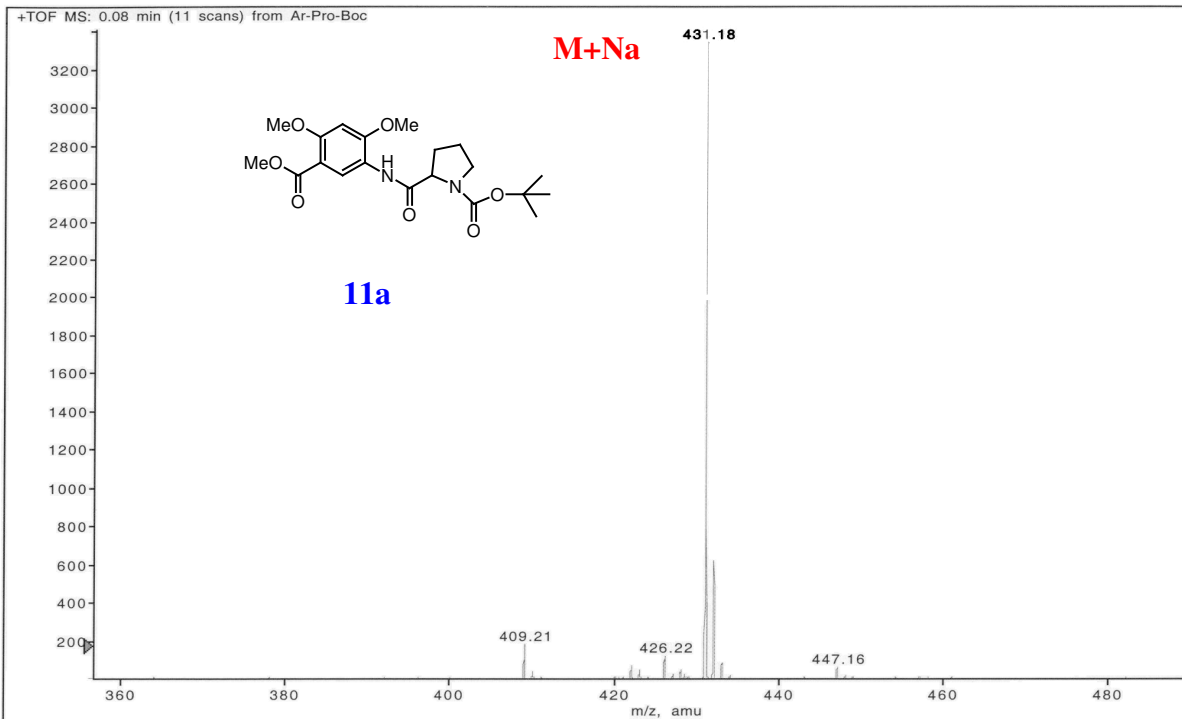
Voyager Spec #1=>AdvBC(32,0.5,0.1)=>NR(2.00)=>DI[BP = 419.4, 122107]

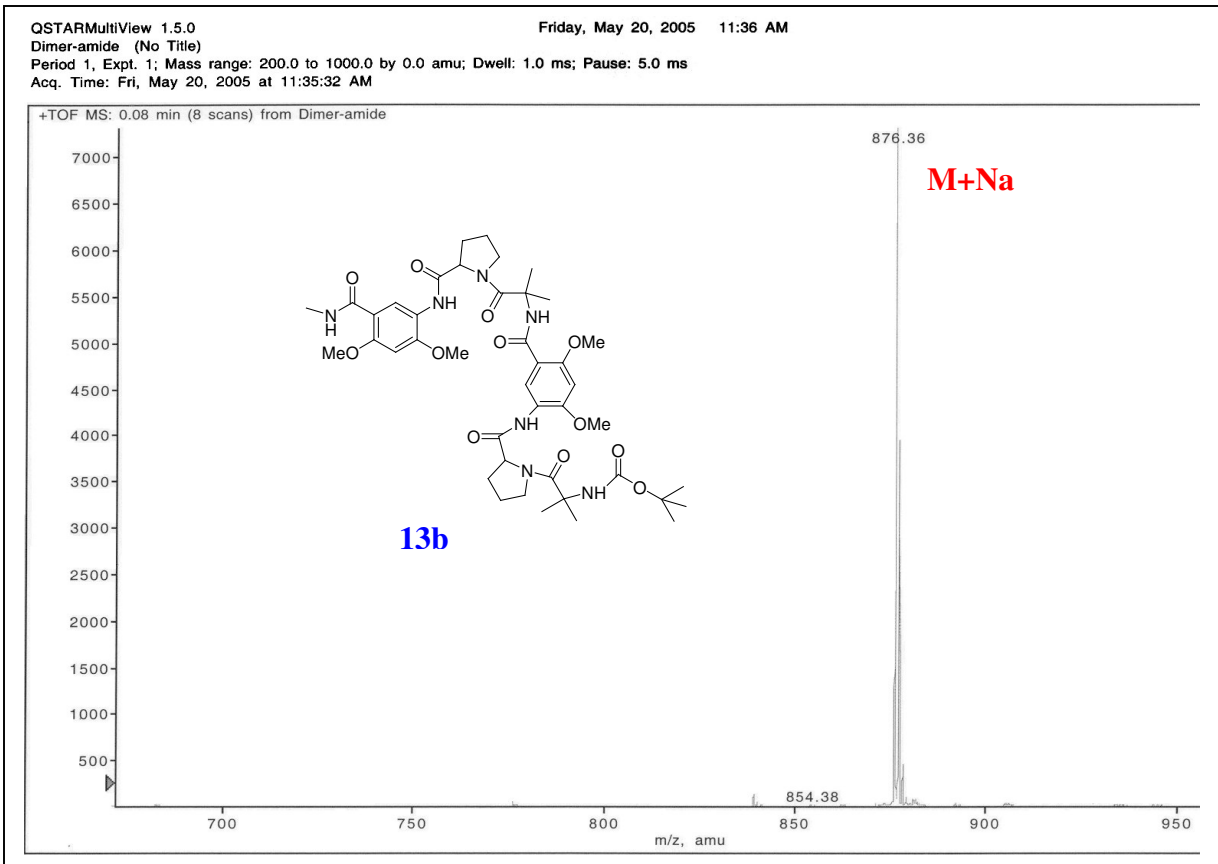
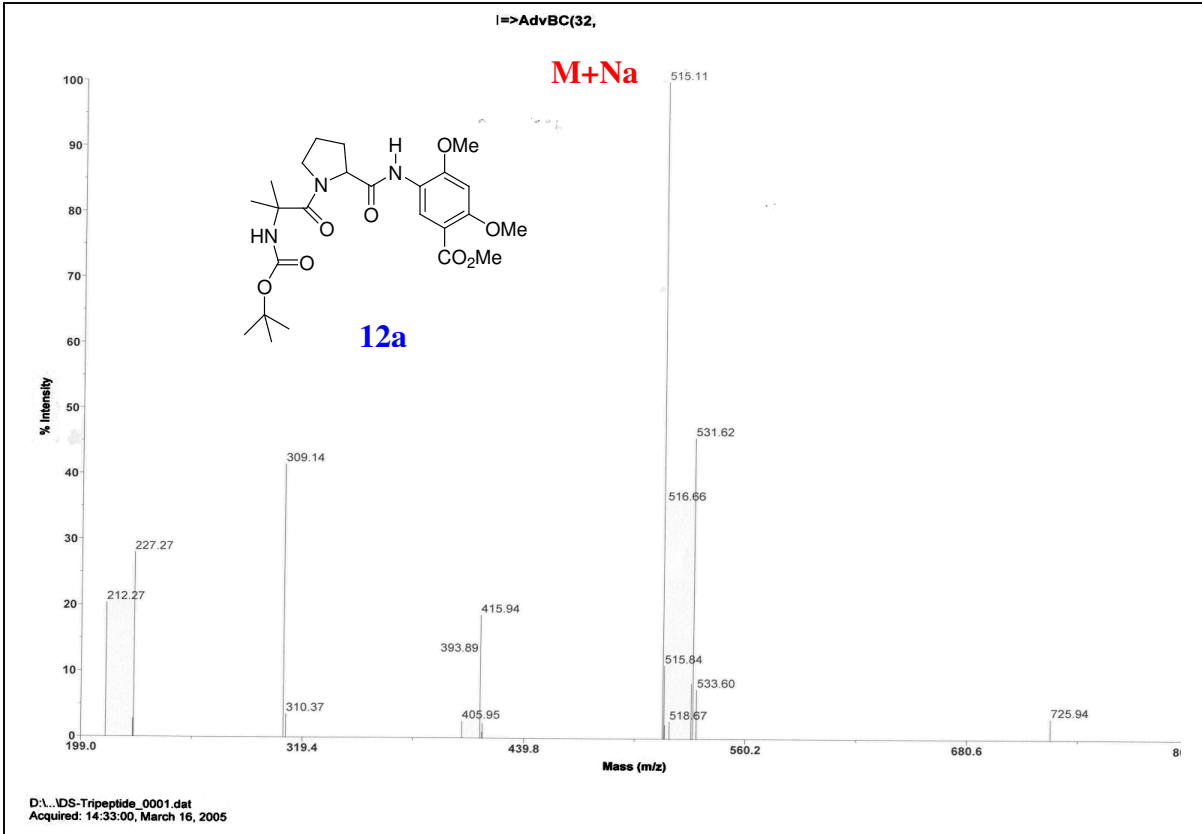


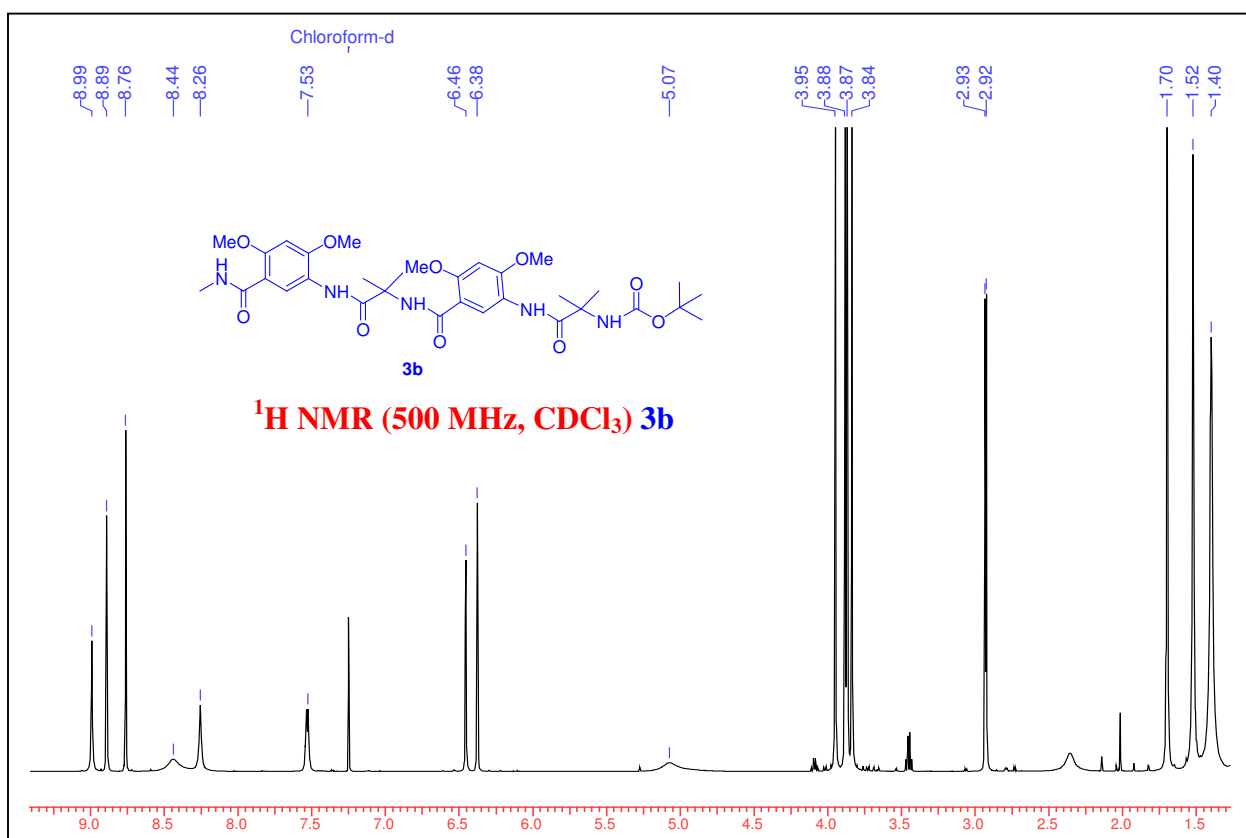
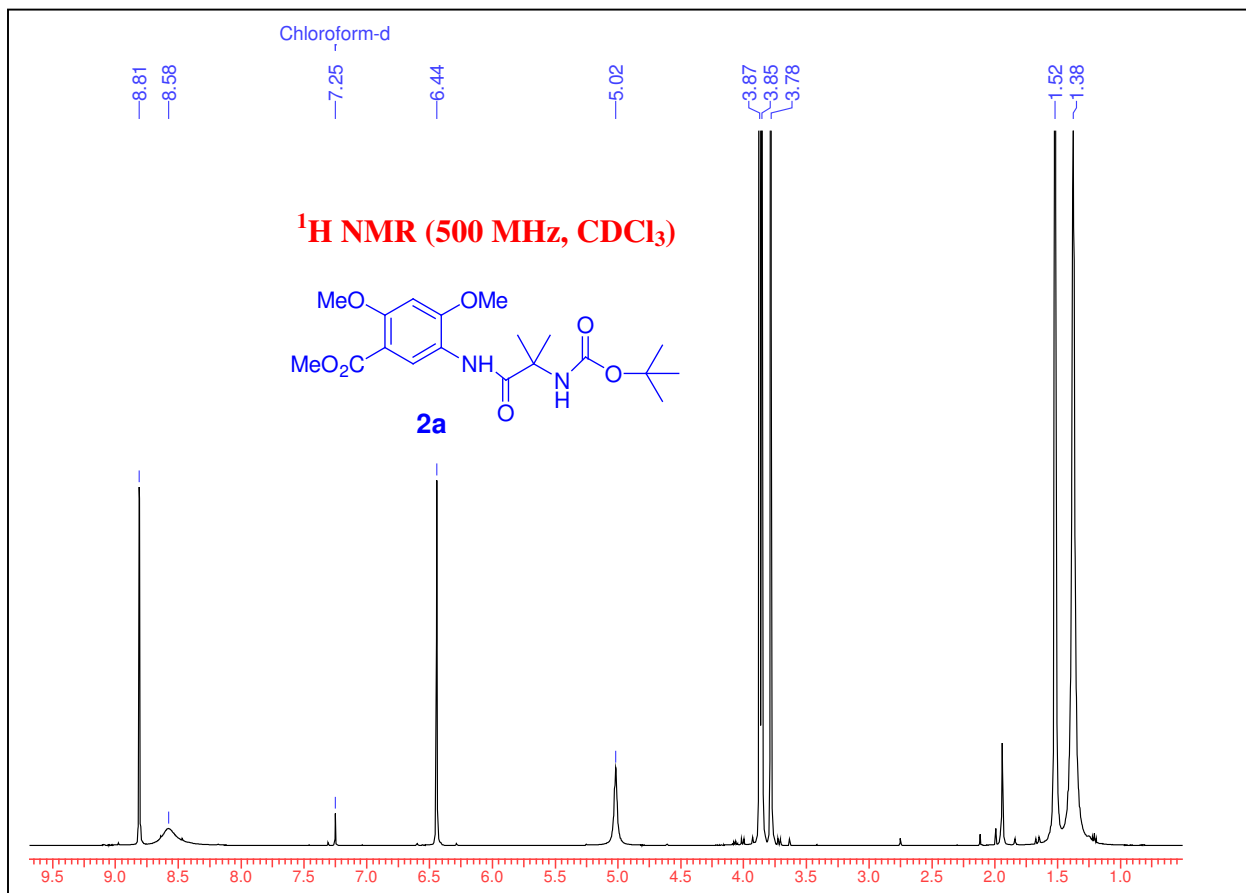
D:\...IDs-Alb-amide_0001.dat
Acquired: 14:31:00, March 16, 2005

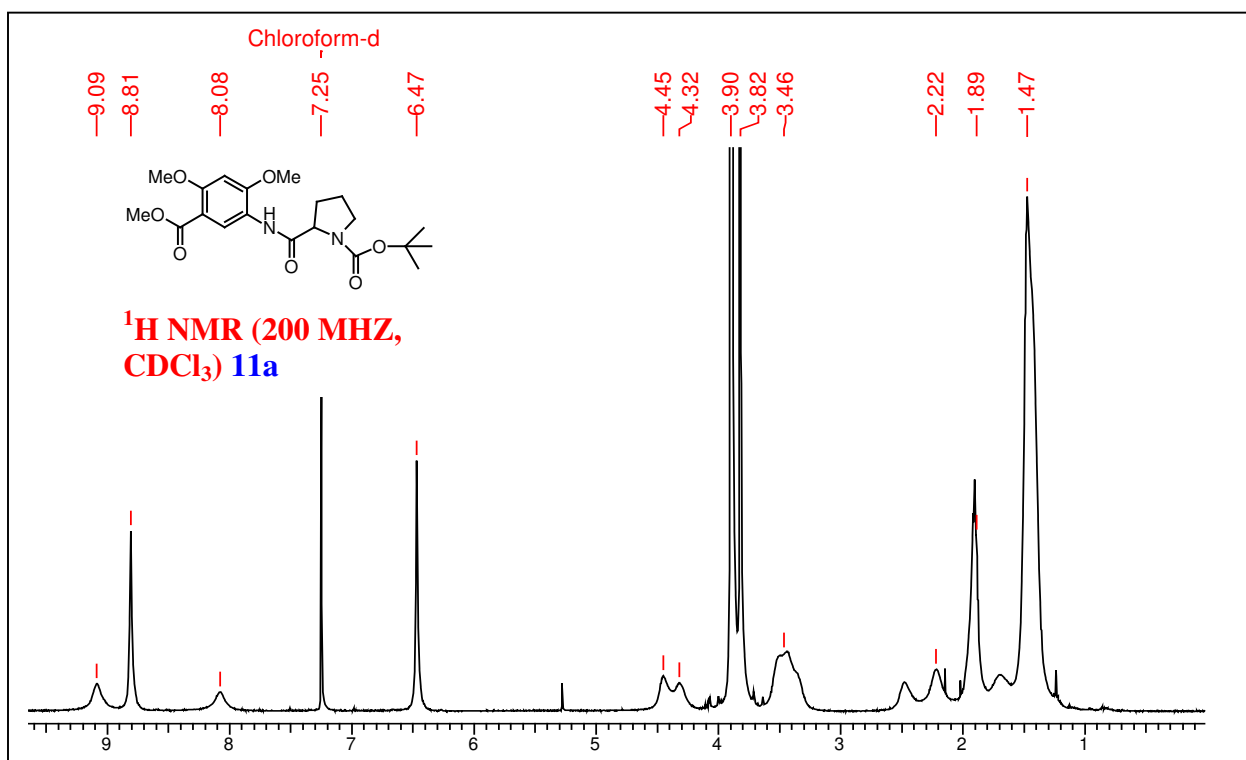
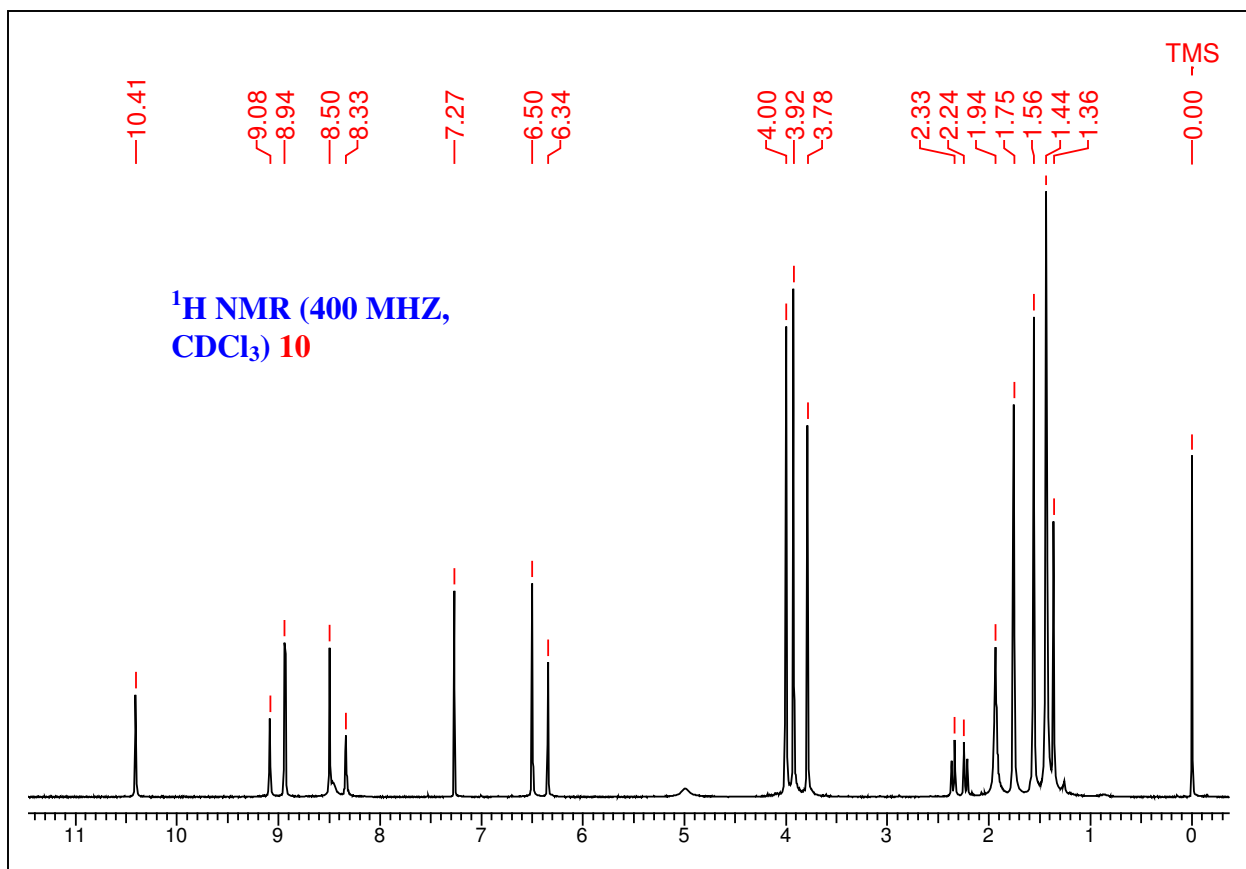


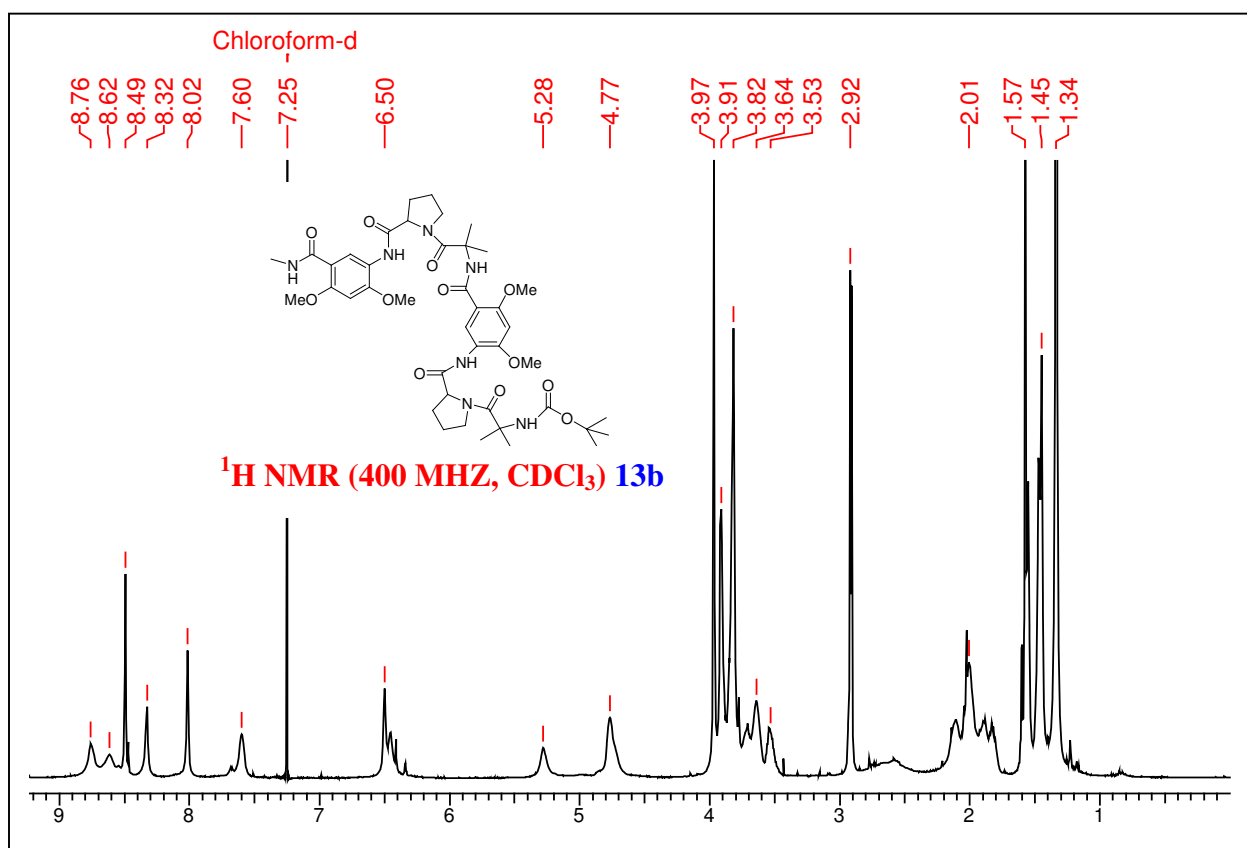
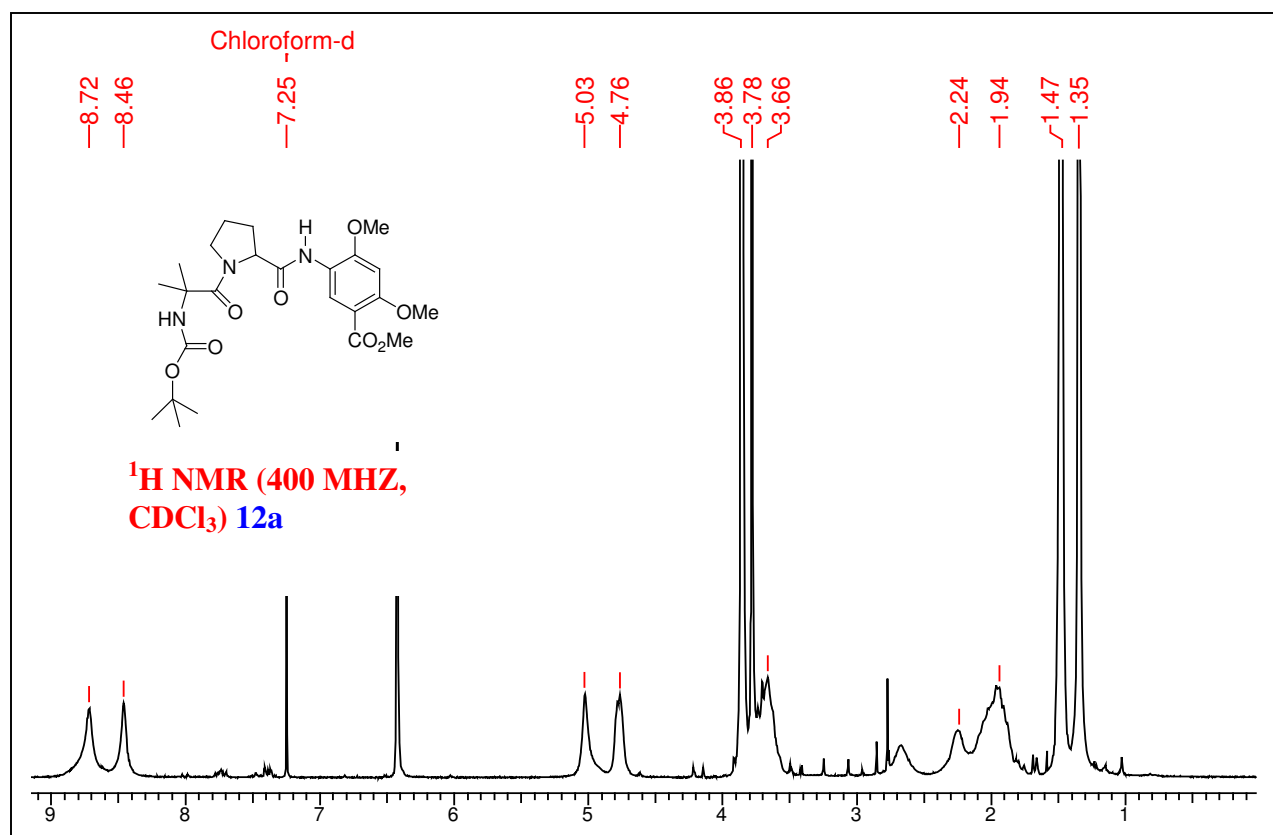
QSTARMultiView 1.5.0 Friday, May 20, 2005 11:30 AM
 Ar-Pro-Boc (No Title)
 Period 1, Expt. 1; Mass range: 200.0 to 900.0 by 0.0 amu; Dwell: 1.0 ms; Pause: 5.0 ms
 Acq. Time: Fri, May 20, 2005 at 11:29:15 AM

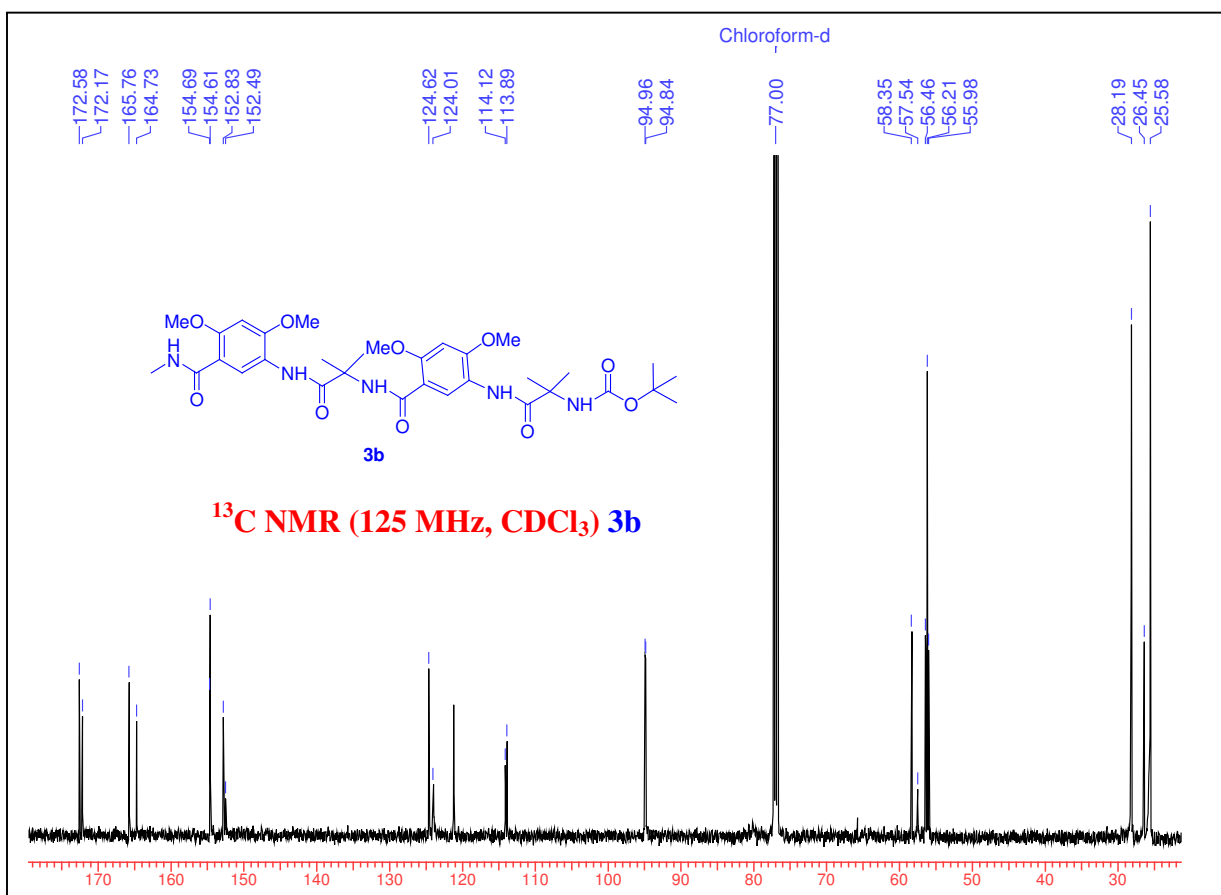
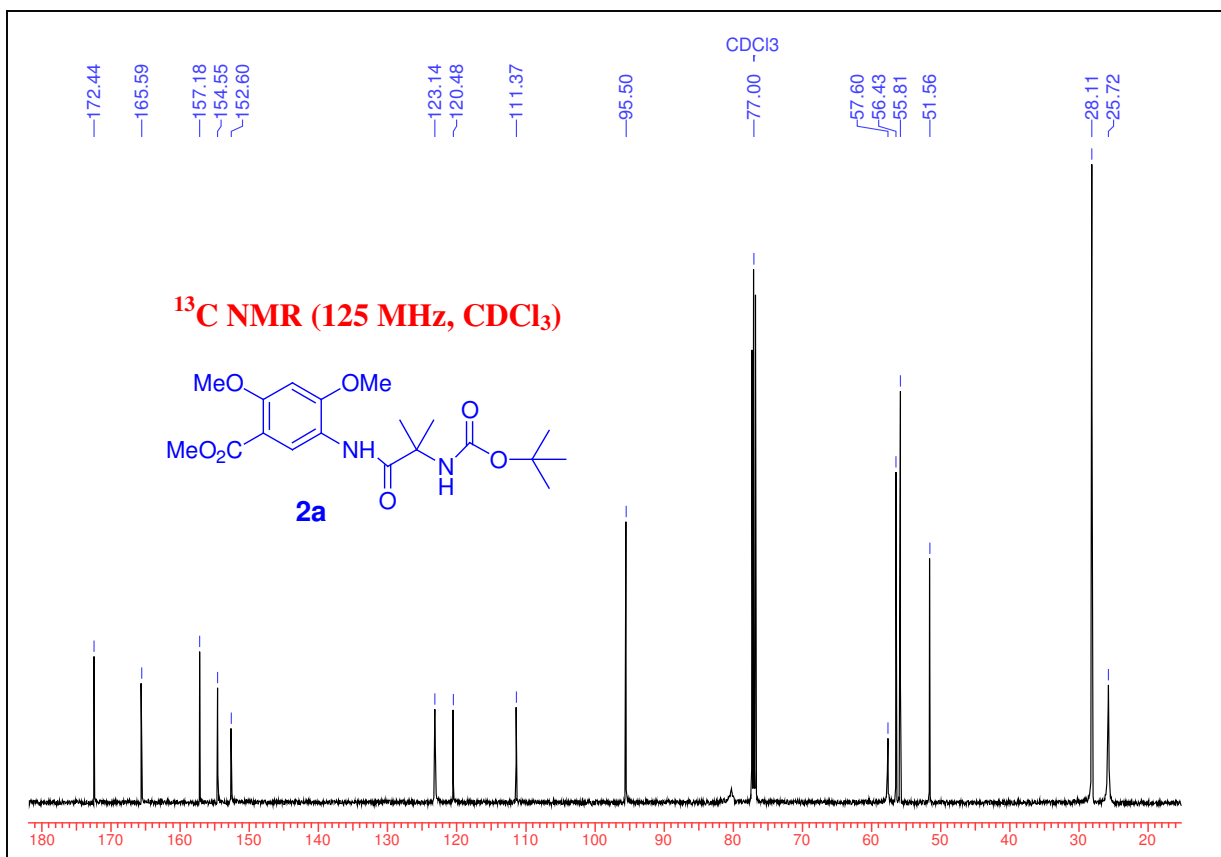


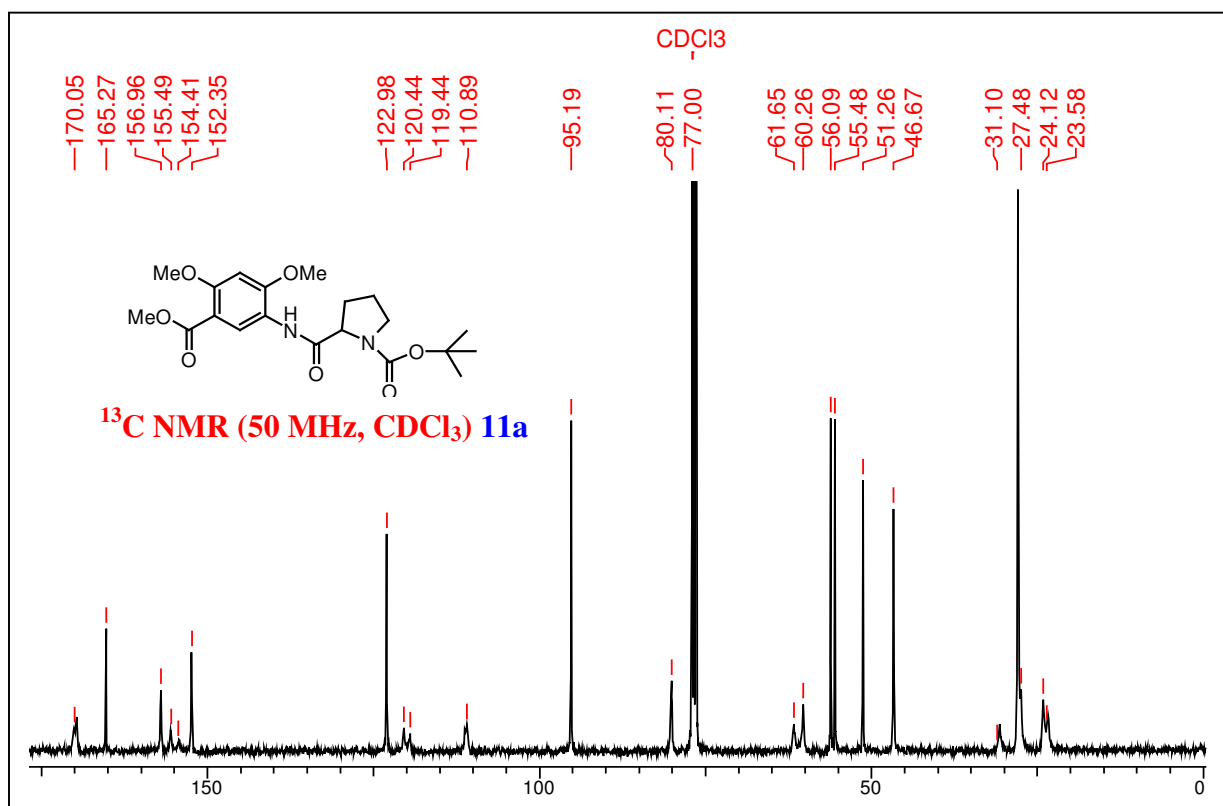
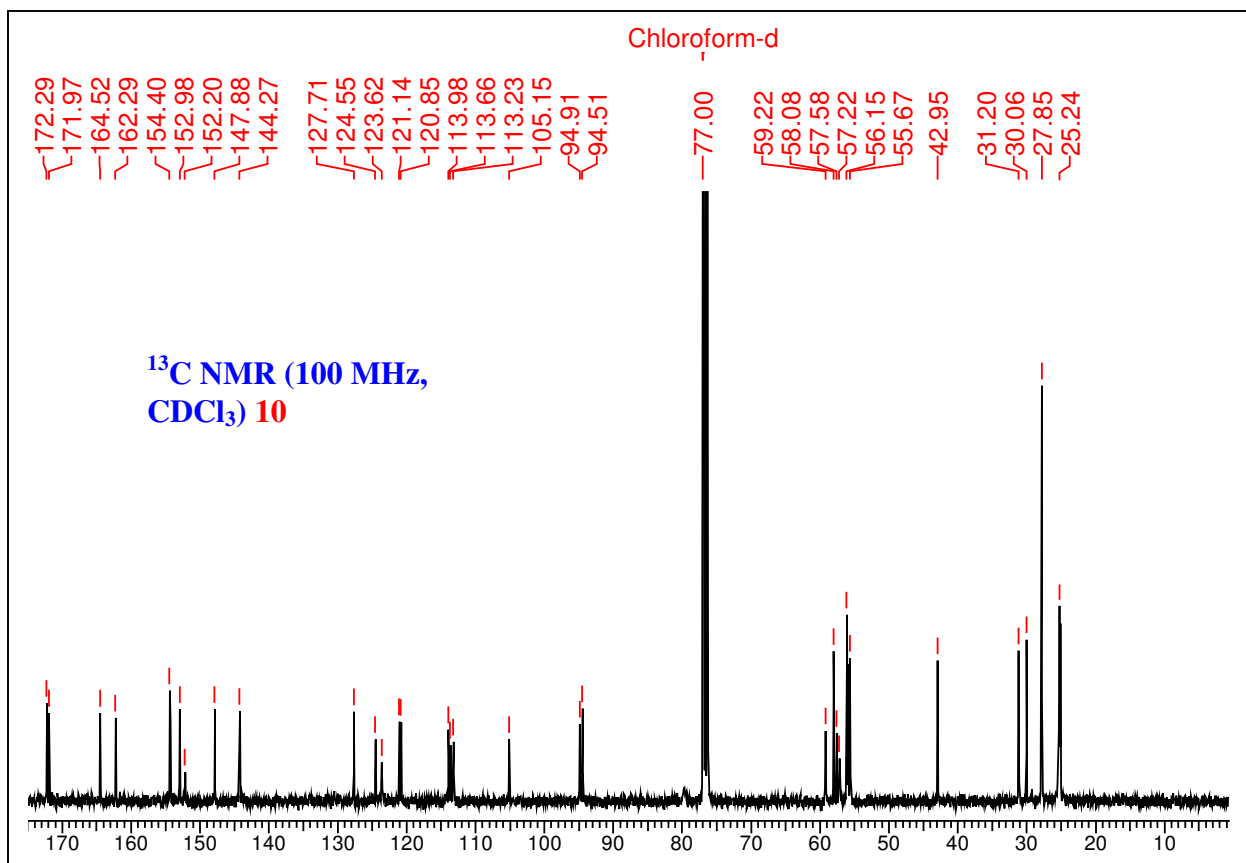


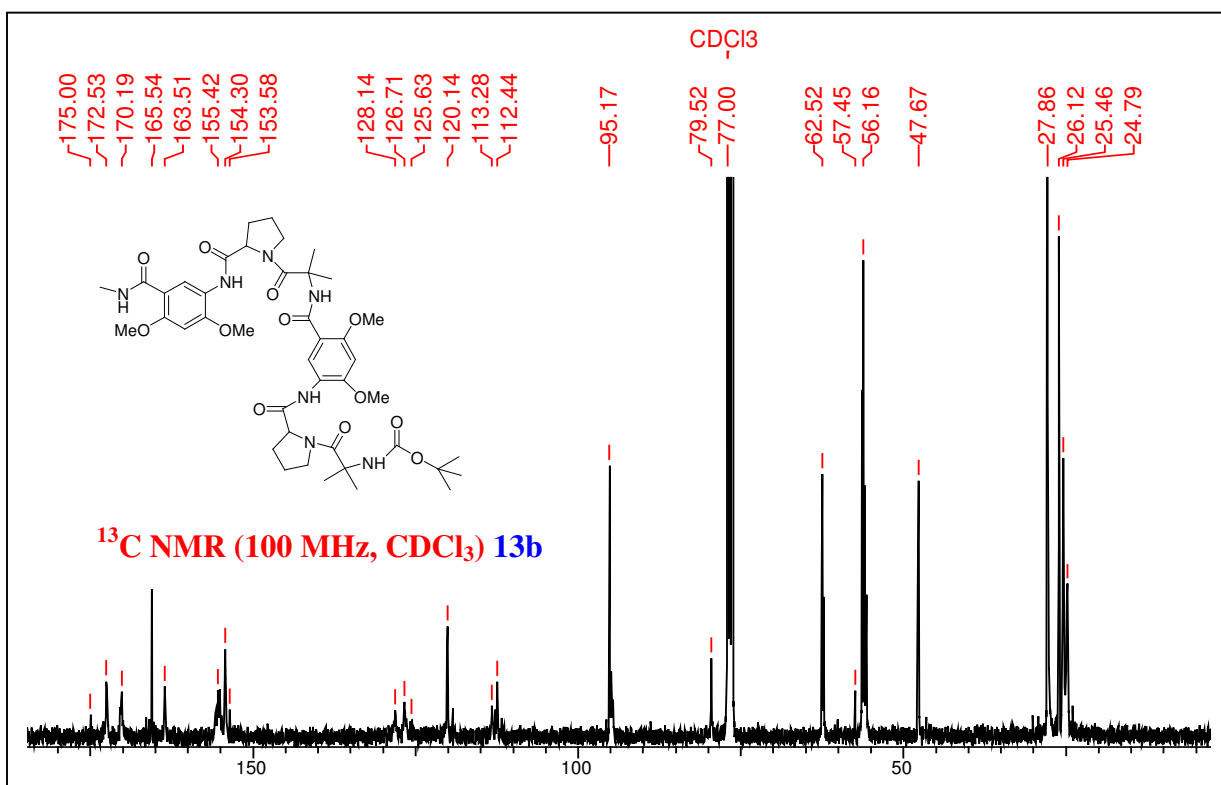
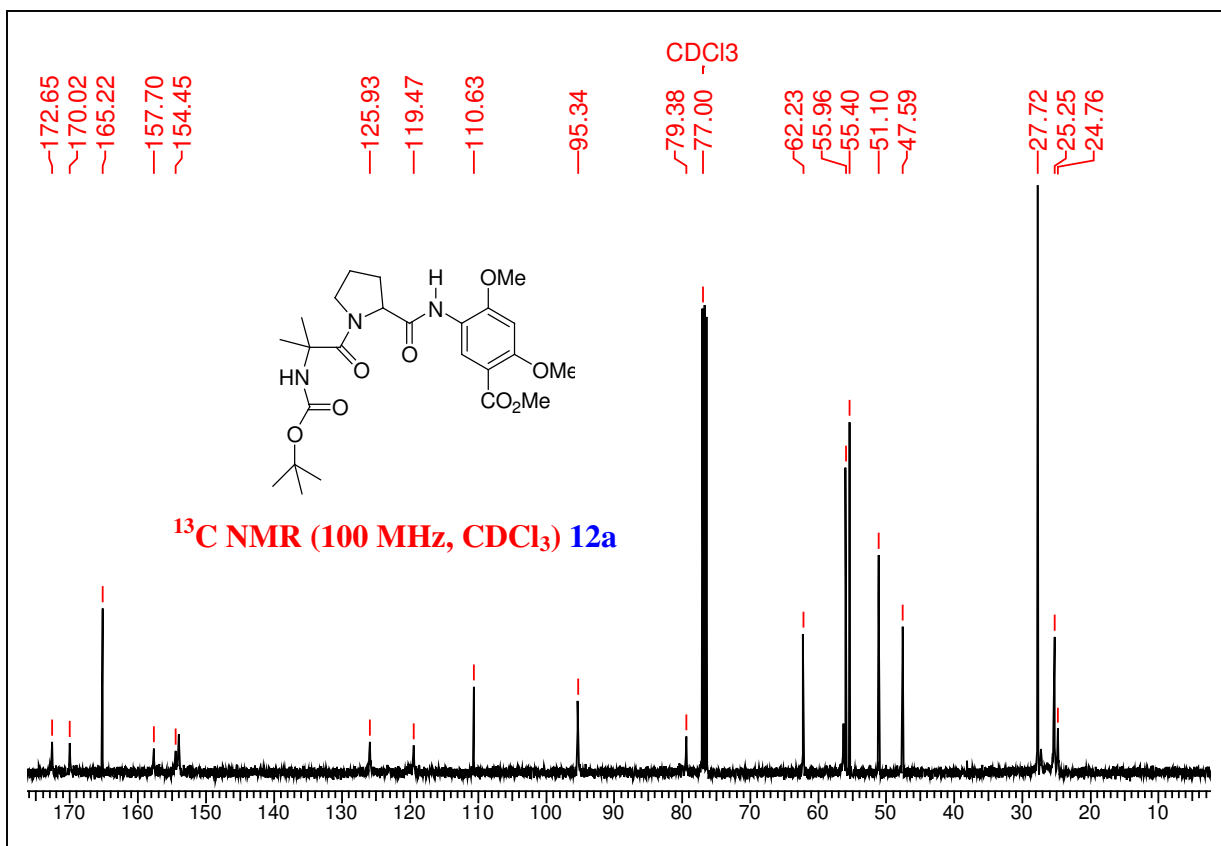












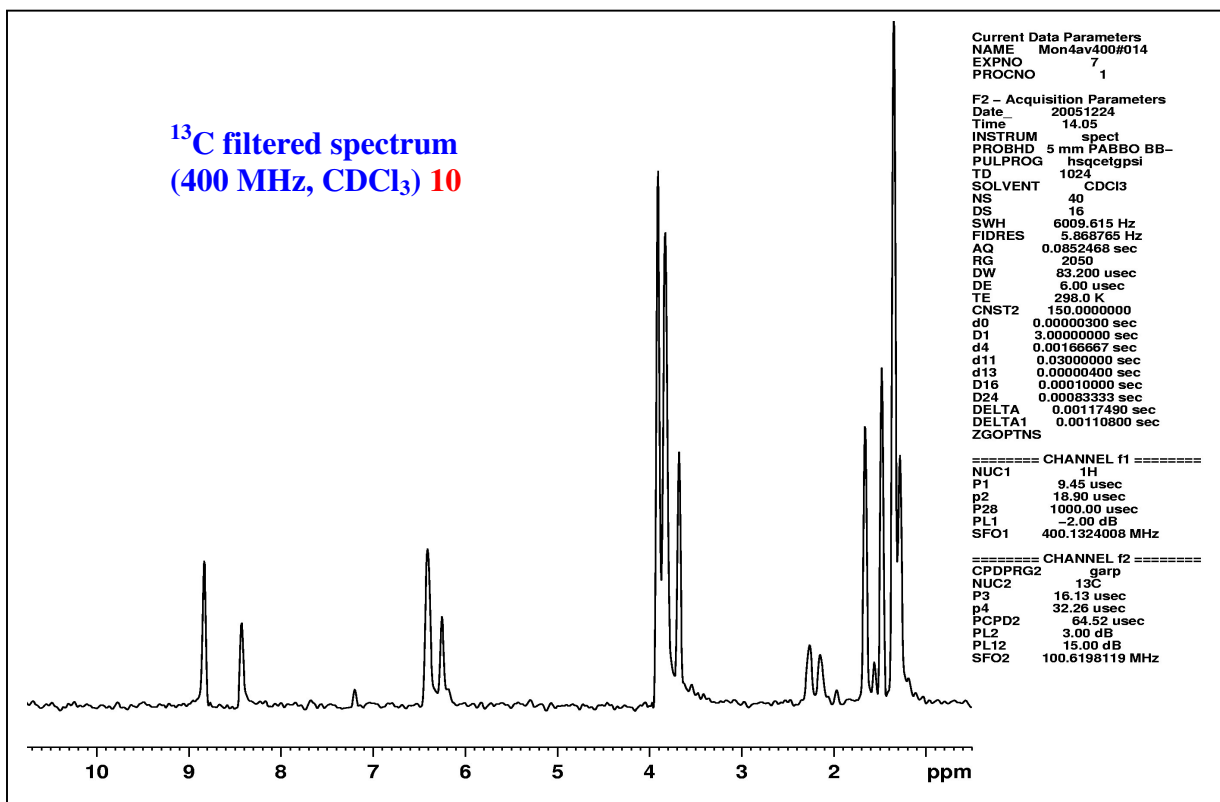
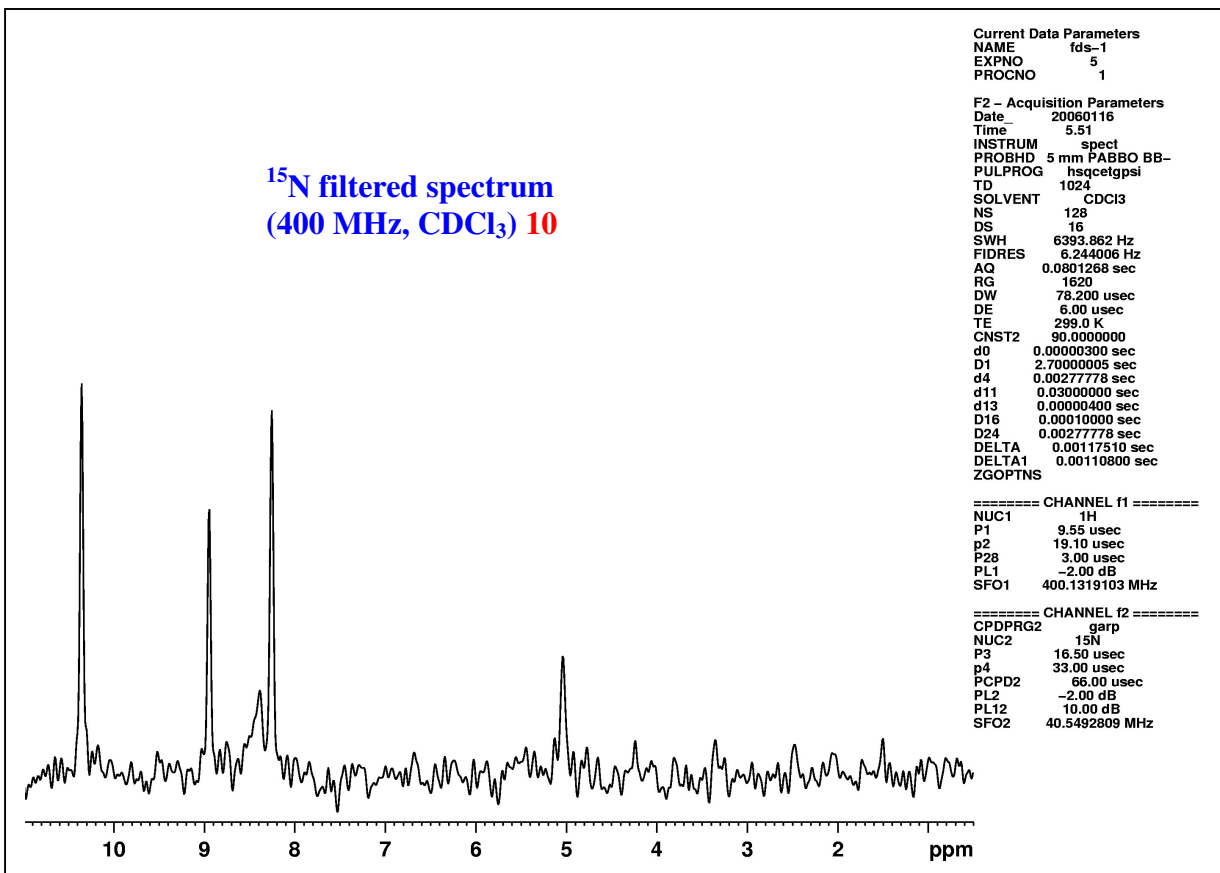


Table 1: Showing chemical shift changes on incremental addition of DMSO-d6 into 0.6 mL CDCl₃ containing the foldamer **3b**.

	DMSO (μ L)	NH1	NH2	NH3	NH4	NH5
1	0	5.05	8.45	8.98	8.26	7.6
2	5	5.08	8.44	8.96	8.24	7.58
3	10	5.14	8.43	8.92	8.21	7.57
4	15	5.17	8.42	8.9	8.2	7.55
5	20	5.22	8.41	8.86	8.17	7.55
6	25	5.26	8.39	8.84	8.16	7.54
7	30	5.31	8.39	8.83	8.15	7.54
8	35	5.35	8.36	8.78	8.11	7.52
9	40	5.39	8.35	8.75	8.09	7.51
10	45	5.41	8.34	8.74	8.08	7.5
11	50	5.45	8.33	8.7	8.06	7.49

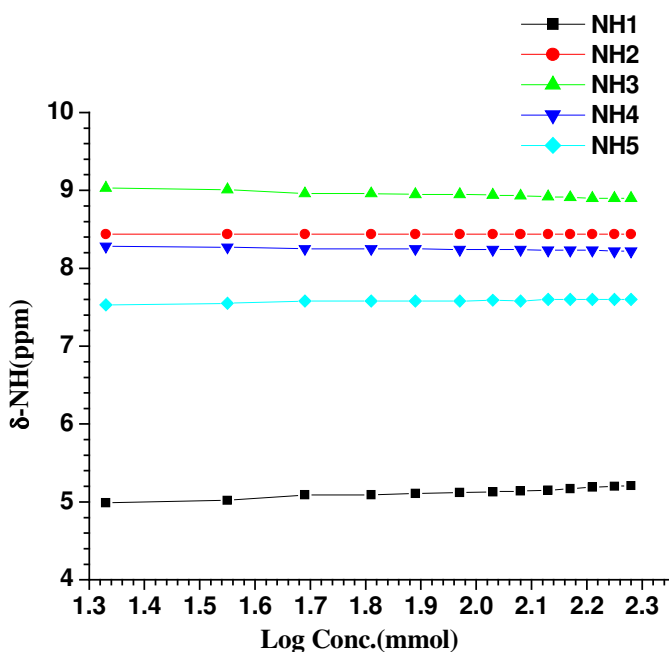


Figure 26: Dilution experiment graph of the foldamer **3b** in chloroform-d

Table 2: CDCl₃ Dilution data for foldamer **3b**

S.No	Log conc. mm	NH1	NH2	NH3	NH4	NH5
1	2.28	5.21	8.44	8.90	8.22	7.60
2	2.25	5.20	8.44	8.90	8.22	7.60
3	2.21	5.19	8.44	8.90	8.23	7.60
4	2.17	5.17	8.44	8.91	8.23	7.60
5	2.13	5.16	8.44	8.92	8.23	7.59
6	2.08	5.14	8.44	8.93	8.24	7.58
7	2.03	5.13	8.44	8.94	8.24	7.58
8	1.97	5.12	8.44	8.95	8.24	7.58
9	1.89	5.11	8.44	8.95	8.25	7.58
10	1.81	5.09	8.44	8.96	8.25	7.58
11	1.69	5.09	8.45	8.96	8.25	7.58

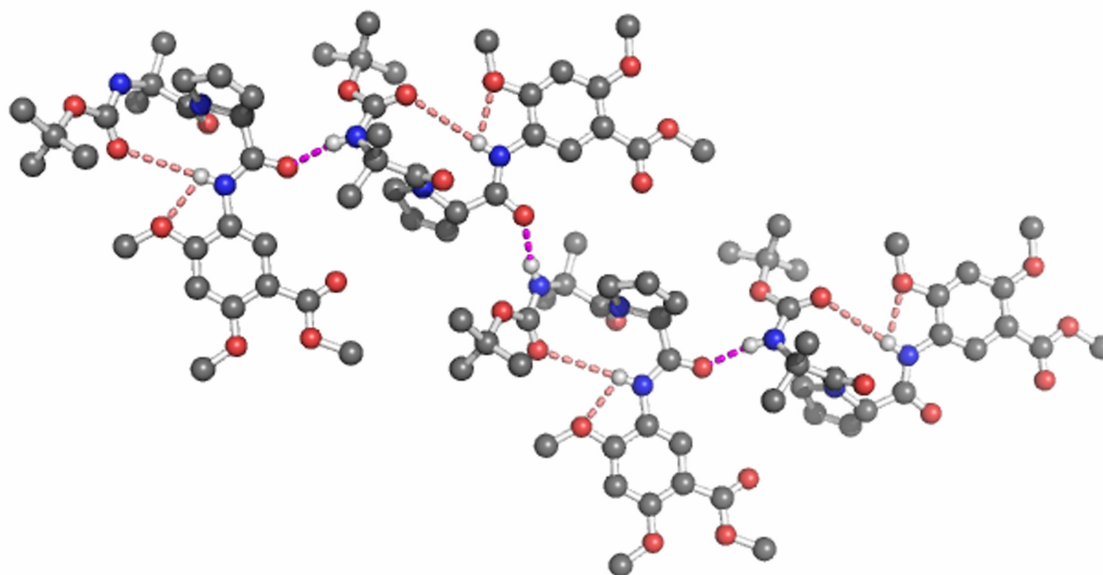


Figure 27: Single crystal X-ray structure of the Boc-Aib-Adb-OMe foldamer **12a** showing self assembly forming extended structure. The intermolecular hydrogen bonding interactions are highlighted in pink colored dashes, for aiding quick identification. Hydrogens, other than at the hydrogen bonding sites, have been deleted for clarity.

1.9 References and notes

(1) (a) Voyer, N.; *Top. Curr. Chem.* **1996**, *184*, 1; (b) Voyer, N.; Lamothe, J. *Tetrahedron* **1995**, *51*, 9241-9284.

(2). for reviews, see: (a) Gellman, S. H. *Acc. Chem. Res.* **1998**, *31*, 173-180; (b) Smith, M. D.; Fleet, G. W. J. *J. Peptide Sci.* **1999**, *5*, 425-441; (c) Hill, D. J.; Mio, M. J.; Prince, R. B.; Hughes, T. S.; Moore, J. S. *Chem. Rev.* **2001**, *101*, 3893-4011; (d) Schmuck, C. *Angew. Chem. Int. Ed.* **2003**, *42*, 2448-2452; (e) Sanford, A. R.; Yamato, K.; Yang, X.; Yuan, L.; Han, Y.; Gong, B. *Eur. J. Biochem.* **2004**, *271*, 1416-1425; (f) Sanford, A. R.; Gong, B. *Curr. Org Chem.* **2003**, *7*, 1649-1659; (g) Huc, I. *Eur. J. Org. Chem.* **2004**, 17-29; (h) Licini, G.; Prins, L. J.; Scrimin, P. *Eur. J. Org. Chem.* **2005**, 969-977; (i) Kirschenbaum, K.; Zuckerman, R. N.; Dill, D. A. *Curr. Opin. Struct. Biol.* **1999**, *9*, 530-535; (j) Stigers, K. D.; Soth, M. J.; Nowick, J. S. *Curr. Opin. Chem. Biol.* **1999**, *3*, 714-723; (k) Cubberley, M. S.; Iverson, B. L. *Curr. Opin. Chem. Biol.* **2001**, *5*, 650-653; (l) Cheng, R. P.; Gellman, S. H.; DeGrado, W. F. *Chem. Rev.* **2001**, *101*, 3219-3232; (m) Martinek, T. A.; Fulop, F. *Eur. J. Biochem.* **2003**, *270*, 3657-3666; (n) Seebach, D.; Hook, D. F.; Glättli, A. *Biopolymers* **2006**, *84*, 23-37; (o) Davis, J. M.; Tsou, L. K.; Hamilton, A. D. *Chem. Soc. Rev.* **2007**, *36*, 326-334; (p) Stone, M. T.; Heemstra, J. M.; Moore, J. S. *Acc. Chem. Res.* **2006**, *39*, 11-20.

(3) Apella, D. H.; Christianson, L. A.; Klein, D. A.; Richards, M. R.; Powell, D. R. Gellman, S. H. *J. Am. Chem. Soc.* **1999**, *121*, 7574-7581.

(4) Cheng, R. P.; Gellman, S. H.; DeGrado, W. F. *Chem. Rev.* **2001**, *101*, 3219-3232.

(5) (a) Gademann, K.; Hintermann, T.; Seebach, D. *Curr. Med. Chem.* **1999**, *6*, 905-925; (b) Seebach, D.; Mathews, J. L. *Chem. Commun.* **1997**, 2015-2022.

- (6) Hintermann, T.; Gademann, K.; Jaun, B.; Seebach, D. *Helv. Chim. Acta.* **1998**, 81.
- (7) Hanessian, S.; Luo, X.; Schaum, R.; Michnick, S. J. *J. Am. Chem. Soc.* **1998**, 120, 8569-8570.
- (8) Szabo, L.; Smith, B. L.; McReynolds, K. D.; Parrill, A. L.; Morris, E. R.; Gervay, J. *J. Org. Chem.* **1998**, 63, 1074-1078.
- (9) Smith, M. D.; Claridge, T. D. W.; Tranter, G. E.; Sansom, M. S. P.; Fleet, G. W. J. *J. Chem. Soc., Chem. Commun.* **1998**, 2041.
- (10) Krishenbaum, K.; Barron, A. E.; Goldsmith, R. A.; Armand, P.; Bradley, E. K.; Truong, K. T. V.; Dill, K. A.; Cohen, F. E.; Zuckermann, R. N. *Proc. Natl. Acad. Sci.* **1998**, 95, 4303-4308.
- (11) Armand, P.; Krishenbaum, K.; Goldsmith, R. A.; Farr-Jones, S.; Barron, A. E.; Truong, K. T. V.; Dill, K. A.; Mierke, D. F.; Cohen, F. E.; Zuckermann, R. N.; Bradley, E. K. *Proc. Natl. Acad. Sci.* **1998**, 95, 4309-4314.
- (12) Nowick, J. S.; Mahrus, S.; Smith, E. M.; Ziller, J. W. *J. Am. Chem. Soc.* **1996**, 118, 1066-1072.
- (13) Smith, A. B.; Guzaman, M. C.; Sprengler, P. A.; Keenan, T. P.; Holcomb, R. C.; Wood, J. L.; Carroll, P. J.; Hirschmann, R. *J. Am. Chem. Soc.* **1994**, 116, 9947-9962;
- (14) Yang, D.; Qu, J.; Li, B.; Ng, F.; Wang, X.; Cheung, K.; Wang, D.; Yu, Y. *J. Am. Chem. Soc.* **1999**, 121, 589-590.
- (15) Gennari, C.; Salom, B.; Potenza, D.; Longari, C.; Fioravanzo, E.; Carugo, O.; Sardone, N. *Chem. Eur. J.* **1996**, 2, 644-655.
- (16) Hagihara, M.; Anthony, N. J.; Stout, T. J.; Clardy, J.; Schreiber, S. L. *J. Am. Chem. Soc.* **1992**, 114, 6568-6570.

- (17) Beier, M.; Reck, F.; Wanger, T.; Krishnamurthy, R.; Eschenmoser, A. *Science* **1999**, 283, 699.
- (18) Nielsen, P. E. *Acc. Chem. Res.* **1999**, 32, 624-630.
- (19) Diederichsen, U.; Schmitt, H. W. *Eur. J. Org.* **1998**, 827-835.
- (20) Hamuro, Y.; Geib, S. J.; Hamilton, A. D. *J. Am. Chem. Soc.* **1996**, 118, 1066-1072.
- (21) Tanatani, A.; Yamaguchi, K.; Azumaya, I.; Fukutomi, R.; Shudo, K.; Kagechika, H. *J. Am. Chem. Soc.* **1998**, 120.
- (22) Bassani, D. M.; Lehn, J-M.; Baum, G.; Fenske, D. *Angew. Chem., Int. Ed.* **1997**, 36, 1845-1847.
- (23) Lokey, R. S.; Iverson, B. L. *Nature* **1995**, 375, 303.
- (24) Nelsen, J. C.; Saven, J. G.; Moore, J. S.; Wolynes, P. G. *Science* **1997**, 277, 1793.
- (25) Gong, B. *Chem. Eur. J.* **2001**, 7, 4336-4342.
- (26) (a) Seebach, D.; Overhand, M.; Ku'hnle, F. N. M.; Martinoni, B.; Oberer, L.; Hommel, U.; Widmer, H. *Helv. Chim. Acta* **1996**, 79, 913; (b) Seebach, D.; Ciceri, P. E.; Overhand, M.; Jaun, B.; Rigo, D.; Oberer, L.; Hommel, U.; Amstutz, R.; Widmer, H. *Helv. Chim. Acta* **1996**, 79, 2043; (c) Hintermann, T.; Seebach, D. *Synlett* **1997**, 437; (d) Hintermann, T.; Seebach, D. *Chimia* **1997**, 51, 244; (e) Guichard, G.; Seebach, D. *Chimia* **1997**, 51, 315. (f) Seebach, D.; Schreiber, J. V.; Abele, S.; Daura, X.; vanGunsteren, W. F. *Helv. Chim. Acta.* **2000**, 83, 34; (g) Hintermann, T.; Gademann, K.; Juan, B.; Seebach, D. *Helv. Chim. Acta.* **1998**, 81, 983-1002; (h) Dado, G. P.; Gellman, S. H. *J. Am. Chem. Soc.* **1994**, 116, 1054-1062. (i) Appella, D. H.; Christianson, L. A.; Karle, I. L.; Powell, D. R.; Gellman, S. H. *J. Am. Chem. Soc.* **1996**, 118, 13071-13072; (j) Appella, D. H.; Christianson, L. A.; Klein, D. A.; Powell, D. R.; Huang, X.; Barchi, J. J.;

Gellman, S. H. *Nature* **1997**, *387*, 381-383; (k) Krauthauser, S.; Christianson, L. A.; Powell, D. R.; Gellman, S. H. *J. Am. Chem. Soc.* **1997**, *119*, 11719-11720; (l) Applequist, J.; Bode, K. A.; Appella, D. H.; Christianson, L. A.; Gellman, S. H. *J. Am. Chem. Soc.* **1998**, *120*, 4891-4892; (m) Appella, D. H.; Christianson, L. A.; Klein, D. A.; Richards, M. R.; Powell, D. R.; Gellman, S. H. *J. Am. Chem. Soc.* **1999**, *121*, 7574-7581; (n) Appella, D. H.; Barchi, J. J.; Durell, S. R.; Gellman, S. H. *J. Am. Chem. Soc.* **1999**, *121*, 2309-2310; (o) Appella, D. H.; LePlae, P. R.; Raguse, T. L.; Gellman, S. H. *J. Org. Chem.* **2000**, *65*, 4766-4769.

(27) (a) Barron, A. E.; Zuckermann, R. N.; *Curr. Opin. Chem. Biol.* **1999**, *3*, 681-687; (b) Kirshenbaum, K.; Zuckermann, R. N.; Dill, K. A. *Curr. Opin. Struct. Biol.* **1999**, *9*, 530-535; (c) Soth, M. J.; Nowick, J. S. *Curr. Opin. Chem. Biol.* **1997**, *1*, 120-129; (d) Gellman, S. H. *Acc. Chem. Res.* **1997**, *31*, 173-180. (e) Hill, D. J.; Mio, M. J.; Prince, R. B.; Hughes, T. S.; Moore, J. S. *Chem. Rev.* **2001**, *101*, 3893-4011.

(28) For some select recent examples see: (a) Hunter, C. A.; Spitaleri, A.; Tomas, S. *Chem. Commun.* **2005**, 3691-3693; (b) Hang, F.; Bai, S.; Yap, G. P. A.; Tarwade, V.; Fox, J. M. *J. Am. Chem. Soc.* **2005**, *127*, 10590-10599; (c) Huck, B. R.; Gellman, S. H. *J. Org. Chem.* **2005**, *70*, 3353-3362; (d) Goto, K.; Moore, J. S. *Org. Lett.* **2005**, *7*, 1683-1686; (e) Licini, G.; Prins, L. J.; Scrimin, P. *Eur. J. Org. Chem.* **2005**, 969-977; (f) Arunkumar, E.; Ajayaghosh, A.; Daub, J. *J. Am. Chem. Soc.* **2005**, *127*, 3156-3164; (g) Gabriel, G. J.; Sorey, S.; Iverson, B. L. *J. Am. Chem. Soc.* **2005**, *127*, 2637-2640; (h) Violette, A.; Averlant-Petit, M. C.; Semetey, V.; Hemmerlin, C.; Casimir, R.; Graff, R.; Marraud, M.; Briand, J. P.; Rognan, D.; Guichard, G. *J. Am. Chem. Soc.* **2005**, *127*, 2156-2164; (i) Chen, F.; Zhu, N. Y.; Yang, D. *J. Am. Chem. Soc.* **2004**, *126*, 15980-15981; (j)

- Farrera, S. J.; Zaccaro, L.; Vidal, D.; Salvatella, X.; Giralt, E.; Pons, M.; Albericio, F.; Royo, M. *J. Am. Chem. Soc.* **2004**, *126*, 6048-6057; (k) De P. S.; Zorn, C.; Klein, C. D.; Zerbe, O.; Reiser, O. *Angew. Chem., Int. Ed.* **2004**, *43*, 511-514; (l) Baldauf, C.; Guenther, R.; Hofmann, H. J. *Helv. Chim. Acta.* **2003**, *86*, 2573-2588.
- (29) (a) Estroff, L. A.; Incarvito, C. D.; Hamilton, A. D. *J. Am. Chem. Soc.* **2004**, *126*, 2-3; (b) Sadowsky, J. D.; Schmitt, M. A.; Lee, H. S.; Umezawa, N.; Wang, S.; Tomita, Y.; Gellman, S. H. *J. Am. Chem. Soc.* **2005**, *127*, 11966-11968; (c) Norgren, A. S.; Arvidsson, P. I. *Org. Biomol. Chem.* **2005**, *3*, 1359-1361; (d) Chang, K. J.; Kang, B. N.; Lee, M. H.; Jeong, K. S. *J. Am. Chem. Soc.* **2005**, *127*, 12214-12215.
- (30) Hayen, A.; Schmitt, M. A.; Ngassa, F. N.; Thomasson, K. A.; Gellman, S. H. *Angew. Chem., Int. Ed.* **2004**, *43*, 505-510.
- (31) (a) Roy, R. S.; Karle, I. L.; Raghothama, S.; Balaram, P. *Proc. Natl. Acad. Sci. U.S.A.* **2004**, *101*, 16478-16482; (b) De Pol, S.; Zorn, C.; Klein, C. D.; Zerbe, O.; Reiser, O. *Angew. Chem., Int. Ed.* **2004**, *43*, 511-514; (c) Sharma, G. V. M.; Nagendar, P.; Jayaprakash, P.; Krishna, P. R.; Ramakrishna, K. V. S.; Kunwar, A. C. *Angew. Chem., Int. Ed.* **2005**, *44*, 5878-5882; (d) C. Baldauf.; R. Gunther.; H-J. Hofmann. *J. Org. Chem.* **2006**, *71*, 1200-1208.
- (32) Cyclic peptides containing proline-aromatic amino acid units have been reported by Kubik et al., see: Otto, S.; Kubik, S. *J. Am. Chem. Soc.* **2003**, *125*, 7804-7805; d) Heinrichs, G.; Kubik, S.; Lacour, J.; X Vial, S. *J. Org. Chem.* **2005**, *70*, 4498-4501.
- (33) Hamuro, Y.; Geib, S. J.; Hamilton, A. D. *J. Am. Chem. Soc.* **1997**, *119*, 10587-10593.
- (34) Nelson, J. C.; Saven, J. G.; Moore, J. S.; Woylnes, P. G. *Science* **1997**, *277*, 1793.

- (35) Zhu, J.; Parra, R. D.; Zeng, H.; Jankun, E. S.; Zeng, X. C.; Gong, B. *J. Am. Chem. Soc.* **2000**, *122*, 4219-4220.
- (36) Yuan, L.; Feng, W.; Yamato, K.; Sanford, A. R.; Xu, D.; Guo, H.; Gong, B. *J. Am. Chem. Soc.* **2004**, *126*, 11120-11121.
- (37) (a) Pavone, V.; Di Blasio, B.; Santini, A.; Benedetti, E.; Pedone, C.; Toniolo, C.; Crisma, M. *J Mol Biol*, **1990**, *214*, 633; (b) Toniolo, C.; Crisma, M.; Bonora, G. M.; Benedetti, E.; Di Blasio, B.; Pavone, V.; Pedone, C.; Santini, A. *Biopolymers* **1991**, *31*, 129.
- (38) (a) Prasad, B. V. V.; Balaram, P. *CRC Crit. Rev. Biochem.* **1984**, *16*, 307; (b) Karle, I. L.; Balaram, P. *Biochemistry* **1990**, *29*, 6747; (c) Toniolo, C.; Benedetti, E. *Trends Biochem. Sci.* **1991**, *16*, 350; (d) Toniolo, C.; Benedetti, E. *ISI Atlas Sci. Biochem.* **1988**, *1*, 225; (e) Benedetti, E. *Biopolymers* **1996**, *40*, 3; (f) Bosch, R.; Schmitt, H.; Jung, G.; Winter, W. *Biopolymers* **1985**, *24*, 961; (g) Bosch, R.; Jung, G.; Schmitt, H.; Winter, W. *Biopolymers* **1985**, *24*, 979; (h) Marshall, G. R.; Hodgkin, E. E.; Langs, D. A.; Smith, G. D.; Zabrocki, J.; Leplawy, M. T. *Proc. Natl. Acad. Sci. U.S.A.* **1990**, *87*, 487; (i) Taga, T.; Itoh, M.; Machida, K.; Fujita, T.; Ichihara, T. *Biopolymers* **1990**, *26*, 1057.
- (39) Toniolo, C.; Crisma, M.; Formaggio, F.; Peggion, C. *Biopolymers*. **2001**, *60*, 396-419.
- (40) Blasio, B. D.; Pavone, V.; Saviano, M.; Lombardi, A.; Nistri, F.; Pedone, C.; Benedetti, E.; Crisma, M.; Anzolin, M.; Toniolo, C. *J. Am. Chem. Soc.* **1992**, *114*, 6273-6278.
- (41) (a) Toniolo, C. *Crit. Rev. Biochem.* **1980**, *9*, 1; (b) Rose, G. D.; Gierasch, L. M.; Smith, J. A. *Adv. Protein Chem.* **1985**, *37*, 1; (c) Vass, E.; Hollsi, E. M.; Besson, F.;

Buchet, R. *Chem. Rev.* **2003**, *103*, 1917; (d) Spatola, A. F. *Bioorganic Chemistry: Peptides and Proteins* Oxford University Press, New York, **1998**, 367 – 394.

(42) Ball, J. B.; Hughes, R. A.; Alewood, P. F.; Andrews, P. R. *Tetrahedron* **1993**, *49*, 3467-3478.

(43) (a) Stanfield, R. L.; Fieser, T. M.; Lerner, R. A.; Wilson, I. A. *Science* **1990**, *248*, 712-719; (b) Marshall, G. R. *Curr. Opin. Struct. Biol.* **1992**, *2*, 904-919.

(44) Chakraborty, T. K.; Srinivas, P. S.; Madhavendra, S.; Kiran Kumar, S.; Kunwar, A. C. *Tetrahedron Letters* **2004**, *45*, 3573-3577.

(45) Chakraborty, T. K.; Jayaprakash, S.; Srinivasu, P.; Madhavendra, S. S.; Ravi Sankar, A.; Kunwar, A.C. *Tetrahedron*. **2002**, *58*, 2853-2859.

(46) Chakraborty, T. K.; Srinivasu, P.; Kiran Kumar, S.; Kunwar, A. C. *J. Org. Chem.* **2002**, *67*, 2093-2100.

(47) Smith, M. D.; Claridge, T. D. W.; Tranter, G. E.; Sansom, M. S. P.; Fleet, G. W. J. *Chem. Commun.* **1998**, 2041-2042.

(48) Baruah, P. K.; Sreedevi, N. K.; Gonnade, R.; Ravindranathan, S.; Damodaran, K.; Hofmann, H.-J.; Sanjayan, G. J. *J. Org. Chem.* **2007**, *72*, 636-639.

(49) Yang, D.; Zhang, D. W.; Hao, Y.; Wu, Y. D.; Luo, S-W.; Zhu, N-Y. *Angew. Chem., Int. Ed.* **2004**, *43*, 6719-6722.

(50) α -aminoisobutyric (Aib) residue is highly conformationally restricted, with allowed conformations lying largely in the region $\phi \pm 60^\circ$, $\psi \pm 30^\circ$, see: $\psi \pm 30^\circ$, see: (a) Kaul, R.; P. Balaram, P.; *Bioorg. Med. Chem.* **1999**, *7*, 105-117.

(51) (a) Barbour, L. J.; Orr, G. W.; Atwood, J. L. *Nature*, **1998**, *393*, 671-673; (b) Barbour, L. J.; Orr, G. W.; Atwood, J. L. *Chem. Commun.*, **2000**, 859–860; (c) Atwood,

- J. L.; Barbour, L. J.; Jerga, A.; Schottel, B. L. *Science* **2002**, 298, 1000 – 1002; (d) Desiraju, G. R. *J. Chem. Soc., Chem. Commun.* **1991**, 426-428; (e) Magazu, S.; Migliardo, F.; Ramirez-Cuesta, A. J., *J. R. Soc. Interface.* **2005**, 2, 527-532.
- (52) Graether, S. P.; Kuiper, M. J.; Gagnes, S. M.; Walker, V. K.; Jia, Z.; Sykes, B. D.; Davies, P. L. *Nature*, **2000**, 406, 325-328.
- (53) For a review, see: Harding, M. M.; Anderberg, P. I.; Haymet, A. D. J. *Eur. J. Biochem.* **2003**, 270, 1381.
- (54) Vishweshwar, P.; Babu, N. J.; Nangia, A.; Mason, S. A.; Puschmann, H.; Mondal, R.; Howard, J. A. K. *J. Phys. Chem. A*, **2004**, 108, 9406-9416.
- (55) For an excellent account on the graph set analysis of H-bonded systems, see: Etter, M. C. *Acc. Chem. Res.* **1990**, 23, 120-126.
- (56) Srinivas, D.; Gonnade, R.; Ravindranathan, S.; Sanjayan, G. J. *Tetrahedron* **2006**, 62, 10141-10146.
- (57) Molteni, V.; Rhodes, D.; Rubins, K.; Hansen, M.; Bushman, F.D.; Siegel, J. S. *J. Med. Chem.* **2000**, 43, 2031-2039.
- (58) Karle, I. L.; Flippen-Anderson, J. L.; Sukumar, M.; Balaram, P. *Proc. Natl. Acad. Sci. USA* **1987**, 84, 5087-5091.
- (59) (a) Venkataram Prasad, B. V.; Balaram, P. *Int J Biol Macromol.* **1982**, 4, 99; (b) Di Blasio, B.; Pavone, V.; Saviano, M.; Lombardi, A.; Nastri, F.; Pedone, C.; Benedetti, E.; Crisma, M.; Anzolin, M.; Toniolo, C. *J Am Chem Soc.* **1992**, 114, 6273–6278.

CHAPTER 2

Concurrent Display of Both α - and β -Turns in a
Semi Synthetic Peptide

2.1 Introduction and significance of reverse turns

One of the important goals in peptide chemistry is to be able to design short peptides that can mimic some important aspects of protein structure and function.¹ Synthetic secondary structural motifs that promote unique / specific conformations are of considerable importance in the design and development of new peptidomimetics.¹ Furthermore, such motifs might also possess enzyme-like catalytic activities.^{2,3} Intense interest in this area during the last two decades have resulted in the generation of a plethora of synthetic structural motifs that mimic / promote various protein secondary structures, in particular reverse turns.⁴ A turn in a protein structure is defined as a site where a polypeptide chain reverses its overall direction. Reverse turns are generally categorized as γ -turn, β -turn, α -turn, and π -turn, which are formed by three-, four-, five-, and six-amino-acid residues, respectively (figure 1).⁵ According to the folding mode and backbone dihedral angles, each of such turns can be further classified into several different sub-types.

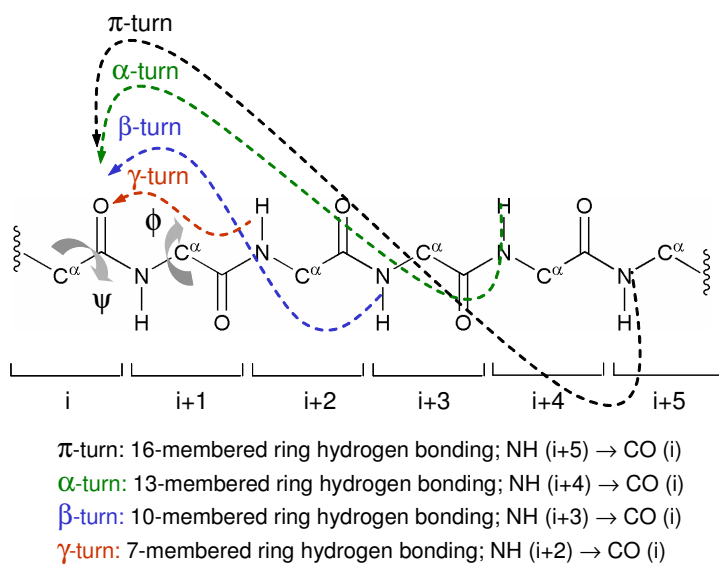


Figure 1: Representation of different reverse turns in a polypeptide chain⁵

Reverse turns are ubiquitous in proteins, and are known to account for nearly one third of the residues in proteins of known structures. Reverse turns play an important role in globular proteins from both the structural and functional points of view.^{5,6} Among the various reverse turns, beta turns are important secondary structural motifs in protein secondary structure. β -turns, usually featuring a 10-membered ring hydrogen-bonded network, has been extensively investigated in the past.⁷

Recent studies suggest that α -turns,^{8,9} although less frequently observed in proteins when compared to β -turns, also play key roles in certain biological functions.¹⁰ For instance, the role of α -turn motifs in molecular recognition processes involving HIV-neutralization has just begun to unfold. Investigations of crystal structure of the antibody F425-B4e8 in complex with a V3 peptide revealed a new binding mode for HIV-1 neutralization, involving a five-residue α -turn around the conserved GPGRA apex of the β -hairpin loop.¹¹ α -turn motif is likely to be one of the crucial structural factors for effecting specific molecular recognition processes involving the recently isolated Asian scorpion toxin (BmK 17[4]).¹² The sustained efforts in the development of reverse turn mimetics as potential peptidomimetics have led to the discovery of structural motifs that display α -turns; although they are very limited in number.^{13,14}

2.2 Importance of three-centered/bifurcated H-bonding

Hydrogen bonding is the favorite intermolecular force in self-assembling systems by virtue of directionality, specificity, and biological relevance. Most natural building blocks, such as carbohydrates, amino acids, and nucleic acids, offer a rich source of H-bond donors and acceptors. There are two types of H-bonds, (i) three-centered H-bond

which involves two H atoms interacting with one acceptor atom (HXH interaction) and (ii) bifurcated H-bond which involves two acceptor atoms interacting with one H atom (XHY interaction figure 2). Molecules of solvent may often participate in three-centered/bifurcated H-bonding as they may act as proton donor as well as proton acceptor. Water (H₂O) may be involved in both types of three-centered/bifurcated H-bondings.¹⁵

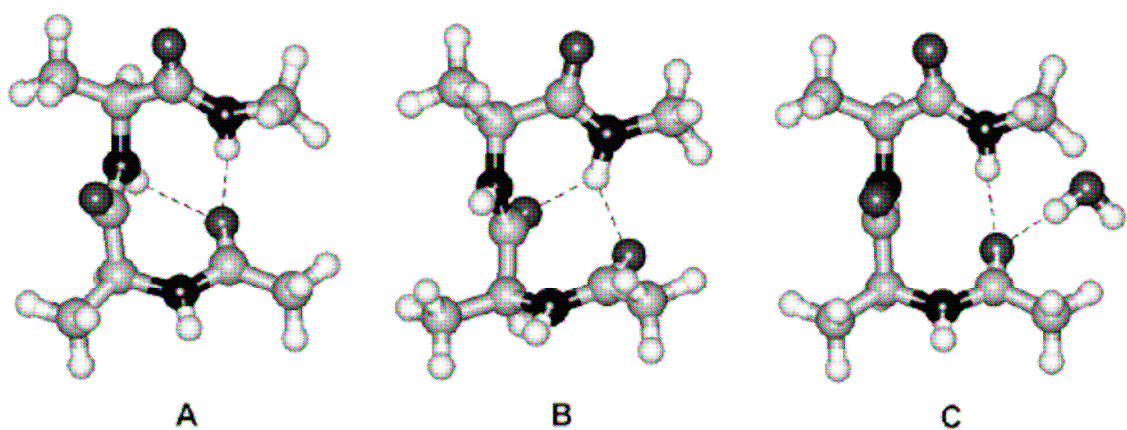


Figure 2: Turn structures with three-centered H-bond between two donor N-H groups and one acceptor C=O (A). Bifurcated hydrogen bond between two acceptor C=O groups and one donor N-H ('inverse bifurcation') (B). Bifurcation with the participation of a water molecule (C)¹⁵

It has been suggested that the three-centered/bifurcated hydrogen bond¹⁶ plays an important role in determining the structure and function of molecules, ranging from inorganic to organic and biological molecules. The three-centered/bifurcated hydrogen bonding is detected in crystal structures of small molecule such as amino acids and carbohydrates¹⁷ as well as large biopolymers such as RNA,¹⁸ DNA¹⁹ and proteins.²⁰ The ubiquitous nature of three-centered/bifurcated H-bonding in biomolecules is further explored in the molecular recognition and self-assembly of designed molecules, together

with normal two-center H-bonding.²¹ Designing a molecular recognition system that utilizes bifurcated H-bonding would provide further understanding of this novel molecular interaction and would expand the scope of molecular recognition by artificial receptors.

Three-center/bifurcated H-bonding has been proposed to play an important role DNA, RNA and protein conformation, small molecule-DNA and protein-DNA recognition, host-guest complexation,^{21a} and self assembly.²² Gellman and other research groups have described three-centered hydrogen bond, in various short peptides and depsipeptides, and extensive studies on model depsipeptides in CH₂Cl₂ and in CHCl₃ and has documented spectroscopic data on various hydrogen-bonding patterns.¹⁴

2.3 Turn induced small peptides and depsipeptides

Gellman^{14a} *et al* have reported the folding of several depsipeptides constructed from α -amino acids [L-proline (P) and L-alanine (A)] and α -hydroxy acids [L-lactic acid (L) and glycolic acid (G)]. These depsipeptides have been examined in methylene chloride solution by variable temperature IR spectroscopy, variable temperature ¹H NMR spectroscopy, and molecular mechanics (figure 3). The depsipeptides include three-residue molecules (PLL, ALL, and PLG) that can form 13-membered-ring amide-to-amide hydrogen bond, which for a peptide backbone, would correspond to a single turn of an α -helix. These depsipeptides can also form 10- membered-ring amide-to-ester hydrogen bonds, which would correspond to β -turn formation for a peptide backbone.

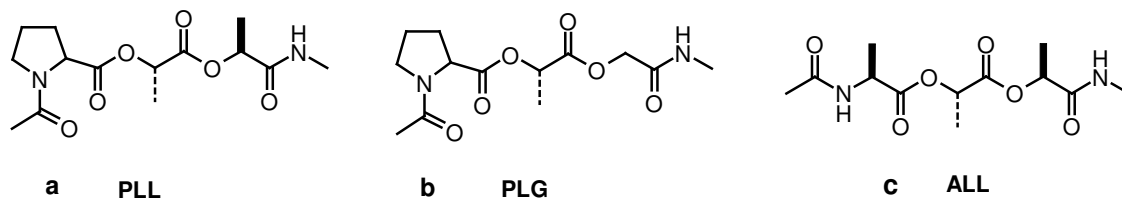


Figure 3: H-Bond-mediated folding in depsipeptide models^{14a}

Gellman *et al*^{14b} examined the relative stability of an HXH three-center hydrogen bond with alternative two-center hydrogen bond in a depsipeptide model system. Modest information is available on the stability of three-center hydrogen bonds relative to two-center hydrogen bonds (figure 4a, 4b and 4c). The results show that there is negative cooperativity between the two components of the HXH interaction.

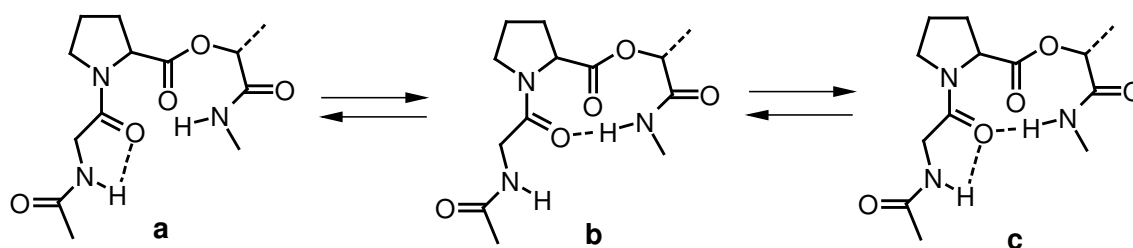


Figure 4: Different folding patterns in depsipeptide^{14b}

Scott J. Miller *et al*^{3a} described the synthesis and conformational studies of His-Pro-Aib peptides (figure 5). Miller *et al* synthesized small peptides (5a, 5b) which differ only at N-terminus. Peptide (5a) possesses a Boc-Phe residue at the N-terminus, where peptide (5b) bears a Boc-(τ -benzyl) His system. The conformation studies revealed that peptide (5a) adopts a regular β -turn conformation, and peptide 5b adopts a well defined, compact structure that resembles the AsX-Pro-turn.

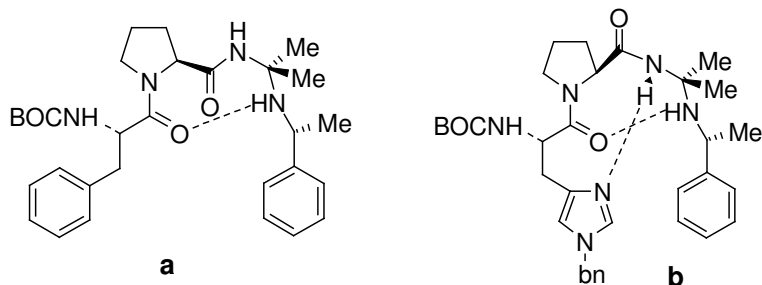


Figure 5: Structural similarity between the Asx-Pro-turn and the imidazole peptide^{3a}

Gung²³ *et al* reported the findings of the difference in the conformational preference between a succinic glycine derivative (a) and a glutaric glycine derivative (d) (figure 6). The two model peptides were prepared during their study of hydrogen bonding cooperativity. Each triamide can form several conformations (a-e) through intramolecular hydrogen bonding. On the basis of the IR and ¹H NMR data, an *Asx turn* type of folding pattern (b) is identified to be the enthalpically favored conformation in chloroform for both triamide a and d.

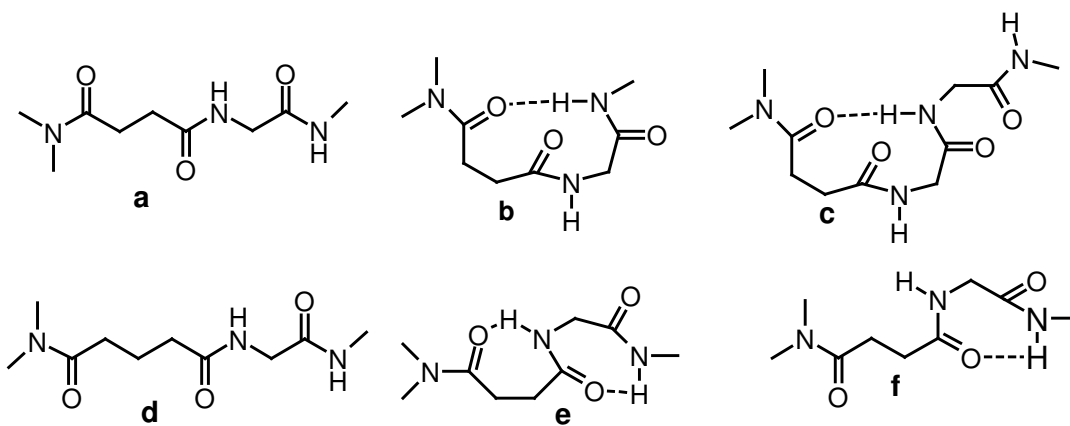


Figure 6: Different folding patterns of succinic glycine and glutaric glycine derivatives²³

Chakraborty²⁴ *et al* reported the synthesis and conformational studies of peptides containing *cis*-3-hydroxy-D-proline (figure 7). Conformational analysis of peptides containing *cis*-3-hydroxy-D-proline (D-*cis*-3-Hyp) by NMR studies revealed that the 3-

hydroxyl group in this amino acid plays a significant role in the overall three-dimensional structures of the peptides. When the *D-cis*-3-Hyp had its 3-hydroxyl group protected as the benzyl (Bn) ether, the peptide displayed a β -hairpin structure in both CDCl_3 and $\text{DMSO-}d^6$ (figure 7a). Even after the removal of the benzyl group, the resulting deprotected compound retained the same structure as in the CDCl_3 . However, in polar solvent $\text{DMSO-}d^6$, the C-terminal strand of the hydroxyl deprotected peptide flipped to the side of the hydroxyl group, breaking the hairpin to form a pseudo β -turn-like nine-membered ring structure involving an intramolecular hydrogen bond between $\text{LeuNH} \rightarrow \text{HypC3-OH}$ (figure 7b).

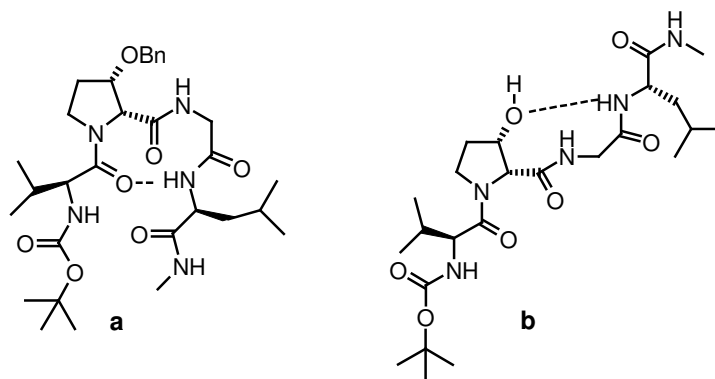


Figure 7: Different folding patterns of *cis*-3-hydroxy D-proline containing peptides²⁴

2.4 Objective of the present work

The main objective of the work described in this chapter is to develop novel structural motifs to study their folding patterns both in solution and solid state.

2.4.1 Design principles

We have been able to develop a semi synthetic peptide motif (Pro-Gly-Gly Ψ [CH₂NH]) that concurrently displays both α - and β -turns within the molecule, as evidenced from

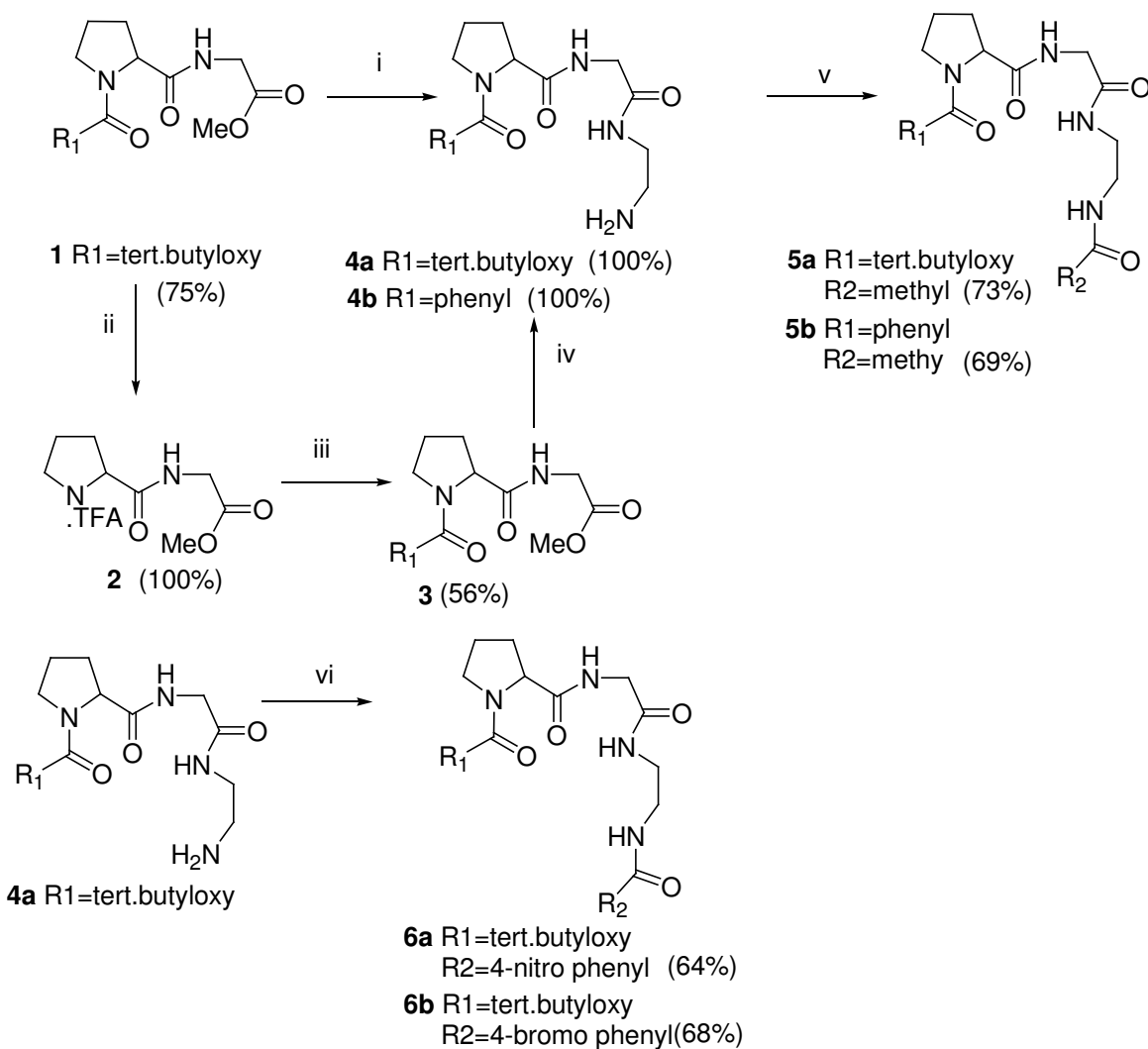
structural investigations by single crystal X-ray crystallography and NMR studies (*vide infra*). In this semi synthetic peptide motif, the amino acid residues proline and Glycine occupies the i+1 and i+2 sites of a typical type-II β -turn

It should be noted that positioning of Pro and Gly at the the i+1 and i+2 sites of peptide segments is known to promote type II β -turn formation.²⁵ However, introduction of a N-acylated Gly Ψ [CH₂NH] at the i+3 site paved the way for additional intramolecular hydrogen bonding interaction forming an α -turn characterized by a three-centered hydrogen bonding, as evident from its crystal structure. The molecule features two intramolecular hydrogen bondings; one coming from the expected type-II β -turn owing to the positioning of the Pro-Gly sequence at i+1 and i+2 sites, respectively, and another intramolecular interaction featuring a 13-membered H bonding arising from the 5 \rightarrow 1 interaction.

2.4.2 Synthesis

The peptide couplings were carried out by using solution-phase peptide synthesis methods and TBTU [O-(Benzotriazol-1-yl)-N,N,N',N'-tetramethyluronium tetrafluoroborate] was used as a peptide coupling reagent and acetonitrile as a solvent. The synthesis started with the dipeptide **1** (Boc-Pro-Gly-OMe) which was prepared from the corresponding protected amino acids of Proline, and Glycine by using standard mixed anhydride protocol,²⁶ in good yield.

Scheme 1



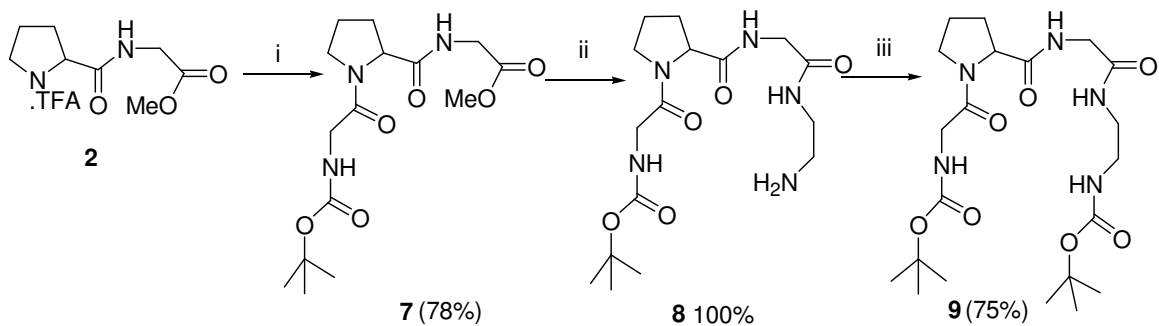
Reagents and conditions: (i) ethylenediamine, methanol, rt, 2h; (ii) trifluoro acetic acid, DCM, rt, 2h; (iii) benzoyl chloride, Et₃N, dry dichloromethane, rt, 5h; (iv) ethylenediamine, methanol, rt, 1h; (v) acetic anhydride, pyridine, rt, 6h; (vi) 4-nitrobenzoic acid, TBTU, DIPEA, dry acetonitrile, rt, 6h; (vi) 4-bromo benzoic acid, TBTU, DIPEA, dry acetonitrile, rt, 6h.

The dipeptide **1** (Boc-Pro-Gly-OMe) which on deprotection of *t*-Boc with 50% TFA-DCM followed by benzoylation with benzoyl chloride (Et₃N-CH₂Cl₂) gave the benzoyl protected dipetide **3**. The Peptides **1** and **3** were treated with ethylenediamine in the

presence of methanol to give the ethylenediamine condensed products **4a** and **4b**, which on acylation followed by amidation gave the peptides **5a** and **5b** in good yield. The peptide **4a** was coupled with 4-nitro benzoic acid and 4-bromo benzoic acid in presence of TBTU and DIPEA to obtain the corresponding nitro and bromo derivatives **6a**, **6b** respectively (scheme 1).

The dipeptide **1** (Boc-Pro-Gly-OMe) which on deprotection of *t*-Boc with (50% TFA-DCM), furnished the TFA salt of dipeptide **2**. The peptide **7** was made by treatment of **2** with Boc-Gly-OH in presence of EDCI and DIPEA in dichloromethane. Peptide **7** was treated with ethylenediamine in the presence of methanol to give the ethylenediamine condensed product **8**, which on reaction with Boc-anhydride furnished **9** with in yield (scheme 2)

Scheme 2



Reagents and conditions: (i) **2**, Boc-Gly-OH, EDCI, triethylamine, dry dichloromethane, rt, 6h; (ii) ethylenediamine, methanol, rt, 2h; (iii) Boc-anhydride, tetrahydrofuran, rt, 3h.

2.4.3 Results and Discussion

All attempts to crystallize the peptides **5a**, **6a** and **6b** were unsuccessful. However the peptide **5b** crystallized from chloroform: pet ether (60:40), in monoclinic space group

P2-1. The unit cell contained two molecules (figure 8). A closer inspection of the crystal structure revealed that the α -turn interaction is relatively more stronger with dihedral angles ($\phi_{i+1}=-58.08$, $\psi_{i+1}=136.16$, $\phi_{i+2}=69.35$, $\psi_{i+2}=15.09$).

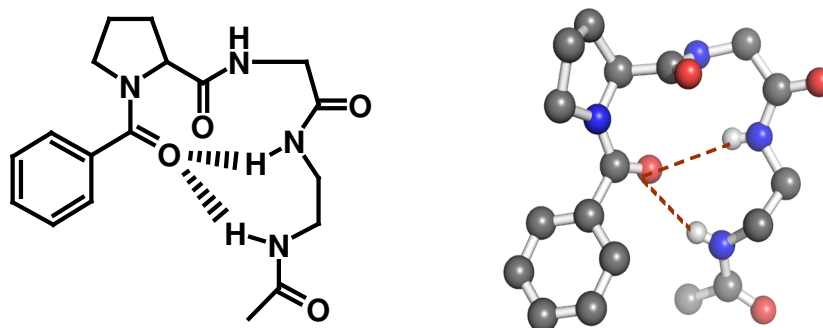


Figure 8: Molecular structure (left) and crystal structure (right) of **5b** in ball and stick representation (right). Hydrogens other than at the hydrogen bonding sites have been deleted for clarity in the crystal structure image.

Further inspection of the crystal structure revealed the formation of self-assembled supramolecular structure involving the amide NH of glycine that does not participate in intramolecular interactions (figure 9).

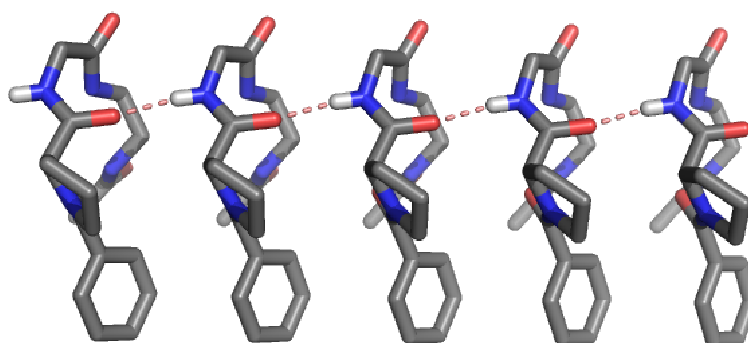


Figure 9: PyMOL-rendered crystal structure of **5b** showing molecular self-assembly in the solid-state. Hydrogens other than at the hydrogen bonding sites have been deleted for clarity.

2.4.4 Conformational analysis of peptide 5a

In order to investigate the solution-state conformation, we undertook a detailed NMR study of **5a**. The analog **5a** with all aliphatic substituents was preferred for solution-state NMR studies to minimize the “aromatic” chemical shift interferences. The three-centered hydrogen bonding interactions and the turn conformations, as observed in the solid-state, were confirmed by the observed dipolar couplings (nOes) from the 2D NOESY NMR spectra (400 MHz, CDCl₃) of **5a** (figure 10).

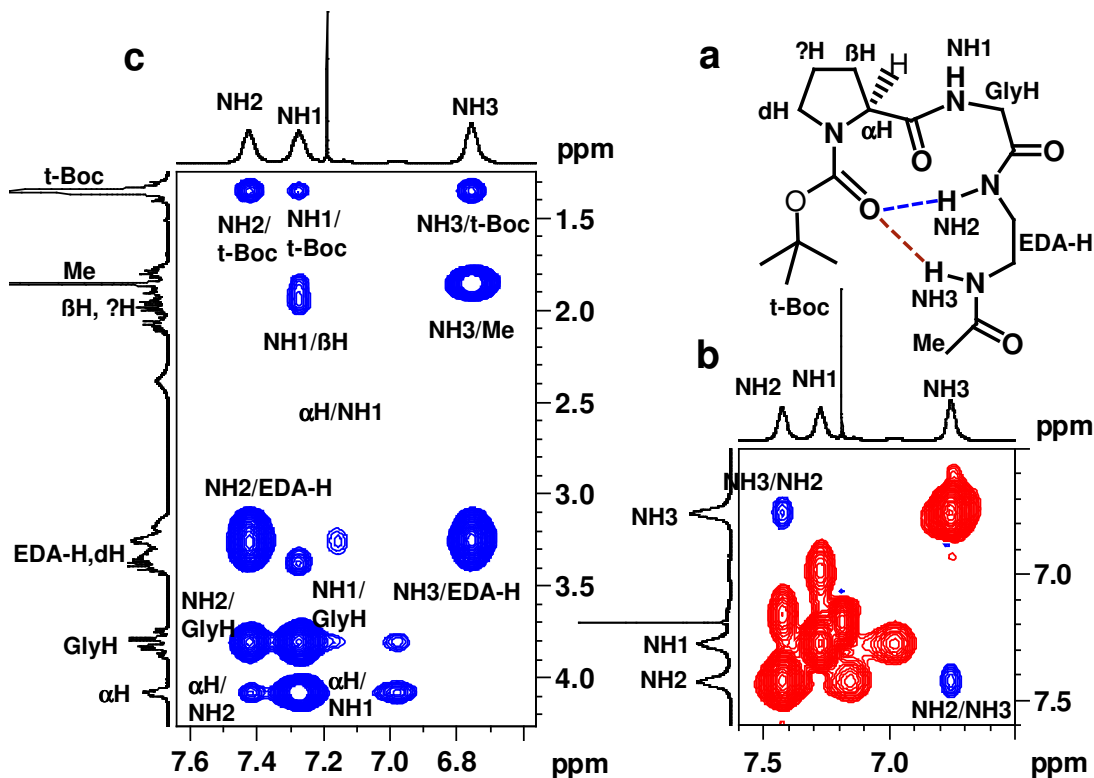


Figure 10: Molecular structure (a), and expanded 2D NOESY NMR spectra (b,c) of **5a**.
Note: The cross-peaks colored in red (figure 10b) are due to chemical exchange.

Analysis of the crystal structure had revealed that the most characteristic nOe that is quintessential to support the three-centered hydrogen bonding interaction, involving

both β - and α -turns, would be the requirement of the diagnostic dipolar coupling between NH2, and NH3 since they are closer in space (2.67 Å), held by the intramolecular turn conformations. Inspection of the 2D NOESY data indeed revealed the observation of the dipolar coupling between NH2 and NH3 (figure 10b), thereby confirming the prevalence of turn conformations and three centered H-bonding in solution-state as well. Other selected nOes that supported the turn conformations were: NH3 *vs* t-Boc, NH2 *vs* GlyH, NH2 *vs* α H (Pro α -H), and NH1 *vs* α H (figure 10c). It is noteworthy that the observed strong nOe between Pro α -H and NH1 is diagnostic of typical type II β -turn,²⁵ since these protons are positioned closely in such a conformation.

Solvent dilution experiment is particularly useful for differentiating the nature of hydrogen bonding interactions (inter *vs* intra) in the solution-state, wherein intermolecular hydrogen bondings (solvent exposed NHs) are relatively more vulnerable to concentration effects.²⁷ Further experimental support for the prevalence of three-centered intramolecular hydrogen bonding interaction, as observed in the solid-state, came from CDCl₃ dilution studies of **5a**. Notably, both the amide NHs participating in three-centered intramolecular H-bondings (NH2 and NH3, (figure 11) show relatively small shift ($\Delta\delta$ NH2: 0.12 ppm, and $\Delta\delta$ NH3: 0.23 ppm) when solutions of **5a** in CDCl₃ was diluted.

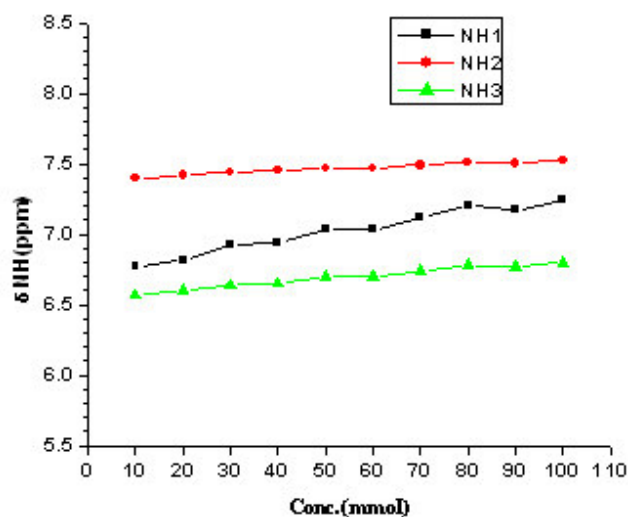


Figure 11: Dilution experiments performed in chloroform-d of peptide **5a**

This observation suggested their involvement in intramolecular hydrogen bonding interactions; consistent with the X-ray structure of **5b**. However, the amide NH (NH1) that does not participate in three-centered intramolecular hydrogen bonding interaction showed relatively larger shift ($\Delta\delta = 0.47$ ppm), obviously because of its intermolecular interaction, again consistent with its crystal structure (*vide supra*).

2.4.5 Conformational analysis of peptide **9**

Steric and electronic interactions often play a crucial role on the conformation of hydrogen bonded systems.²⁸ In an effort to investigate the effect of chain elongation from N-terminal on the overall conformation, we synthesized the peptide **9**. The peptide **9** was crystallized from a mixture of dichloromethane and water (85:15); the unit cell contained four molecules. Curiously enough, crystal structure studies showed the absence of α -turn structure in **9**, although the β -turn conformation was still retained with dihedral angles ($\phi_{i+1} = -62.20$, $\psi_{i+1} = 129.13$, $\phi_{i+2} = 72.49$, $\psi_{i+2} = 26.25$, figure 12).

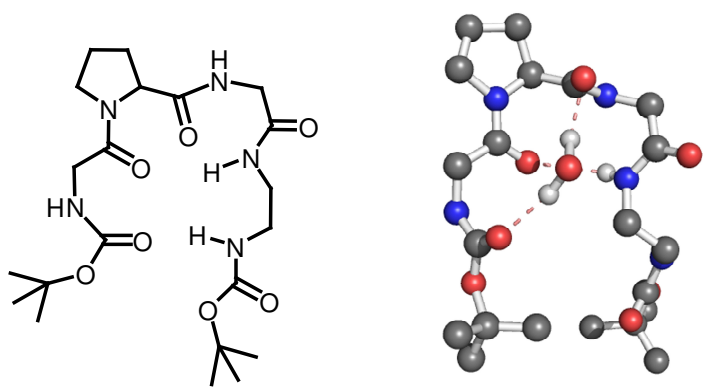


Figure 12: Molecular structure (left) and single crystal X-ray crystal structure (right) of **9**. *Note:* Hydrogens other than at the hydrogen bonding sites have been deleted for clarity.

Further, a water molecule was found interacting with the peptide backbone, connecting the amide carbonyls. The strong interaction of the water molecules with the back bone amide groups, were also substantiated by 2D NOESY and DOSY NMR (diffusion ordered spectroscopy) experiments (*vide infra*). It is noteworthy that water molecules strongly interacting with the peptide backbone have been shown to be playing crucial roles in modulating the conformation and function of the host peptides / proteins.²⁹

Intrigued by the absence of α -turn structure in **9** as evident from its crystal structure, we undertook a detailed NMR study that would provide insights into its structural features in the solution-state. ¹H NMR studies at various temperatures, coupled with 2D NOESY NMR studies in various concentrations (figure 14), unambiguously suggested that the peptide **9** exists in multiple conformations in solutions state, presumably arising out of the *cis-trans* isomerisation of proline; a known property associated with N-acyl prolines lacking a compact conformation.³⁰ Variable temperature NMR experiments carried out in dichloromethane (CD₂Cl₂, 400 MHz) at 100 mg/ml concentration (298 K down to 243 K) suggested that the two conformers freezes at 243 K. The existence of multiple conformers was also evident in polar solvents such as

acetone-d₆. Interaction of water molecules with amide backbones of **9** was evident in solution-state as well, as could be substantiated by 2D NOESY and DOSY studies. 2D NOESY studies carried out with varying parameters such as concentration, and temperature were suggestive of water interactions with the amide backbone of **9** (figure 13).

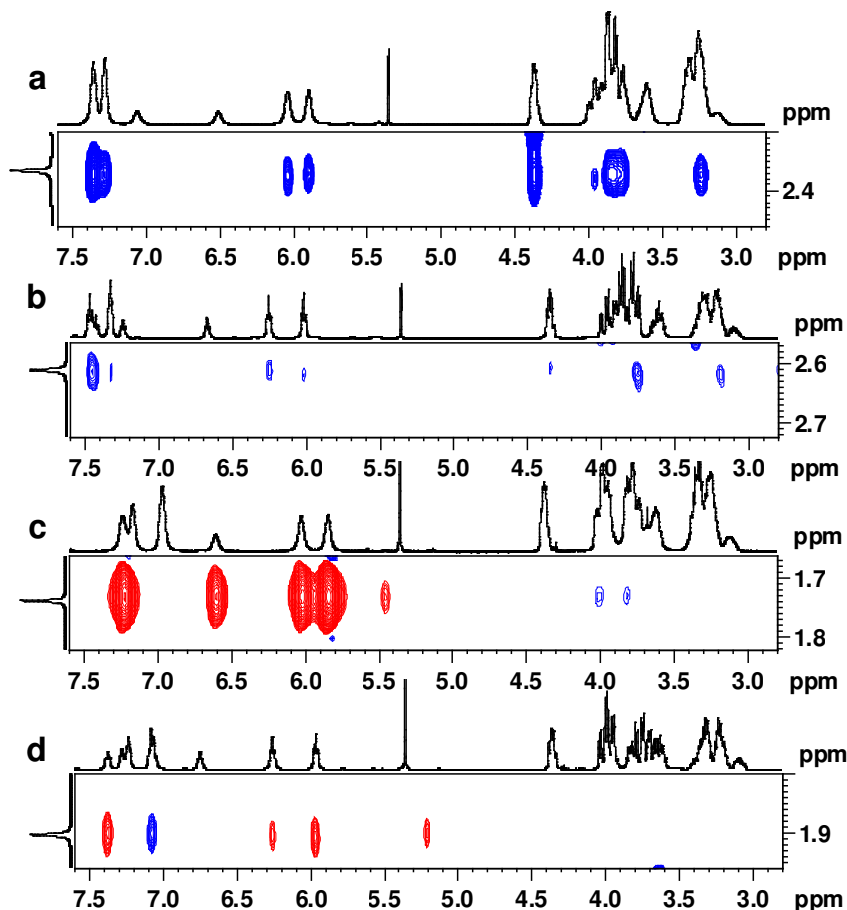


Figure 13: Expanded 2D NOESY NMR spectra of **9** showing interaction of water with peptide backbone. (a) 2D NOESY at 298 K in 265 mmol concentration; (b) 278 K in 265 mmol concentration; (c) 298 K in 53 mmol concentration; (d) 278 K in 53 mmol concentration). *Note:* The cross-peaks colored in red (figure c, d) are due to chemical exchange at low concentration.

Strong interaction of water molecules with backbone protons (amide as well as glycine CH₂s), as evident from negative nOes (marked in blue), were consistently

observed in the concentration of 265 mmol in CD₂Cl₂, (figure 14a). Interestingly, the interactions were observable even at a low concentration of 53 mmol in CD₂Cl₂, as evident from negative nOes with backbone CH₂s, (marked red, figure14b). However, positive cross peaks (marked red) are observed between water and all the amide protons since the exchange interactions dominate over the nOe interaction at low substrate concentration. As anticipated, the water-backbone interactions strengthen (re-appearance of negative nOes with amide NH) as the system is cooled from 298 K down to 278 K, obviously because of thermodynamic stabilization.

The water-peptide interaction was further substantiated by the results of DOSY NMR (figure14) (diffusion ordered spectroscopy) experiments.³¹ Diffusion coefficient measurements at two concentrations at 298K showed significant decrease in self-diffusion coefficient of water with increase in the substrate concentration, an observation which is also suggestive of water-substrate interaction in solution-state.

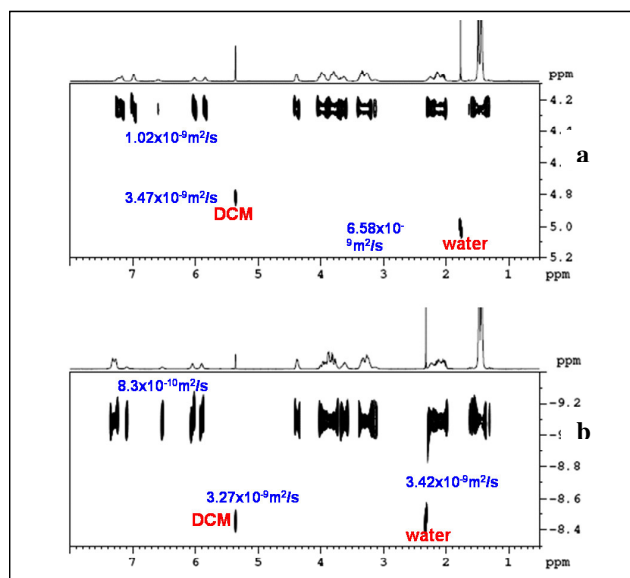


Figure 14: DOSY experiments of peptide **9** (a) 20mg/mL (b) 100mg/mL³¹

2.4.6 Conclusions

In summary, we have developed a semi synthetic peptide motif, Boc-Pro-Gly-Gly Ψ [CH₂NH]Boc that concurrently displays both α - and β -turns within the molecule, as evidenced from structural investigations by single crystal X-ray crystallography and NMR studies. The present findings also attest to the importance of utilizing three-centered hydrogen bonding interactions in stabilizing peptide / protein conformations which would also have a bearing on practical utility; for instance in the development of novel peptidomimetics that feature multiple reverse turns. The semi synthetic peptide motif described here in could become the starting point for the design of novel ordered

2.5 Experimental Procedures

General Methods

Unless otherwise stated, all the chemicals and reagents were obtained commercially. Acetonitrile was dried by distilling over calcium hydride and kept it over 4 Å mol sieves, prior to use. Chromatography was done on pre-coated silica gel plates (kieselgel 60F₂₅₄, Merck). Column chromatographic purifications were done with 100-200 Mesh Silica gel. NMR spectra were recorded in CDCl₃ on Ac 200 MHz or DRX-500 MHz Bruker NMR spectrometers. All chemical shifts are reported in δ ppm downfield to TMS and peak multiplicities are reported as singlet (s), doublet (d), quartet (q), broad (br), broad singlet (bs) and multiplet (m). Elemental analyses were performed on a Elementary-Vario- EL (Heraeus Company Ltd., Germany). IR spectra were recorded in nujol or CHCl₃ using Shimadzu FTIR-8400 spectrophotometer. Melting points were determined on a Buchi Melting Point B 540. MALDI-TOF Mass spectra were obtained from Voyager-PE, Voyager DEPRO and Voyager-DE STR Models. Single crystal X-ray data were collected on a Bruker SMART APEX CCD Area diffractometer with graphite monochromatized (Mo K_α = 0.71073 Å) radiation at room temperature. All the data were corrected for Lorentzian, polarization and absorption effects using Bruker's SAINT and SADABS programs. SHELX-97 was used for structure solution and full matrix least squares refinement on F^2 . Hydrogen atoms were included in the refinement as per the riding model.

Crystallographic data of 5b: (C₁₈H₂₄N₄O₄): $M = 360.41$, crystal dimensions 0.76 x 0.27 x 0.18 mm³, monoclinic, space group $P 2_1$, $a = 4.7957(14)$, $b = 19.605(6)$, $c = 9.913(3)$ Å, $\beta = 100.076(4)^\circ$, $V = 917.7(5)$ Å³, $Z = 2$, $\rho_{\text{calcd}} = 1.304$ gcm⁻³, μ (Mo-K_α) = 0.094 mm⁻¹

¹, $F(000) = 384$, $2\theta_{\max} = 50.00^\circ$, $T = 297(2)$ K, 10080 reflections collected, 4092 unique, 3811 observed ($I > 2\sigma(I)$) reflections, 248 refined parameters, R value 0.0505, $wR2 = 0.1348$ (all data $R = 0.0537$, $wR2 = 0.1377$), $S = 1.070$, minimum and maximum transmission 0.970 and 0.983; maximum and minimum residual electron densities +0.269 and $-0.195 \text{ e } \text{\AA}^{-3}$.

Crystallographic data of 9: ($\text{C}_{21}\text{H}_{39}\text{N}_5\text{O}_8 \cdot \text{H}_2\text{O}$): $M = 489.57$, crystal dimensions $0.54 \times 0.38 \times 0.07 \text{ mm}^3$, orthorhombic, space group $P 2_1$, $a = 9.0917(8)$, $b = 9.8531(9)$, $c = 29.228(2) \text{ \AA}$, $V = 2618.3(4) \text{ \AA}^3$, $Z = 4$, $\rho_{\text{calcd}} = 1.242 \text{ gcm}^{-3}$, $\mu (\text{Mo-K}\alpha) = 0.095 \text{ mm}^{-1}$, $F(000) = 1056$, $2\theta_{\max} = 50.00^\circ$, $T = 297(2)$ K, 13265 reflections collected, 4607 unique, 3636 observed ($I > 2\sigma(I)$) reflections, 321 refined parameters, R value 0.0641, $wR2 = 0.1324$ (all data $R = 0.0855$, $wR2 = 0.1411$), $S = 1.116$, minimum and maximum transmission 0.9501 and 0.9938; maximum and minimum residual electron densities +0.221 and $-0.142 \text{ e } \text{\AA}^{-3}$.

2-(Methoxycarbonylmethyl-carbamoyl)-pyrrolidine-1-carboxylic acid tert-butyl ester 1: To an ice-cold stirred solution of the Boc-Pro-OH (1.2 g, 5.58 mmol, 1 equiv.) in dry dichloromethane (15 mL) was added Et_3N (1.94 mL, 13.9 mmol, 2.5equiv) and isobutyl chloroformate (0.51 mL, 3.95 mmol, 1 equiv.). The resulting mixture was stirred vigorously for 5 min, and glycine methyl ester (0.62 g, 5.02 mmol, 0.9equiv) was added. The resulting reaction mixture was stirred for 5 h. The reaction mixture was diluted with dichloromethane and washed sequentially with potassium hydrogen sulphate solution, saturated sodium bicarbonate, and water. Drying and concentration of the dichloromethane extract under reduced pressure gave the crude product which on column

chromatography (40% EtOAc/Hexane) afforded the desired pure product **1** (1.2 g, 75%).²⁶

[(Pyrrolidine-2-carbonyl)-amino]-acetic acid methyl ester, trifluoro acetate 2. To an ice-cold stirred solution of **1** (1.0 g, 3.49 mmol) in dichloromethane (10 mL) was added, 50% trifluoro acetic acid-dichloromethane mixture (6 mL). The resulting reaction mixture was stirred at room temperature for 2h. The solvent was stripped of under reduced pressure, and the resultant residue was dissolved in methanol. Methanol was removed under reduced pressure; the process was repeated for two times to remove the excess trifluoro acetic acid from the reaction mixture. The residue was dried under vacuum to yield the desired product **2** as a white gummy liquid (1.0 g, quantitative), which was used for the next reaction, without further purification.

[(1-Benzoyl-pyrrolidine-2-carbonyl)-amino]-acetic acid methyl ester 3. To an ice-cold stirred solution of **2** (2.0 g, 6.68 mmol, 1 equiv.) in dry dichloromethane (15 mL) was added Et₃N (2.78 mL, 20.0 mmol, 3 equiv.) followed by benzoyl chloride (1.1 mL, 8.0 mmol, 1.2 equiv.). The resulting reaction mixture was stirred at room temperature for 6h. The reaction mixture was diluted with dichloromethane (80 mL) and washed sequentially with saturated sodium bicarbonate solution and water. Drying and concentration of the dichloromethane extract under reduced pressure gave the crude product which on column chromatography (60% EtOAc/Hexane) afforded the desired pure product **3** (1.1 g, 56%), $[\alpha]_D^{26} -9.5$ (CHCl₃); IR (CHCl₃) ν (cm⁻¹): 3018, 1749, 1679, 1602, 1215, 759; ¹H NMR (400 MHz, CDCl₃): δ 7.60-7.30 (m, 5H), 4.90-4.70 (m, 1H), 4.10-3.95 (m, 2H), 3.72 (s, 3H), 3.65-3.30 (m, 2H), 2.55-1.70 (m, 4H); ¹³C NMR

(100 MHz, CDCl₃): δ 171.5, 170.9, 170.0, 135.9, 130.1, 128.2, 127.0, 59.5, 52.0, 50.2, 41.0, 27.4, 25.1; ESI Mass: 313.3 (M+Na); Anal. Calcd. for C₁₅H₁₈N₂O₄: C, 62.06; H, 6.25; N, 9.65. Found: C, 62.15; H, 6.19; N, 9.59.

2-[[2-Amino-ethylcarbamoyl]-methyl]-carbamoyl]-pyrrolidine-1-carboxylic acid

tert-butyl ester 4a: To an ice-cold stirred solution of **1** (1.0 g, 3.49 mmol, 1 equiv.) in methanol (20 mL) was added ethylenediamine (3 mL). The resulting reaction mixture was stirred at 0°C for 30 min, and continued at room temperature for 1 hr. The solvent was stripped of under reduced pressure, the resultant residue was taken in toluene, and toluene was stripped of under reduced pressure. The process was repeated for two times to remove excess ethylenediamine. The residue was dried under vacuum to yield the desired product **4a** as a thick liquid (1.09 g, 100%) which was used for the next reaction, without further purification.

1-Benzoyl-pyrrolidine-2-carboxylic acid [(2-amino-ethylcarbamoyl)-methyl]-amide

4b: To an ice-cold stirred solution of **3** (0.5 g, 1.72 mmol, 1 equiv.) in methanol (10 mL) was added ethylenediamine (1.5 mL). The resulting reaction mixture was stirred at 0°C for 30 min, and continued at room temperature for 30 min. The solvent was stripped of under reduced pressure, the resultant residue was taken in toluene, and toluene was stripped of under reduced pressure, the process was repeated two times to remove excess ethylenediamine. The residue was dried under vacuum to yield the desired product **4b** as thick liquid (0.54 g, 100%) which was used for the next reaction, without further purification.

2-[[2-Acetylamino-ethylcarbamoyl)-methyl]-carbamoyl]-pyrrolidine-1-carboxylic acid tert-butyl ester 5a: To a solution of **4a** (3.0 g, 9.55 mmol, 1equiv.) in dry pyridine (15 mL) was added acetic anhydride (2.71 mL, 28.66 mmol, 3equiv.). The resulting reaction mixture was stirred at room temperature for 5h. The solvent was stripped of under reduced pressure get the crude product which on column chromatography (80% EtOAc: Pet. ether) afforded the desired pure product **5a** as thick liquid (2.5 g, 73%) $[\alpha]_D^{26} -10.7$ (CHCl₃); IR (CHCl₃) ν (cm⁻¹): 3323, 3016, 1668, 1533, 1411, 1215, 756; ¹H NMR (400 MHz, CDCl₃): δ 7.56 (bs, 1H), 7.49 (bs, 1H), 7.10 (bs, 1H), 4.17 (bs, 1H), 4.00-3.75 (m, 2H), 3.50-3.0 (m, 6H), 2.20-1.80 (m, 4H), 1.94 (s, 3H), 1.42 (s, 9H); ¹³C NMR (100 MHz, CDCl₃): δ 173.6, 171.1, 170.3, 155.5, 80.7, 60.8, 47.3, 43.2, 39.2, 29.8, 28.4, 24.6, 23.0; ESI Mass: 395.3 (M+K); Anal. Calcd. for C₁₆H₂₈N₄O₅: C, 53.92; H, 7.92; N, 15.72. Found: C, 53.65; H, 7.70; N, 15.63.

1-Benzoyl-pyrrolidine-2-carboxylic acid [(2-acetylamino-ethylcarbamoyl)-methyl]-amide 5b: To a solution of **4b** (0.5 g, 1.57 mmol, 1equiv.) in dry pyridine (5 mL) was added acetic anhydride (0.44 mL, 4.71 mmol, 3equiv.). The resulting reaction mixture was stirred at room temperature for 5h. The solvent was stripped of under reduced pressure to get the gave the crude product which on column chromatography (100% EtOAc) afforded the desired pure product **5b** (0.39 g, 69%); mp 157-160⁰C; $[\alpha]_D^{26} -11.5$ (CHCl₃); IR (CHCl₃) ν (cm⁻¹): 3336, 3018, 1662, 1612, 1217, 771; ¹H NMR (400 MHz, CDCl₃): δ 8.24 (bs, 1H), 8.07 (bs, 1H), 8.05-7.95 (m, 2H), 7.88 (bs, 1H), 7.85-7.70 (m, 3H), 4.95-4.75 (m, 1H), 4.75-4.55 (m, 1H), 4.30-3.60 (m, 7H), 2.70-1.90 (m, 4H), 2.15 (s, 3H), 3; ¹³C NMR (100MHz, CDCl₃): δ 172.5, 170.8, 170.0, 135.5, 130.6, 128.5,

126.9, 61.6, 50.7, 43.3, 39.6, 39.1, 29.4, 25.6, 22.7; ESI Mass: 383.17 (M+Na); Anal. Calcd. for C₁₈H₂₄N₄O₄: C, 59.99; H, 6.71; N, 15.55. Found: C, 59.82; H, 6.69; N, 15.40.

2-([2-(4-Nitro-benzoylamino)-ethylcarbamoyl]-methyl)-carbamoyl-pyrrolidine-1-carboxylic acid tert-butyl ester 6a : To an ice-cold stirred solution of 4-nitro-benzoic acid (0.5 g, 3.04 mmol, 1.2 equiv.) and amine **4a** (0.8 g, 2.54 mmol, 1 equiv.) in dry acetonitrile (15mL) was added DIPEA (1.09 mL, 6.09 mmol, 2.4 equiv.) followed by TBTU (1.14 g, 3.55 mmol, 1.4 equiv.) The resulting reaction mixture was stirred for overnight at room temperature. The solvent was stripped off under reduced pressure; the resultant residue was dissolved in dichloromethane (100 mL) and washed sequentially with potassium hydrogen sulphate solution, saturated sodium bicarbonate and water. Drying and concentration in vacuo yielded the crude product which on column chromatography (70% ethyl acetate/pet-ether) afforded **6a** (0.75 g, 64%); mp 173-176⁰C; $[\alpha]_D^{26}$ -9.0 (CHCl₃); IR (CHCl₃) ν (cm⁻¹): 3325, 3018, 1666, 1527, 1215, 756; ¹H NMR (400 MHz, CDCl₃): δ 8.30-8.15 (d, 2H), 8.10-7.95 (d, 2H), 7.90 (bs, 1H), 7.79 (bs, 1H), 6.87 (bs, 1H), 4.20-3.85 (m, 3H), 3.65-3.30 (m, 6H), 2.30-1.75 (m, 4H), 1.40 (s, 9H); ¹³C NMR (100 MHz, CDCl₃): δ 173.6, 170.9, 165.6, 155.7, 149.3, 139.7, 128.4, 123.4, 80.9, 60.9, 47.3, 43.2, 40.8, 39.0, 29.8, 28.3, 24.5 ; ESI Mass: 486.20 (M+Na); Anal. Calcd. for C₂₁H₂₉N₅O₇: C, 54.42; H, 6.31; N, 15.11. Found: C, 54.27; H, 6.19; N, 14.99.

2-([2-(4-Bromo-benzoylamino)-ethylcarbamoyl]-methyl)-carbamoyl-pyrrolidine-1-carboxylic acid tert-butyl ester 6b: To an ice-cold stirred solution of 4-bromo-benzoic acid (0.5 g, 3.04 mmol, 1.2 equiv.) and amine **4a** (0.8 g, 2.54 mmol, 1 equiv.) in dry acetonitrile (15mL) was added DIPEA (1.09 mL, 6.09 mmol, 2.4 equiv.) followed by the addition of TBTU (1.14 g, 3.55 mmol, 1.4 equiv.) The resulting reaction mixture was

stirred for overnight at room temperature. The solvent was stripped off under reduced pressure; the resultant residue was dissolved in dichloromethane (100 mL) and washed sequentially with potassium hydrogen sulphate solution, saturated sodium bicarbonate and water. Drying and concentration in vacuo yielded the crude product which on column chromatography. (90% ethyl acetate/pet-ether) afforded **6b** (0.79 g, 68%); mp 180-182⁰C; $[\alpha]_D^{26} -5.0$ (CHCl₃); IR (CHCl₃) ν (cm⁻¹): 3334, 3018, 1662, 1411, 1215, 756; ¹H NMR (400 MHz, CDCl₃): δ 7.85-7.40 (m, 6H), 7.02 (bs, 1H), 4.20-3.75 (m, 3H), 3.65-3.25 (m, 6H), 2.25-1.70 (m, 4H), 1.40 (s, 9H) ; ¹³C NMR (100 MHz, CDCl₃): δ 173.3, 170.7, 166.7, 155.5, 132.9, 131.4, 128.8, 125.8, 80.7, 60.8, 47.2, 43.1, 40.6, 39.1, 29.7, 28.2, 24.5 ; ESI Mass: 520.25 (M+Na); Anal. Calcd. for C₂₁H₂₉N₄O₅Br: C, 50.71; H, 5.88; N, 11.26. Found: C, 50.65; H, 5.80; N, 11.19.

{[1-(2-tert-Butoxycarbonylamino-acetyl)-pyrrolidine-2-carbonyl]-amino}-acetic acid methyl ester 7: To an ice-cold stirred solution **2** (0.5 g, 1.67 mmol, 1 equiv.) and Boc-Gly-OH (0.29 g, 1.67 mmol, 1 equiv.) in dry dichloromethane (10 mL) was added DIPEA (1.19 mL, 6.68 mmol, 4 equiv.) followed by EDCI (0.44 g, 2.33 mmol, 1.4 equiv.) The resulting reaction mixture was stirred overnight at room temperature. The reaction mixture was diluted with dichloromethane (80mL) and washed sequentially with potassium hydrogen sulphate solution, saturated sodium bicarbonate and water. Drying and concentration in vacuo yielded the crude product which on column chromatography (70% EtOAc/Hexane) afforded the desired product **7** (0.45 g, 78%).

[2-(2-[(2-Amino-ethylcarbamoyl)-methyl]-carbamoyl)-pyrrolidin-1-yl]-oxo-ethyl]-carbamic acid tert-butyl ester 8: To an ice-cold stirred solution of **7** (1.0 g, 3.49 mmol, 1 equiv.) in methanol (10 mL) was added ethylenediamine (2 mL). The resulting reaction

mixture was stirred at 0°C for 30 min, and continued at room temperature for 30 min. The solvent was stripped of under reduced pressure, then the residue was taken in toluene, and again stripped of the solvent under reduced pressure. The residue was dried under vacuum to yield the desired product **8** as a thick liquid (1.09 g, 100%) which was used for the next reaction, without further purification.

[2-(2-[(2-tert-Butoxycarbonylamino-ethylcarbamoyl)-carbamoyl]-pyrrolidin-1-yl)-2-oxo-ethyl]-carbamic acid tert-butyl ester **9**: To an ice cold solution of the compound **8** (0.54 g, 1.45 mmol, 1 equiv.) in tetrahydrofuran (10 mL) Boc anhydride (0.63 g, 2.91 mmol, 2equiv.) was added and the resulting reaction mixture was stirred at room temperature for one hour. The reaction mixture was diluted with ethyl acetate (50 mL) and washed with water and saturated sodium chloride solution. Drying and concentration of the ethyl acetate extract under reduced pressure gave the crude product which on column chromatography (100% EtOAc) afforded the desired pure product **9** (0.55 g, 75%); mp 195-198°C; $[\alpha]_D^{26} -11.2$ (CHCl₃); IR (CHCl₃) ν (cm⁻¹): 3325, 3018, 1666, 1612, 1215, 756; ¹H NMR (400 MHz, CDCl₃): δ 8.30-8.15 (d, 2H), 8.10-7.95 (d, 2H), 7.90 (bs, 1H), 7.79 (bs, 1H), 6.87 (bs, 1H), 4.20-3.85 (m, 3H), 3.65-3.30 (m, 6H), 2.30-1.75 (m, 4H), 1.40 (s, 9H); ¹³C NMR (100 MHz, CDCl₃): δ 171.8, 169.8, 169.6, 157.5, 156.6, 156.0, 79.8, 79.5, 61.3, 47.0, 43.0, 40.1, 29.0, 28.2, 24.9 ; ESI Mass: 494.20 (M+Na); Anal. Calcd. for C₂₁H₃₇N₅O₇: C, 53.49; H, 7.91; N, 14.85 Found: C, 53.15; H, 7.75; N, 14.67.

Table 1: Dilution data for 5a at high concentration in chloroform-d

S.No	Conc. (mmol)	NH1	NH2	NH3
1	10	6.77	7.4	6.57
2	20	6.82	7.42	6.6
3	30	6.92	7.44	6.64
4	40	6.94	7.45	6.65
5	50	7.03	7.47	6.7
6	60	7.03	7.47	6.7
7	70	7.12	7.49	6.74
8	80	7.2	7.51	6.78
9	90	7.17	7.5	6.77
10	100	7.24	7.52	6.8

Table 2: Self diffusion coefficient table for 9 in CD₂Cl₂

Conc. mmol	Self diffusion coefficient (10 ⁻⁹ m ² sec ⁻¹)		
	Substrate	Water	DCM
--	--	6.58	3.57
70	1.02	5.86	3.47
350	0.82	3.42	3.27

Table 3: Dilution data for 5a at low concentration in chloroform-d

S.No	Conc. (mmol)	NH1	NH2	NH3
1	10	6.77	7.40	6.57
2	9.5	6.75	7.40	6.56
3	9	6.75	7.40	6.56
4	8.5	6.74	7.40	6.56
5	8	6.74	7.40	6.55
6	7.5	6.74	7.40	6.55
7	7.0	6.73	7.40	6.55
8	6.5	6.73	7.40	6.55
9	6.0	6.72	7.40	6.55
10	5.5	6.72	7.40	6.55

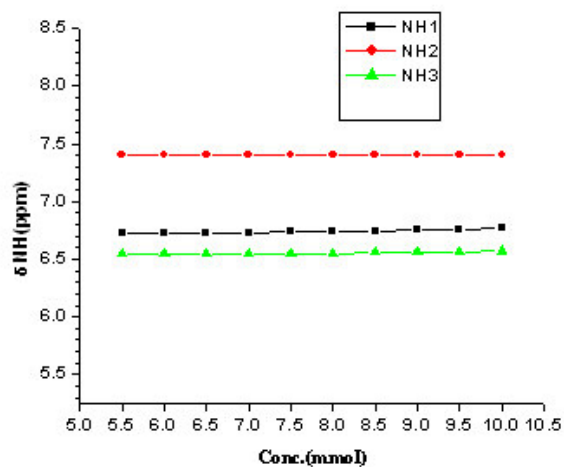


Figure 15: Dilution experiments performed (low concentration) in chloroform-d of peptide 5a

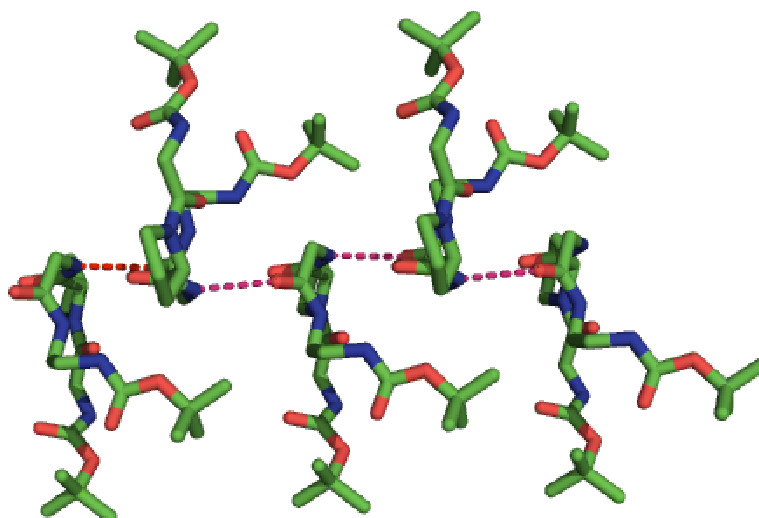


Figure 16: Single crystal X-ray structure of the peptide **9** showing self assembly forming extended structure: The intermolecular hydrogen bonding interactions are highlighted in pink colored dashes, for aiding quick identification. Hydrogens have been deleted for clarity.

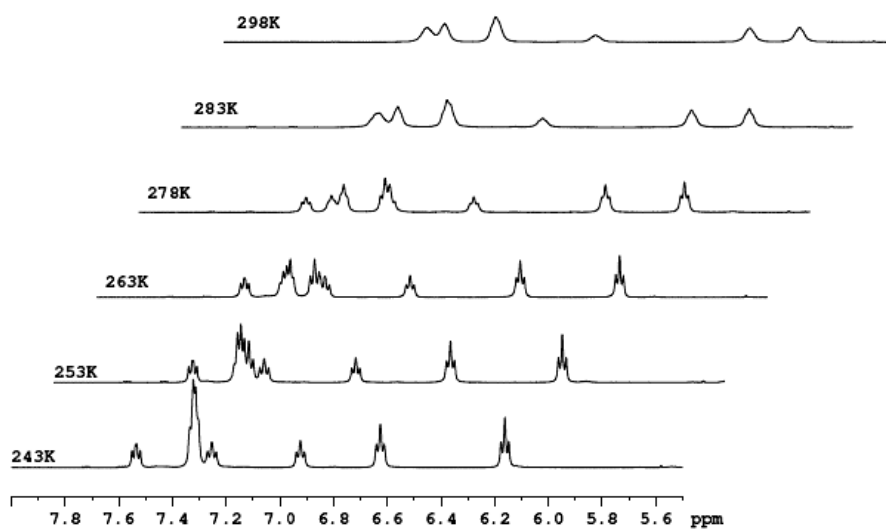


Figure 17: Variable temperature ¹H NMR spectra of **9** (NH region); 298K – 243K (400 MHz, CD₂Cl₂) 20 mg/ml (53 mmol)

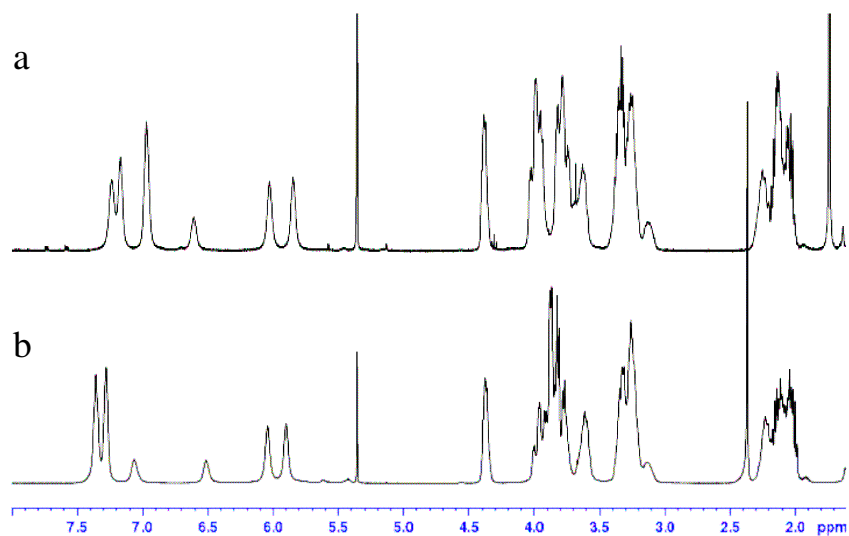


Figure 18: ^1H NMR spectra of **9** in CD_2Cl_2 (a) 20 mg/ml (b) 100 mg/ml

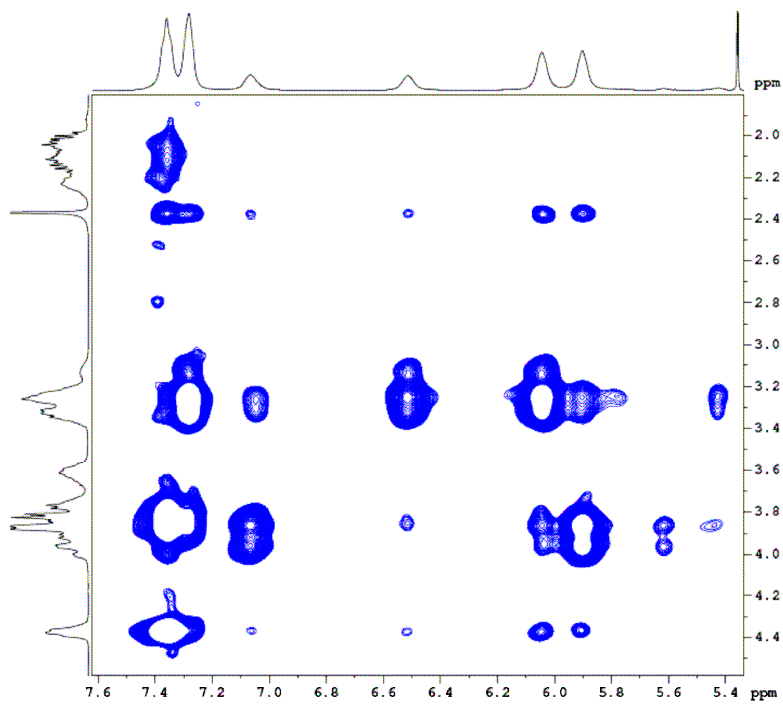


Figure 19: 2D NOESY of **9** in CD_2Cl_2 (100 mg/ml) with 1.25 s Mixing time at 298K

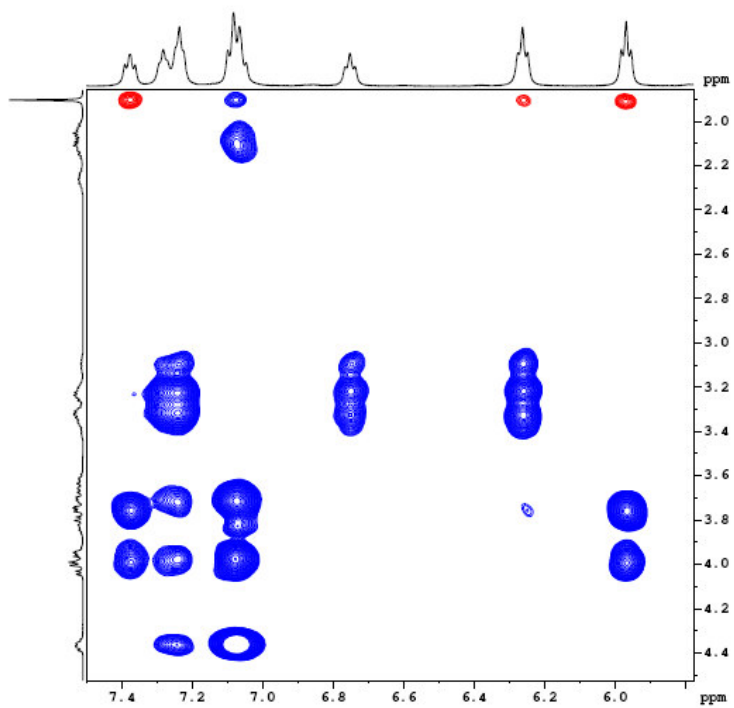
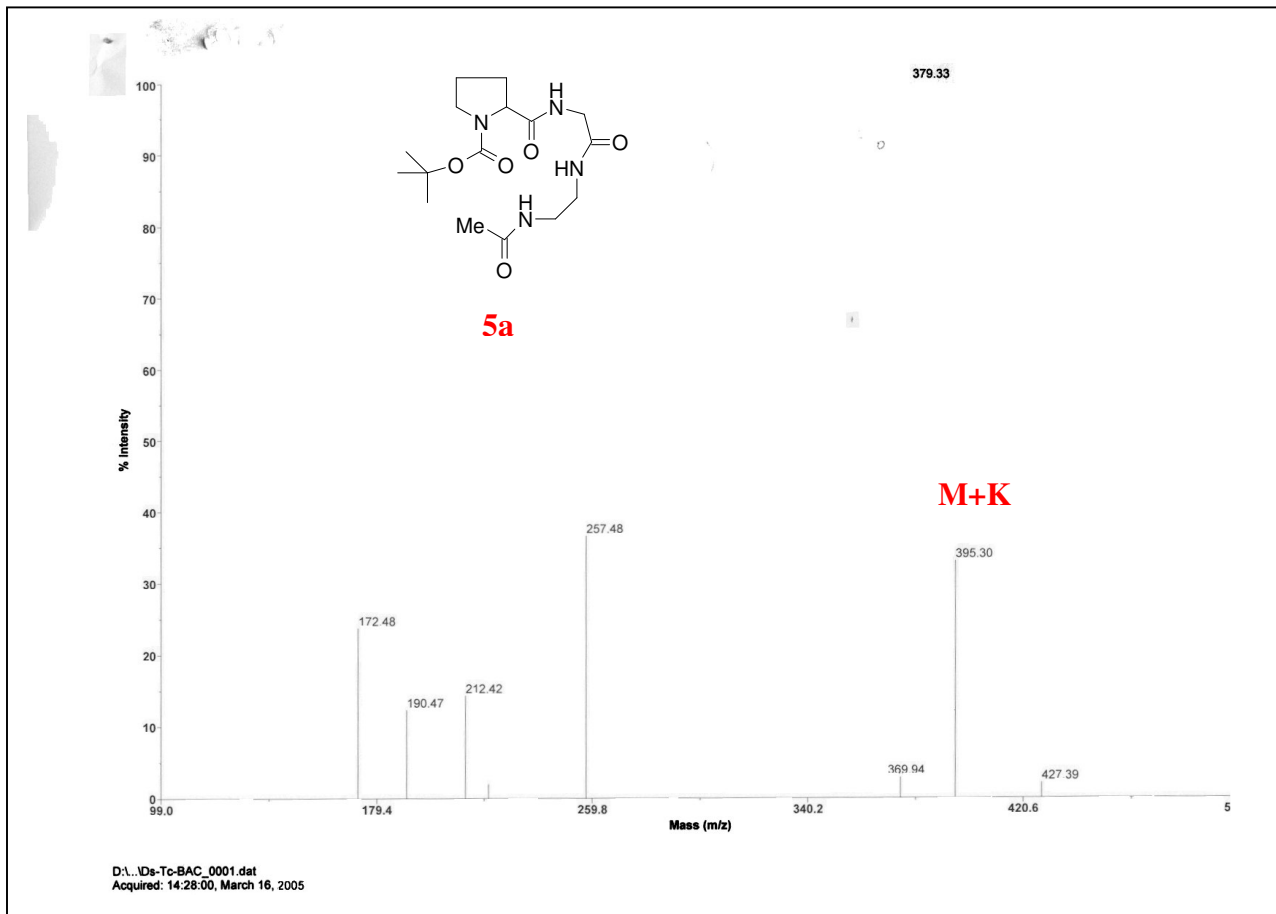
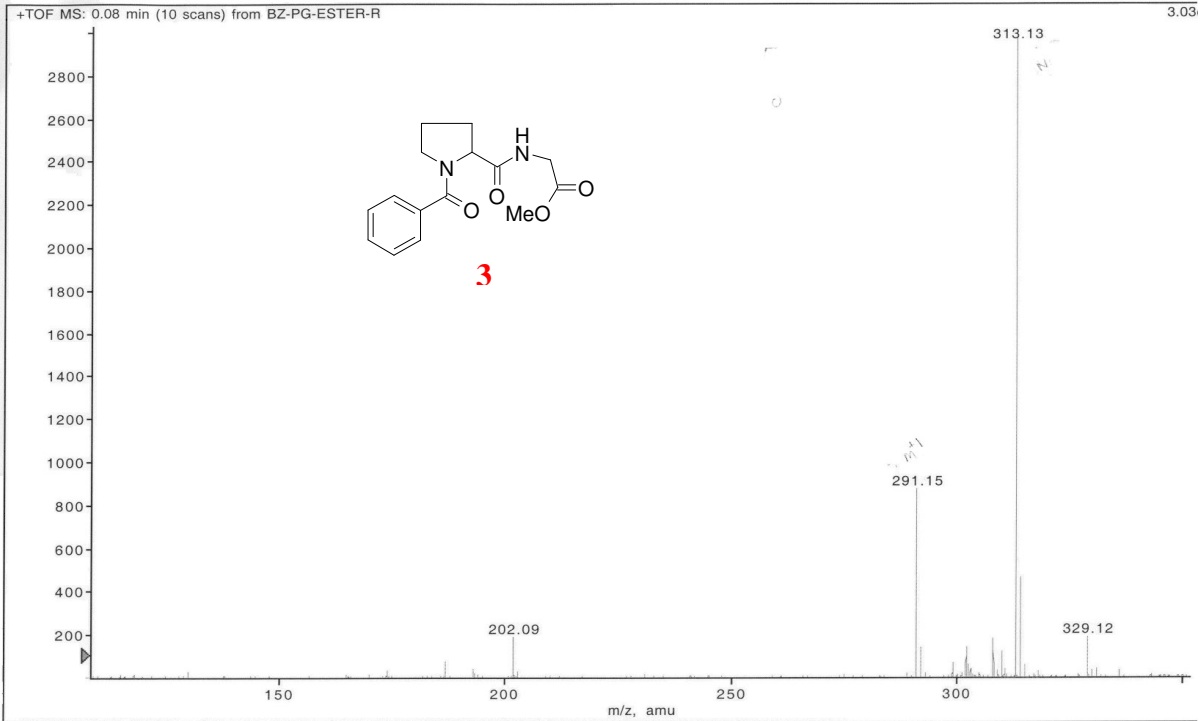


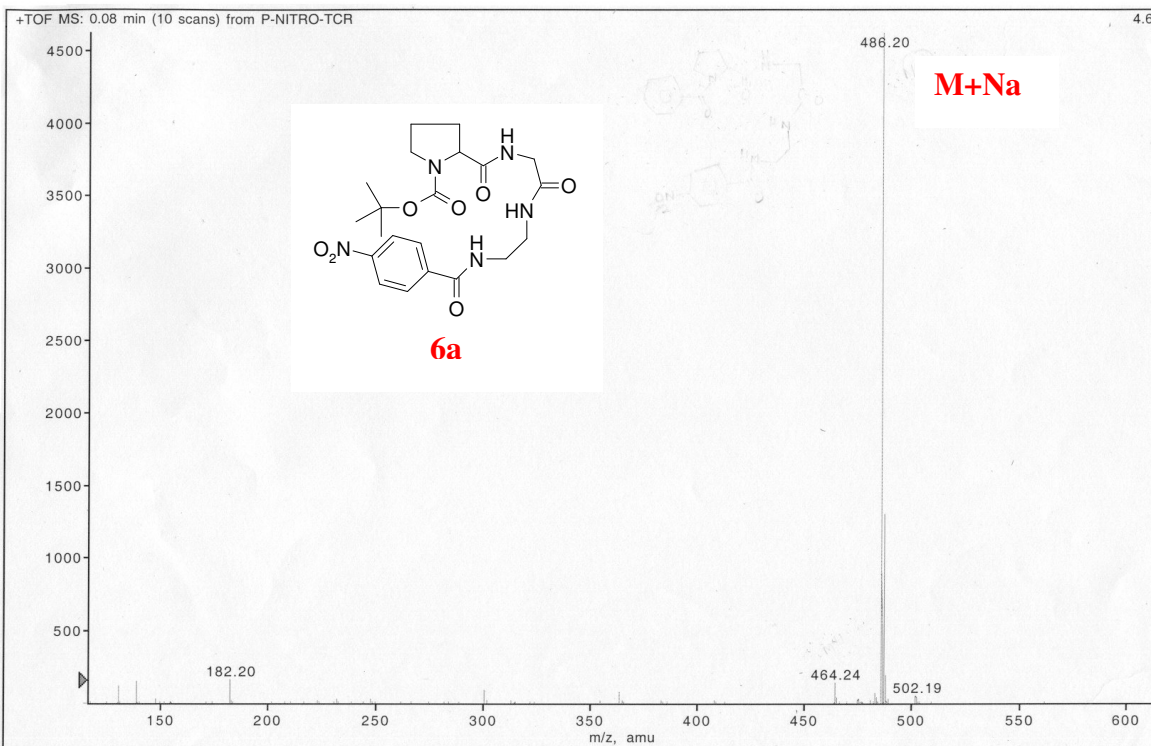
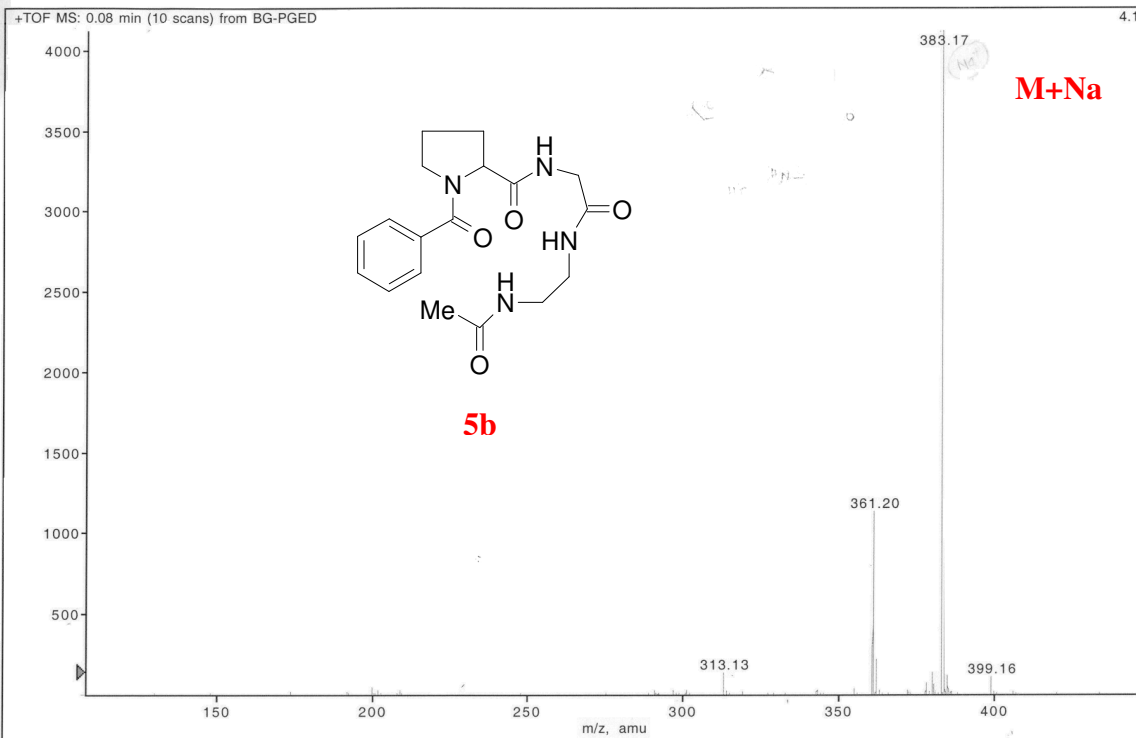
Figure 20: 2D NOESY of **9** (NH region) in CD₂Cl₂ (20 mg/ml) with 1.25 s Mixing time at 278K

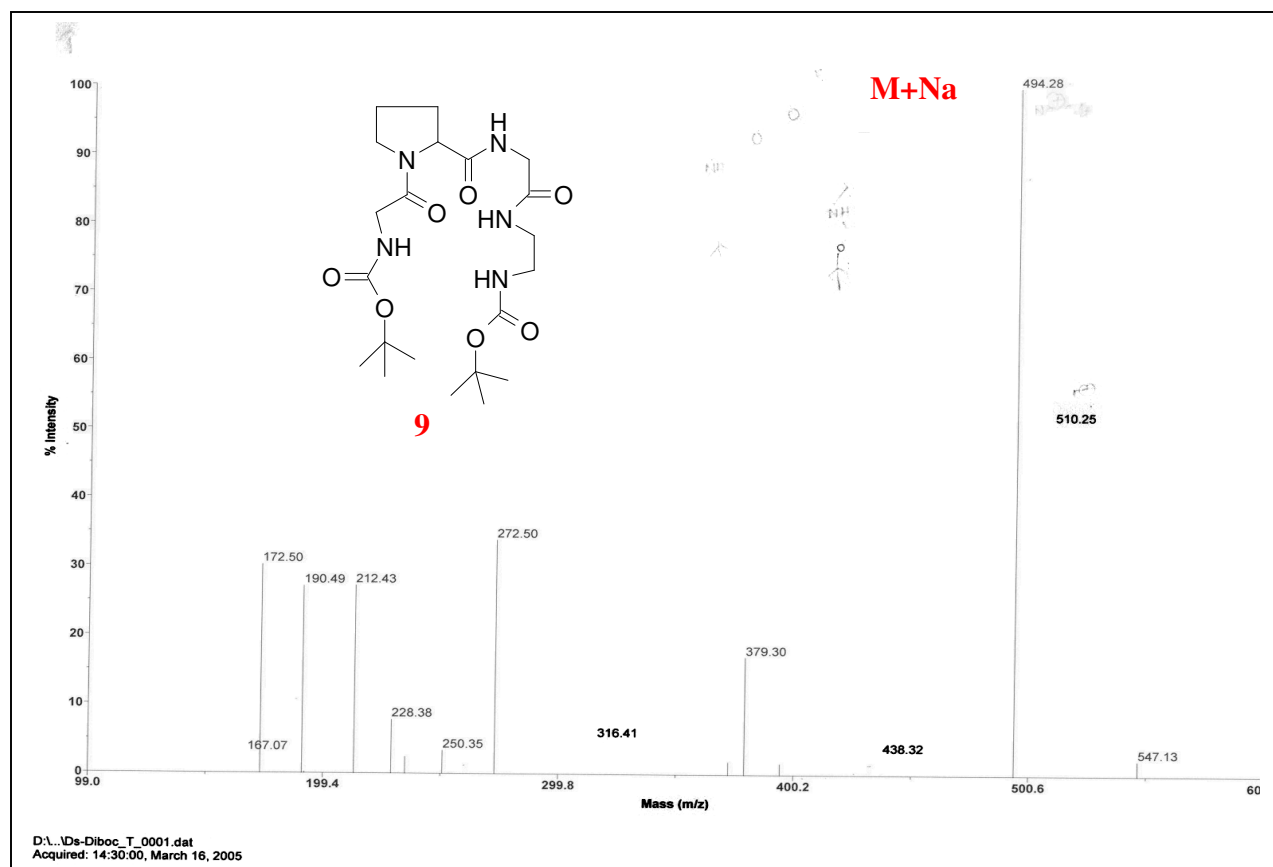
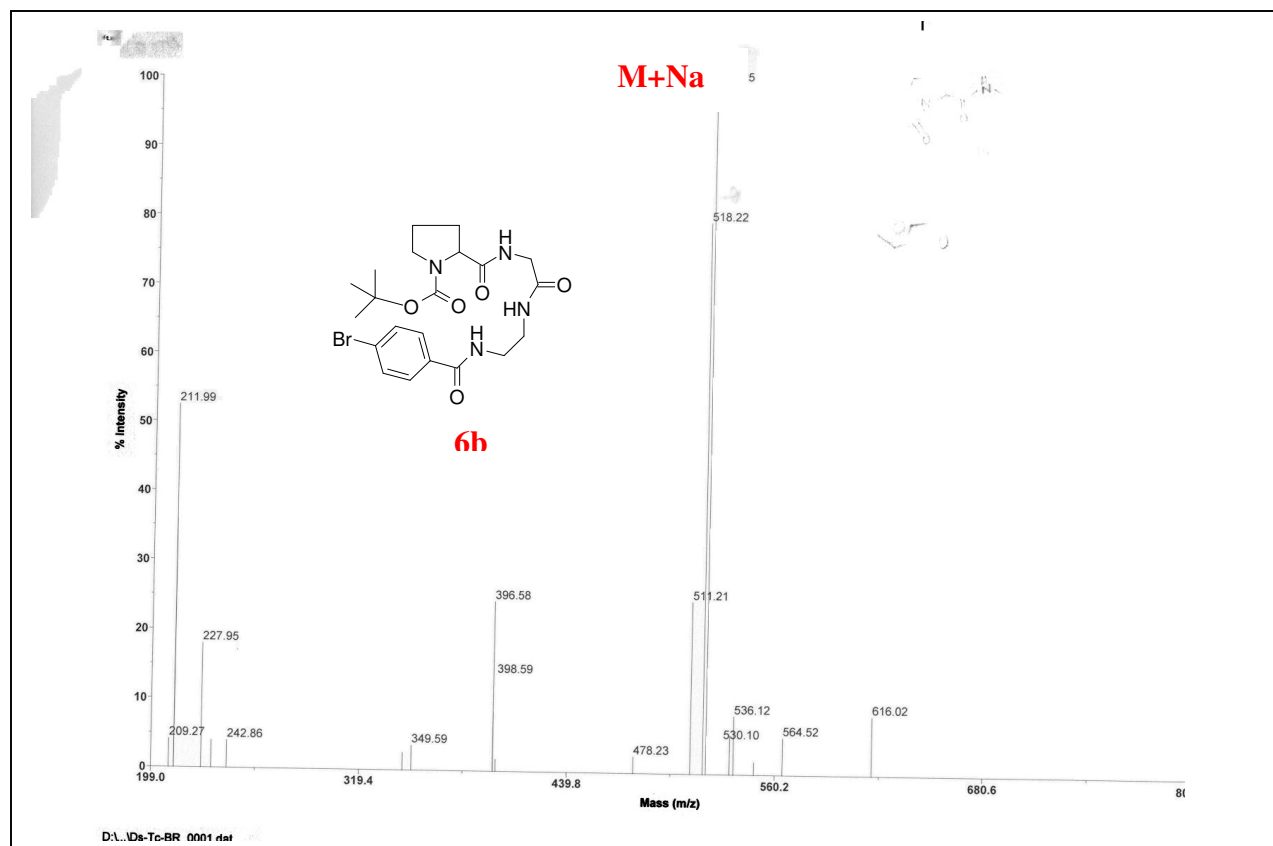
BZ-PG-ESTER-R (No Title)

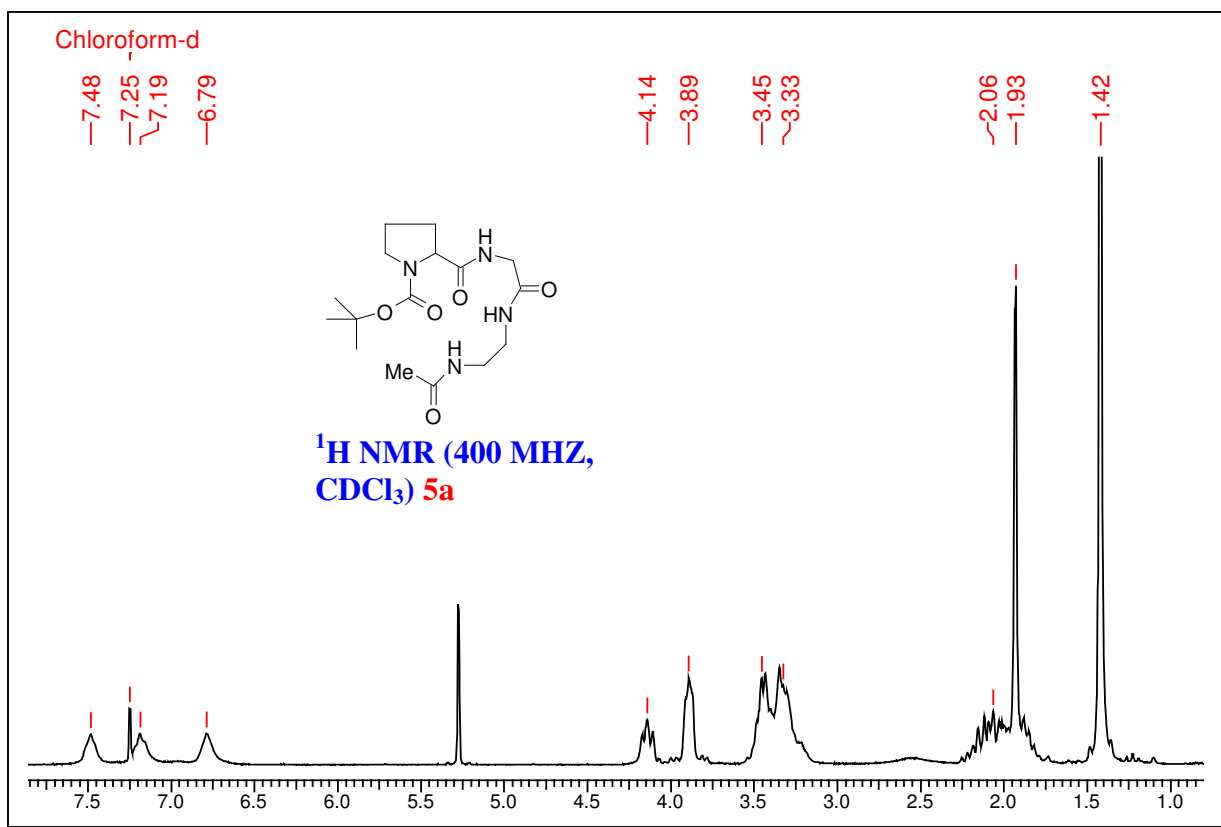
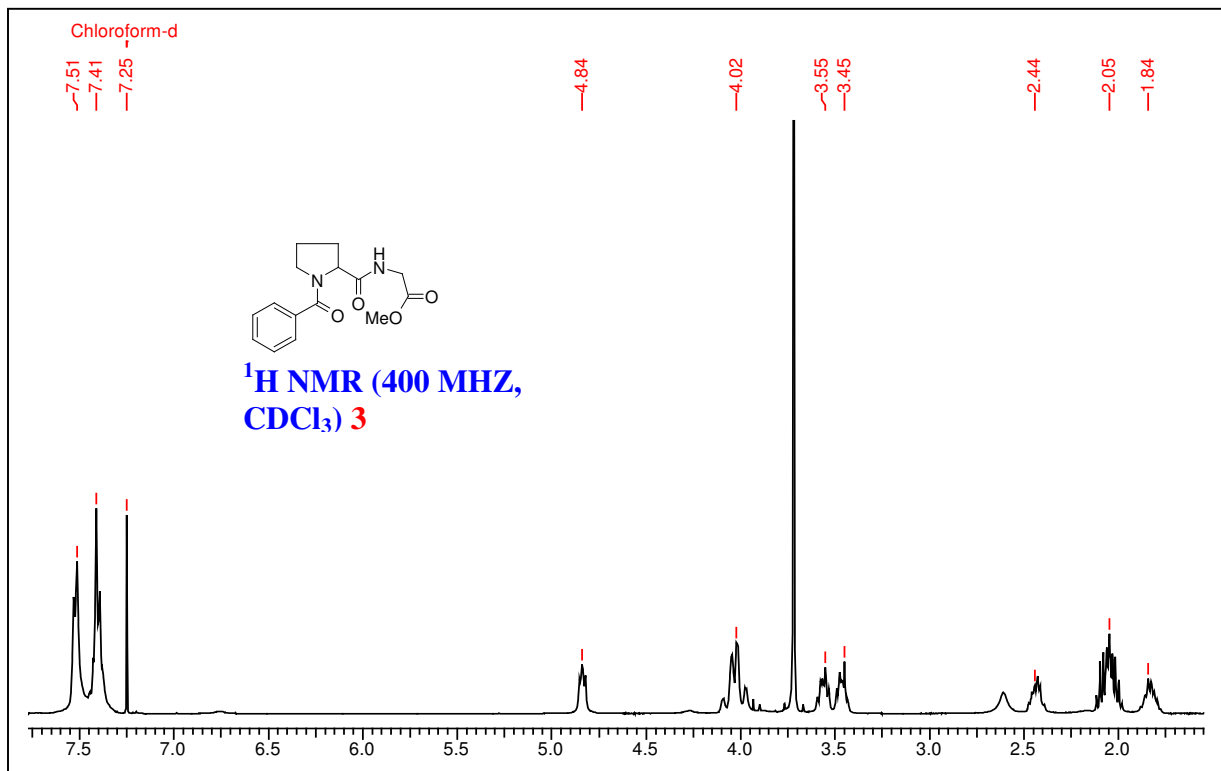
Period 1, Expt. 1; Mass range: 100.0 to 800.0 by 0.0 amu; Dwell: 1.0 ms; Pause: 5.0 ms

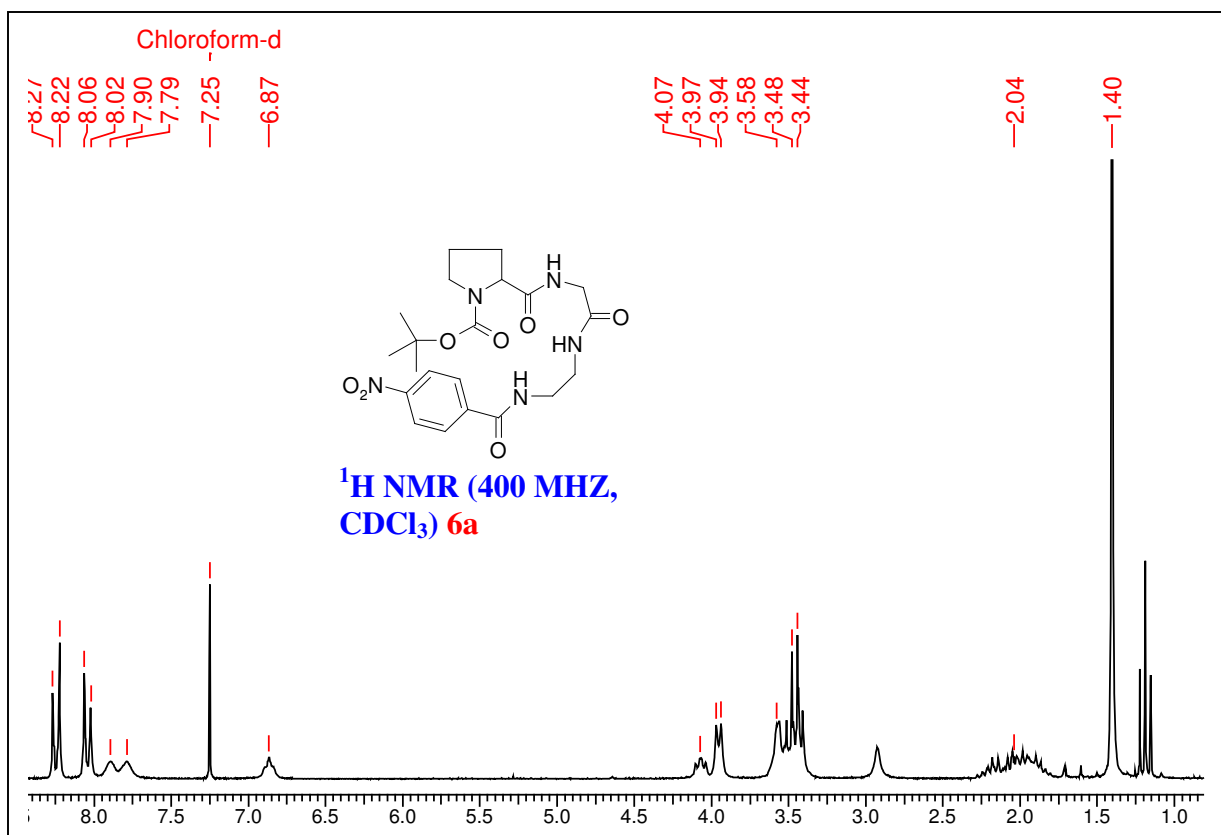
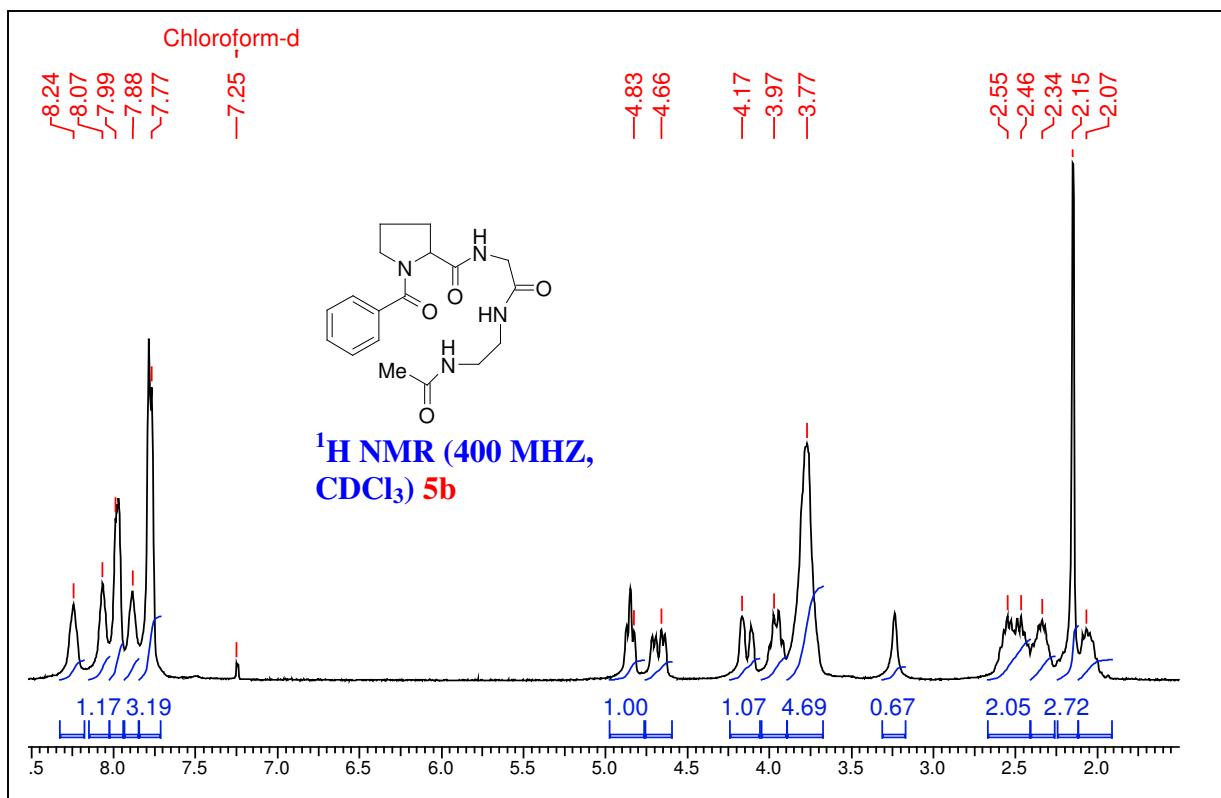
Acq Time: Mon, Apr 25, 2005 at 3:47:37 PM

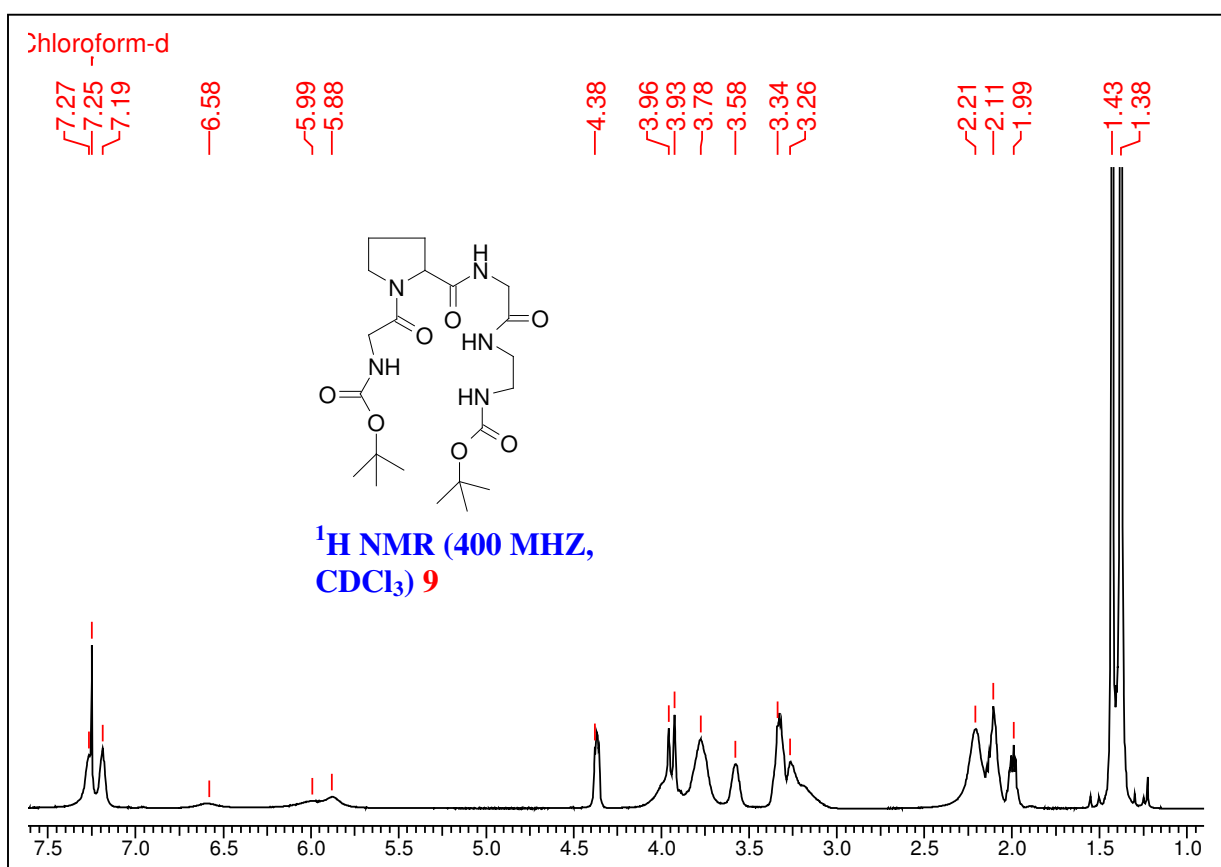
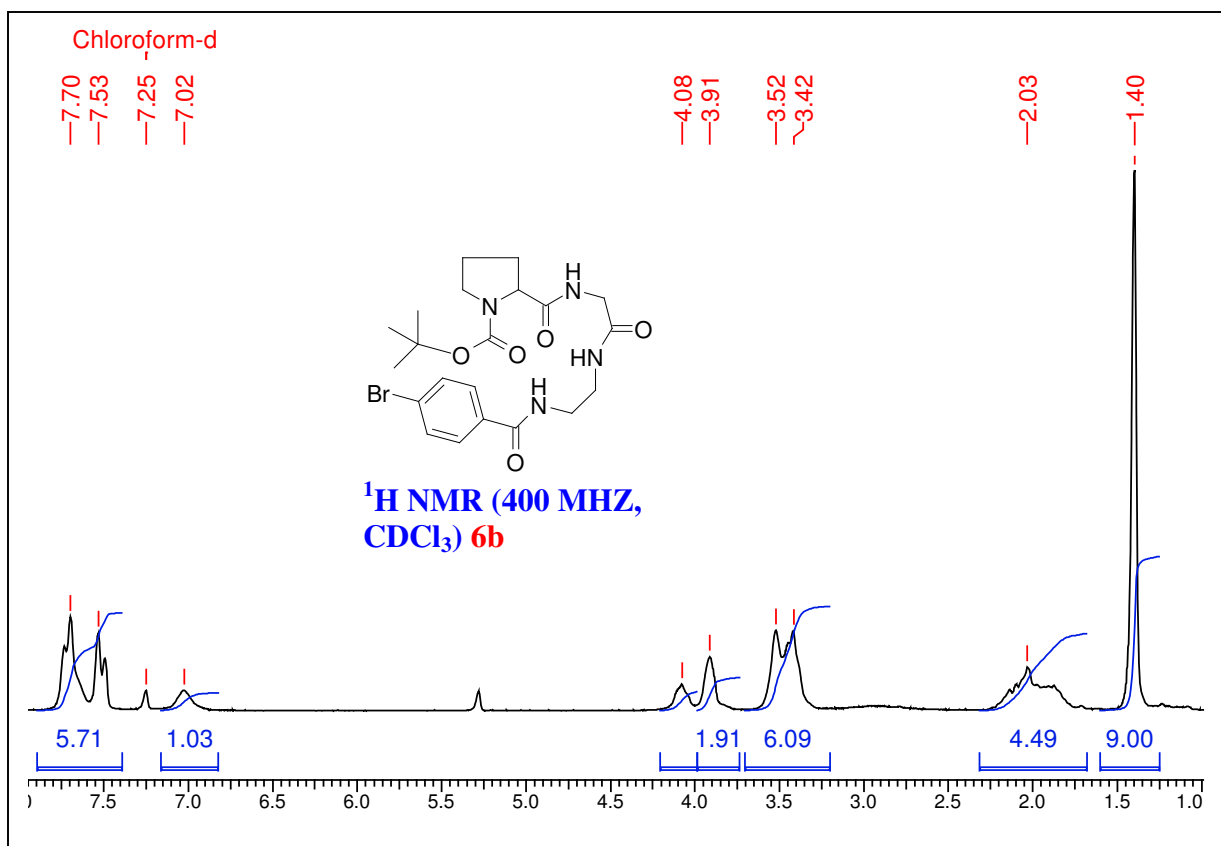


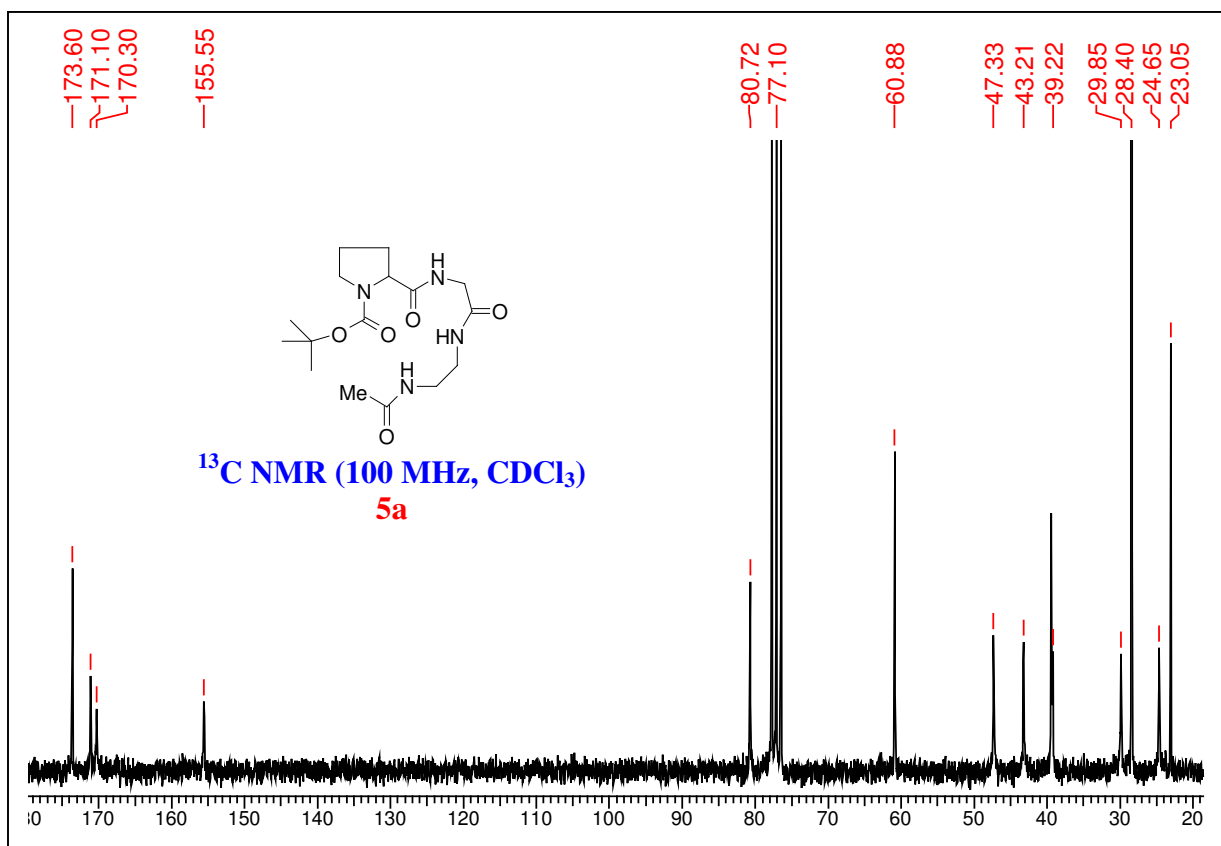
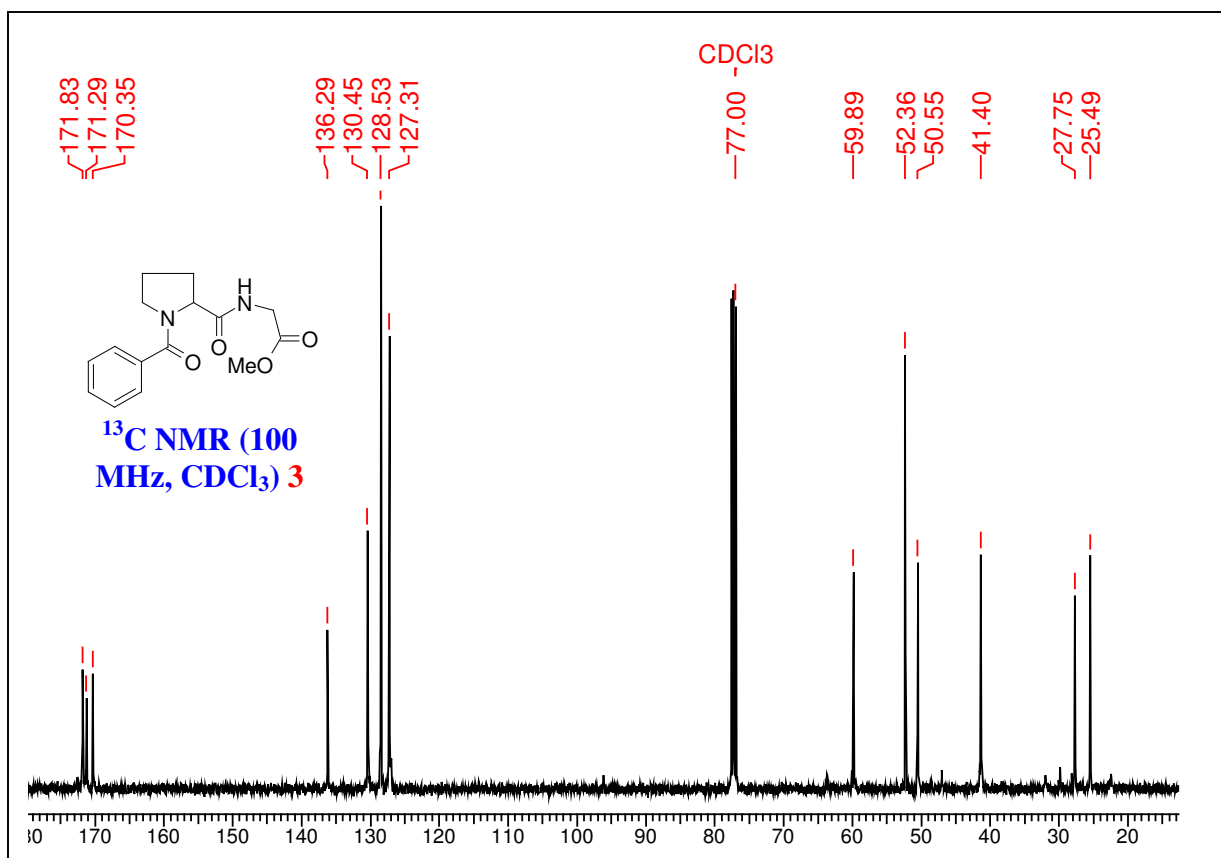


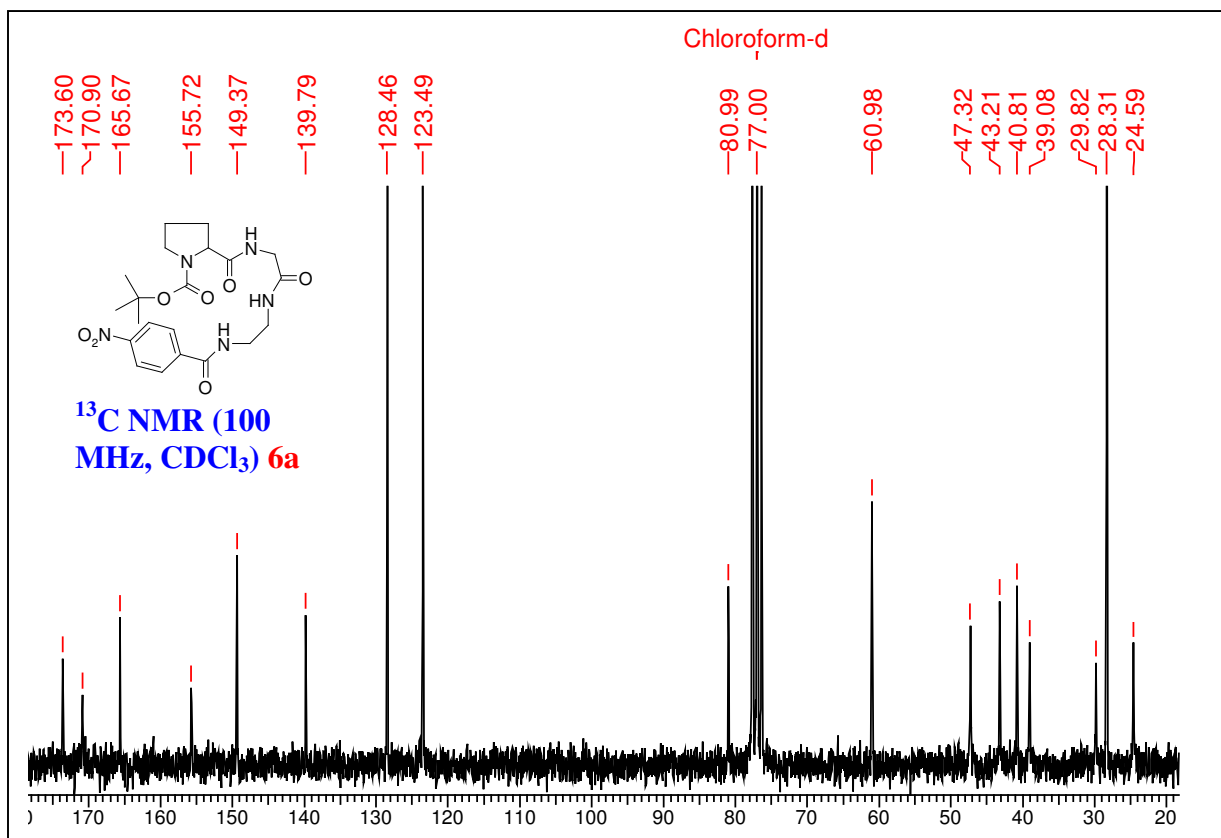
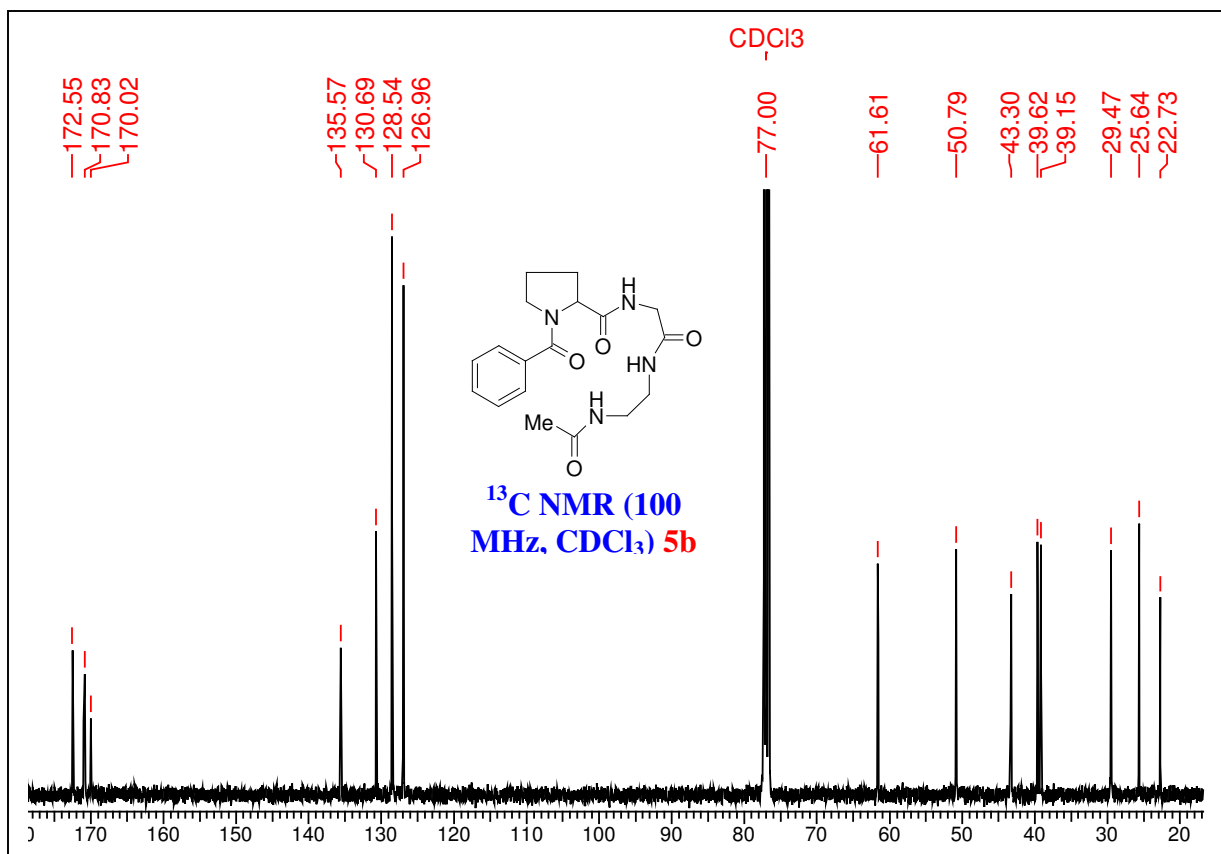


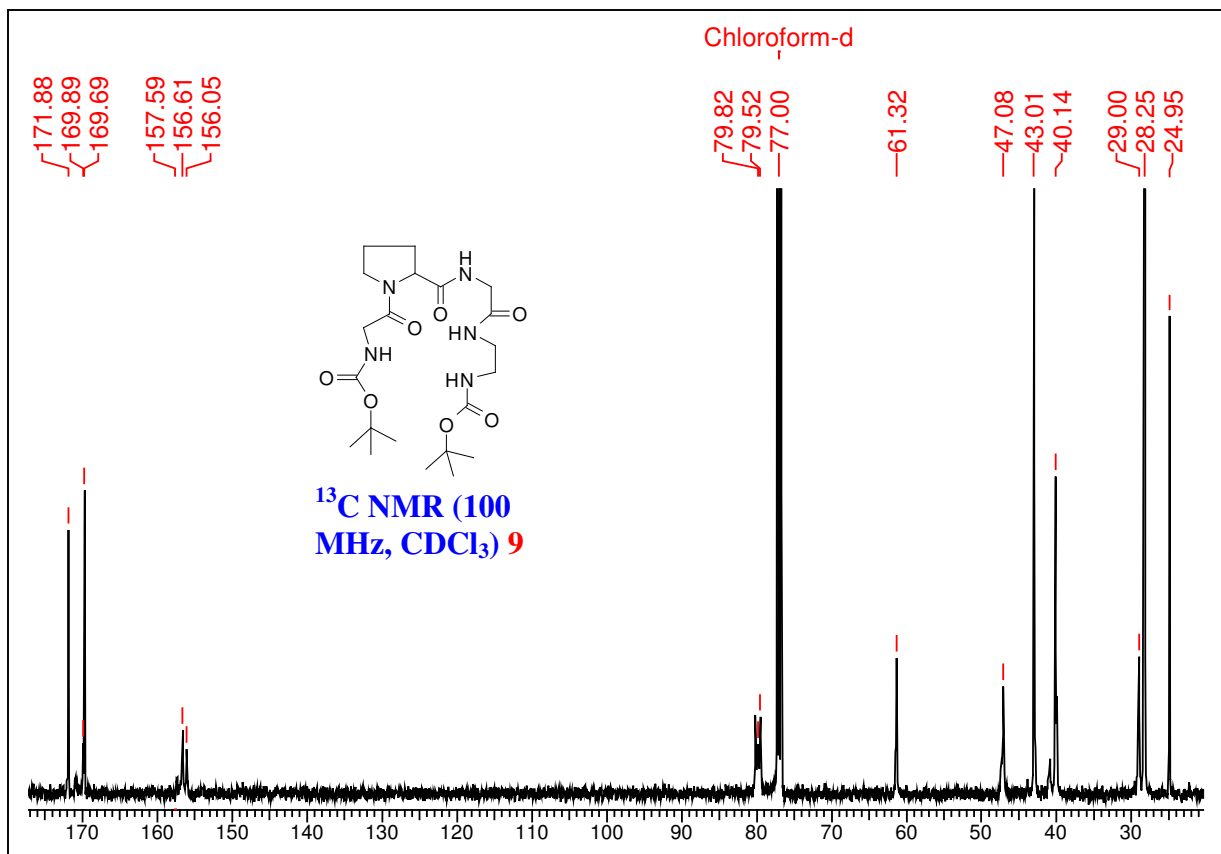
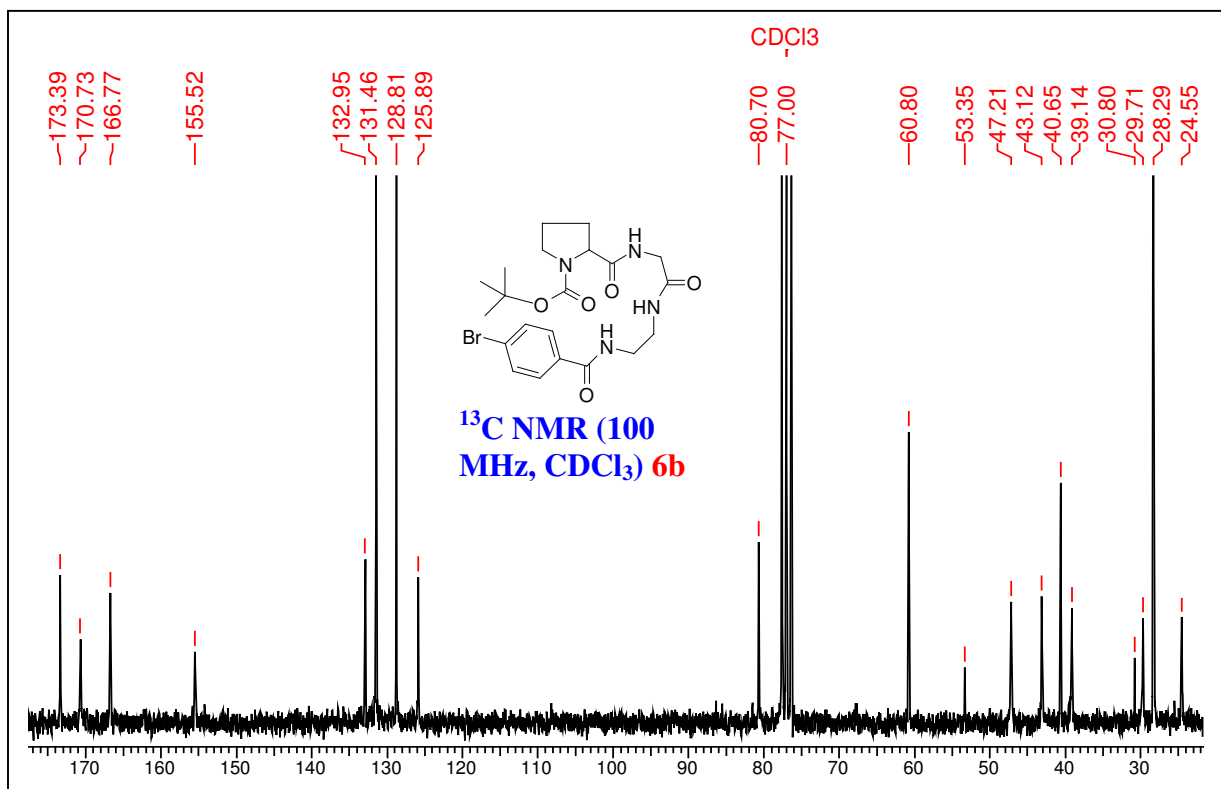












2.6 References and notes

(1) For reviews, see: (a) Jeffrey, G. A.; Saenger, W. *Hydrogen Bonding in Biological Structures*; Springer-Verlag: New York, 1991; (b) Synthesis of Peptides and Peptidomimetics. Murray Goodman (San Diego, CA). Georg Thieme Verlag: Stuttgart and New York. 2002; (c) Loughlin, W. A.; Tyndall, J. D. A.; Glenn, M. P.; Fairlie, D. P. *Chem. Rev.*, **2004**, *104*, 6085-6118; (d) Davis, J. M.; Tsou, L. K.; Hamilton, A. D. *Chem. Soc. Rev.*, **2007**, *36*, 326–334.

(2) Elia, V. D.; Zwickngal, H.; Reiser, O. *J. Org. Chem.* **2008**, 10.1021/jo800168h

(3) (a) Blank, J. T.; Guerin, D. J.; Miller, S. J. *Org. Lett.*, **2000**, *2*, 1247-1249; (b) Miller, S. J. *Acc. Chem. Res.*, **2004**, *37*, 601-610.

(4) For an excellent recent review see: Che, Y.; Marshall, G. R.; Expert Opinion on Therapeutic Targets, Volume 12, **2008**, pp. 101-114, and references cited therein.

(5) Chou, K. C. *Analytical Biochemistry.* **2000**, *286*, 1–16.

(6) (a) Fasman, G. D. In *Prediction of Protein Structure and the Principles of Protein Conformation.*, 1989, pp. 317–358. Plenum, New York; (b) Liu, W.; Chou, K. C.; *Protein Eng.*, **1999**, *12*, 1041–1050.

(7) Secondary structure mimetics based on diverse sugar scaffolds have been reported, see: (a) Smith, M. D.; Claridge, T. D. W.; Tranter, G. E.; Sansom, M. S. P.; Fleet, G. W. *J. Chem. Com.*, **1998**, 2041-2042; (b) Well, R. M. V.; Marinelli, L.; Altona, C.; Erkelens, K.; Siegal, G.; Raaij, M. V.; Saiz, A. L. L.; Kessler, H.; Novellino, E.; Lavecchia, A.; van Boom, J. H.; Overhand, M. *J. Am. Chem. Soc.*, **2003**, *125*, 10822-10829; (c) Sharma, G. V. M.; Ravinder Reddy, K.; Radha Krishna, P.; Ravi Sankar, A.; Jayaprakash, P.; Jagannadh, B.; Kunwar, A. C. *Angew. Chem. Int. Ed.*, **2004**, *43*, 3961 – 3965; (c)

Sharma, G. V. M.; Nagender, P.; Radha Krishna, P.; Jayaprakash, P.; Ramakrishna, K. V. S.; Kunwar, A. C. *Angew. Chem. Int. Ed.*, **2005**, *44*, 5878 – 5882; (d) Heller, M.; Sukopp, M.; Tsomaia, N.; John, M.; Mierke, D. F.; Reif, B.; Kessler, H. *J. Am. Chem. Soc.*, **2006**, *128*, 13806-13814; (e) Kothari, A.; Qureshi, M. K. N.; Beck, E. M.; Smith, M. D. *Chem. Com.*, **2007**, 2814-2816; (f) Chakraborty, T. K.; Arora, A.; Roy, S.; Kumar, N.; Maiti, S.; *J. Med. Chem.* **2007**, *50*, 5539-5542.

(8) (a) Nataraj, D. V.; Srinivasan, N.; Sowdhamini, R.; Ramakrishnan, C. *Current Science.*, **1995**, *69*, 434–447; (b) Pavone, V.; Geata, G.; Lombardi, A.; Natri, F.; Maglio, O.; Isernia, C.; Saviano, M. *Biopolymers.*, **1996**, *38*, 705–721; (c) Dasgupta, B.; Pal, L.; Basu, G.; Chakrabarti, P.; *Proteins: Structure, Function, and Bioinformatics.*, **2004**, *55*, 305-315.

(9) For theoretical methods of predicting α -turns in proteins, see: (a) H. Kaur, G. P. Raghava, *Structure, Function, and Bioinformatics.*, 2004, **55**, 83-90; (b) Wang, Y.; Xue, Z.; Xu, J.; *Structure, Function, and Bioinformatics.*, **2006**, *65*, 49-54.

(10) Prabakaran, P.; Gan, J.; Wu, Y. O.; Zhang, M. Y.; Dimitrov, D. S.; Ji, X. *J. Mol. Biol.*, **2006**, *357*, 82-99.

(11) Cavacini, L. A.; Stanfield, R. L.; Burton, D. R.; I. A. Wilson, I. A. *J. Mol. Biol.*, **2008**, *375*, 969-978.

(12) Hahin, R.; Chen, Z.; Wang, D.; Reddy, G.; L. Mao, L. *Cell Biochemistry and Biophysics.*, **2002**, *37*, 169-186.

(13) (a) Maji, S. K.; Haldar, D.; Bhattacharyya, D.; Banerjee, A. *J. Mol. Stru.*, **2003**, 111-123; (b) Shepherd, N. E.; Hoang, H. N.; Desai, V. S.; Letouze, E.; Young, P. R.; D. P. Fairlie, D. P. *J. Am. Chem. Soc.*, **2006**, *128*, 13284-13289; (c) Wang, D.; Chen, K.;

Dimartino, G.; Arora, P. S. *Org. Biomol. Chem.*, **2006**, *4*, 4074-4081; (d) Vasudev, G. P.; Ananda, K.; Chatterjee, S.; Aravinda, S.; Shamala, N.; Balaram, P. *J. Am. Chem. Soc.*, **2007**, *129*, 4039-4048.

(14) (a) Gallo, A. E; Gellman, S. H. *J. Am. Chem. Soc.* **1993**, *115*, 9774-9788; (b) Yang, J.; Gellman, S. H. *J. Am. Chem. Soc.* **1998**, *120*, 9090-9091; (c) Yang, J.; Christianson, A. L.; Gellman, S. H. *Org. Lett.* **1999**, *1*, 11-13; (d) Fisk, J. D.; Powell, D. R.; Gellman, S.H. *J. Am. Chem. Soc.* **2000**, *122*, 5443-5447; (e) Gellman, S. H.; Adams, B.R.; Dado, G. P. *J. Am. Chem. Soc.* **1990**, *112*, 460-461; (f) Haque, T. S.; Little, J. C.; Gellman, S. H. *J. Am. Chem. Soc.* **1996**, *118*, 6975-6985; (g) Langenhan, J. M.; Fisk, J. D.; Gellman, S. H. *Org. Lett.* **2001**, *3*, 2559-2562; (h) Liang, G. B.; Rito, C. J.; Gellman, S. H. *J. Am. Chem. Soc.* **1992**, *114*, 4440-4441; (i) Chakraborty, T. K.; Srinivasu, P.; Vengal Rao, R.; Kiran Kumar, S.; Kunwar, A. C. *J. Org. Chem.* **2002**, *67*, 2093-2100; (j) Krishna Prasad, K.; Purohit, C. S.; Jain, A.; Sankararama krishnan, R.; Verma, S. *Chem. Com.* **2005**, 2564-2566.

(15) Vass, E.; Hollo'csi, M.; Besson, F.; Buchet, R. *Chem. Rev.* **2003**, *103*, 1917-1954.

(16) for reviews, see: (a) Jeffrey, G. A.; Saenger, W. *Hydrogen Bonding in Biological Structures*; Springer-Verlag: New York, 1991; Chapter 2.2. (b) Aakero'y, C. B.; Seddon, K. R. *Chem. Soc. rev.* 1993, 397-407. (c) Bernstein, J.; Davis, R. E.; Shimoni, L.; Chang, N.-L. *Angew. Chem., Int. Ed. Engl.* **1995**, *34*, 1555-1573. (d) Steiner, T. *Angew. Chem., Int. Ed.* **2002**, *41*, 48-76.

(17) (a) Taylor, R.; Kennard, O.; Versichel, W. *J. Am. Chem. Soc.* **1984**, *106*, 244-248.

(b) Jeffery, G. A.; Mitra, J. *J. Am. Chem. Soc.* **1984**, *106*, 5546-5553.

(18) Auffinger, P.; Westhol, E. *J. Mol. Biol.* **1999**, *292*, 467-483.

- (19) (a) Nelson, H. C. M.; Finch, J. T.; Luisi, B. F. Klug, A. *Nature* **1987**, *330*, 221-226
(b) Taberero, L.; Bella, J.; Alema'n, C. *Nucleic Acids Res.* **1996**, *24*, 3458-3466.
- (20) (a) Sundaralingam, M.; Sekharudu, Y. C. *Science* **1989**, *244*, 1333-1337. (b) Prei'ner, R.; Egner, U.; Saenger, W. *FEBS Lett.* **1991**, *288*, 192-196.
- (21) (a) Askew, B.; Ballester, P.; Buhr, C.; Jeong, K. S.; Jones, S.; Parris, K.; Williams, K.; Rebek, J., Jr. *J. Am. Chem. Soc.* **1989**, *111*, 1082-1094. (b) Zimmerman, S. C.; Murray, T. J. *Tetrahedron Lett.* **1994**, *35*, 4077-4080.
- (22) Conn, M. M.; Rebek, J. *Chem. ReV.* **1997**, *97*, 1647.
- (23) (a) Gung, B.W.; Zhu, Z. *J. Org. Chem...* **1996**, *61*, 6482-6483; (a) Gung, B. W.; Zhu, Z. *Tetrahedron Lett.* **1996**, *37*, 2189.
- (24) Chakraborty, T. K.; Srinivasu, P.; Vengal Rao, R.; Kiran Kumar, S.; Kunwar, A. C. *J. Org. Chem.* **2004**, *69*, 7399-7402.
- (25) (a) Raghothama, S. R.; Awasthi, S. K.; Balaram, P. *J. Chem. Soc., Perkin Trans. 2* **1998**, 137-143; (b) Gil, A. M.; Bunuel, E.; Jimenez, A. I.; Cativiela, C. *Tetrahedron Letters.*, **2003**, *44*, 5999-6002.
- (26) Bodanszky, M; Bodanszky, A. *The Practice of Peptide Synthesis* 2nd Edition.
- (27) For leading references, see: (a) Gellman, S. H.; Dado, G. P.; Liang, G-B.; Adams, B. R. *J. Am. Chem. Soc.* **1991**, *113*, 1164-1173.; (b) Dado, G. P.; Gellman, S. H. *J. Am. Chem. Soc.* **1993**, *115*, 4228-4245; (c) Gardner, R.; Liang, G. B.; Gellman, S. H. *J. Am. Chem. Soc.*, **1999**, *121*, 1806.
- (28) (a) Baruah, P. K.; Gonnade, R.; Phalgune, U. D.; Sanjayan, G. J. *J. Org. Chem.*, **2005**, *70*, 6461-6467; (b) Prabhakaran, P.; Puranik, V. G.; Sanjayan, G. J. *J. Org. Chem.*, **2005**, *70*, 10067-10072.

(29) (a) Graether, S. P.; Kuiper, M. J.; Gagnes, S. M.; Walker, V. K.; Jia, Z.; Sykes, B. D.; Davies, P. L. *Nature*, **2000**, *406*, 325; (b) Harding, M. M.; Anderberg, P. I.; Haymet, A. D. J. *Eur. J. Biochem.* **2003**, *270*, 1381.

(30) The peptide bond preceding proline has relatively high probability of accommodating a *cis* configuration as compared to other peptide bonds, particularly in the absence of a compact conformation; see: (a) Dugave, C.; Demange, L.; *Chem. Rev.*, **2003**, *103*, 2475-2532; (b) Kang, Y. K.; Byun, B. J. *J. Phys. Chem., B* **2007**, *111*, 5377.

(31) Morris, G. A. in *Encyclopedia of Nuclear Magnetic Resonance*, ed. Grant, D. M.; Harris, R. K. John Wiley & Sons Ltd, Chichester, *Advances in NMR*, **2002**, *9*, pp. 35–44.

CHAPTER 3

Efficient synthesis and structural investigations of
BINOL-*m*-phenylenediamine-derived macrocycles

3. 1 Aromatic oligoamide foldamers: Overview and significance

Intense interest in constructing the foldamers,¹ with well defined secondary structures triggered the design and synthesis of large number of artificial systems,¹⁻⁴ such as aliphatic α -, β -, γ -, and δ -peptides,⁴⁻⁷ and single-stranded and multistranded abiotic oligomers.⁸ Foldamers as a class of conformationally ordered synthetic oligomers assume similarity to natural peptides. The challenges for folding synthetic oligomers include the ease of synthesis, folding stability, tunability, and the control of conformational changes under different environmental conditions that enable the molecules to adopt various secondary structures or to undergo host-guest complexation.⁹ Among the reported foldamer system aromatic oligoamides seem to be one class of promising candidates to satisfy many of these requirements and some of which have already displayed interesting activities.

Aromatic oligoamide foldamers possess a high potential for mimicking the secondary structures of biopolymers. These oligomers are efficiently designed, easy to synthesize, and allow one to reach a wide range of stable folded states. The aryl amide bond rotation can be restricted through specific attractive and repulsive interactions between the amide and the other functional groups at the *ortho* position on the aryl moiety. The overall conformation of an oligomer results from the simple linear combination of the local conformational preferences at each amide bond.

Synthetic foldamers, or oligomers that fold into well-defined conformations in solution, have been the object of great attention and very active research over the past ten years.¹⁰ Aromatic oligoamide foldamers were constructed based on anthranilic acids,¹¹ pyridines,¹² pyridine oxides,¹¹ pyrazines,¹³ and so on. A few less studied aromatic

oligomers were designed based on the ureas¹⁴ or hydrazides.¹⁵ β -sheet like structures¹⁶ and well-defined molecular duplexes,^{4,17} were developed based on the combination of both α -peptide backbone and aromatic rings with alkoxy substituents to form adjacent hydrogen bonding.¹⁶

Rotations about NHCO-aryl and CONH-aryl bonds are not as free as rotations about NHCO-alkyl and CONH-alkyl bonds, because of the conjugation between the amide and aromatic groups (figure 1). Energy minima are found in both the *syn* and *anti* conformations where aryl and amide groups are coplanar or close to coplanar.¹⁸

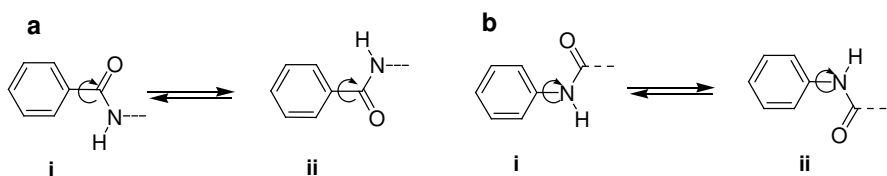


Figure 1: Rotation around (a) aryl-CONH bond and (b) aryl-NHCO bond

The stability of particular conformer e.g. *syn* or *anti* can be further increased by using specific attractive and repulsive interaction between the amide and other functional groups in the aryl moiety.

Intramolecular hydrogen bonding provides the most-simple, efficient, and reliable approach for this purpose.^{4a,3} figure-2 shows the typical intramolecular hydrogen-bonding patterns that have been used to restrict the rotation of the Ar-CONHAr bond in folding oligomers. The six- and five-membered rings formed by O \cdots H-N and N \cdots H-N hydrogen bonding (figure 2a–e) are well-established.^{11a,7d} Replacement of the OR (figure 2a) with an OH group lowers the stability of the conformation shown, because the OH proton can also form a six-membered hydrogen bond with the neighboring carbonyl oxygen atom. On the other hand, a phenoxide salt (figure 2d, M=K) was reported to form the expected

intramolecular hydrogen bonding that is used to induce the formation of ionic foldamers.¹⁹ It is well-established that fluoride ion is a strong proton acceptor. Covalently bound fluorine is considered a very weak hydrogen bond acceptor.²⁰ But Li *et al*²¹ has demonstrated that intramolecular F...H-N hydrogen bonding, as shown in figure 2f, can be readily formed.

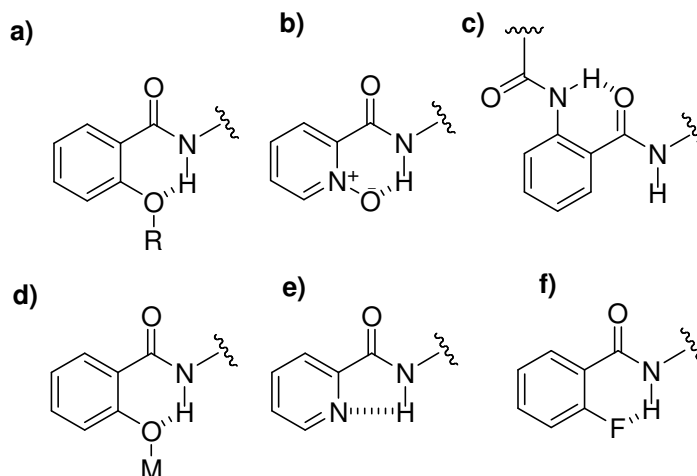


Figure 2: Typical example of intramolecular bond in aromatic units for restriction of Ar-CONHAr bond

Some representative examples of intramolecular hydrogen-bonding patterns in aromatic foldamers that restrict the rotation of the Ar-NHCOAr bond in foldamers are shown in figure 3.

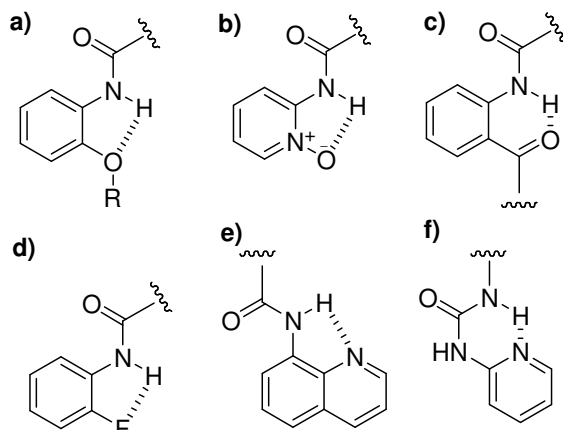


Figure 3: Typical example of intramolecular hydrogen bond in aromatic units for restriction of Ar-NHCOAr bond

These rotational restrictions are strong enough to design an aromatic oligomer with predictable conformation. This has been well demonstrated in the case of oligomers derived from pyridine diamines and pyridine carboxylic acid^{7c} or those derived from 4, 6-dimethoxy-3-amino-benzoic acid.¹⁷

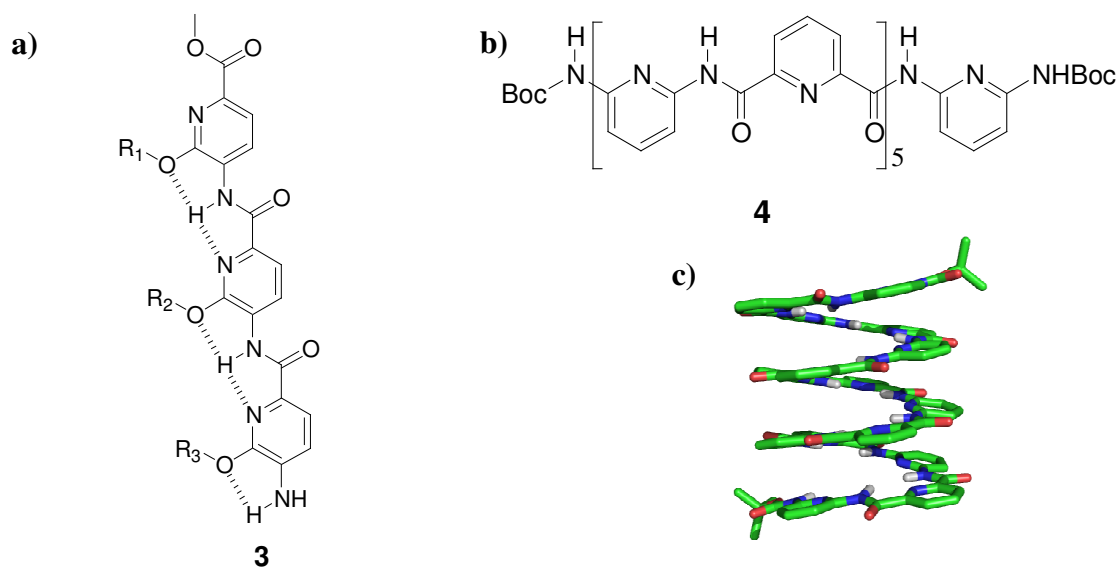


Figure 4: (a) Oligomers of 6-alkoxy-5-aminopicolinic acid adopting linear structure.^{7g} (b) Molecular structure of oligomer derived from 2,6-diaminopyridine and 2,6-pyridinedicarboxylic acid. (c) X-ray structure of **4** adopting helical structure.^{7c}

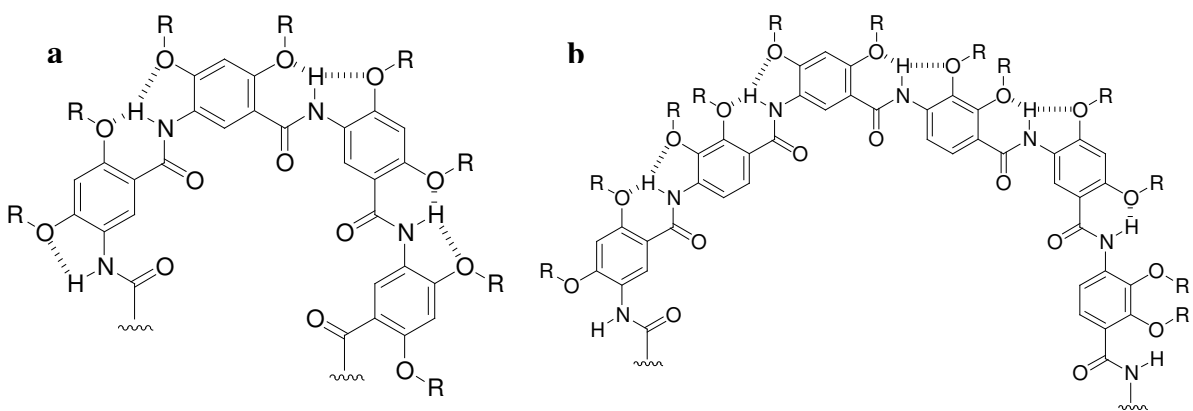


Figure 5: The diameter of the helical backbone can be easily tuned by changing the substituents¹⁷ in the monomeric building blocks; (a) backbone with *meta, meta, meta* sequence and (b) backbone with *meta, para, meta* sequence

3.2 Synthesis and characterization of the oligomers

The ease of synthesis of aromatic oligoamide foldamers is one of the attractive aspects of this field. Research groups have usually applied similar simple synthetic strategies. Although solid-supported synthesis of aromatic oligoamides has been reported²² a convergent solution-phase strategy is generally adopted. Carboxylic acids are activated as high yielding acid chlorides before couplings are performed. They are protected as esters, which can be easily saponified. Amines may be obtained from the reduction of nitro groups, or from the deprotection of simple carbamates (Fmoc, Cbz). A convergent segment-doubling strategy is generally adopted²³ where a dimer is obtained from two monomers, a tetramer from two dimers and so on. More than two blocks may also be assembled in one step as in a convergent dendrimer synthesis. For example, two oligomers bearing a free amine group may be coupled to a diacid chloride core.

The aromatic oligoamide foldamers usually crystallize easily. Therefore, the main technique of characterization is single-crystal X-ray diffraction. However, crystallinity often requires the absence of long alkyl chains and is not always compatible with high solubility, so structural studies in solution are often performed using NMR spectroscopy. The well-defined conformations give rise to sharp spectra, from which deshielding of hydrogen-bonded amide groups and/or shielding of aromatic protons involved in π - π stacking are easily observable. A detailed conformational analysis in solution using the NMR techniques developed for peptides cannot be used in every case because the spectra are not always easy to assign completely.

3.3 Macrocycles: An overview

The importance of conformational pre-organization in successful macrocyclization reactions has been recognized ever since Eschenmoser's synthesis of vitamin B12 and Woodward's synthesis of erythromycin. Different approaches to productive preorganization are possible depending on mainly on the degree of freedom in the choice of structural elements.

Inspired by prevalence of cyclic macro molecules in nature, including cyclic antibiotics, cyclodextrins and ionophores, chemists are interested in synthesizing macrocycles with preorganized binding sites and cavities large enough to complex organic or inorganic guest molecules.²⁴ Macrocycles are commonly synthesized by reactions of bifunctional monomers but the kinetic competition between macrocyclization and polymerization often plague synthetic yields.²⁴ To overcome these deleterious polymerization reactions, chemists use high-dilution and templating techniques.^{25,26} In some cases dynamic (reversible) covalent chemistry provides an attractive synthetic strategy to yield thermodynamically favored macrocyclic products.^{27,28} Directed conformational preorganization is a powerful approach for macrocyclization reactions.²⁹

Hunter *et al* developed a series of macrocycles and catenanes to evaluate the role of hydrogen bonding in macrocycle synthesis.³⁰ By taking the advantage of hydrogen bonding, macrocycles can be prepared from one step irreversible reactions without the need for external templates. For example, Gong and co-workers recently reported highly efficient, one-step macrocyclization reactions assisted by the folding and preorganization of precursor oligomers.³¹ Likewise, Huc and co-workers attribute the high yield obtained for the cyclization of oligoamide macrocycles to precursor preorganization.³²

The extraordinary importance of hydrogen-bonding interactions in determining the conformation of molecules is highlighted by the vast diversity of spatial arrangements adopted by peptides and proteins in which hydrogen bonding plays a crucial role. Their secondary structures are induced by a multitude of directional changes and folding patterns stabilized by hydrogen bonds across the chains, the so-called “turn units.”^{33,34} Obviously, hydrogen bonding has special importance in the context of the design of effective conformation directed macrocyclization reactions. Intramolecular hydrogen bonding can lead to one conformation being favored over another, thereby enabling or preventing the two cyclization sites to achieve productive proximity.

Conformationally constrained cyclic foldamers constructed from chiral building blocks represent an attractive class of macrocycles that may be exploited to create functional self-assembling systems through noncovalent interactions. Among the various methods developed for preparing macrocycles,³⁵⁻³⁷ one step, multicomponent cyclizations are particularly attractive because of the simplicity of the method and the easy availability of starting materials. Except for systems that involve reversible covalent bond formation, most one step cyclizations described thus far are complicated by the entropically disfavored nature of the process, which usually leads to numerous side products and low yields of the targeted macrocycles.

Shape-persistent macrocycles are structures with rigid noncollapsible backbones and lumens of various sizes. These structures are interesting because of their unique properties that differ from their linear analogues. However, examples of these molecules are rare mainly due to the difficulty of their preparation. Most of the shape-persistent macrocycles reported thus far have been based on the oligo (*meta*-phenylene ethylene)

backbone or its analogues. Similar to other one step cyclizations, one step synthesis led to very low yields of the *m*-PE cyclic hexamer.

3.3.1 Macrocycles- A Short History

Bing Gong *et al*³¹ reported the highly efficient formation of a new class of shape-persistent, cyclic hexa (aramides) from one-step macrocyclization of monomeric building blocks. Because of the three-center intramolecular hydrogen bond consisting of the S (5) and S (6) type, the corresponding oligoamides form shape-persistent macrocycles (figure 6).

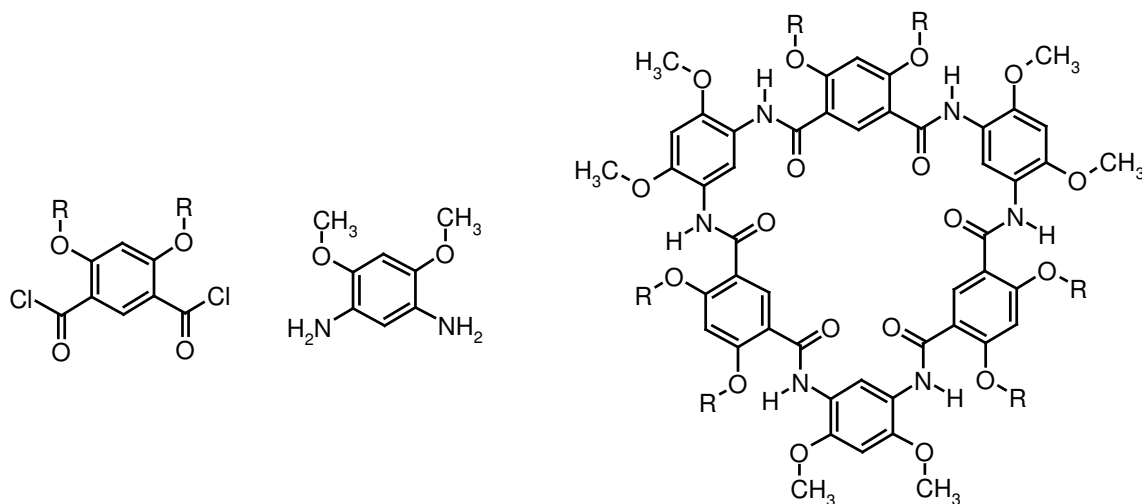


Figure 6: Pre-organized oligoarylamide macrocycles³¹

Bing Gong *et al*³⁸ described aromatic oligourea that are forced into well-defined conformation by incorporating intramolecular hydrogen bonds. Shape-persistent tetra urea macrocycles were obtained in a one-step [2+2] reaction in good yield (figure 7).

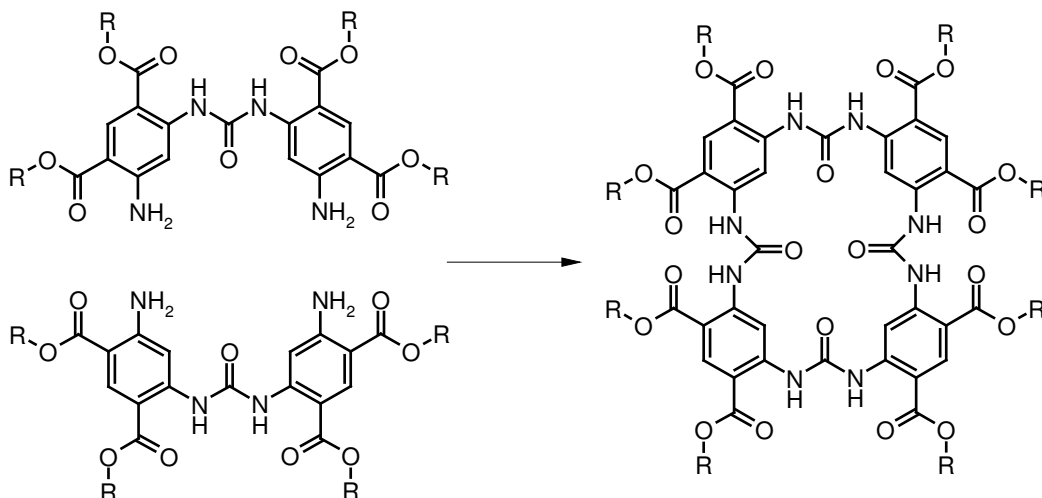


Figure 7: Aromatic oligourea macrocycles³⁸

Cuccia *et al*³⁹ reported one-step synthesis of pyridazine and naphthyridine containing macrocycles directed by intramolecular hydrogen-bonding (figure 8). The naphthyridine moieties are connected via urea or formamidine linkages, and the pyridazine moieties are connected either by tolyl or phenyl groups *via* urea linkages.

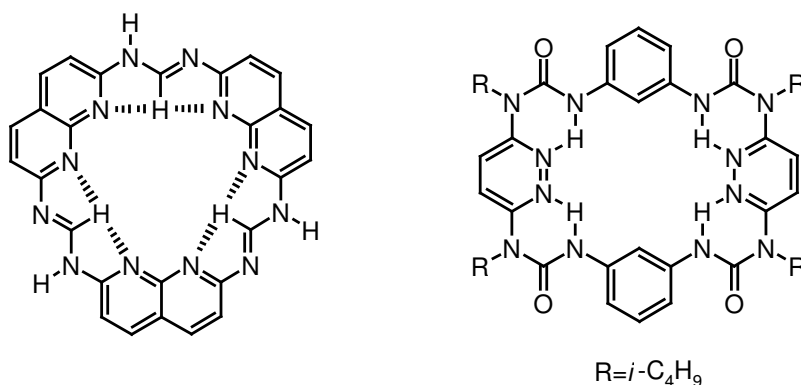


Figure 8: Pyridazine and naphthyridine pre-organized macrocycles³⁹

Ivan Huc *et al*³² described macrocyclic saddle-shaped bifunctional clip molecule that self-assembles into discrete circular dodecamers in the solid state and shows potential for binding aromatic acid guests in solution.

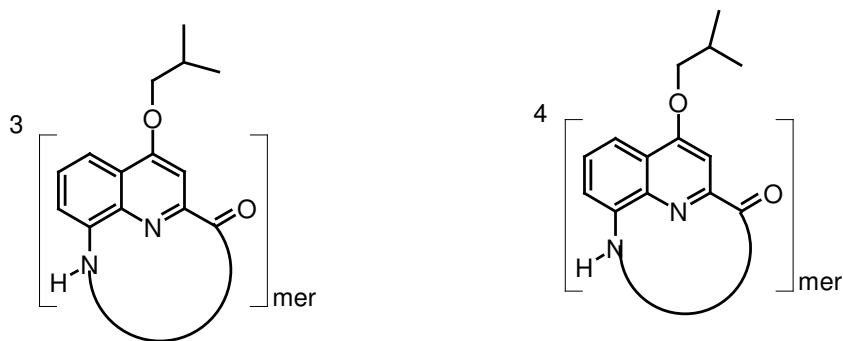


Figure 9: Quinoline based macrocycles³²

8-amino-2-quinolinecarboxylic acid upon polymerization afforded cyclic trimer and cyclic tetramer in moderate yield (figure 9). The cyclic tetramer has potential for binding aromatic acid guest molecules.

3.4 Present work

In this chapter we describe a serendipitous discovery of an efficient synthetic route to BINOL-*m*-phenylenediamine and 2, 6 diamino pyridine derived macrocycles. These macrocycles are quickly accessible in a one-pot procedure by the direct condensation of (R) and (S) BINOL bis-acids with suitably substituted *m*-phenylenediamine analogs. Structural investigations by single crystal X-ray crystallography and solution-state NMR studies provided convincing evidence of their intramolecular hydrogen bonding arrangement and rigid structural architecture. The striking feature of these macrocycles is their ready accessibility in optically pure form coupled with their ease of synthesis.

Encouraged by the dazzling foldamer structural architectures (figure10),⁴⁰ obtained from the hybrid sequences derived from optically pure BINOL and 2,6-diamino

pyridine residues as subunits, we set out to generate larger oligomers derived from similar building blocks, but without protecting the terminal amino groups during synthesis, contrary to the ^tBOC protecting strategy we adopted earlier.⁴⁰

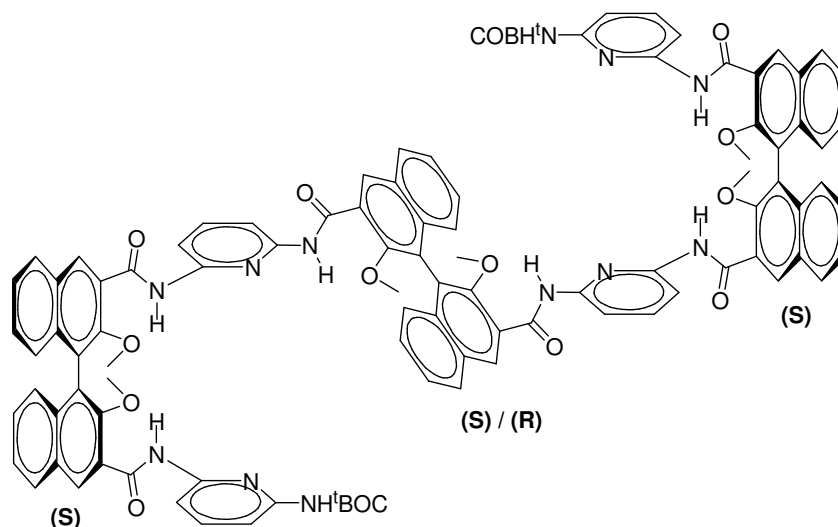


Figure 10: Hybrid foldamer of BINOL-2, 6-diamino pyridine units⁴⁰

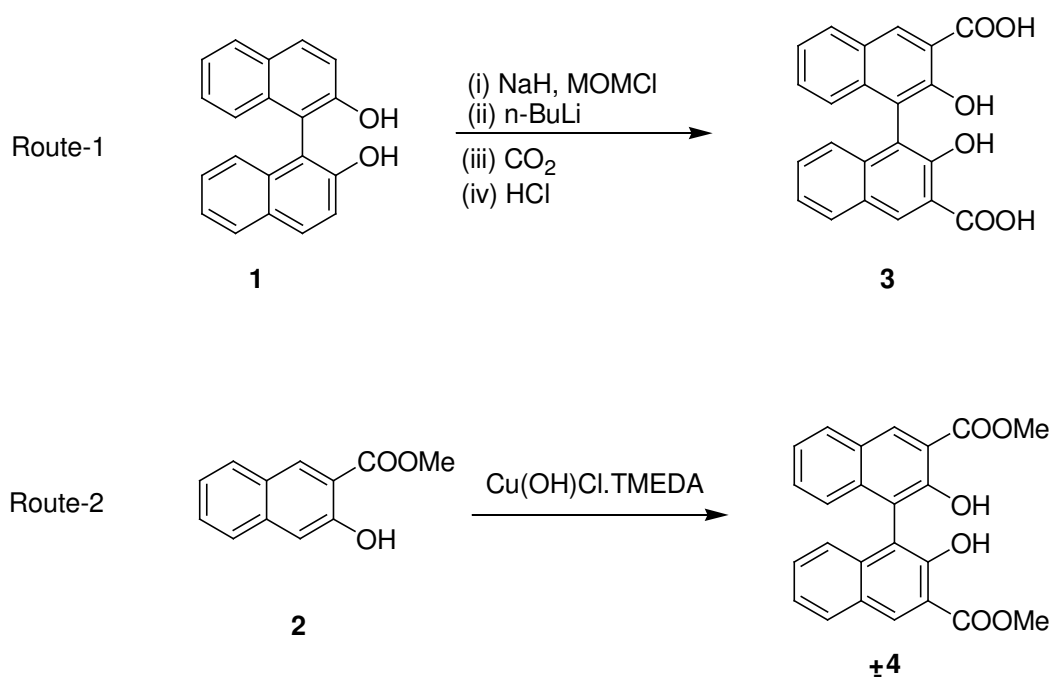
The research work from the laboratories of Lehn^{12b} and Huc^{41,42} have shown that synthetic oligomers of considerable size can be readily obtained by segment doubling strategy without resorting to the protection of the terminal amino groups of the building blocks. 2-methoxy-5-methyl-benzene-1,3-diamine, a *m*-phenylene diamine analog, having similar H-bonding directional effect as that of 2,6-diamino pyridine was chosen due to its improved nucleophilicity as compared to its pyridine analog.

3.4.1 Synthesis

The monomeric building block **3** can in principle be accessed by two routes as shown in scheme **1**. The protection of hydroxyl group of commercially available optically pure BINOL **1** by methoxymethyl chloride, *ortho* lithiation with *n*-butyllithium followed by carboxylation and acidification affords compound **3**.⁴³ Alternatively compound **4**,

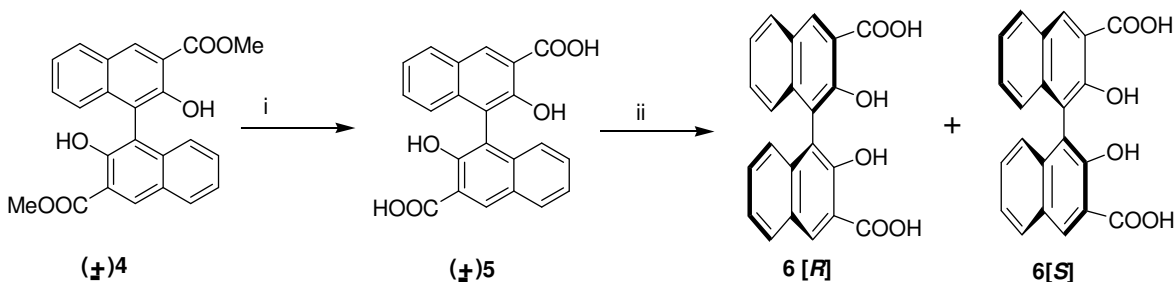
dimethyl ester of 3, 3- dicarboxylic acid, can be obtained in a single step by oxidative coupling⁴⁴ of methyl ester of 3-hydroxy-2-naphthoic acid **2** using Cu(OH)Cl.TMEDA as a catalyst in multigram scale. We chose the second route as it does not involve use of pyrophoric reagents like sodium hydride, n-butyllithium, etc. and can be scaled up very easily.

Scheme 1



The racemic BINOL ester **4**, obtained by the oxidative coupling of methyl ester of 3-hydroxy-2-naphthoic acid **2**, was saponified to furnish the BINOL bis-acid **5**, which was subjected to kinetic resolution⁴⁵ using leucine methyl ester as the base to afford both [*R*] and [*S*] antipodes of **6** (scheme 2).

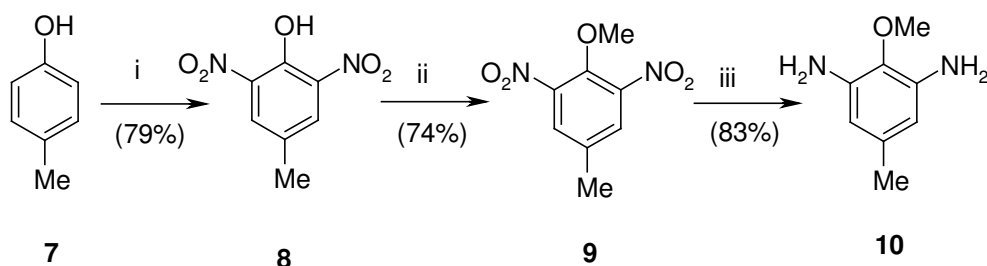
Scheme 2



Reagents and conditions: (i) KOH, MeOH, reflux, 2h; (ii) leucine methyl ester (resolution)⁴⁵

The *m*-phenylenediamine derivative **10** was prepared in three steps. The synthesis started with commercially available 4-methyl phenol. Compound **7** upon nitration furnished the dinitro compound **8**. The compound **9** was made by treatment of **8** with dimethylsulphate and potassium carbonate in acetone. Hydrogenation of **9** in the presence of palladium charcoal under hydrogen atmosphere, afforded *m*-phenylenediamine derivative **10** in good yield (scheme 3).

Scheme 3



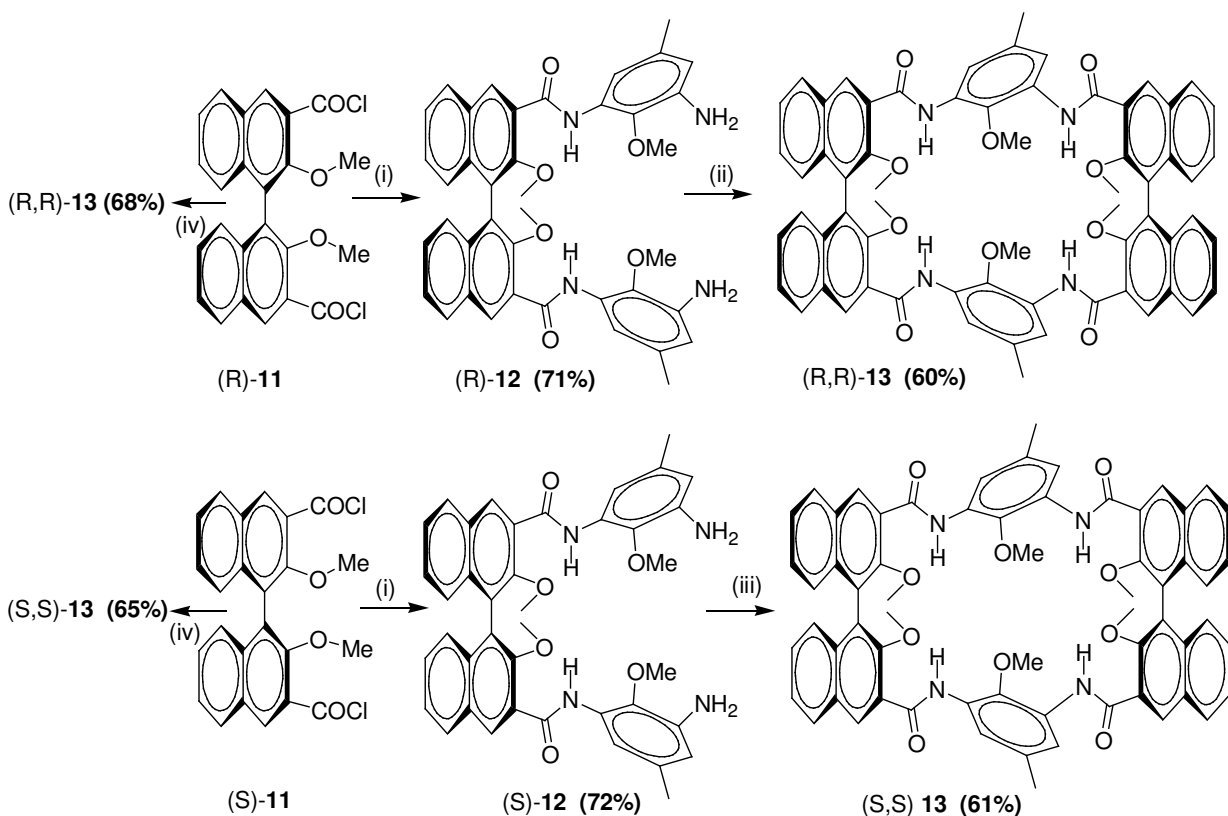
Reagents and conditions: (i) nitric acid, sulphuric acid, dichloromethane, rt, 5h; (ii) dimethyl sulphate, K₂CO₃, acetone, rt, 8h; (iii) 10% Pd/C, methanol, rt, 12h.

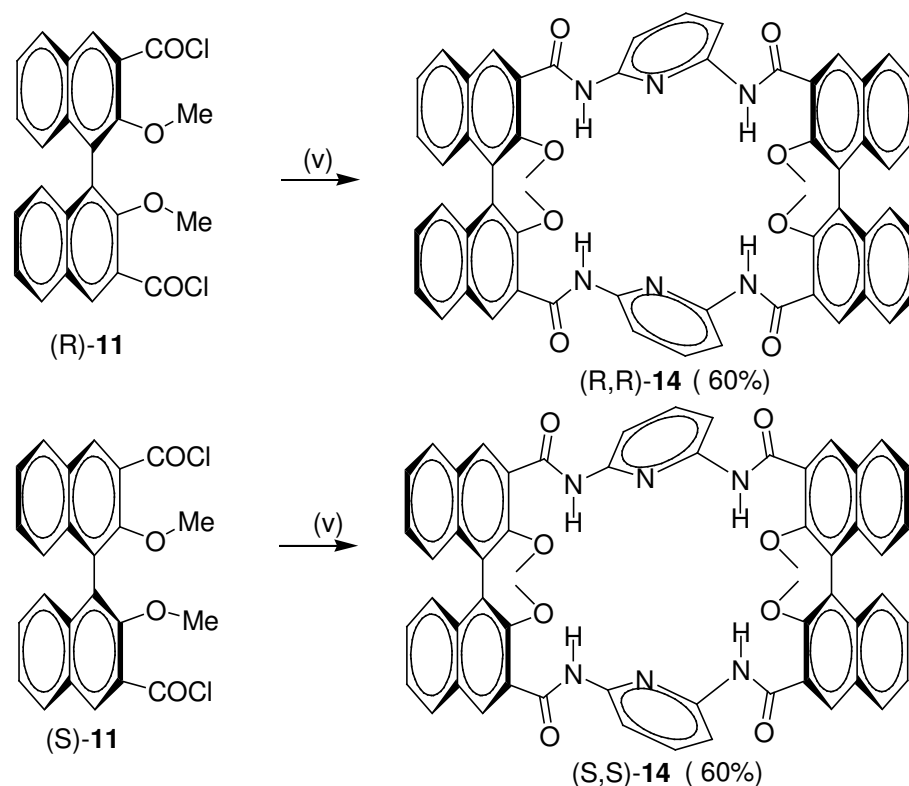
In accordance with our plan for linear oligomer synthesis, we first synthesized the diamine precursor **12**, both enantiomers **12(R)** and **12(S)**, by reacting excess *m*-

phenylenediamine with optically pure BINOL bis-acid chloride (scheme 4). Iteration of the same sequence, however, gave an unexpected result, which was extensively investigated further.

Instead of furnishing a longer oligomer, as we anticipated, this reaction afforded a cyclic product **13**, despite the fact that excess of amine **12** was used for the linear oligomerization. Interestingly, an one-pot reaction of 2-methoxy-5-methyl-benzene-1,3-diamine **10** with BINOL acid chloride **11**⁴⁰ also furnished the same macrocycle in good yield, without much difficulty of isolation. After this interesting observation we carried out one-pot reaction of 2, 6 dimaino pyridine and BINOL acid chloride **11**,⁴⁰ where we obtained macrocycles (R,R)-**14**, (S,S)-**14** in good yield.

Scheme4





Reagents and conditions: (i) 2-Methoxy-5-methyl-benzene-1, 3-diamine (5 equiv.), (R)-11 / (S)-11 (1 equiv.), Et₃N, dry dichloromethane, rt, 6 h; (ii) (R)-12, (3 equiv.), (R)-11 (1 equiv.), Et₃N, dry dichloromethane, rt, 12 h; (iii) (S)-12, (3 equiv.), (S)-11 (1 equiv.), Et₃N, dry dichloromethane, rt, 12 h; (iv) 2-Methoxy-5-methyl-benzene-1, 3-diamine (1 equiv.), (R)-11 / (S)-11 (1 equiv.), Et₃N, dry dichloromethane, rt, 12 h. (v) 2,6 diamino pyridine, (1.2 equiv.), (R)-11 / (S)-11 (1 equiv.), Et₃N, dry dichloromethane, rt, 6 h.

3.4.2 Results and discussions

The exclusive formation of the macrocycles **13** and **14** is presumably due to the combined effect of the conformational restrictions of the residues (BINOL, *m*-phenylenediamine and diamino pyridine units) coupled with the intramolecular hydrogen bonding in their coupled intermediates that preorganize the structural architectures for macrocyclization. Indeed recent years have witnessed a multitude of reports that reveal such preorganization-mediated macrocyclizations.⁴⁶⁻⁴⁹

In order to gain insights into the structural features of the macrocycles **13**, **14**, studies were undertaken in solid- and solution-state by single crystal X-ray crystallography, and NMR spectroscopy, respectively. Extensive efforts to crystallize the macrocycles **13**, **14** gave fruitful results eventually. Good quality crystals macrocycles **13**, and **14** could be grown from a solvent mixture comprising dichloromethane: methanol (40:60) and acetonitrile: methanol (35:65) respectively.

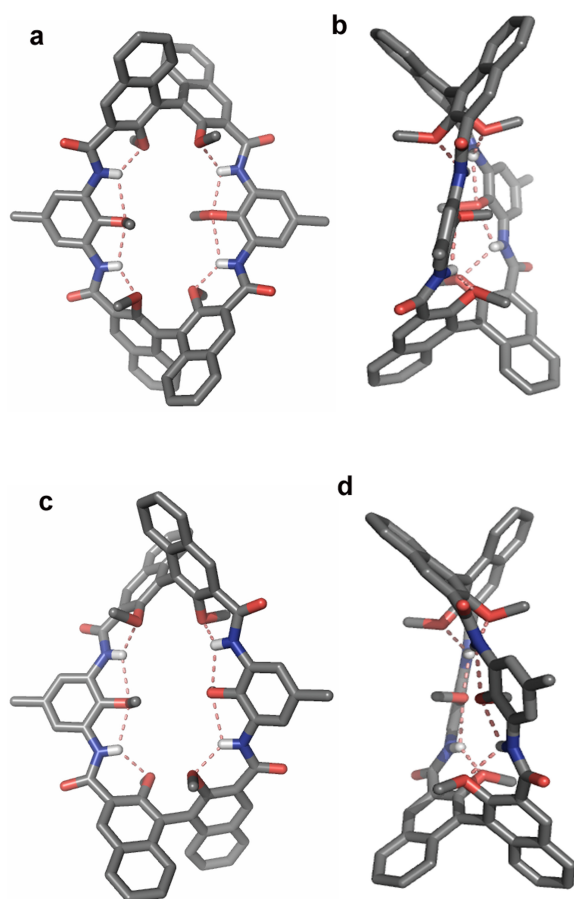


Figure 11: Various views of the crystal structures of macrocycles **13**. (a,b,c,d): Single crystal structures of macrocycle (R,R)-**13** displayed in two different orientations (a,b), and single crystal structures of macrocycle (S,S)-**13** displayed in two different orientations (c,d). *Note:* Comparison of the crystal structures of the macrocycle (R,R)-**13** and (S,S)-**13** reveals their mirror image structural architecture. Hydrogens, other than at the hydrogen bonding sites, have been deleted for clarity.

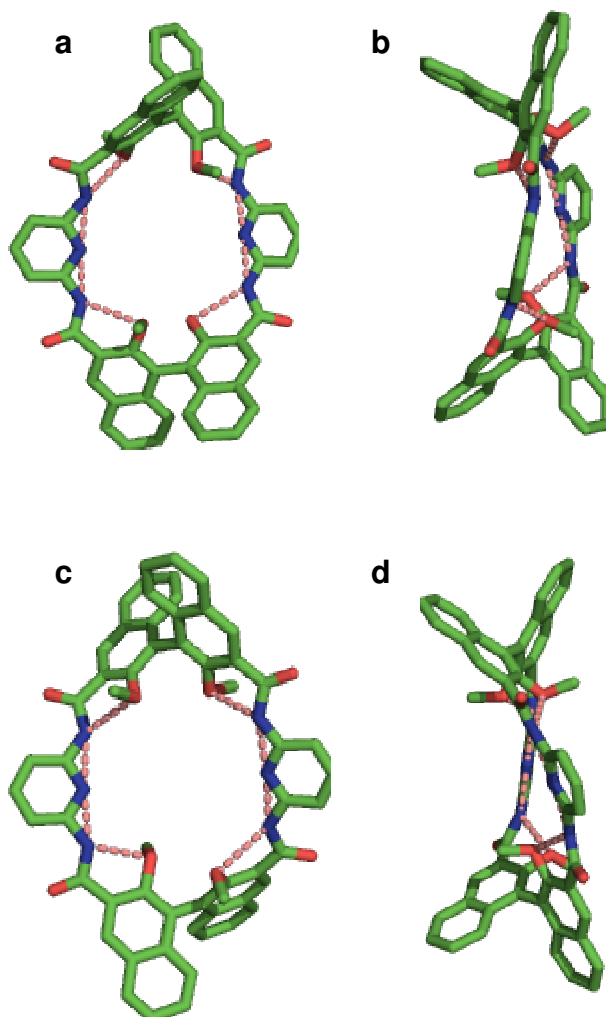


Figure 12: Various views of the crystal structures of macrocycles **14**. (a,b,c,d): Single crystal structures of macrocycle (R,R)-**14** displayed in two different orientations (a,b) and single crystal structures of macrocycle (S,S)-**14** displayed in two different orientations (c,d). *Note:* Comparison of the crystal structures of the macrocycle (R,R)-**14** and (S,S)-**14** reveals their mirror image structural architecture. Hydrogens, other than at the hydrogen bonding sites, have been deleted for clarity.

Analysis of the crystal data of macrocycles **13** and **14** revealed that the amide protons are tightly held by extensive intramolecular bifurcated hydrogen bonding interactions.⁵⁰ In the macrocycle **13**, the aryl amide protons are flanked from both sides

by the alkoxy oxygen's from the adjacent *m*-phenylenediamine and BINOL residues. The aryl amide protons of macrocycle **14** are tightly held between alkoxy group of BINOL and N of the pyridyl moiety, giving these macrocycles a robust structural architecture. Further, the periplanar arrangement of the naphthyl rings in the BINOL rings are clearly observed, which is in agreement with the crystal structures of the common BINOL derivatives.⁵¹ A closer comparison of the crystal structures [(R,R)-**13** vs (S,S)-**13**] and [(R,R)-**14** vs (S,S)-**14**] further reveals their mirror image structural architecture.

3.4.3 NMR studies of the Macrocycles

The macrocycles [(R,R)-**13**, (S,S)-**13**] and [(R,R)-**14** vs (S,S)-**14**] were highly soluble in nonpolar organic solvents (>>100 mM in chloroform) at ambient temperature. This observation suggested that the polar hydrogen-bonding groups of **13** and **14** were strongly protected (solvent shielded) by intramolecular hydrogen bonding, preventing the formation of polymeric hydrogen-bonded aggregates.^{52,53} To confirm that intramolecular hydrogen bonds are clearly prevalent in solution, we also performed [D₆]DMSO titration study of (S,S)-**13** (figure 13). The NH signal that appears at downfield region (10.10 ppm) suggests its involvement in strong hydrogen bonding interactions. Indeed, the NH proton shows little shift when solutions of (S,S)-**13** are titrated gradually with [D₆]DMSO ($\Delta\delta \sim 0.01$ ppm) suggesting their strong involvement in intramolecular hydrogen bonding.

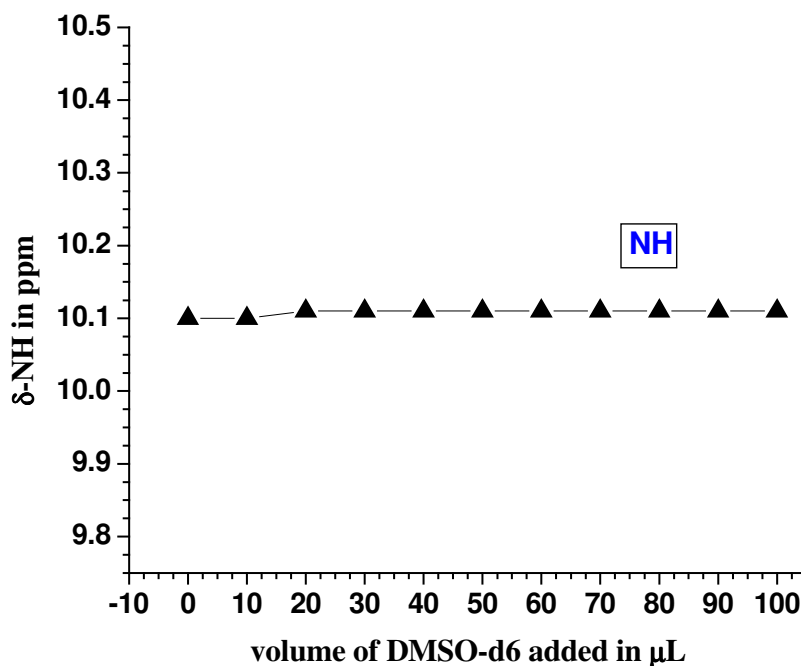


Figure 13: $[D_6]$ DMSO titration graph of the Macrocycle (S,S)-**13**. The initial concentration of the sample in $CDCl_3$ was 16.0 mM, and the total amount of $[D_6]$ DMSO used was 16.8.% of the total volume.

1H and ^{13}C NMR (500 and 125 MHz, respectively) spectra of the macrocycles (R,R)-**13**, (S,S)-**13** and (R,R)-**14**, (S,S)-**14** in $CDCl_3$ showed single set of well-resolved signals⁵⁴ suggesting the existence of a single conformation in solution state at ambient environments. In order to provide insights into the conformational features of these macrocycles, 2D NOESY studies were undertaken (figure 14 and 15).

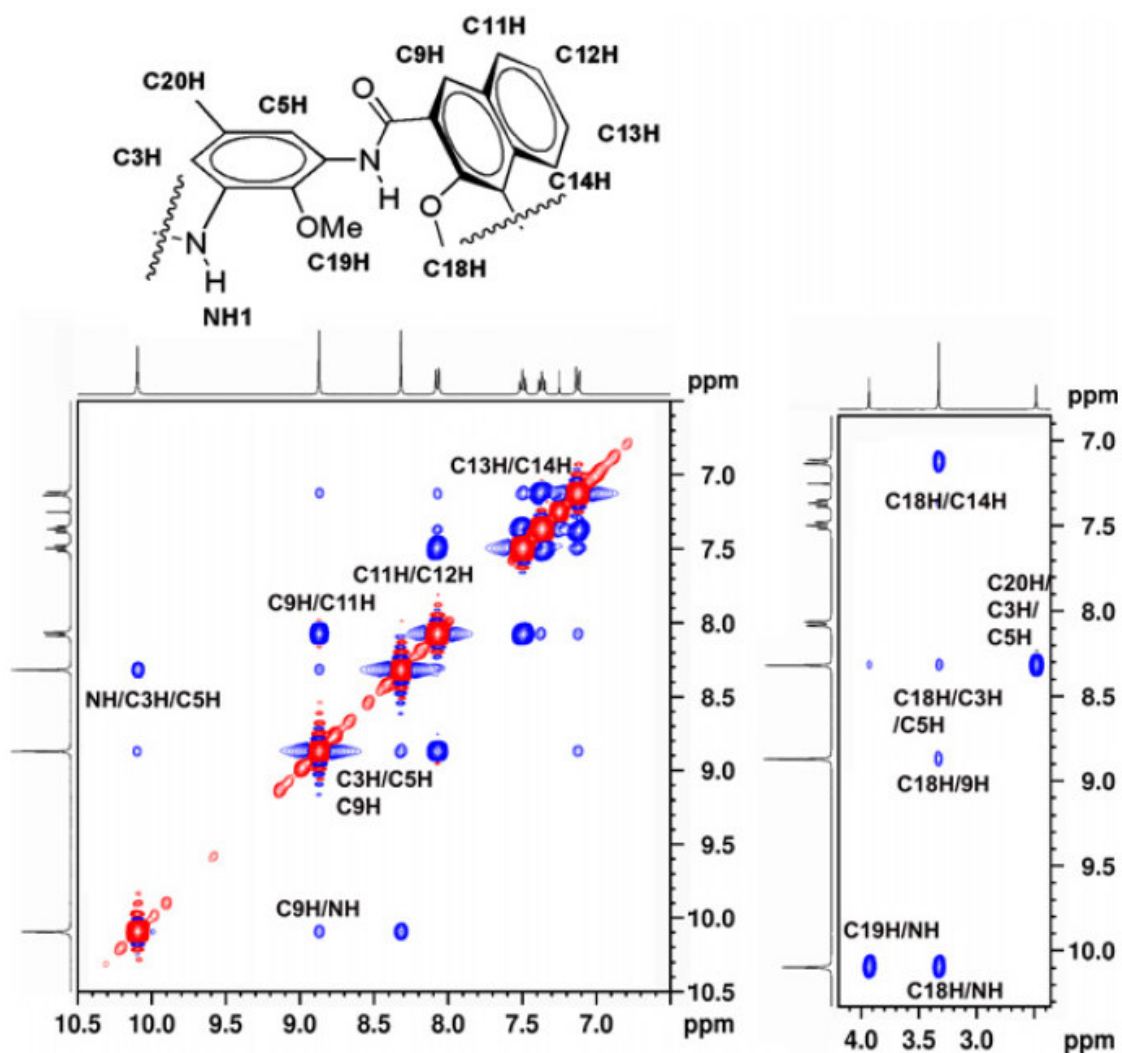


Figure 14: Partial 2D NOESY NMR spectra of (S,S)-**13** (CDCl₃, 500 MHz)

The observed dipolar couplings (nOes) strongly support the bifurcated hydrogen bonding interaction, as seen in their crystal structures in the solid-state (figure 14). One of the most characteristic nOes that would clearly indicate the synchronized (S-5)- and (S-6)-type⁵⁰ bifurcated hydrogen bonding interactions, as observed in the solid-state, would be the requirement of dipolar couplings of both the alkoxy substituents with the NH group that participates in such interactions.^{40,55} Analysis of the 2D data set of (S, S)-**13**

clearly reveals that such an interaction (C19H/NH; C18H/NH; figure 14) is prevalent that clearly confirms the bifurcated H-bonding arrangement in solution-state as well.

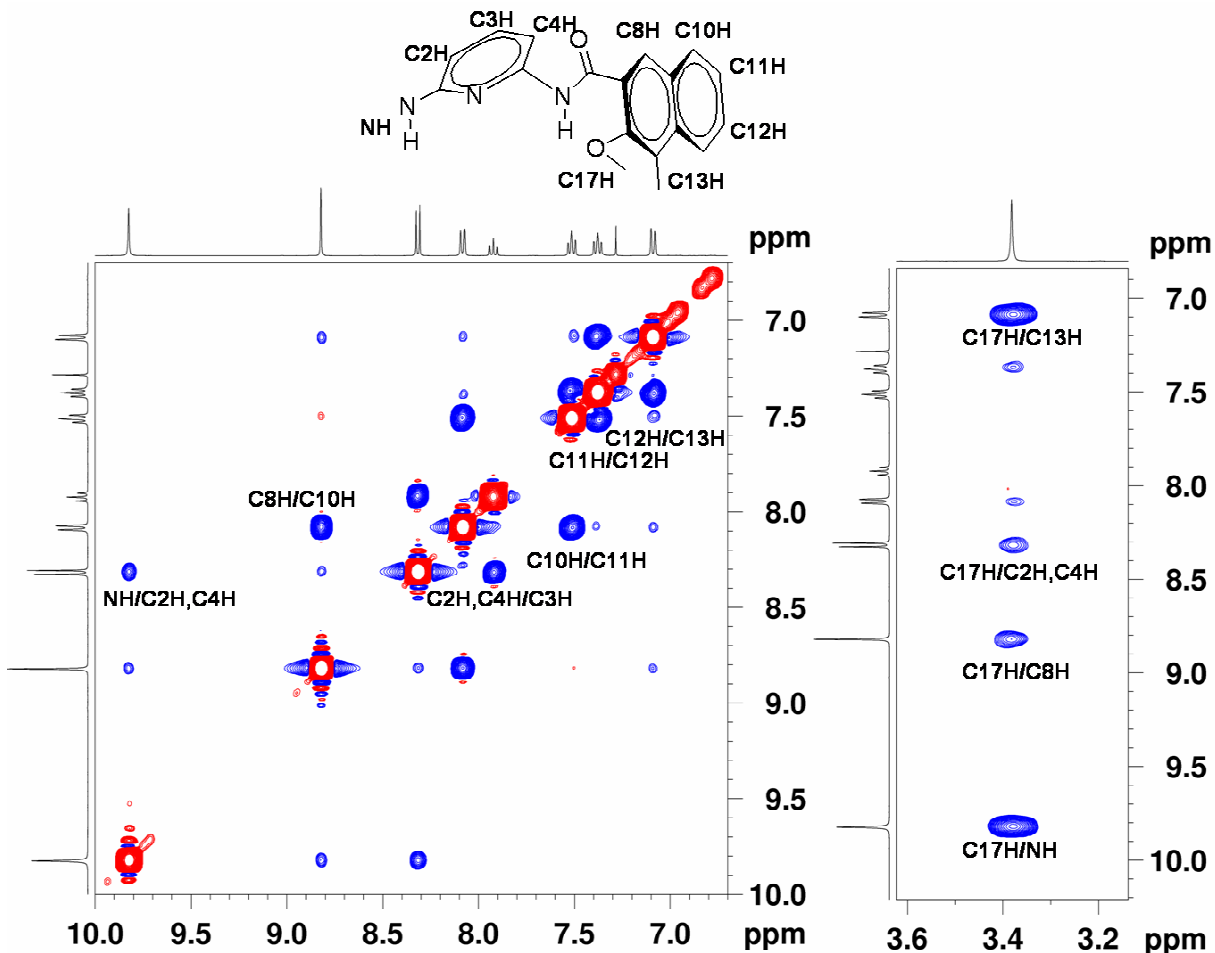


Figure 15: Partial 2D NOESY NMR spectra of (R,R)-**14** (CDCl₃, 500 MHz)

Analysis of the 2D data of (R,R)-**14** (CDCl₃, 500 MHz) (figure 15) clearly indicates that the observed dipolar couplings (nOes) strongly support the bifurcated hydrogen bonding interaction, as seen in their crystal structures in the solid-state. One of the most characteristic nOes that would clearly indicate the synchronized bifurcated hydrogen bonding interactions, as observed in the solid-state, would be the requirement of dipolar couplings of the alkoxy substituents and C2H, C4H of the pyridyl moiety

with the NH group that participates in such interactions.^{40,55} Analysis of the 2D data set of (R,R)-**14** clearly reveals that such an interaction (C17H/NH; C2H,C4H/NH; figure 15) is prevalent that clearly confirms the bifurcated H-bonding arrangement in solution-state as well.

3.4.4 Attempted synthesis of large hybrid oligomers (R) –17

Since our earlier strategy of objective away with N-protecting groups did not furnish the anticipated linear oligomers, we reverted back to the strategy of using N-protecting groups. Unfortunately, herein too, we met with failures, and the oligomer **R-**(**17**) could not be obtained, presumably because of steric reasons. (close proximity of the termini).

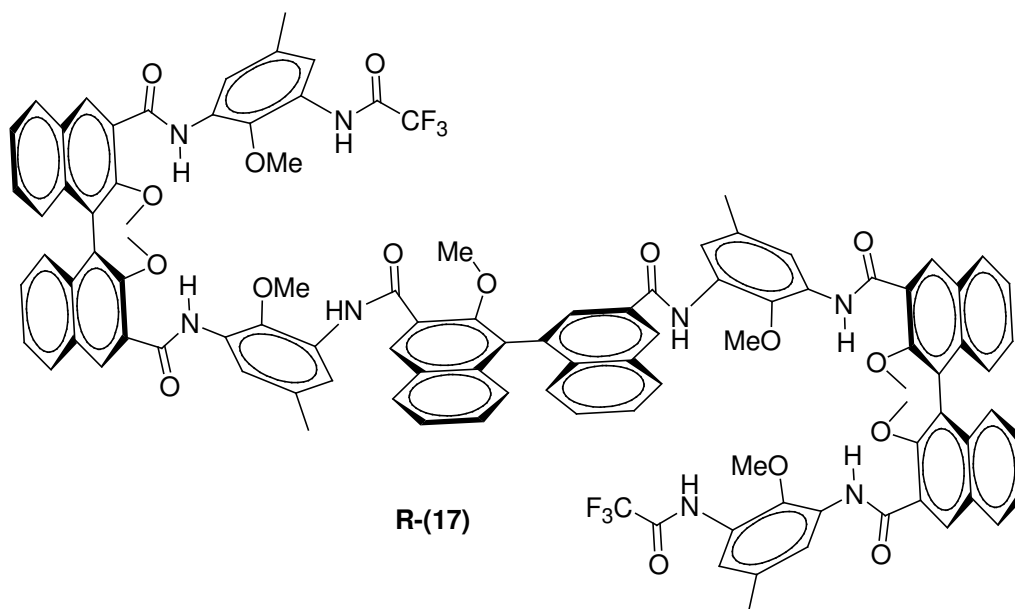
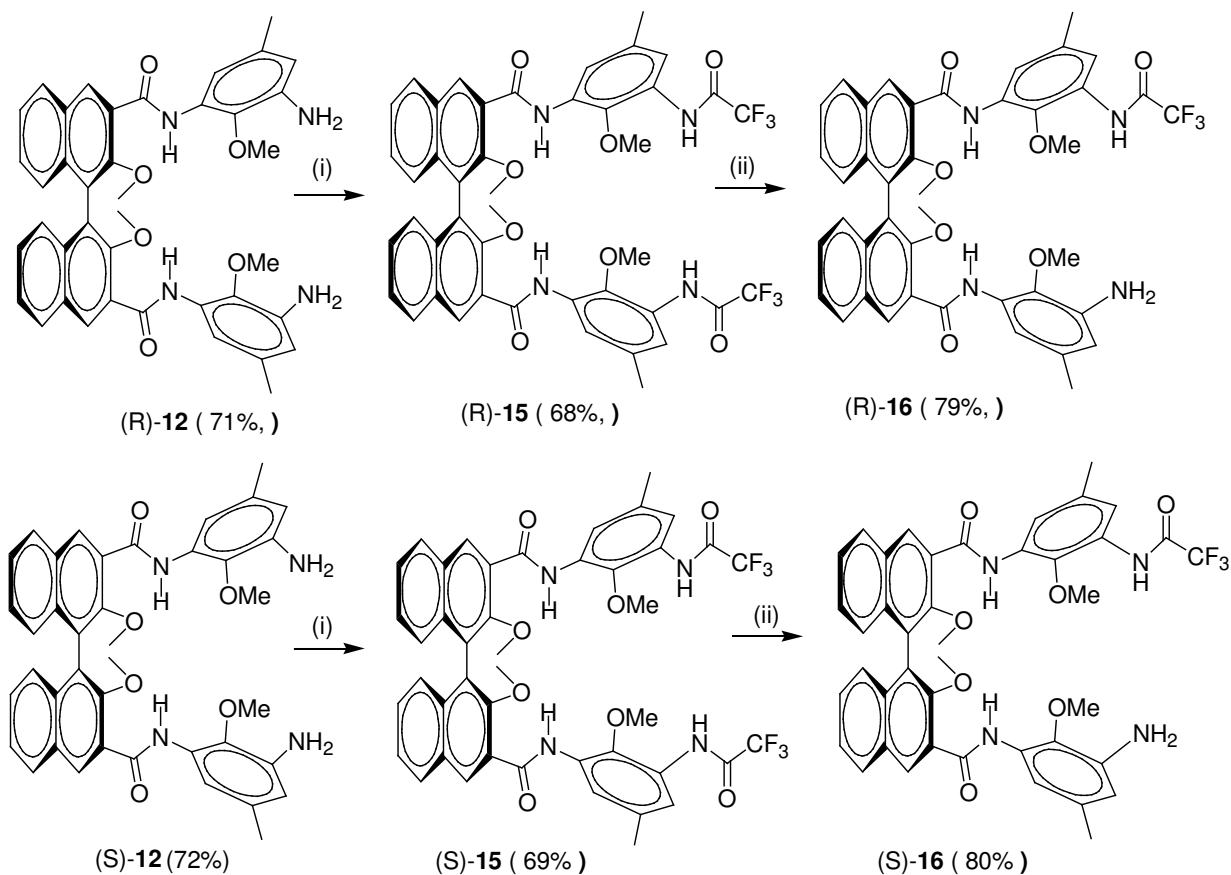


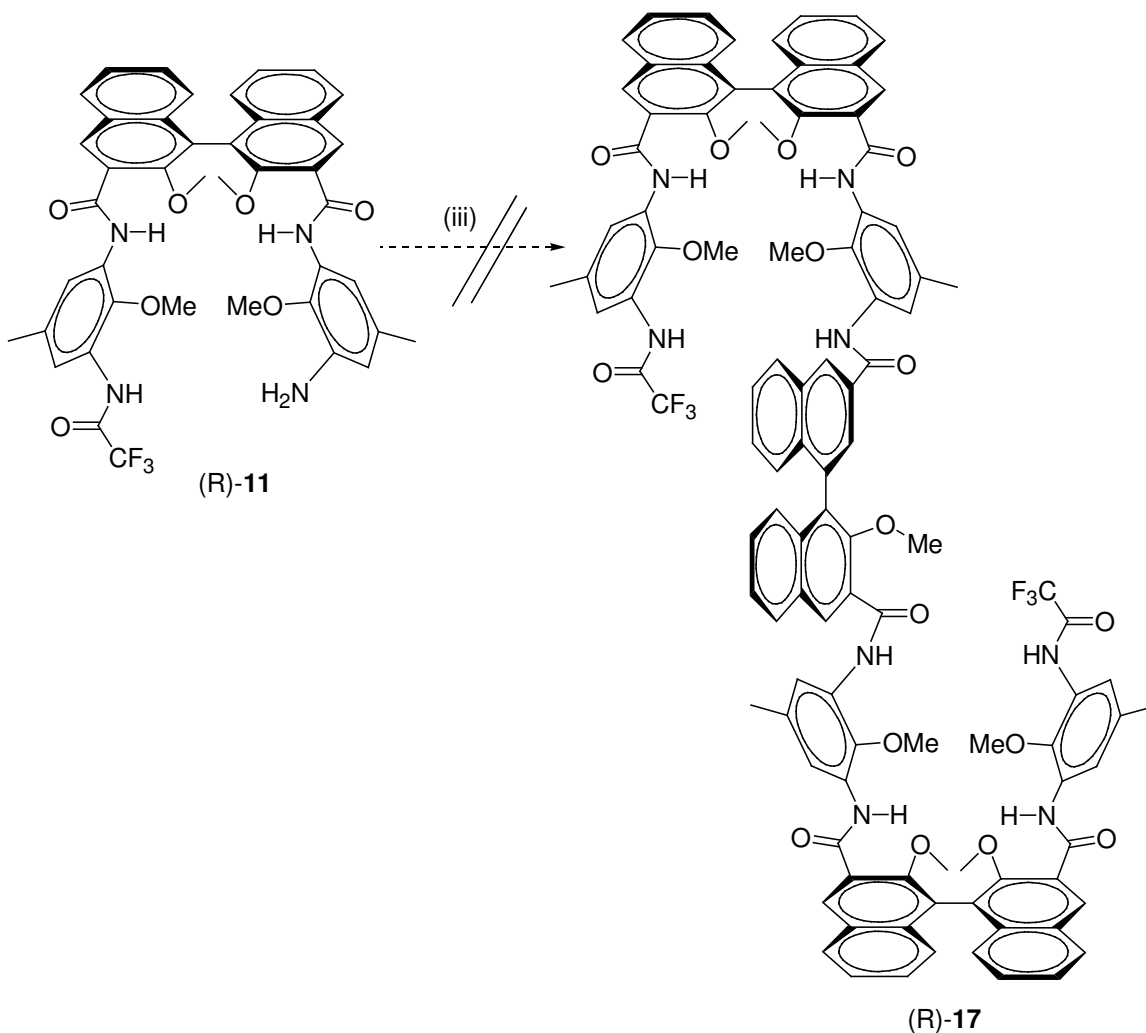
Figure 16: Hybrid foldamer from BINOL and 2-Methoxy-5-methyl-benzene-1, 3-diamine building blocks

3.4.5 Synthesis

The diprotected compounds **R-15** and **S-15** were achieved by treatment of **R/S** diamine **12** with trifluoro acetic acid and Et_3N in the presence EDCI of in dry dichloromethane. Compound **15** upon treatment with K_2CO_3 , methanol and few drop of water for two days at room temperature, furnished mono protected compound **16** and some amount of **15**, and unreacted starting materials (scheme 5). Unfortunately all attempts towards the preparation of linear oligomer **R-(17)** were not successful, as the reaction gave intractable mixture of products under a variety of conditions.

Scheme 5





Reagents and conditions: (i) trifluoro acetic acid, EDCI Et₃N, dry dichloromethane, rt, 12 h; (ii) K₂CO₃, methanol, 0.3 mL water, 48 h; (iii) (S)-11, Et₃N, dry dichloromethane, rt, 12 h.

3.4.6 Conclusion

In summary, we have described novel BINOL-*m*-phenylenediamine and 2,6-diamino pyridine derived macrocycles that feature conformational ordering both in solid- and solution-state. Structural investigations provide convincing evidence of their intramolecular hydrogen bonding arrangement and rigid structural architecture. Attempts towards the preparation of linear oligomer **R-(17)** were not successful.

3.5 Experimental procedures

General Methods

Unless otherwise stated, starting materials were obtained from commercial suppliers and used without further purification. Dry dichloromethane (DCM) were freshly prepared by distillation over P₂O₅ and CaH₂, respectively. Dry acetone was freshly distilled over KMnO₄ followed by K₂CO₃. Dry reactions were performed under argon atmosphere. Purification by column chromatography was performed in 100-200-mesh silica, unless otherwise stated. NMR spectra were recorded in CDCl₃ or DMSO-d₆ on 200, 400 or 500 MHz NMR spectrometers. Reactions were monitored by thin layer chromatography (TLC) carried out on 0.25 mm silica gel plates.

Crystal data for (R,R)-13: C₆₄H₅₂N₄O₁₀·2.5(CH₂Cl₂)·CH₃OH): M=1277.42, crystal dimensions 0.56 x 0.11 x 0.07 mm³, monoclinic, space group *P* 2₁, *a*=17.003(2), *b*=9.1398(13), *c*=21.745(3) Å, β=108.902(3) °; *V*=3197.0(7) Å³; *Z*=2; ρ_{calcd}=1.327 gcm⁻³, μ (Mo-K_α)=0.290 mm⁻¹, *F*(000)=1326, 2θ_{max}=50.00°, 23042 reflections collected, 11122 unique, 9190 observed (*I* > 2σ(*I*)) reflections, 857 refined parameters, *R* value 0.0821, *wR*2=0.2067 (all data *R*=0.0992, *wR*2=0.2269), *S*=1.115, minimum and maximum transmission 0.8544 and 0.9805; maximum and minimum residual electron densities +1.037 and -0.825 e Å⁻³.

Crystal data for (S,S)-13: C₆₄H₅₂O₁₀N₄·2.5(CH₂Cl₂)·H₂O): M=1266.92, crystal dimensions 0.56 x 0.11 x 0.07 mm³, monoclinic, space group *P* 2₁, *a* =16.933(2), *b*=9.1812(11), *c* = 21.721(2) Å, β =108.712(2) °; *V* =3198.4(6) Å³; *Z* =2; ρ_{calcd} =1.316 gcm⁻³, μ (Mo-K_α)= 0.289 mm⁻¹, *F*(000) =1317, 2θ_{max}=50.00°, 38586 reflections

collected, 11227 unique, 8279 observed ($I > 2\sigma(I)$) reflections, 834 refined parameters, R value 0.0729, $wR2=0.1888$ (all data $R=0.1045$, $wR2=0.2170$), $S=1.060$, minimum and maximum transmission 0.8478 and 0.9865; maximum and minimum residual electron densities $+0.790$ and $-0.724 \text{ e } \text{\AA}^{-3}$.

Crystal data for (R,R)-14: ($\text{C}_{58}\text{H}_{42}\text{N}_6\text{O}_8 \cdot 3.5(\text{CH}_3\text{CN}) \cdot 2.25(\text{H}_2\text{O})$): $M=1120.08$, crystal dimensions $0.79 \times 0.50 \times 0.24 \text{ mm}^3$, orthorhombic, space group $P 2_12_12_1$, $a = 21.704(2)$, $b = 17.2552(19)$, $c = 32.978(4) \text{ \AA}$, $V = 12351(2) \text{ \AA}^3$, $Z = 8$, $\rho_{\text{calcd}} = 1.205 \text{ g cm}^{-3}$, $\mu(\text{Mo-K}\alpha) = 0.084 \text{ mm}^{-1}$, $F(000) = 4644$, $2\theta_{\text{max}} = 50.00^\circ$, $T = 133(2) \text{ K}$, 89715 reflections collected, 21684 unique, 17038 observed ($I > 2\sigma(I)$) reflections, 1433 refined parameters, R value 0.0870, $wR2=0.2330$ (all data $R=0.1088$, $wR2=0.2517$), $S=1.033$, minimum and maximum transmission 0.9368 and 0.9802; maximum and minimum residual electron densities $+0.981$ and $-0.431 \text{ e } \text{\AA}^{-3}$.

Crystal data for (S,S)-14: ($\text{C}_{58}\text{H}_{42}\text{N}_6\text{O}_8 \cdot 1.25(\text{H}_2\text{O}) \cdot 0.5(\text{CH}_3\text{OH})$): $M=1084.59$, crystal dimensions $0.71 \times 0.31 \times 0.25 \text{ mm}^3$, orthorhombic, space group $C 222_1$, $a = 17.2153(14)$, $b = 32.837(3)$, $c = 21.7445(17) \text{ \AA}$, $V = 12292.2(17) \text{ \AA}^3$, $Z = 8$, $\rho_{\text{calcd}} = 1.172 \text{ g cm}^{-3}$, $\mu(\text{Mo-K}\alpha) = 0.081 \text{ mm}^{-1}$, $F(000) = 4520$, $2\theta_{\text{max}} = 50.00^\circ$, $T = 133(2) \text{ K}$, 58702 reflections collected, 10779 unique, 8915 observed ($I > 2\sigma(I)$) reflections, 783 refined parameters, R value 0.0691, $wR2=0.1856$ (all data $R=0.0838$, $wR2=0.1980$), $S=1.074$, minimum and maximum transmission 0.9448 and 0.9801; maximum and minimum residual electron densities $+0.851$ and $-0.259 \text{ e } \text{\AA}^{-3}$.

4-Methyl-2,6-dinitro-phenol 8 : To an ice-cold stirred solution of the 4-methyl phenol 7 (10 g, 92.5 mmol, 1 equiv.) in dry dichloromethane (80 mL) was added nitration mixture

(1 mL sulphuric acid, 10 mL nitric acid) drop wise. The resulting mixture was stirred at room temperature for overnight. The reaction mixture was diluted with dichloromethane (200 mL) and washed sequentially with water and saturated sodium chloride solution. Drying and concentration of the dichloromethane extract under reduced pressure gave the crude product which on column chromatography (20% EtOAc/Hexane) afforded the desired pure product **8** (14.5 g, 79%).

2-Methoxy-5-methyl-1,3-dinitro-benzene 9: To an ice-cold stirred solution of the **8** (5 g, 25.20 mmol, 1 equiv.) and potassium carbonate (8.71 g, 63.13 mmol, 2.5 eq) in dry acetone (60 mL) was added dimethyl sulphate drop wise (5.97 mL, 63.13 mmol, 2.5 eq). The resulting reaction mixture was stirred for 8 h at room temperature. The reaction mixture was filtered and washed with excess acetone. The filtrate was concentrated under reduced pressure gave the crude product which on column chromatography (20% EtOAc/Hexane) afforded the desired product **9** (4.0 g, 74%). mp 56-59⁰C; IR (CHCl₃) vcm⁻¹): 3020, 1541, 1346, 1215, 769; ¹H NMR (200 MHz, CDCl₃): δ 7.84 (s, 2H), 4.02 (s, 3H), 2.46 (s, 3H); ¹³C NMR (50 MHz, CDCl₃): δ 145.2, 144.9, 135.0, 129.3, 64.6, 20.5; Anal. Calcd. for C₈H₈N₂O₅: C, 45.29; H, 3.80; N, 13.20. Found: C, 45.21; H, 3.77; N, 13.18.

2-Methoxy-5-methyl-benzene-1, 3-diamine 10: To a stirred solution of the **9** (4.0 g, 18.86 mmol, 1 equiv.) in methanol (20 mL) was added 10% Pd/C (0.4 g). The resulting mixture was stirred at room temperature in hydrogen atmosphere for 8 hrs. The reaction mixture was filtered through celite pad and washed with excess methanol. The filtrate was concentrated and dried obtained the product as a thick liquid **10**. (2.4 g, 83%). IR

(CHCl₃) vcm⁻¹): 3285, 3018, 1608, 1512, 1215, 757; ¹H NMR (200 MHz, CDCl₃): δ 6.36 (s, 2H), 4.10 (s, 3H), 4.05 (bs, 4H), 2.50 (s, 3H); ¹³C NMR (50 MHz, CDCl₃): δ 139.2, 133.9, 132.0, 106.3, 57.9, 20.5; ESI Mass: 153 (M + 1); Anal. Calcd. for C₈H₁₂N₂O: C, 63.13; H, 7.95; N, 18.41. Found: C, 63.09; H, 7.89; N, 18.35.

2,2'-Dimethoxy-[1,1]binaphthalenyl-3,3'-dicarboxylic acid bis-[(3-amino-2-methoxy-5-methyl-phenyl)-amide] (R)-12: To a solution of 2,2'-dimethoxy-1,1'-binaphthyl-3,3'-dicarboxylic acid (0.8 g, 1.99 mmol, 1 equiv.), in dry dichloromethane (15 mL), oxaloyl chloride (1.04 mL, 11.94 mmol, 6 eq.) and a catalytic amount of dry DMF were added. The reaction mixture was stirred for 2 h at room temperature. The solvent was stripped off under reduced pressure and dried under high vacuum. The resulting acid chloride (**R**)-**11** was dissolved in dry dichloromethane (8 mL) and slowly added to a solution of 2-methoxy-5-methyl-benzene-1, 3-diamine (1.51 g, 9.95 mmol, 5 equiv.) in dry dichloromethane (15 mL) containing triethylamine (1.38 mL, 9.95 mmol, 5 eq.). The resulting mixture was stirred at room temperature for 8h. The reaction mixture was diluted with dichloromethane and washed sequentially with water and saturated sodium chloride solution. Drying and concentration of the dichloromethane extract under reduced pressure gave the crude product which on column chromatography (50% EtOAc/Hexane) afforded the desired product (**R**)-**12** (0.95 g, 71%, mp 160-162⁰C; [α]_D = -158.0 (c = 1.0, chloroform); IR (CHCl₃) vcm⁻¹): 3018, 1663, 1541, 1473, 1215, 757; ¹H NMR (400 MHz, CDCl₃): δ 10.49 (s, 2H), 8.97 (s, 2H), 8.09 (d, J=8.24 Hz, 2H), 7.95 (s, 2H), 7.50 (m, 2H), 7.37 (m, 2H), 7.17 (d, J=8.25 Hz, 2H), 6.40 (s, 2H), 3.68 (s, 6H) 3.48 (s, 6H), 2.29 (s, 6H); ¹³C NMR (100 MHz, CDCl₃): Eδ 163.0, 153.3, 138.7, 135.4, 134.9, 134.3, 131.8, 130.3, 129.6, 128.6, 126.2, 125.9, 125.4, 125.2, 112.4, 111.5, 62.1, 59.3, 21.52;

ESI Mass: 671 (M + 1); Anal. Calcd. for C₄₀H₃₈N₄O₆: C, 71.63; H, 5.71; N, 8.35. Found: C, 71.60; H, 5.69; N, 8.32.

2,2'-Dimethoxy-[1,1]binaphthalenyl-3,3'-dicarboxylic acid bis-[(3-amino-2-methoxy-5-methyl-phenyl)-amide] (S)-12: compound **(S)-12** was synthesized according to the procedure described for **(R)-12** (scheme 4) 0.90 g, (72%). mp160-162⁰C; [α]_D = +155.9 (c = 0.34, chloroform); IR (CHCl₃) ν (cm⁻¹) : 3018, 1663, 1541, 1473, 1215, 757; ¹H NMR (400 MHz, CDCl₃): δ 10.48 (s, 2H), 8.97 (s, 2H), 8.09 (d, J=8.24 Hz, 2H), 7.96 (s, 2H), 7.50 (m, 2H), 7.37 (m, 2H), 7.16 (d, J=8.25 Hz, 2H), 6.41 (s, 2H), 3.68 (s, 6H) 3.47 (s, 6H), 2.29 (s, 6H); ¹³C NMR (100 MHz, CDCl₃): δ 163.0, 153.3, 138.0, 135.4, 135.0, 134.7, 134.4, 131.9, 130.3, 129.7, 128.7, 126.2, 125.9, 125.4, 125.2, 112.7, 112.0, 62.1, 59.6, 21.50; ESI Mass: 671 (M + 1); Anal. Calcd. for C₄₀H₃₈N₄O₆: C, 71.63; H, 5.71; N, 8.35. Found: C, 71.59; H, 5.68; N, 8.31.

Synthesis of (R,R)-13: To a solution of 2,2'-dimethoxy-1,1'-binaphthyl-3,3'-dicarboxylic acid (0.04 g, 0.099 mmol, 1 equiv.), in dry dichloromethane (5 mL), oxaloyl chloride (0.05 mL, 0.59 mmol, 6 eq.) and a catalytic amount of dry DMF were added. The reaction mixture was stirred for 2 h at room temperature. The solvent was stripped off under reduced pressure and dried under high vacuum. The resulting acid chloride **(R)-11** was dissolved in dry dichloromethane (8 mL) and slowly added to a solution of **(R)-12** (0.2 g, 0.29 mmol, 3 equiv.) in dry dichloromethane (10 mL) containing triethylamine (0.11 mL, 0.79 mmol, 8 eq.). The resulting mixture was stirred at room temperature for 8h. The reaction mixture was diluted with dichloromethane and washed sequentially with water and saturated sodium chloride solution. Drying and concentration of the

dichloromethane extract under reduced pressure gave the crude product which on column chromatography (40% EtOAc/Hexane) afforded the macrocycle **(R, R)-13** (63 mg, 60%).

One pot synthesis of (R, R)-13: To a solution of 2,2'-dimethoxy-1,1'-binaphthyl-3,3'-dicarboxylic acid (0.2 g, 0.49 mmol, 1 equiv.), in dry dichloromethane (5 mL), oxaloyl chloride (0.26 mL, 2.98 mmol, 6 eq.) and a catalytic amount of dry DMF were added. The reaction mixture was stirred for 2 h at room temperature. The solvent was stripped off under reduced pressure and dried under high vacuum. The resulting acid chloride **(R)-11** was dissolved in dry dichloromethane (8 mL) and slowly added to a solution of 2-methoxy-5-methyl-benzene-1,3-diamine (0.07 g, 0.49 mmol, 1 equiv.) in dry dichloromethane (5 mL) containing triethylamine (0.55 mL, 3.97 mmol, 8 eq.). The resulting mixture was stirred at room temperature for 8h. The reaction mixture was diluted with dichloromethane and washed sequentially with water and saturated sodium chloride solution. Drying and concentration of the dichloromethane extract under reduced pressure gave the crude product which on column chromatography (40% EtOAc/Hexane) afforded the desired pure product **(R,R)-13** (0.17g, 68%). Mp 295-297⁰C; [α]_D = -200.0 (c = 1.0, chloroform); IR (CHCl₃) vcm⁻¹: 3336, 3020, 1670, 1596, 1508, 1217, 757; ¹H NMR (400 MHz, CDCl₃): δ 10.10 (s, 4H), 8.87 (s, 4H), 8.32 (s, 4H), 8.08 (d, J=7.79 Hz, 4H), 7.50 (m, 4H), 7.37 (m, 4H), 7.13 (d, J=8.71 Hz, 4H), 3.93 (s, 6H) 3.32 (s, 12H), 2.48 (s, 6H); ¹³C NMR (100 MHz, CDCl₃): δ 163.4, 153.3, 136.5, 135.2, 134.0, 131.1, 130.3, 129.7, 128.8, 126.7, 125.9, 125.3, 125.0, 117.0, 62.1, 61.4, 21.9; ESI Mass: 1059 (M +Na); Anal. Calcd. for C₆₄H₅₂N₄O₁₀: C, 74.12; H, 5.05; N, 5.40. Found: C, 74.09; H, 4.99; N, 5.38.

Synthesis of (S, S)-13: compound **(S, S)-13** was synthesized according to the procedure described for **(R, R)-13** (scheme 4) 0.44g, (69; mp 295-297⁰C; [α]_D = +196.0 (c = 1.0, chloroform); IR (CHCl₃) vcm⁻¹): 3336, 3020, 1670, 1596, 1508, 1217, 757; ¹H NMR (400 MHz, CDCl₃): δ 10.10 (s, 4H), 8.87 (s, 4H), 8.32 (s, 4H), 8.06 (d, J=7.79 Hz, 4H), 7.50 (m, 4H), 7.37 (m, 4H), 7.12 (d, J=8.71 Hz, 4H), 3.93 (s, 6H) 3.32 (s, 12H), 2.48 (s, 6H); ¹³C NMR (100 MHz, CDCl₃): δ 163.7, 153.6, 136.9, 135.5, 134.3, 131.4, 130.6, 130.0, 129.1, 127.0, 126.3, 125.3, 117.3, 62.5, 61.7, 22.2; ESI Mass: 1059 (M +Na); Anal. Calcd. for C₆₄H₅₂N₄O₁₀: C, 74.12; H, 5.05; N, 5.40. Found: C, 74.09; H, 4.99; N, 5.38.

Synthesis of (R,R)-14: To a solution of 2,2'-dimethoxy-1,1'-binaphthyl-3,3'-dicarboxylic acid (0.8 g, 1.99 mmol, 1 equiv.), in dry dichloromethane (12 mL), oxaloyl chloride (1.0 mL, 11.94 mmol, 6 eq.) and a catalytic amount of dry DMF were added. The reaction mixture was stirred for 2 h at room temperature. The solvent was stripped off under reduced pressure and dried under high vacuum. The resulting acid chloride **(R)-11** was dissolved in dry dichloromethane (15 mL) and slowly added to a solution of pyridine-2,6-diamine (0.23 g, 2.18 mmol, 1.1 equiv.) in dry dichloromethane (10 mL) containing triethylamine (2.21 mL, 15.92 mmol, 8 eq.). The resulting mixture was stirred at room temperature for 8h. The reaction mixture was diluted with dichloromethane and washed sequentially with water and saturated sodium chloride solution. Drying and concentration of the dichloromethane extract under reduced pressure gave the crude product which on column chromatography (45% EtOAc/Hexane) afforded the desired pure product **(R,R)-14** (0.57 g, 60%); mp 284-286⁰C; [α]_D = -173.0 (c = 0.8, chloroform); IR (CHCl₃) v (cm⁻¹): 3355, 3018, 1674, 1583, 1514, 1203, 1085, 757; ¹H NMR (400 MHz, CDCl₃): δ 9.79

(s, 4H), 8.79 (s, 4H), 8.27 (d, J=7.79 Hz, 4H), 8.04 (d, J=8.71Hz, 4H), 7.89 (t, 2H), 7.48 (t, 4H), 7.35 (t, 4H), 7.05 (d, J=8.71 Hz, 4H) 3.35 (s, 12H); ^{13}C NMR (100 MHz, CDCl_3): δ 164.1, 153.1, 150.0, 140.7, 135.5, 134.0, 130.3, 129.7, 128.8, 126.8, 125.9, 125.3, 125.2, 110.5, 62.2; ESI Mass: 973.8 (M +Na); Anal. Calcd. for $\text{C}_{58}\text{H}_{42}\text{N}_6\text{O}_8$: C, 73.25; H, 4.45; N, 8.84. Found: C, 73.15; H, 4.39; N, 8.74.

Synthesis of (S,S)-14: compound **(S,S)-14** was synthesized according to the procedure described for **(R,R)-14** (scheme 4) (0.6 g, 58%); mp 284-286 $^{\circ}\text{C}$; $[\alpha]_{\text{D}} = +170.0$ (c = 0.8, chloroform); IR (CHCl_3) ν (cm^{-1}): 3355, 3018, 1674, 1583, 1514, 1450, 1203, 1085, 757; ^1H NMR (400 MHz, CDCl_3): δ 9.80 (s, 4H), 8.79 (s, 4H), 8.27 (d, J=7.79 Hz, 4H), 8.04 (d, J=8.71 Hz, 4H), 7.89 (t, 2H), 7.48 (t, 4H), 7.34 (t, 4H), 7.06 (d, J=8.71 Hz, 4H) 3.34 (s, 12H); ^{13}C NMR (100 MHz, CDCl_3): δ 164.1, 153.1, 150.1, 140.7, 135.5, 134.0, 130.3, 129.7, 128.8, 126.8, 125.9, 125.3, 125.2, 110.5, 62.2; ESI Mass: 973.8 (M +Na); Anal. Calcd. for $\text{C}_{58}\text{H}_{42}\text{N}_6\text{O}_8$: C, 73.25; H, 4.45; N, 8.84. Found: C, 73.11; H, 4.35; N, 8.70.

2,2'-Dimethoxy-[1,1]binaphthalenyl-3,3'-dicarboxylic acid bis-{{2-methoxy-5-methyl-3-(2,2,2-trifluoro-acetylamino)-phenyl]-amide}(R)-15 : To an ice-cold stirred solution of **(R)-12** (0.9 g, 1.34 mmol, 1 equiv.) and trifluoro acetic acid (0.4 mL, 5.37mmol, 4 equiv) in dry dichloromethane (20 mL) was added Et_3N (0.74 mL, 5.37mmol, 4 equiv) and EDCI (1.03 g, 5.37 mmol, 4 equiv.) in dichloromethane. The resulting mixture was stirred at room temperature for overnight. The reaction mixture was diluted with dichloromethane and washed sequentially with water and saturated sodium chloride solution. Drying and concentration of the dichloromethane extract under reduced pressure gave the crude product which on column chromatography (35% EtOAc/Hexane) afforded

the desired pure product **(R)-15** (0.8 g, 68%); mp 162-165⁰C; [α]_D = -100.0 (c = 0.96, chloroform); IR (CHCl₃) v cm⁻¹): 3406, 3309, 3020, 1733, 1670, 1521, 1217, 763; ¹H NMR (400 MHz, CDCl₃): δ 10.49 (s, 2H), 9.02 (s, 2H), 8.35 (s, 2H), 8.23 (s, 2H), 8.12 (d, 2H), 7.80 (s, 2H), 7.54 (m, 2H), 7.41 (m, 2H) 7.18 (d, 2H), 3.72 (s, 6H) 3.48 (s, 6H), 2.41 (s, 6H); ¹³C NMR (100 MHz, CDCl₃): δ 163.1, 154.6, 154.2, 153.2, 137.0, 135.9, 135.6, 134.8, 131.5, 130.3, 129.8, 129.1, 128.0, 126.2, 125.4, 125.1, 119.1, 116.8, 114.1, 62.2, 61.1, 21.7; ESI Mass: 885 (M +Na); Anal. Calcd. for C₄₄H₃₆F₆N₄O₈: C, 61.25; H, 4.21; N, 6.49. Found: C, 61.18; H, 4.19; N, 6.50.

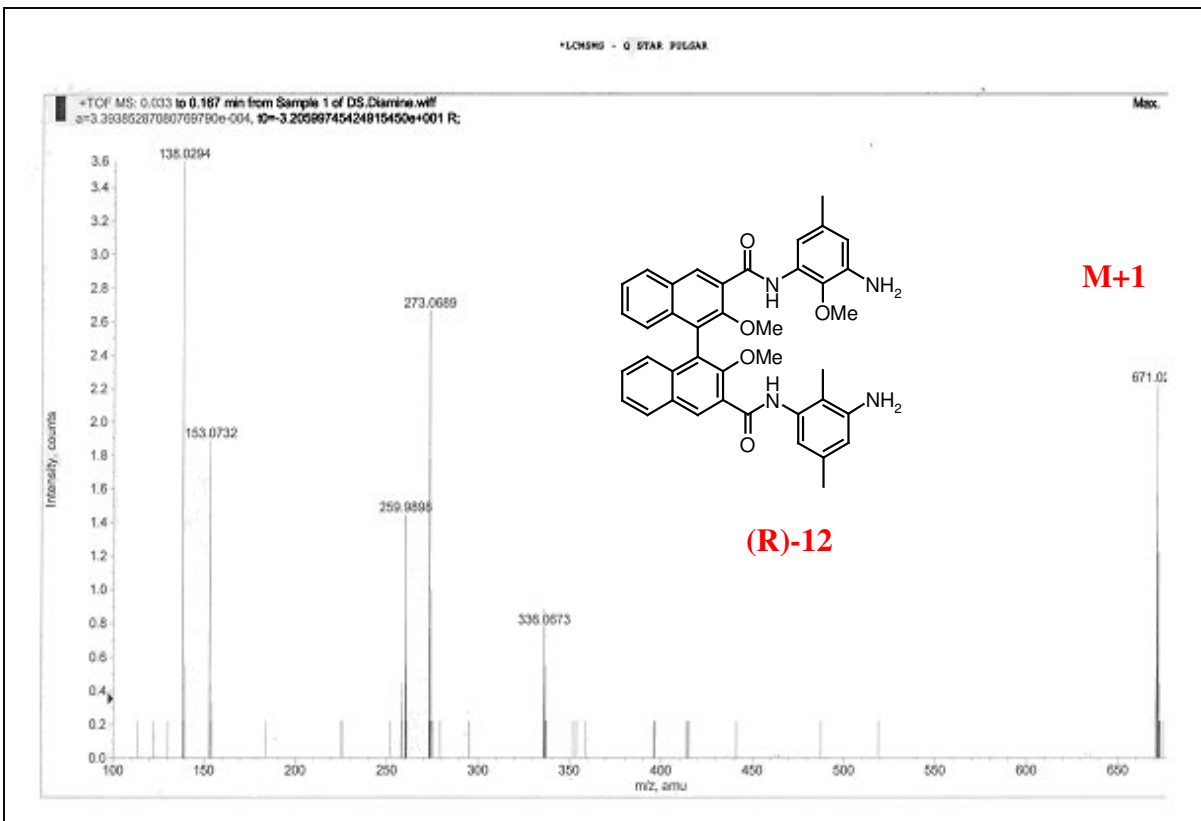
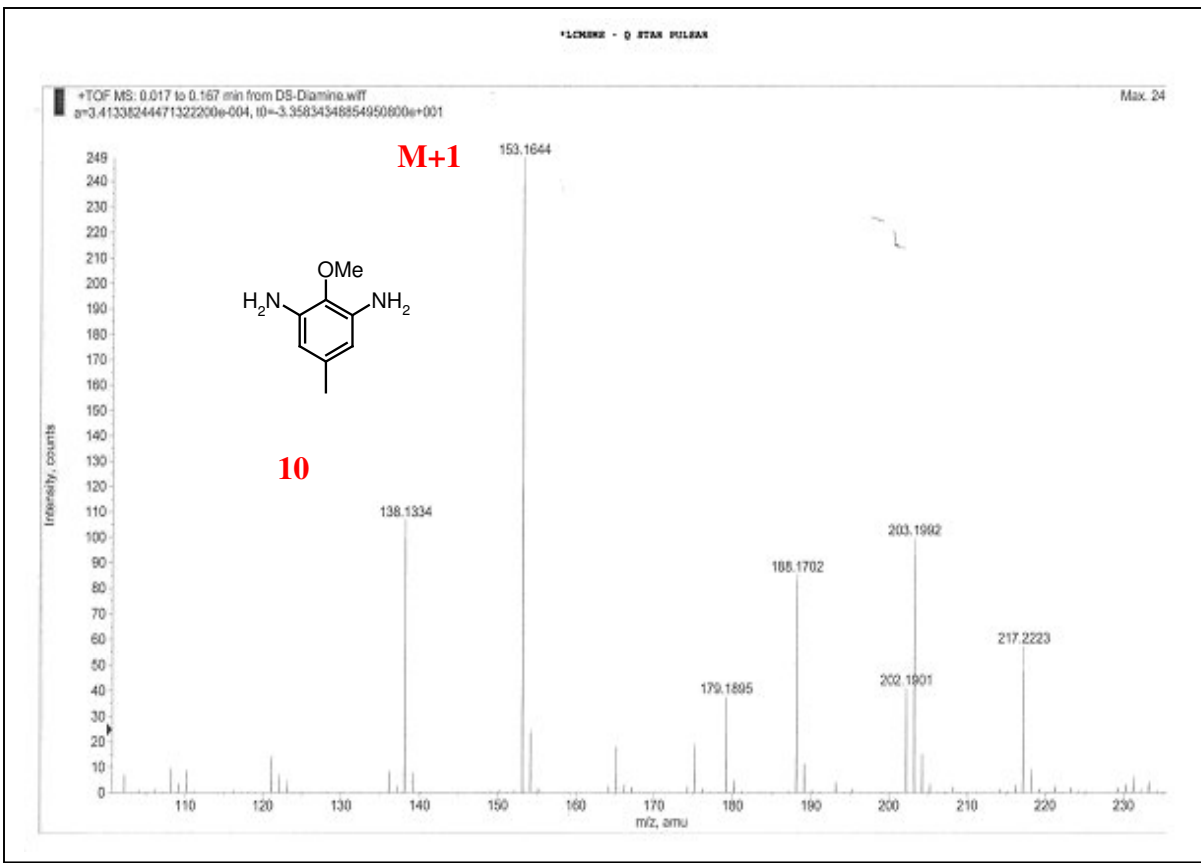
2,2'-Dimethoxy-[1,1]binaphthalenyl-3,3'-dicarboxylic acid bis-{{2-methoxy-5-methyl-3-(2,2,2-trifluoro-acetylamino)-phenyl]-amide}(S)-15: compound **(S)-15** was synthesized according to the procedure described for **(R)-15** (scheme 5) (0.9 g, 69%); mp 162-165⁰C; [α]_D = -97.3 (c = 1.2, chloroform); IR (CHCl₃) vcm⁻¹): 3406, 3309, 3018, 1739, 1674, 1508, 1215, 757; ¹H NMR (400 MHz, CDCl₃): δ 10.49 (s, 2H), 9.02 (s, 2H), 8.35 (s, 2H), 8.24 (s, 2H), 8.10 (d, 2H), 7.79 (s, 2H), 7.54 (m, 2H), 7.41 (m, 2H) 7.17 (d, 2H), 3.72 (s, 6H) 3.48 (s, 6H), 2.41 (s, 6H); ¹³C NMR (100 MHz, CDCl₃): δ 163.4, 154.9, 154.5, 153.5, 137.4, 136.2, 135.9, 135.1, 131.8, 130.6, 130.1, 129.4, 128.3, 126.5, 125.7, 125.4, 119.4, 117.2, 114.4, 62.5, 61.4, 22.0; ESI Mass: 885 (M +Na); Anal. Calcd. for C₄₄H₃₆F₆N₄O₈: C, 61.25; H, 4.21; N, 6.49. Found: C, 61.20; H, 4.15; N, 6.53.

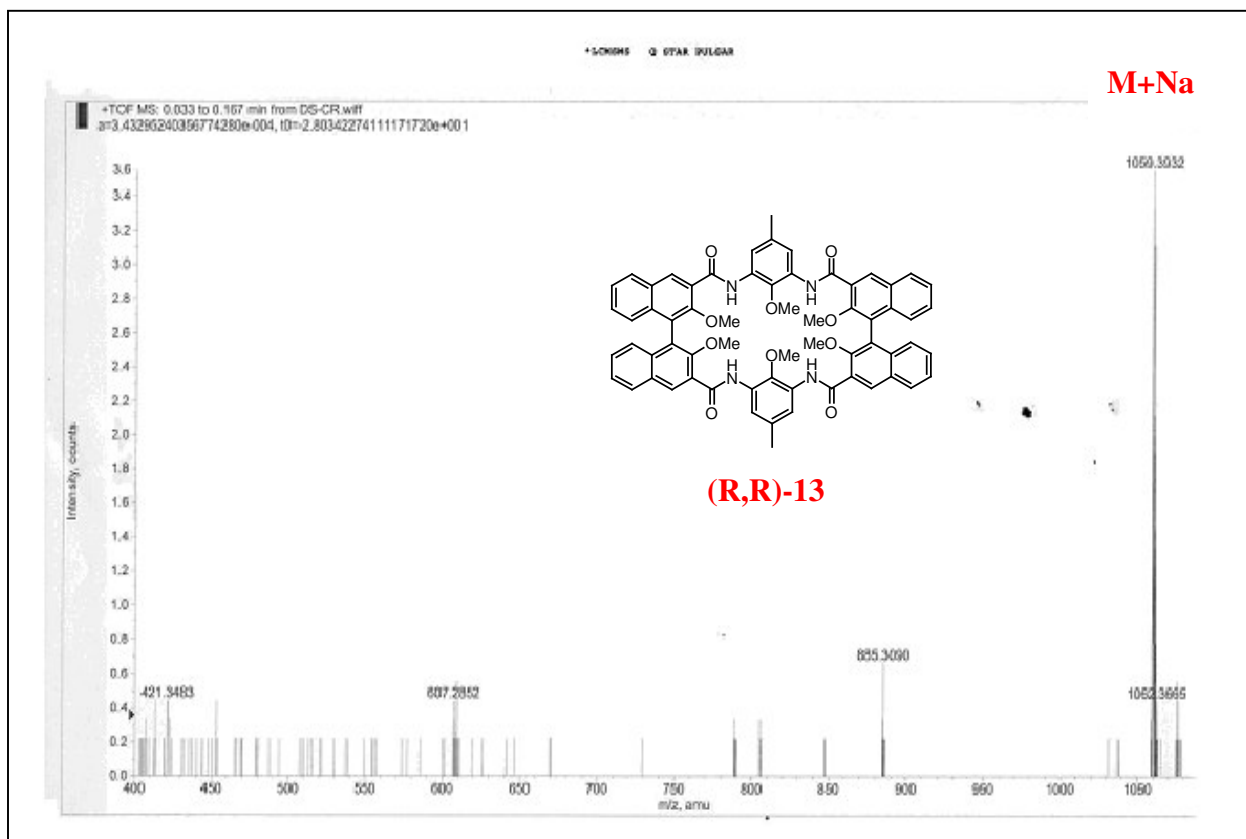
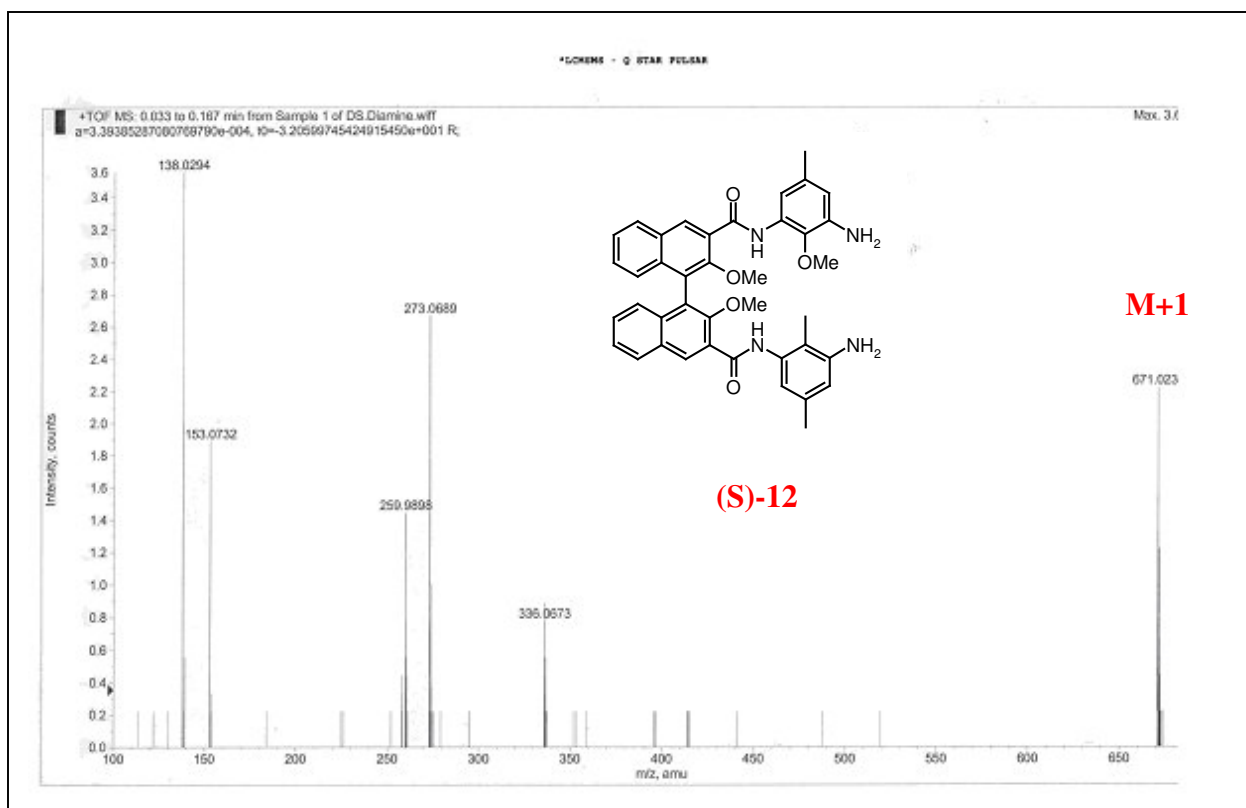
2,2'-Dimethoxy-[1,1']binaphthalenyl-3,3'-dicarboxylic acid 3-[(3-amino-2-methoxy-5-methyl-phenyl)-amide]3'-[[2-methoxy-5-methyl-3-(2,2,2,-trifluoro-acetylamino)-phenyl]-amide} **(R)-16**: To a stirred solution of **(R)-15** (0.55 g, 0.63 mmol, 1 equiv.) in methanol (25 mL) containing potassium carbonate (0.35 g, 2.54 mmol, 4 equiv) and 0.3

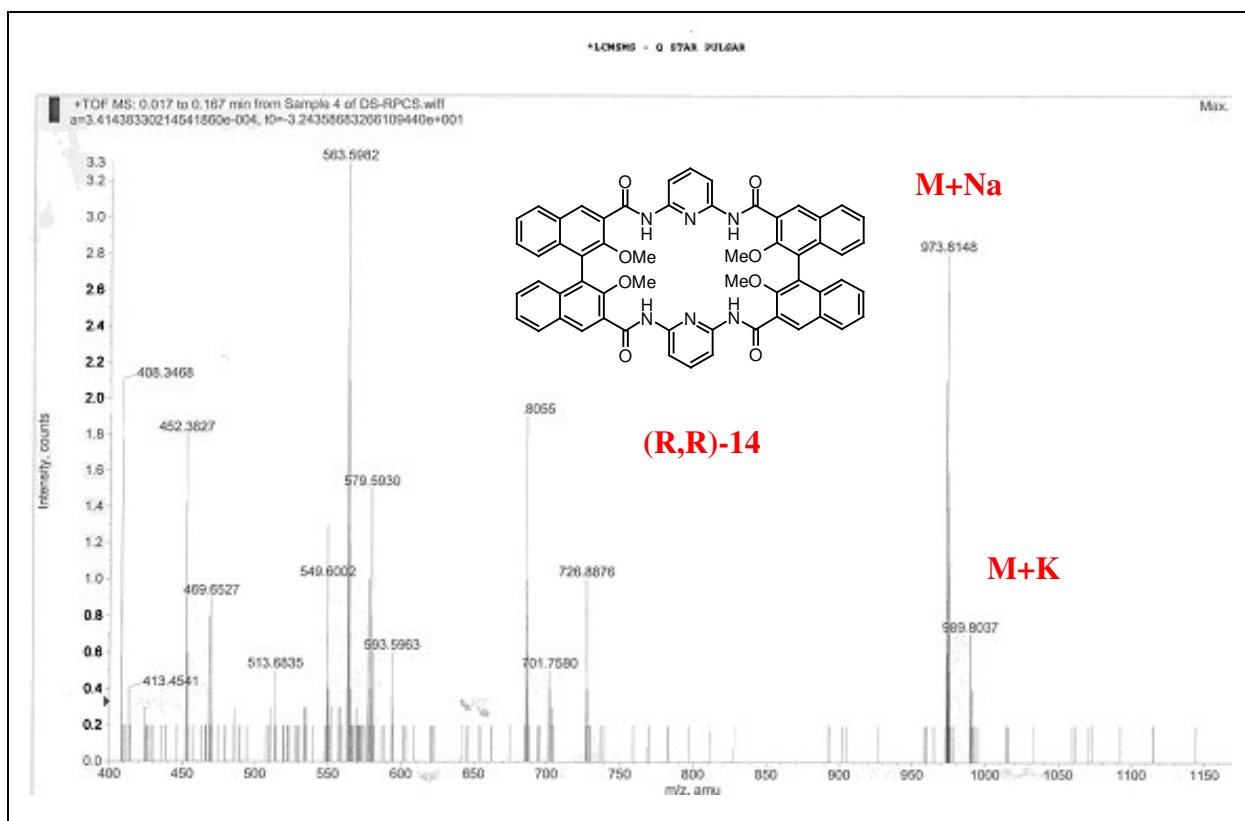
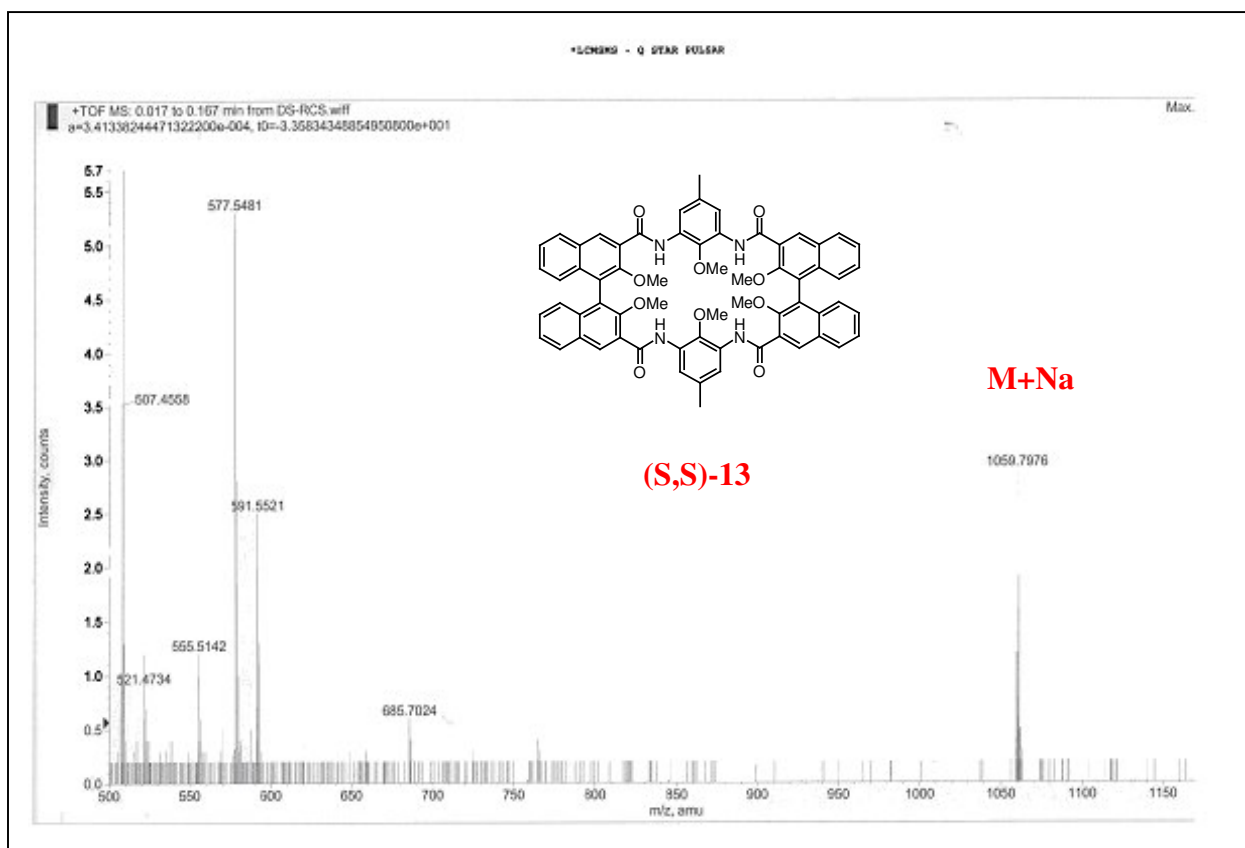
mL of water was added. The resulting mixture was stirred at room temperature for two days. The solvent was completely striped of under reduced pressure and diluted with dichloromethane and washed sequentially with water and saturated sodium chloride solution. Drying and concentration of the dichloromethane extract under reduced pressure gave the crude product which on column chromatography (40% EtOAc/Hexane) afforded the desired pure product **(R)-16** (0.39 g, 79%); mp170-173⁰C; [α]_D = -147.2 (c=0.2, chloroform); IR (CHCl₃) vcm⁻¹): 3313, 3018, 1733, 1668, 1519, 1215, 757; ¹H NMR (400 MHz, CDCl₃): δ 10.56 (s, 1H), 10.41(s, 1H), 9.0 (d, 2H), 8.36 (s, 1H), 8.27 (s, 1H), 8.10 (d, 2H), 7.94 (s, 1H), 7.79 (s, 1H) 7.52 (m, 2H), 7.40 (m, 2H) 7.17 (t, 2H), 6.39 (s, 1H) 3.72 (s, 3H), 3.67 (s, 3H), 3.48 (s, 3H), 3.47 (s, 3H), 2.41 (s, 3H), 2.29 (s, 3H); ¹³C NMR (100 MHz, CDCl₃): δ 163.2, 163.0, 154.7, 154.2, 153.3, 153.2, 137.0, 135.9, 135.7, 135.4, 135.1, 134.6, 131.8, 131.5, 130.4, 129.8, 129.0, 128.8, 128.1, 126.2, 125.3, 125.0, 119.0, 116.7, 112.8, 112.2, 62.2, 61.2, 59.5, 21.8, 21.5; ESI Mass: 789 (M +Na); Anal. Calcd. for C₄₂H₃₇F₃N₄O₇: C, 65.79; H, 4.86; N, 7.31. Found: C, 65.71; H, 4.82; N, 7.28.

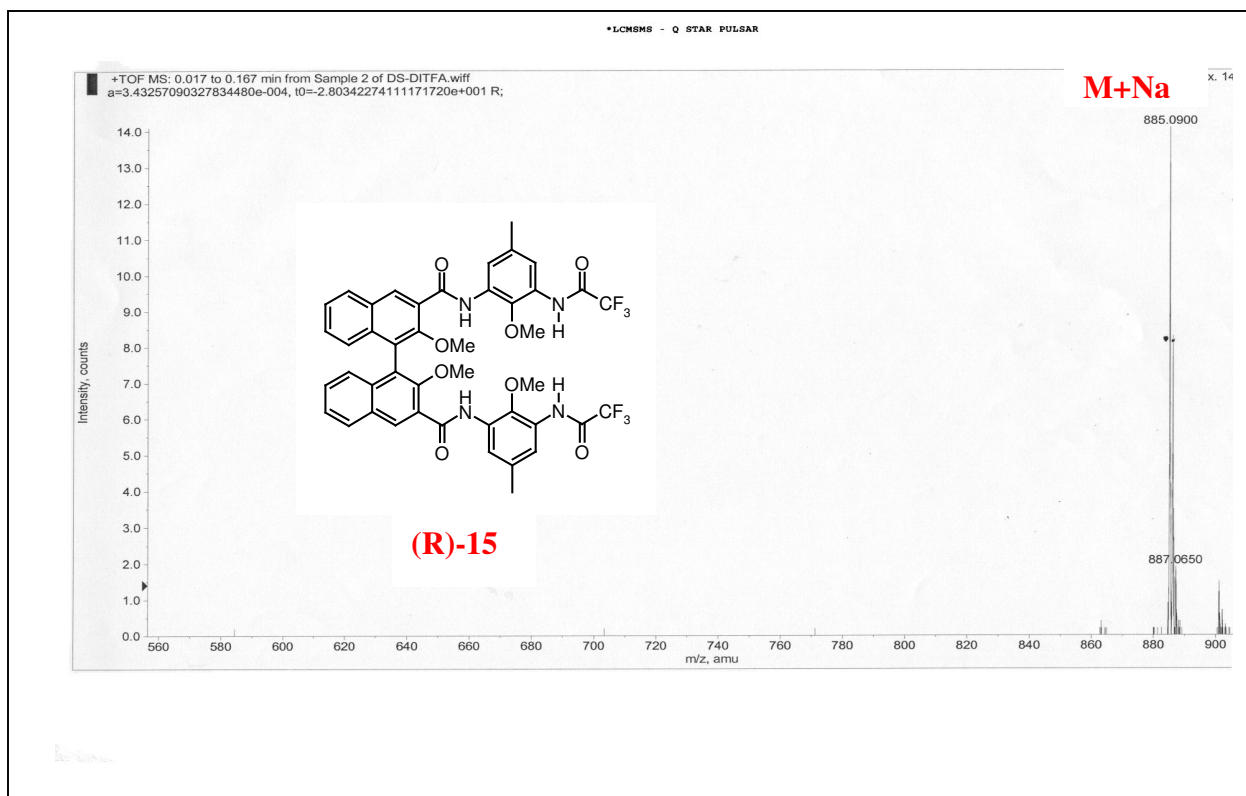
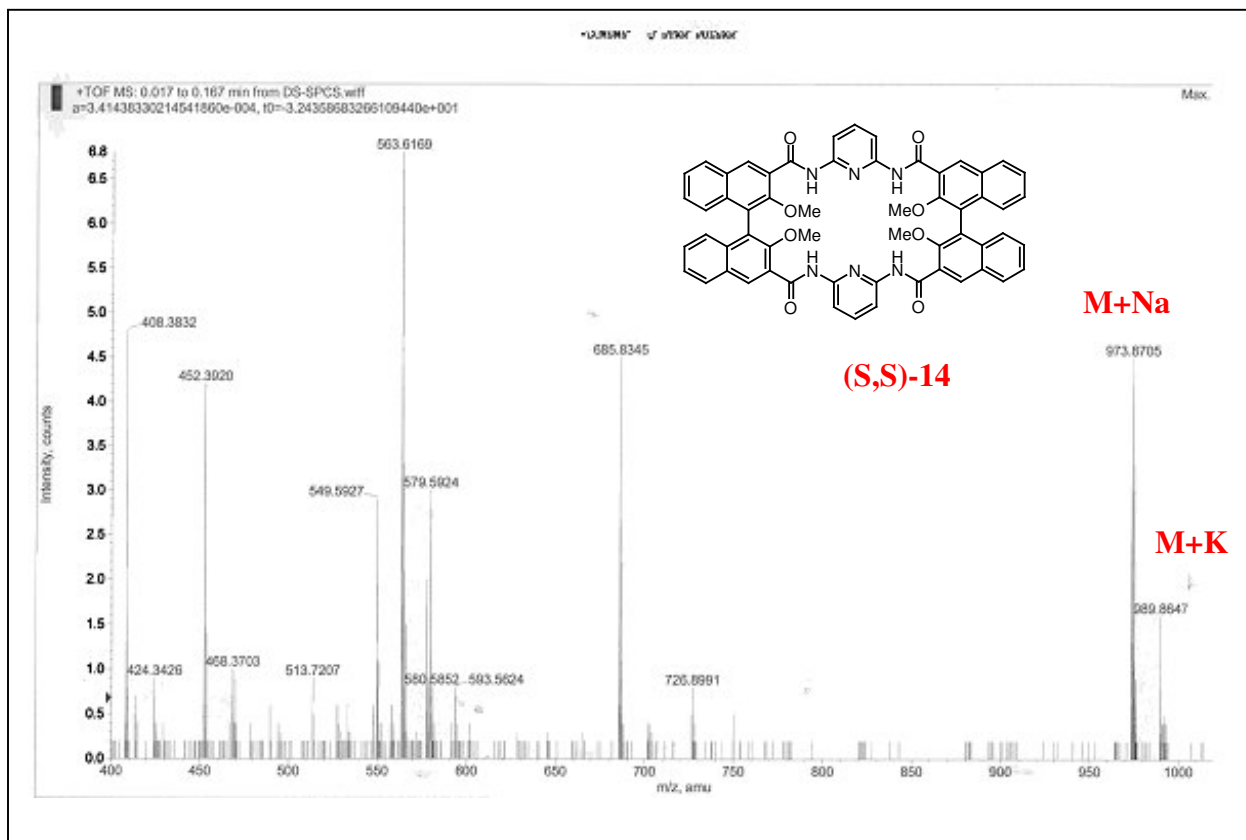
2,2'-Dimethoxy-[1,1']binaphthalenyl-3,3'-dicarboxylic acid 3-[(3-amino-2-methoxy-5-methyl-phenyl)-amide]3'-{[2-methoxy-5-methyl-3-(2,2,2,-trifluoro-acetylamino)-phenyl]-amide} (S)-16 : compound **(S)-16** was synthesized according to the procedure described for **(R)-16** (scheme 5). (0.2 g, 80%); mp170-173⁰C; [α]_D = +144.0 (c = 1.0, chloroform); IR (CHCl₃) vcm⁻¹): 3313, 3018, 1733, 1670, 1541, 1245, 763; ¹H NMR (400 MHz, CDCl₃): δ 10.55 (s, 1H), 10.40 (s, 1H), 9.0 (d, 2H), 8.35 (s, 1H), 8.25 (s, 1H), 8.10 (dd, 2H), 7.92 (s, 1H), 7.80 (s, 1H) 7.53 (m, 2H), 7.41 (m, 2H) 7.18 (t, 2H), 6.37 (s, 1H) 3.74 (s, 3H), 3.68 (s, 3H), 3.50 (s, 3H), 3.49 (s, 3H), 2.42 (s, 3H), 2.31(s, 3H); ¹³C NMR (100 MHz, CDCl₃): δ 163.1, 162.9, 153.3, 153.2, 138.7, 137.1, 135.6, 135.4, 135.0,

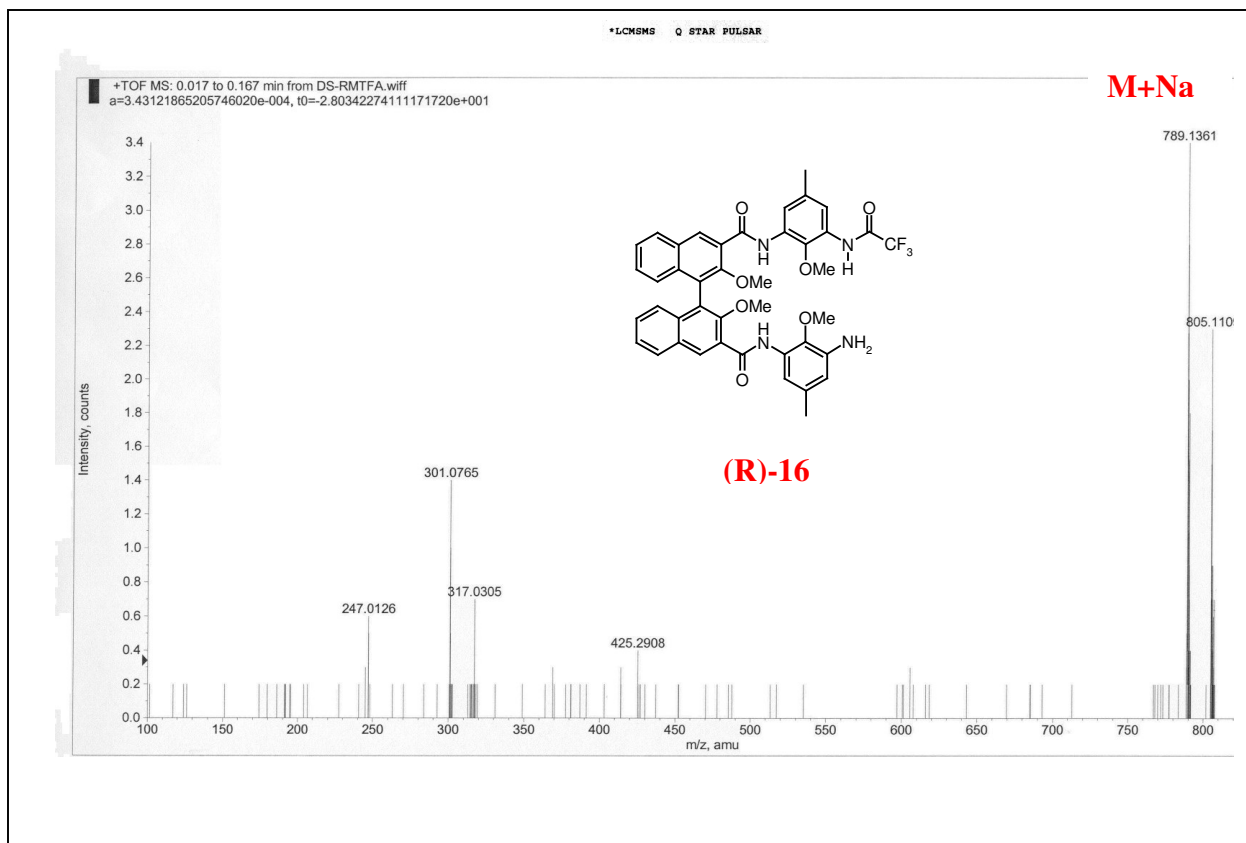
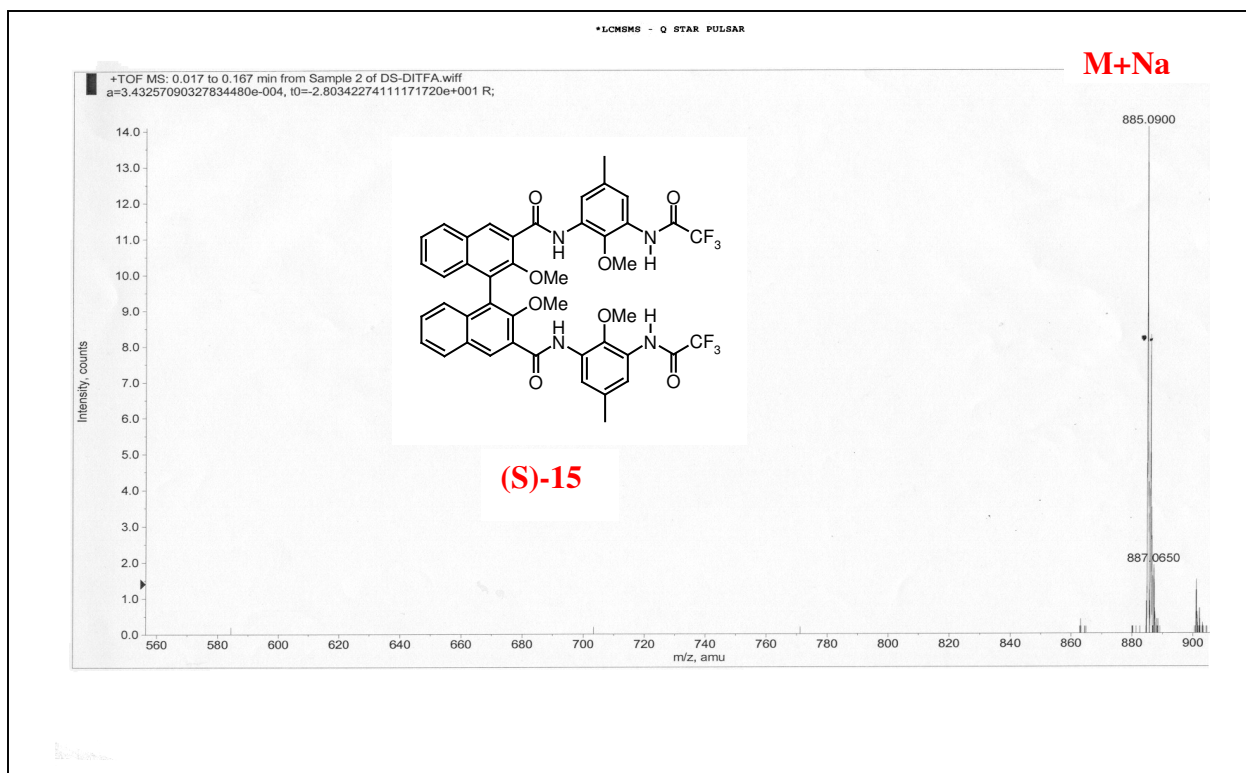
134.5, 131.7, 131.5, 130.3, 129.7, 128.9, 128.7, 128.0, 126.1, 125.4, 119.0, 116.8, 112.5, 111.6, 62.1, 61.1, 59.3, 21.7, 21.4; ESI Mass: 789 (M +Na); Anal. Calcd. for $C_{42}H_{37}F_3N_4O_7$: C, 65.79; H, 4.86; N, 7.31. Found: C, 65.69; H, 4.80; N, 7.26.







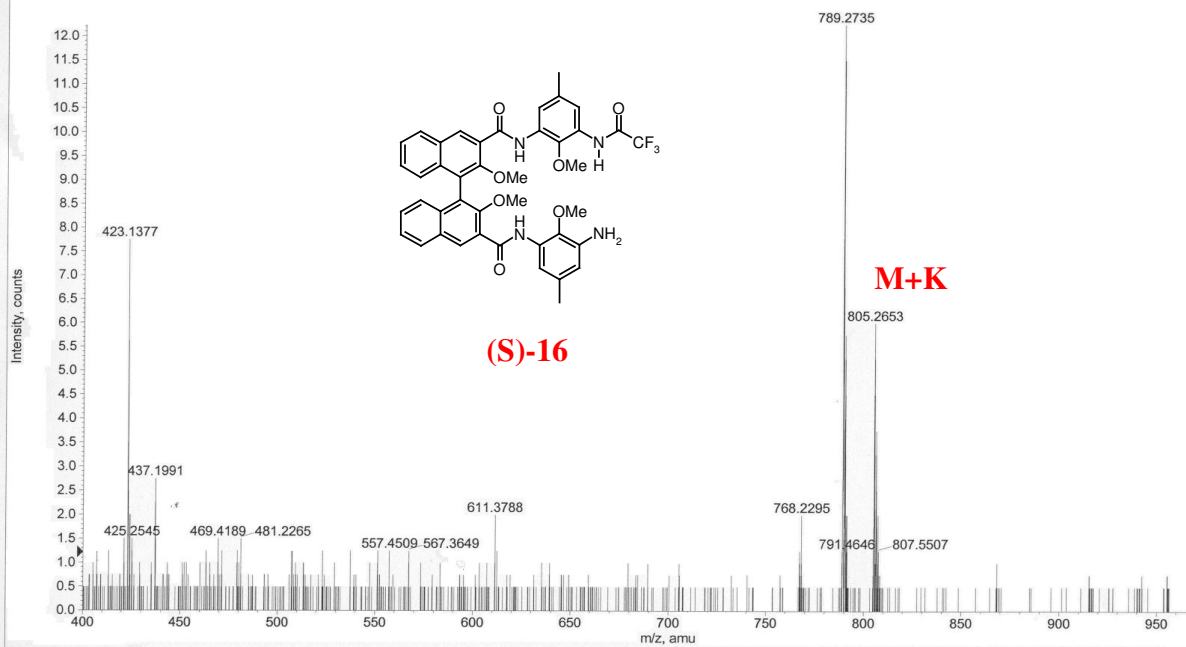


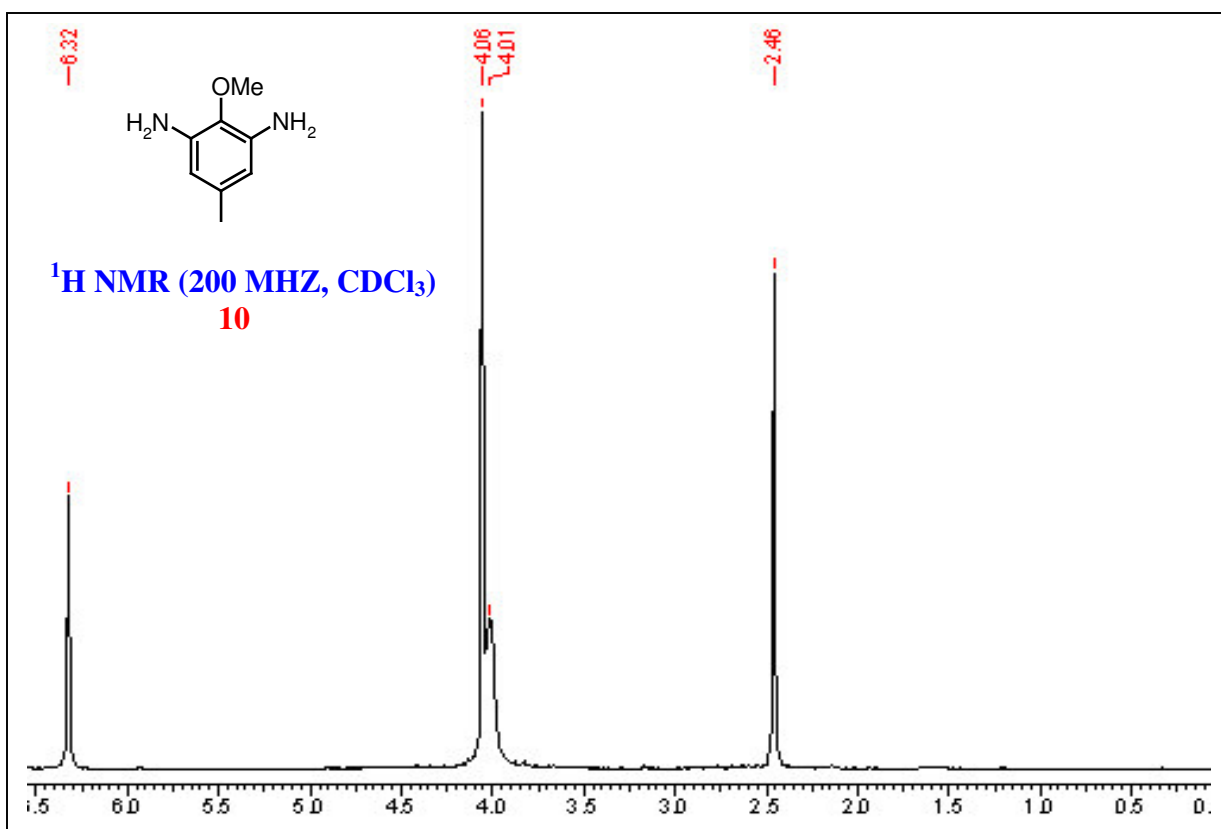
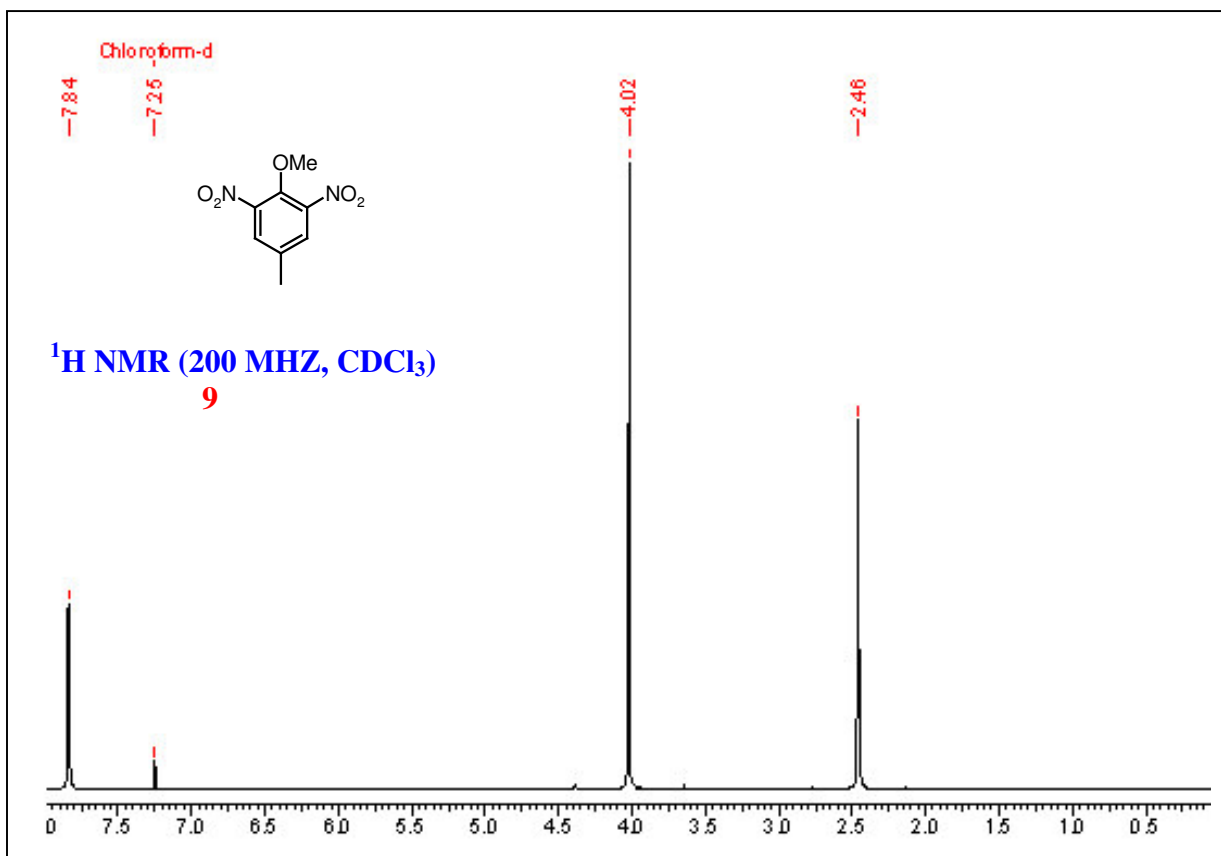


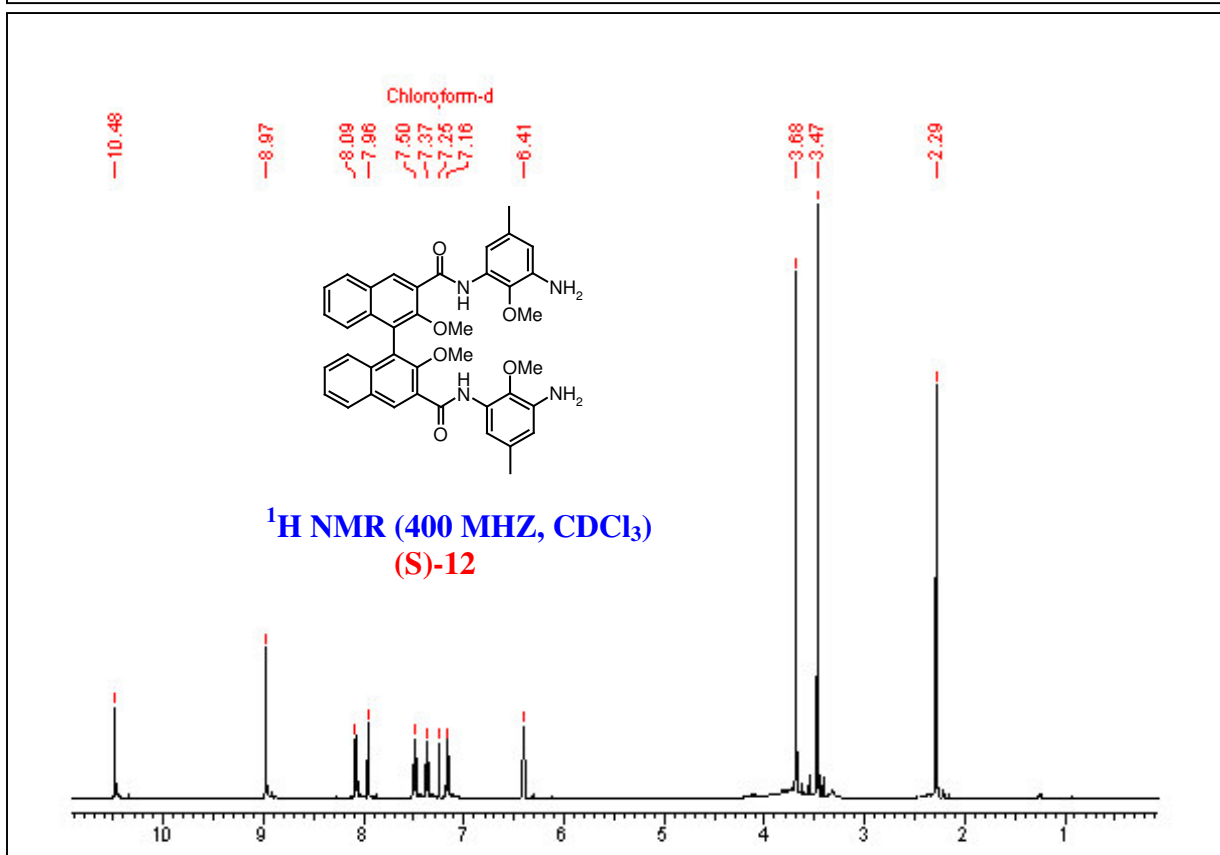
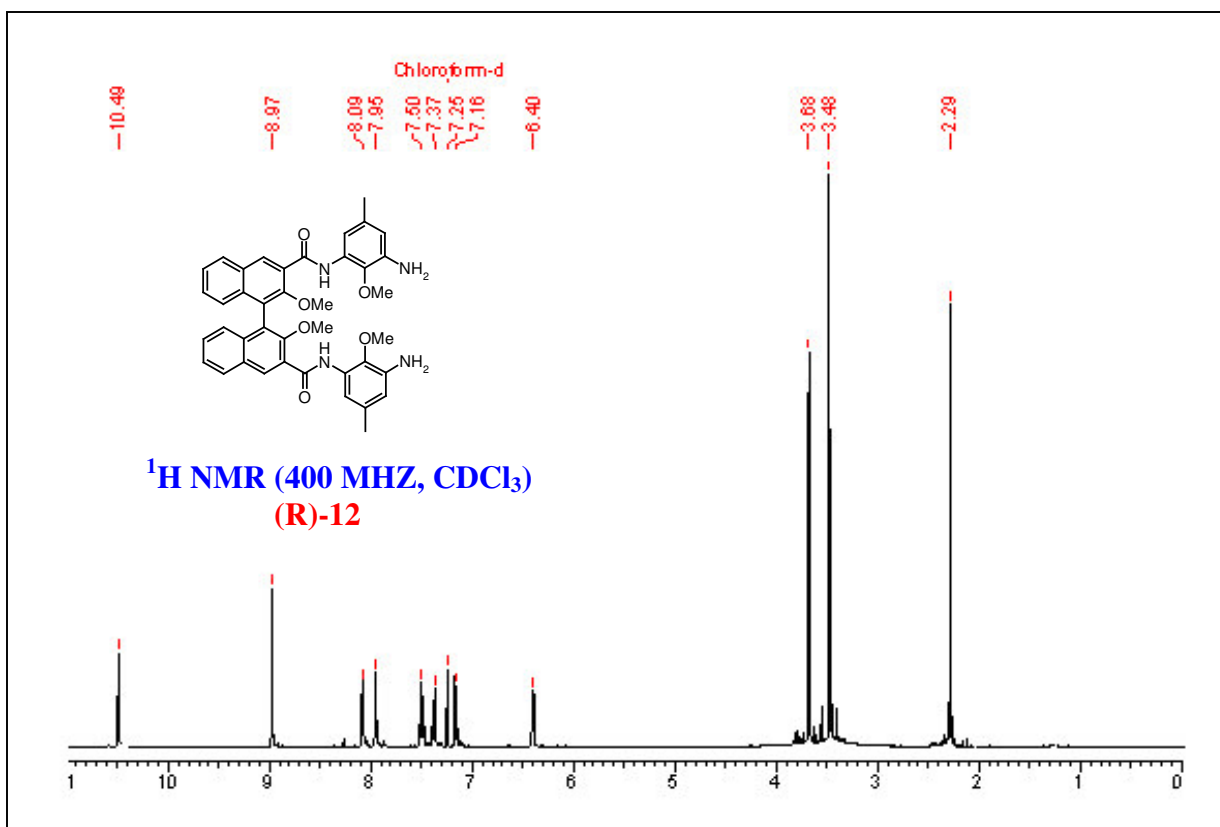
+TOF MS: 0.117 to 0.167 min from DS-S-MTFA.wiff
a=3.43121865205746020e-004, t0=-2.80342274111171720e+001

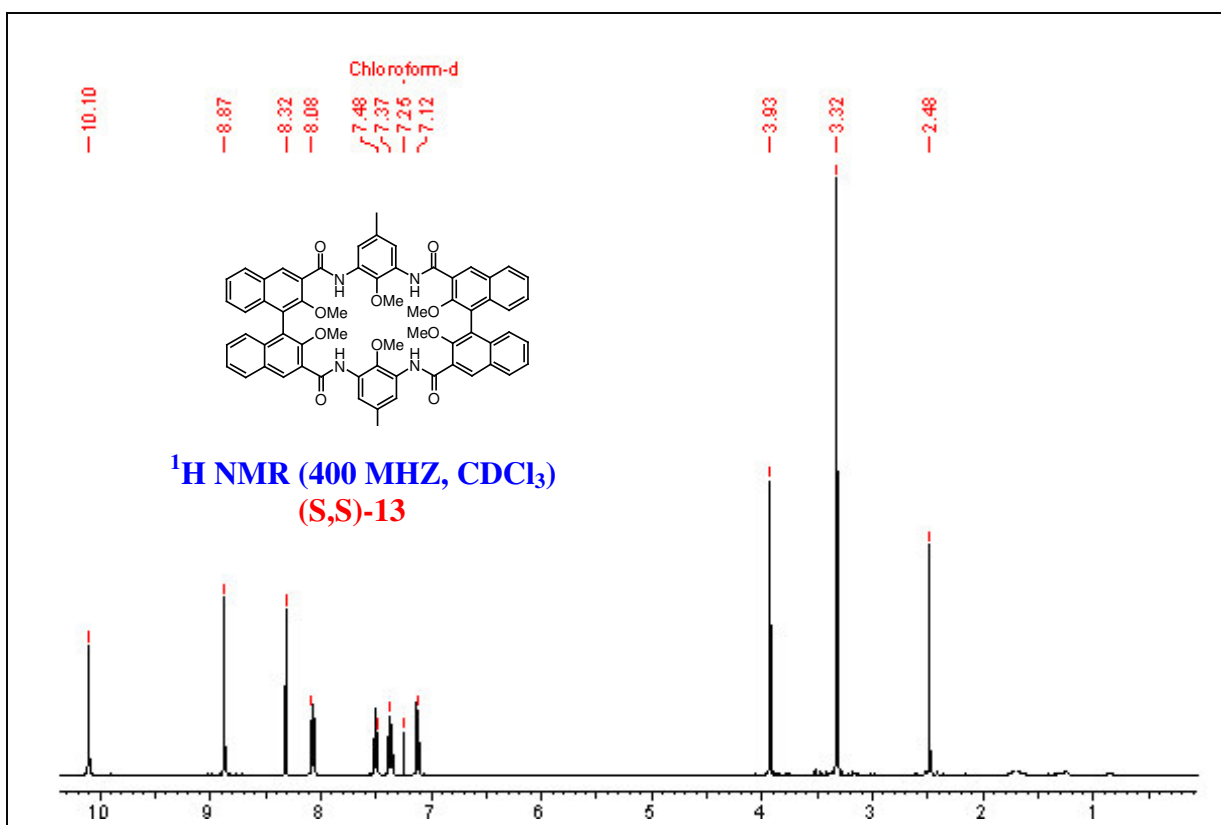
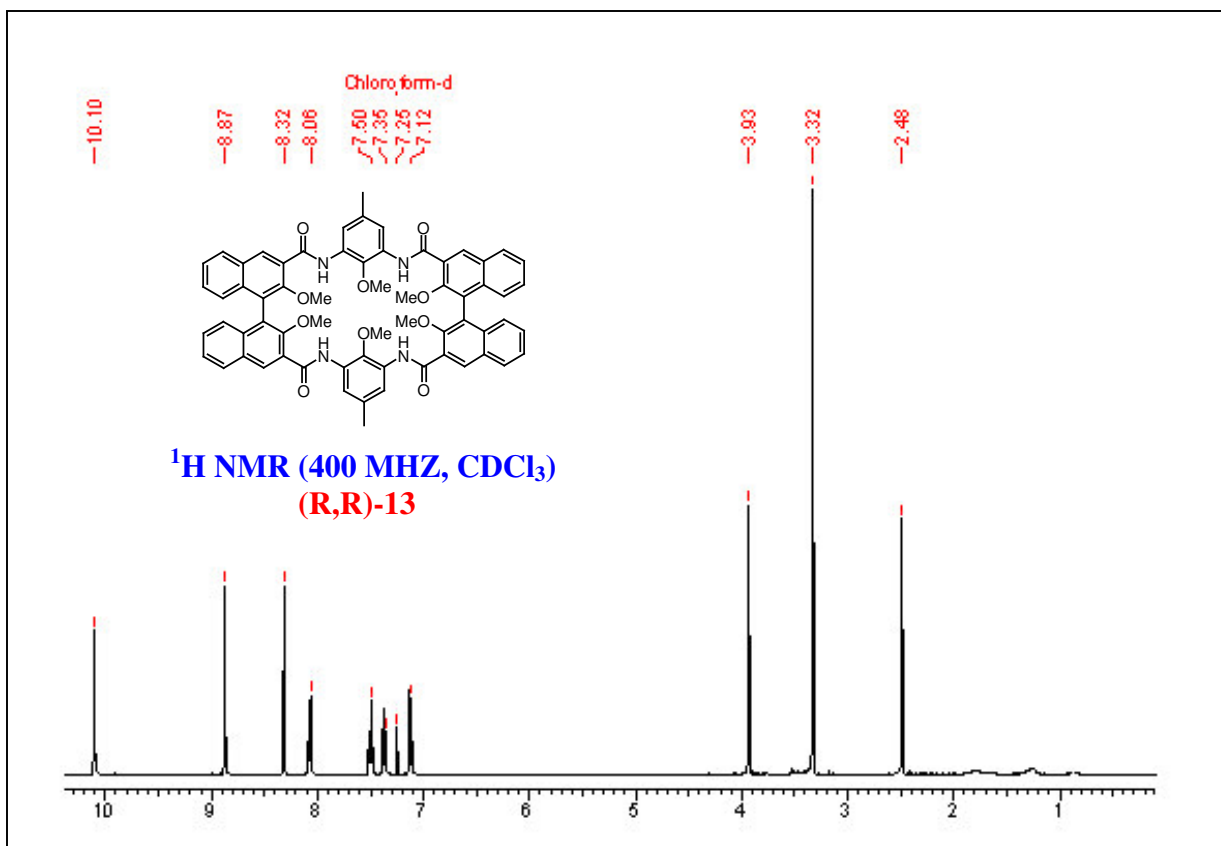
M+Na

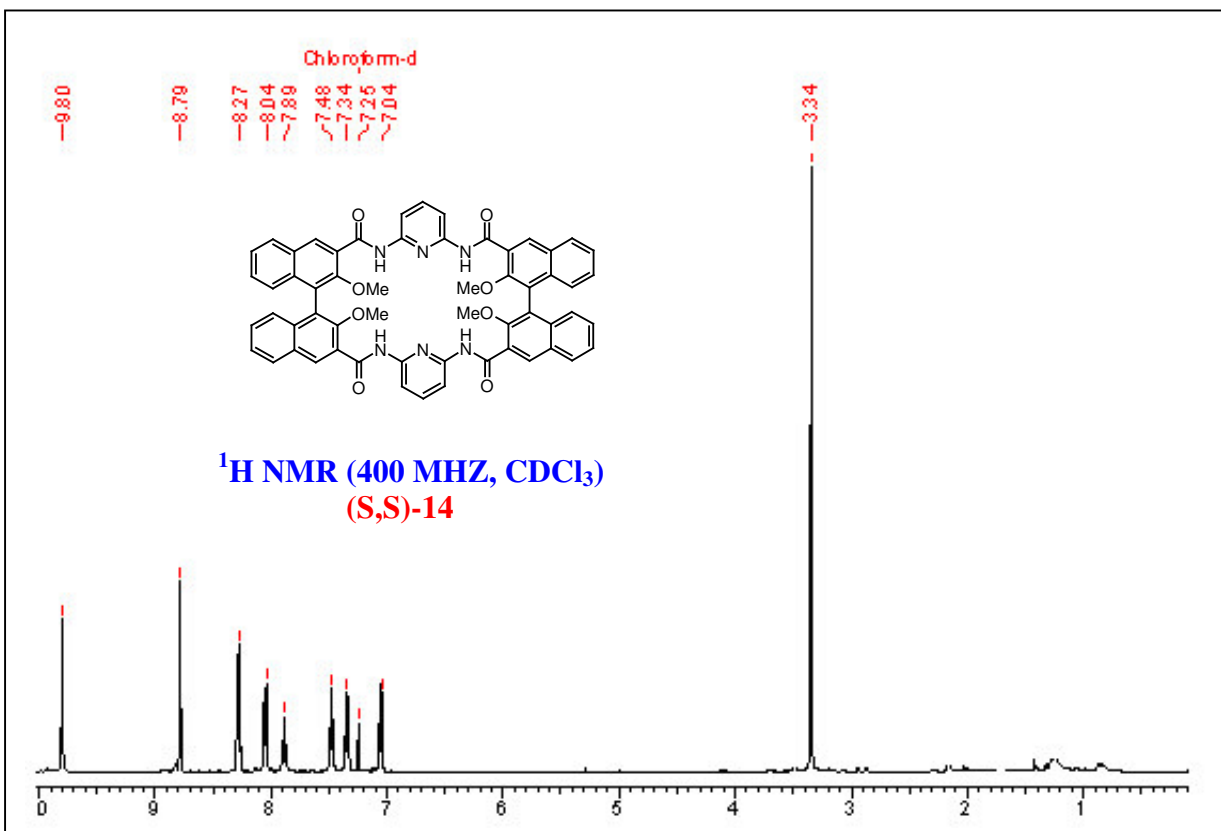
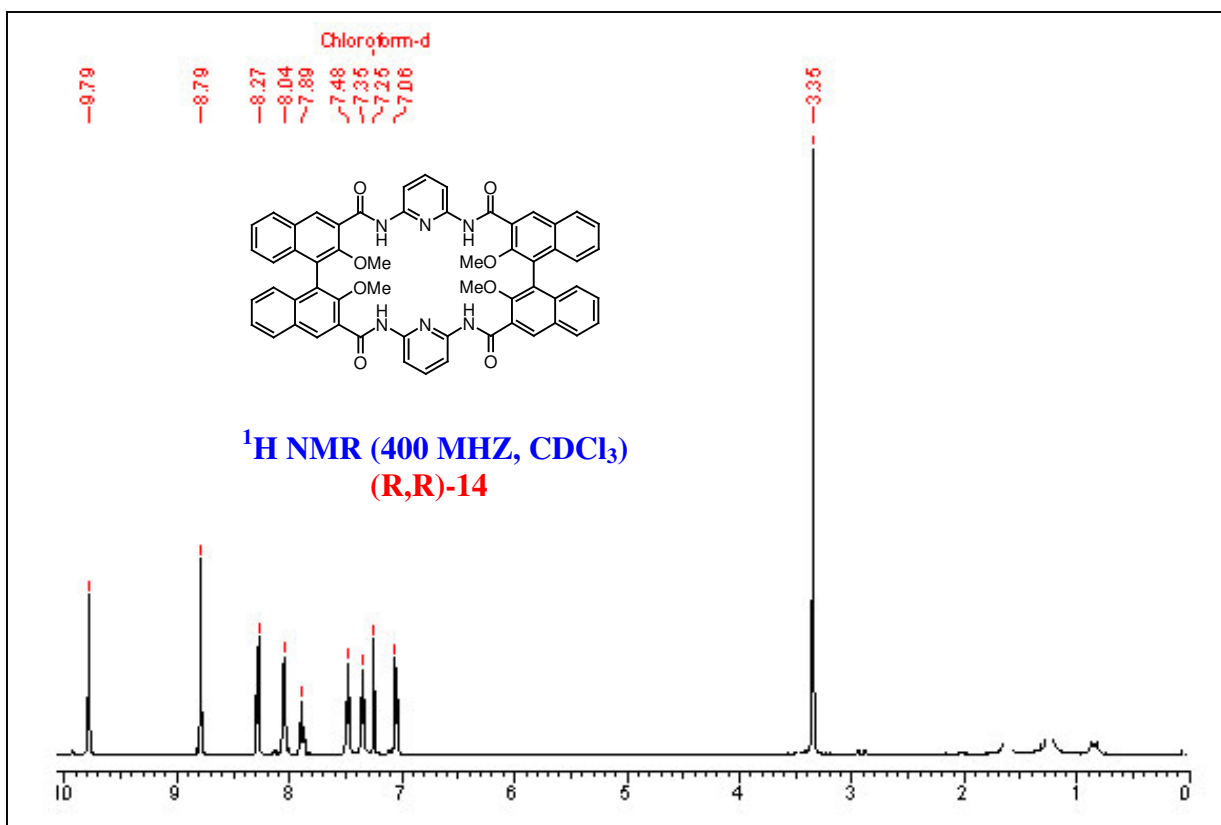
Ma>

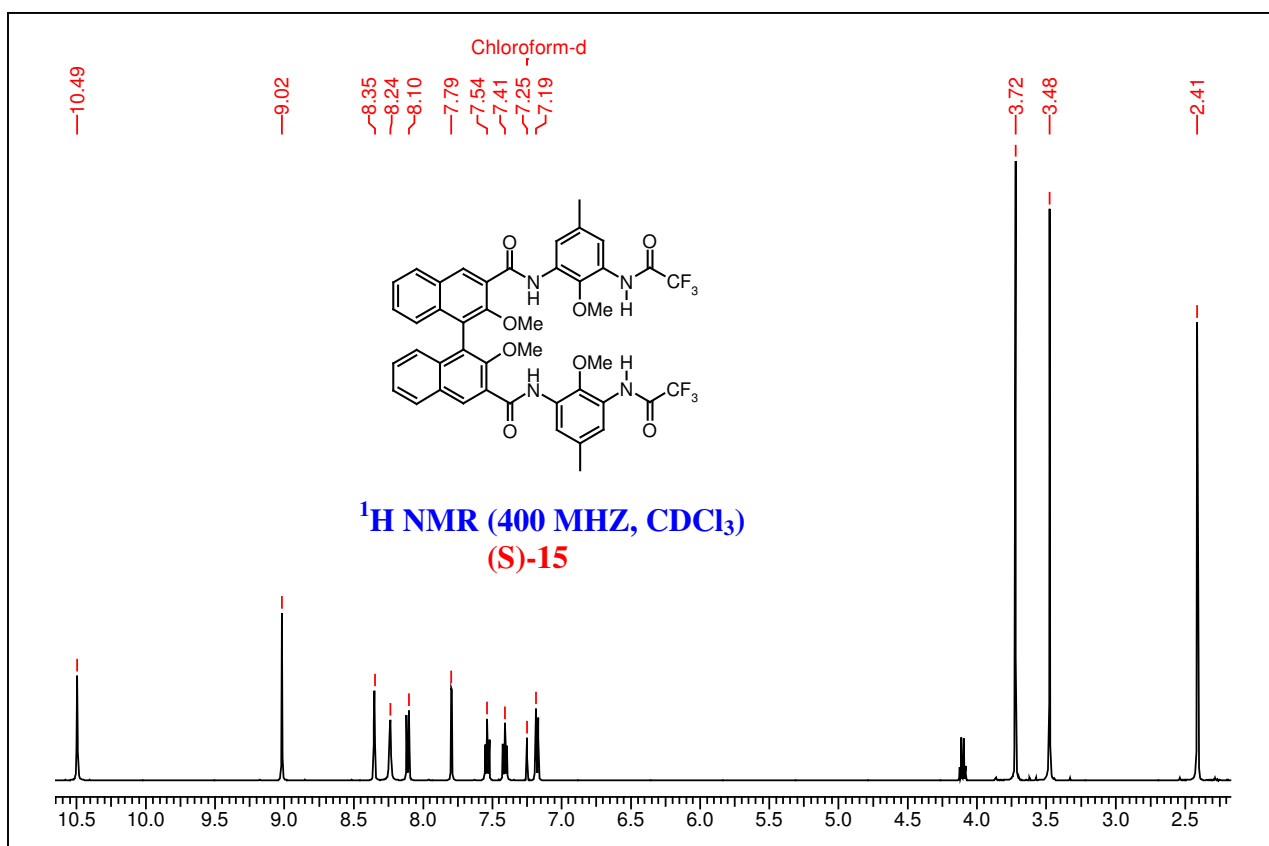
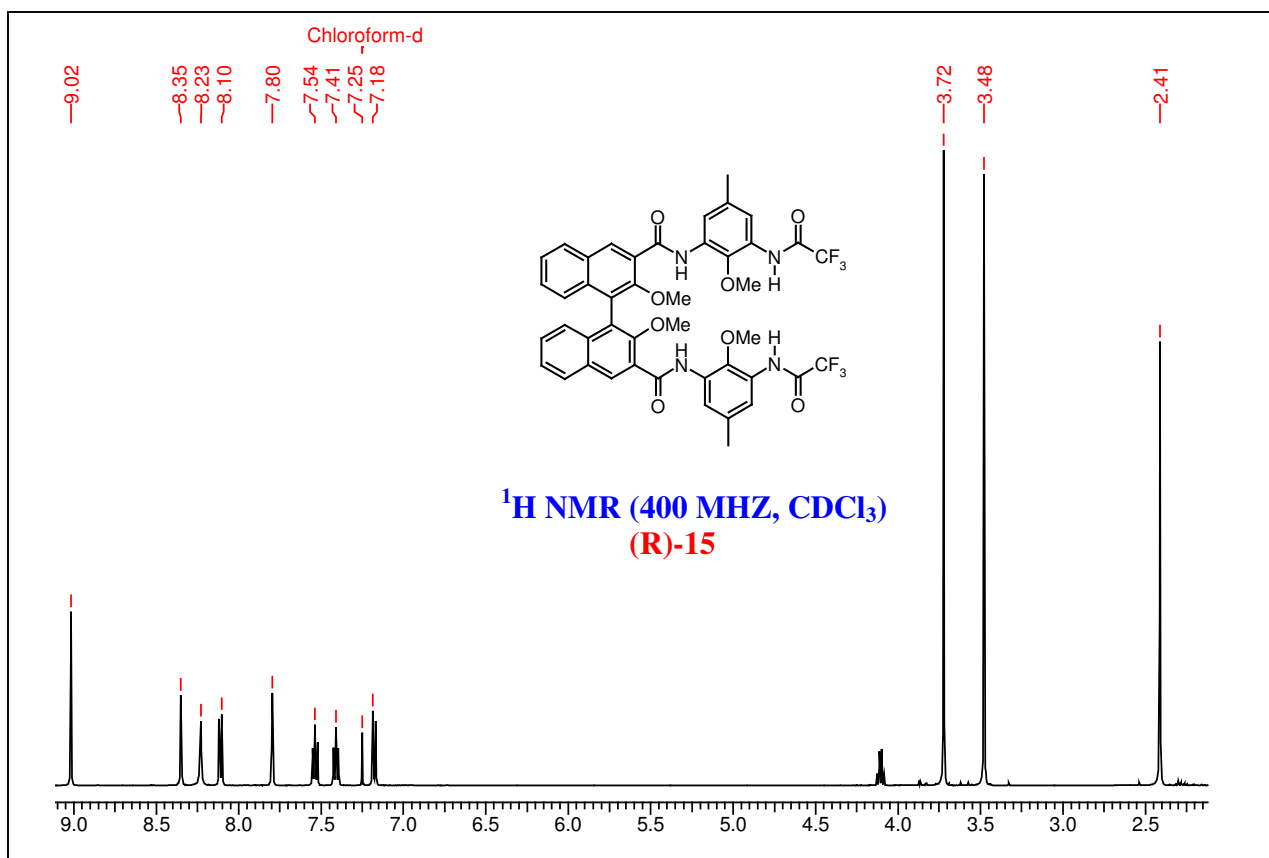


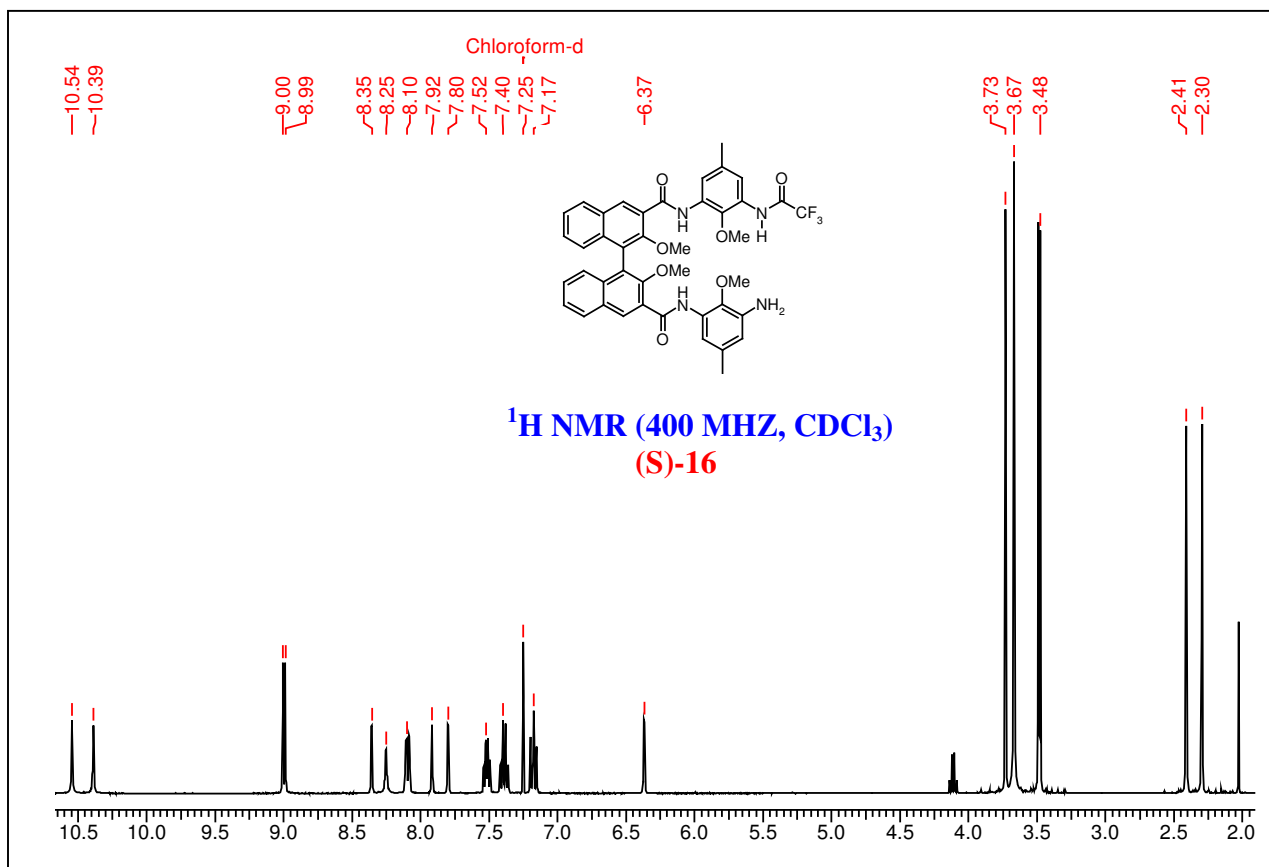
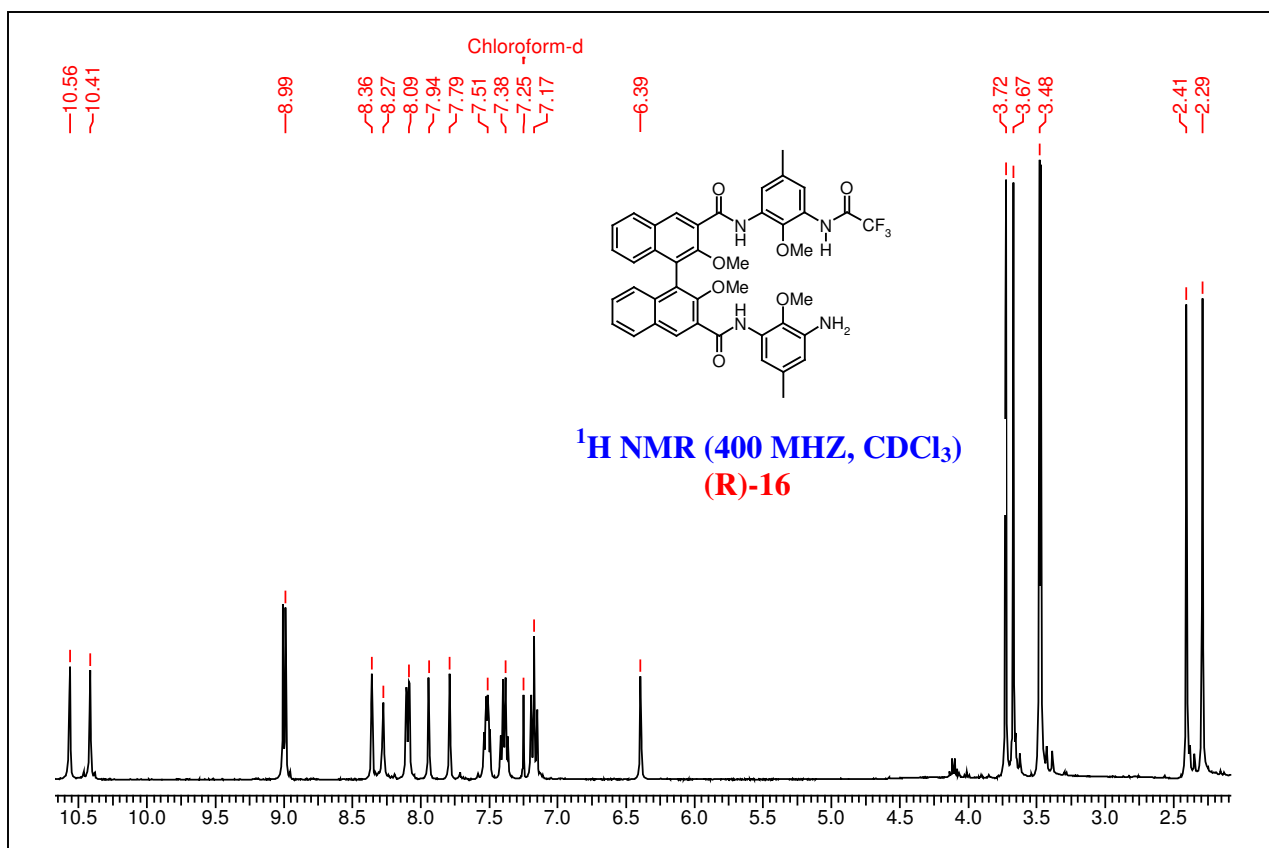


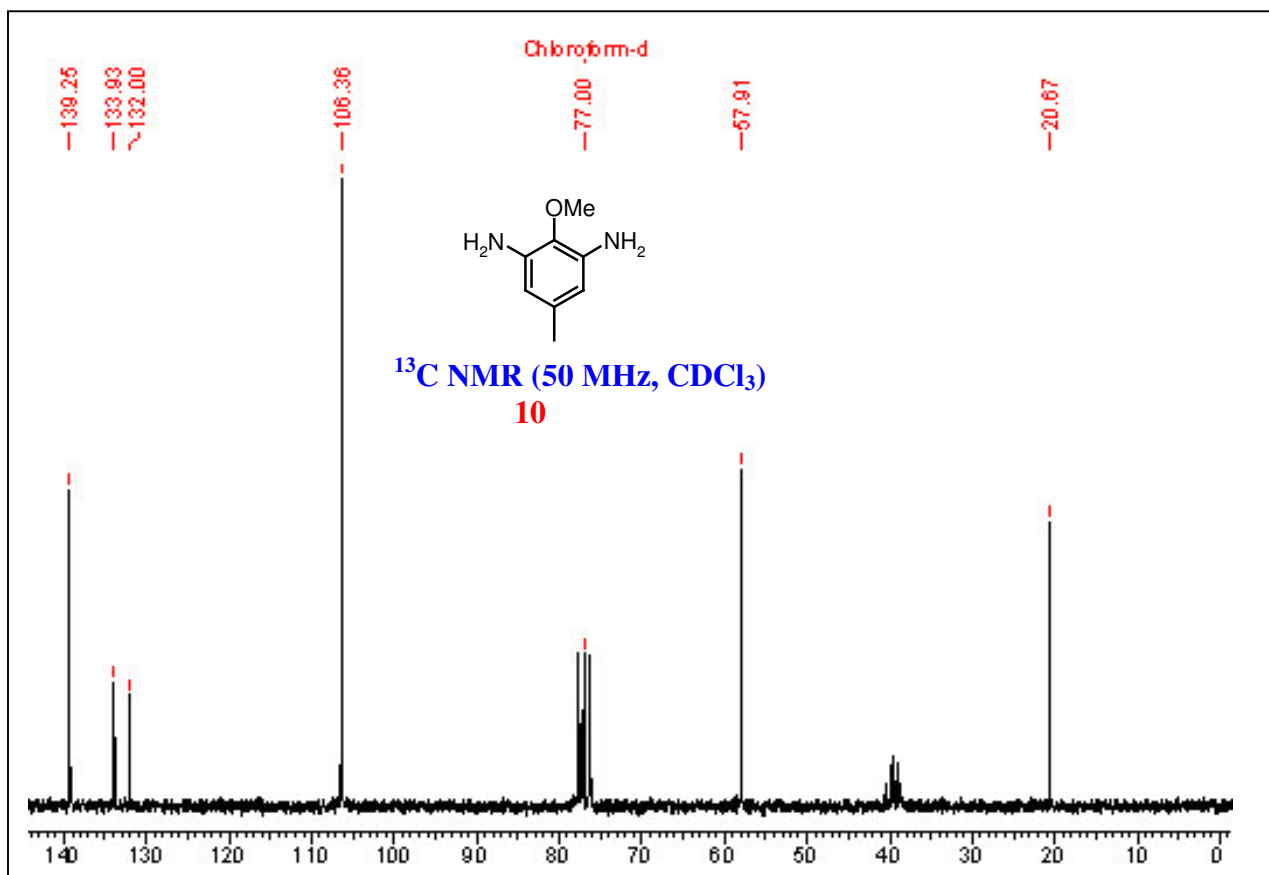
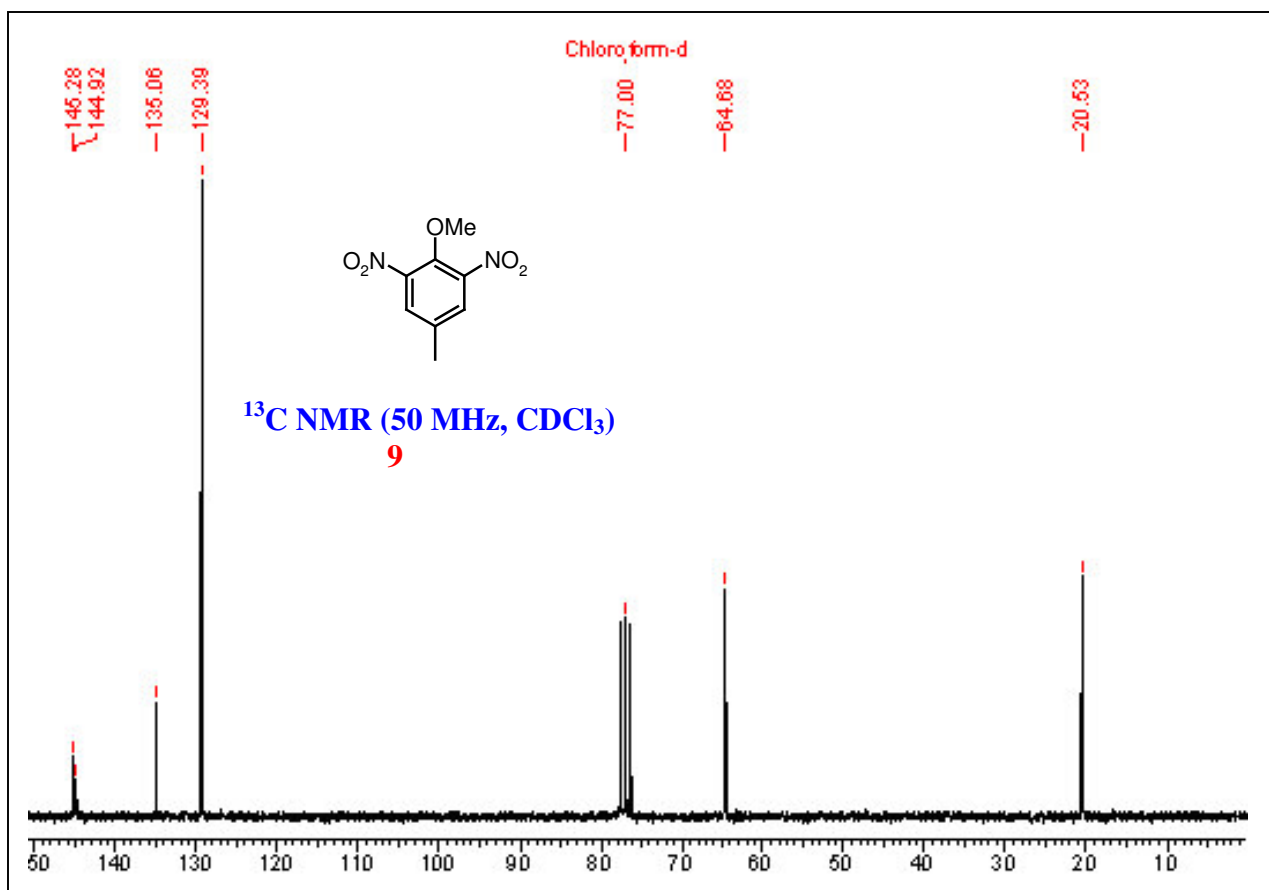


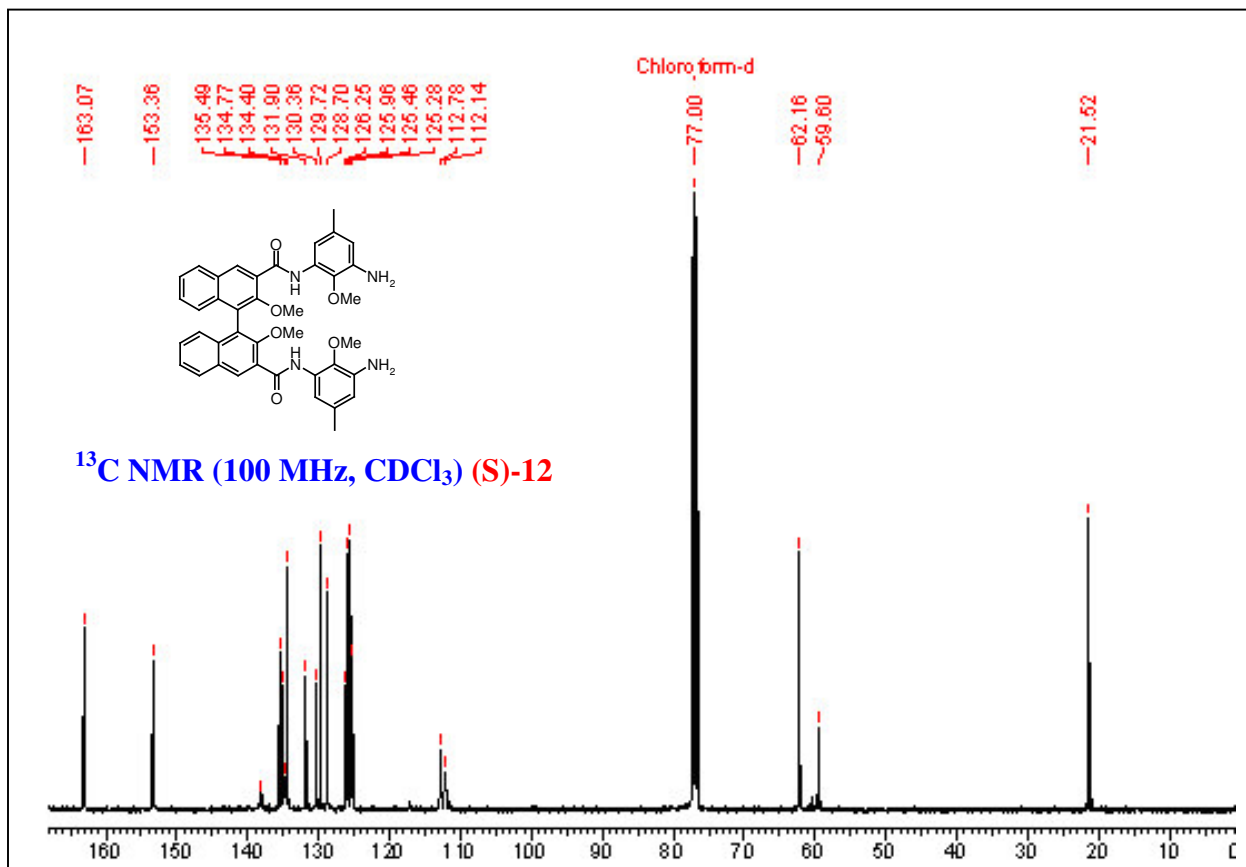
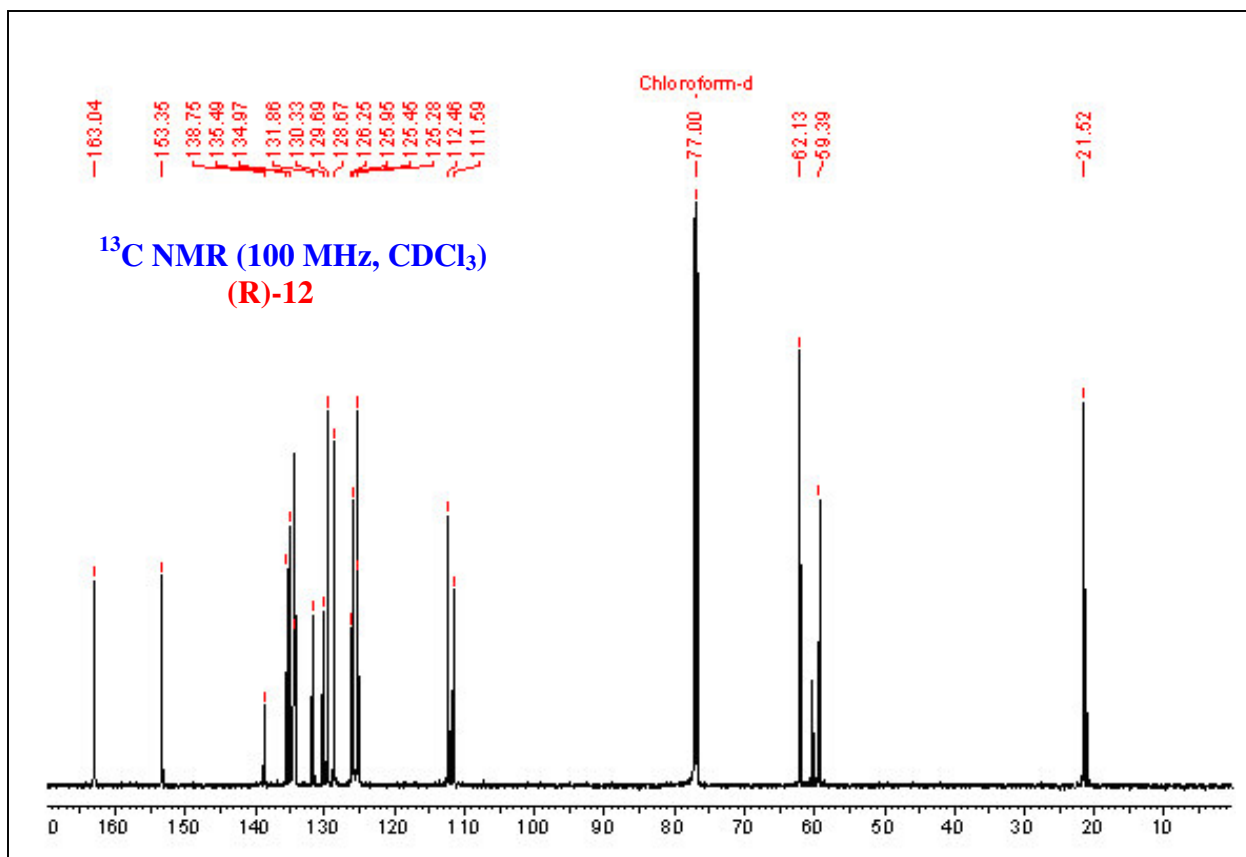


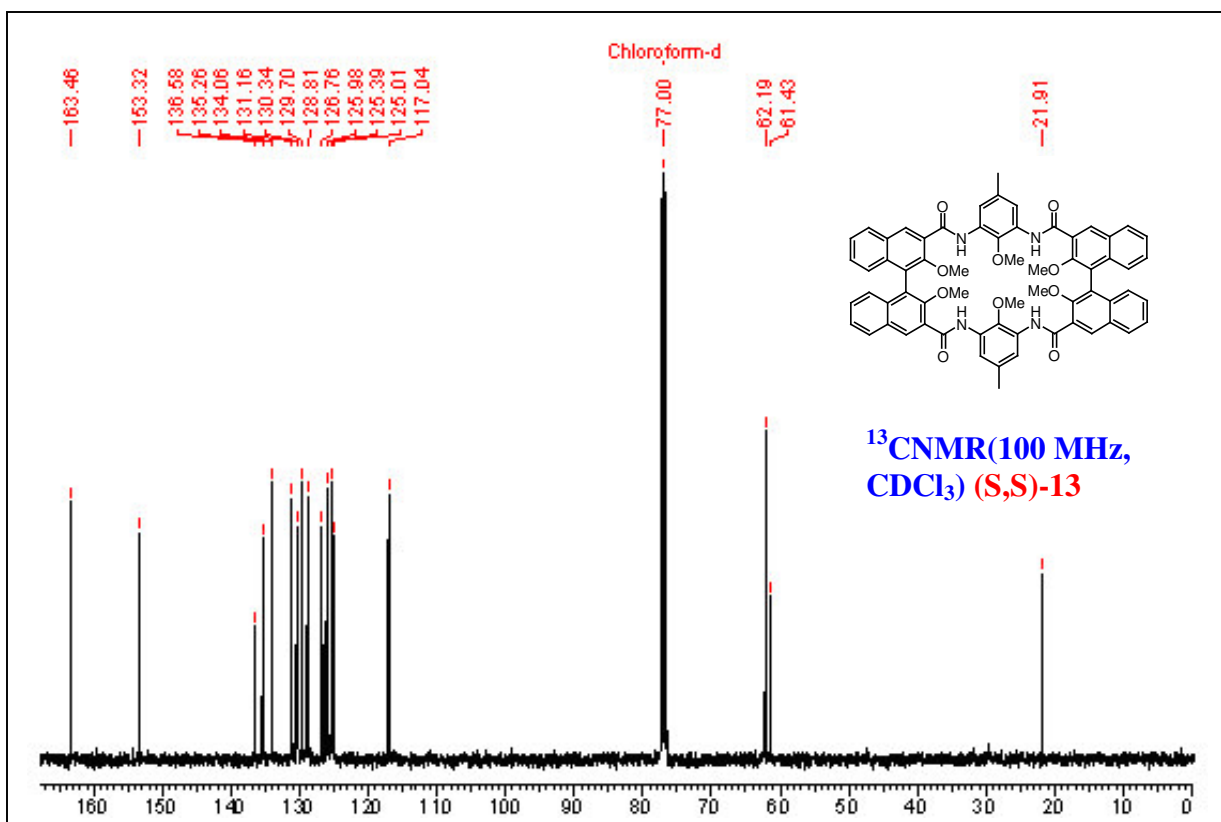
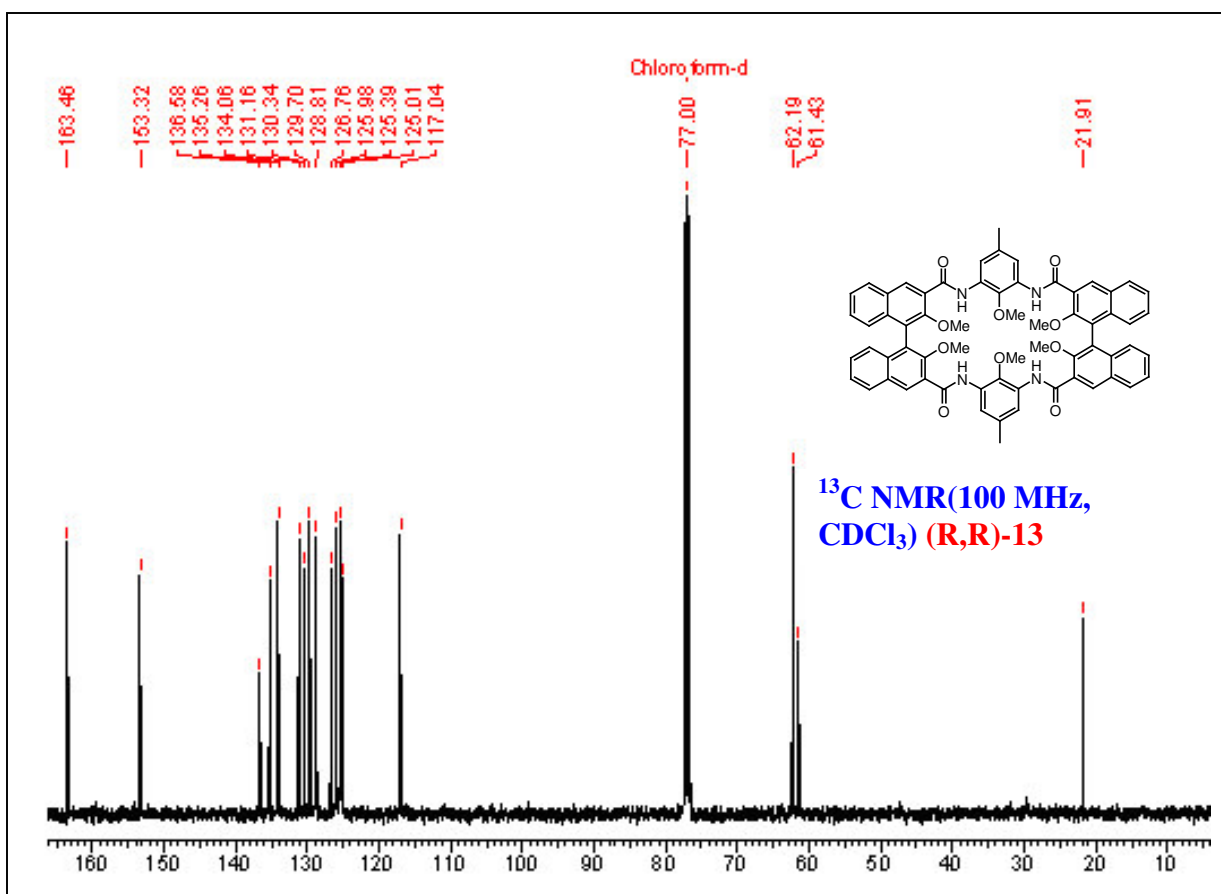


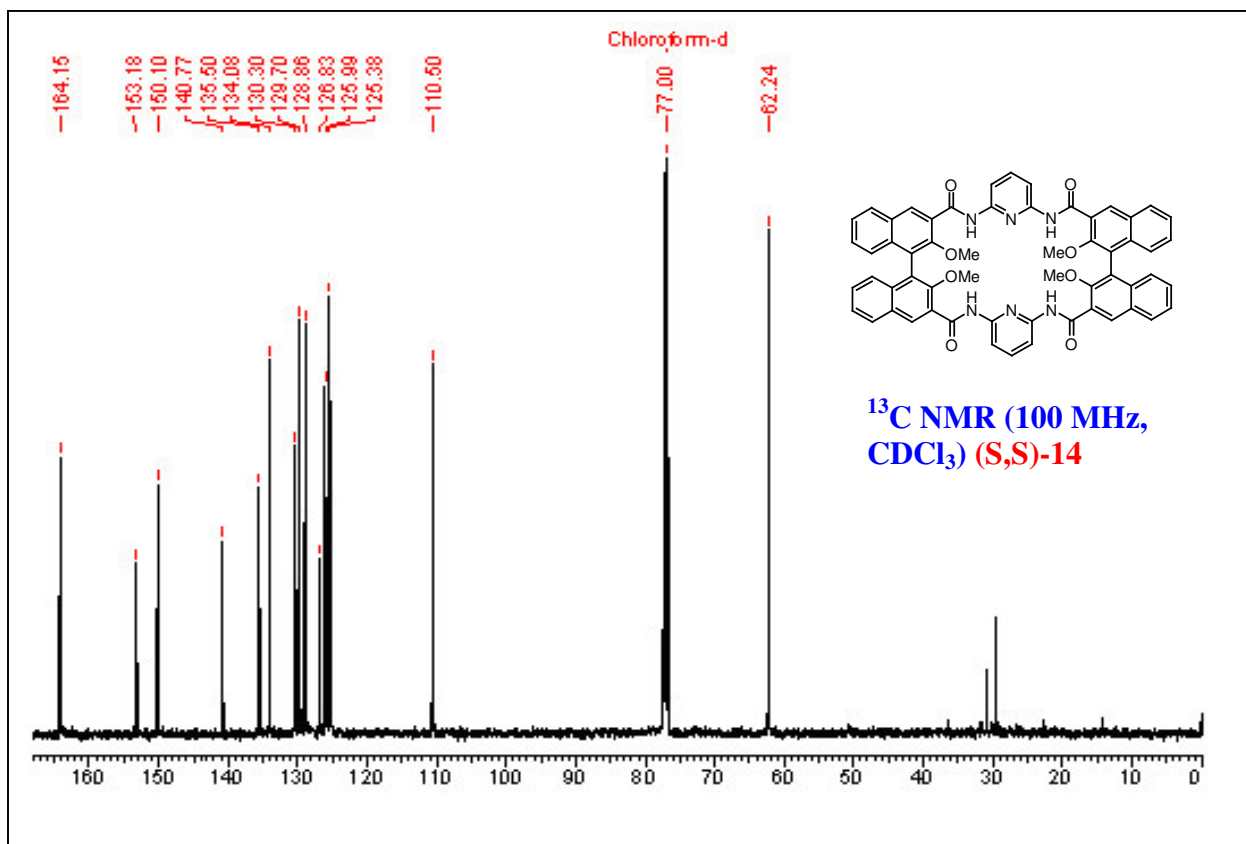
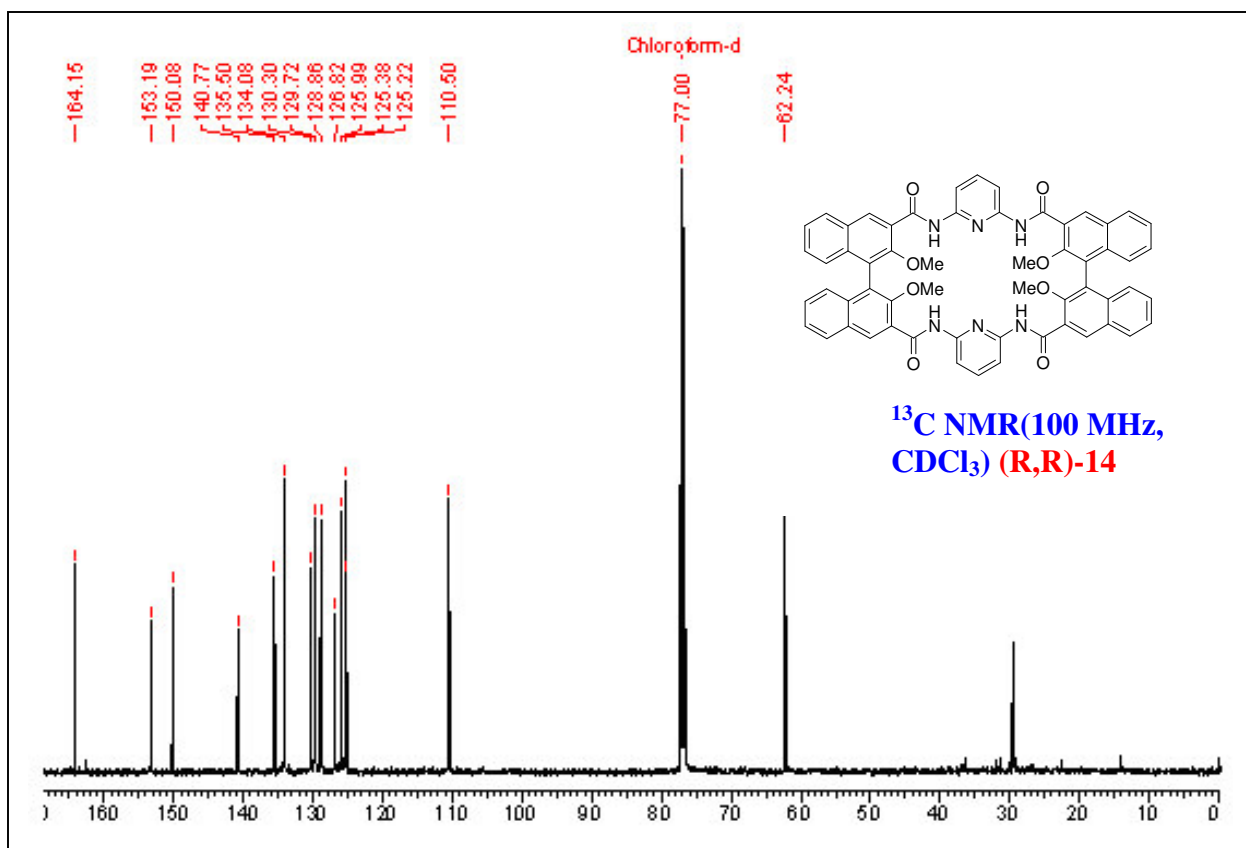


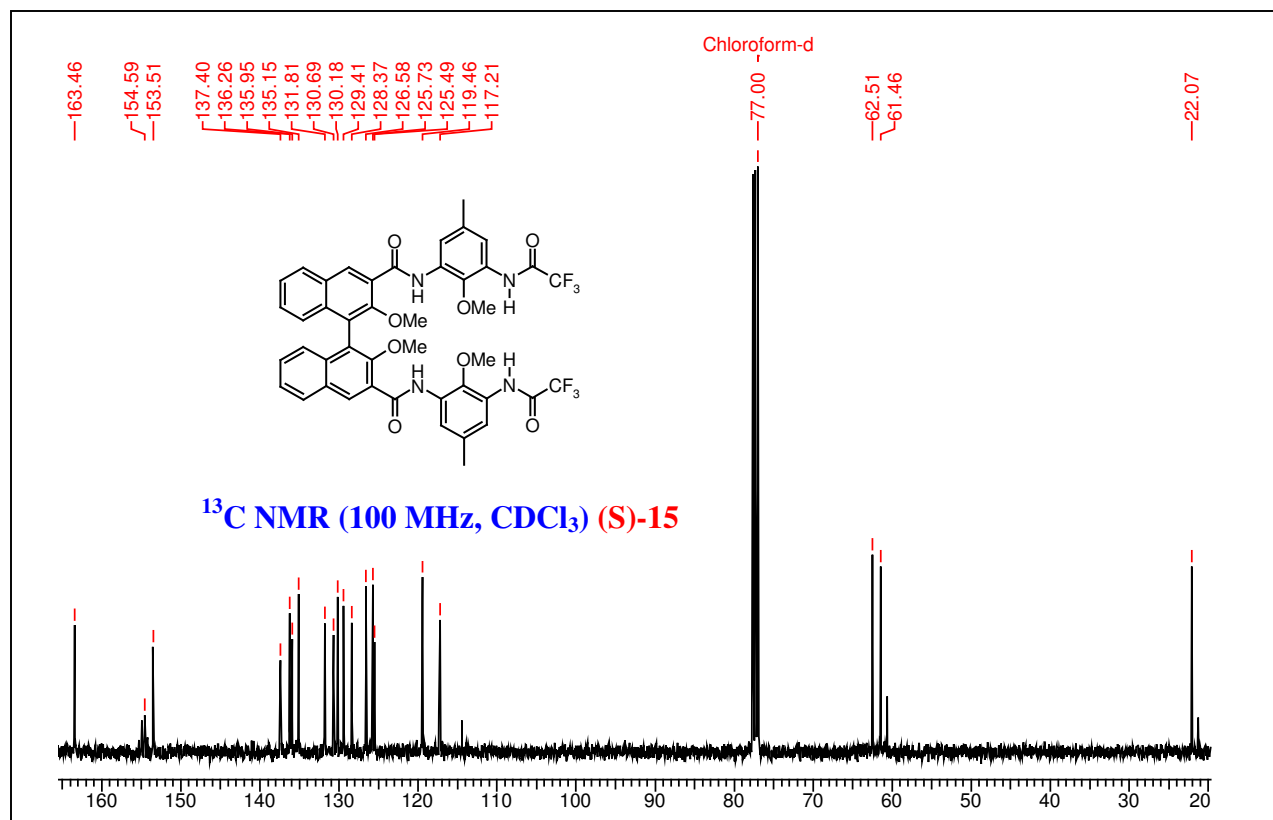
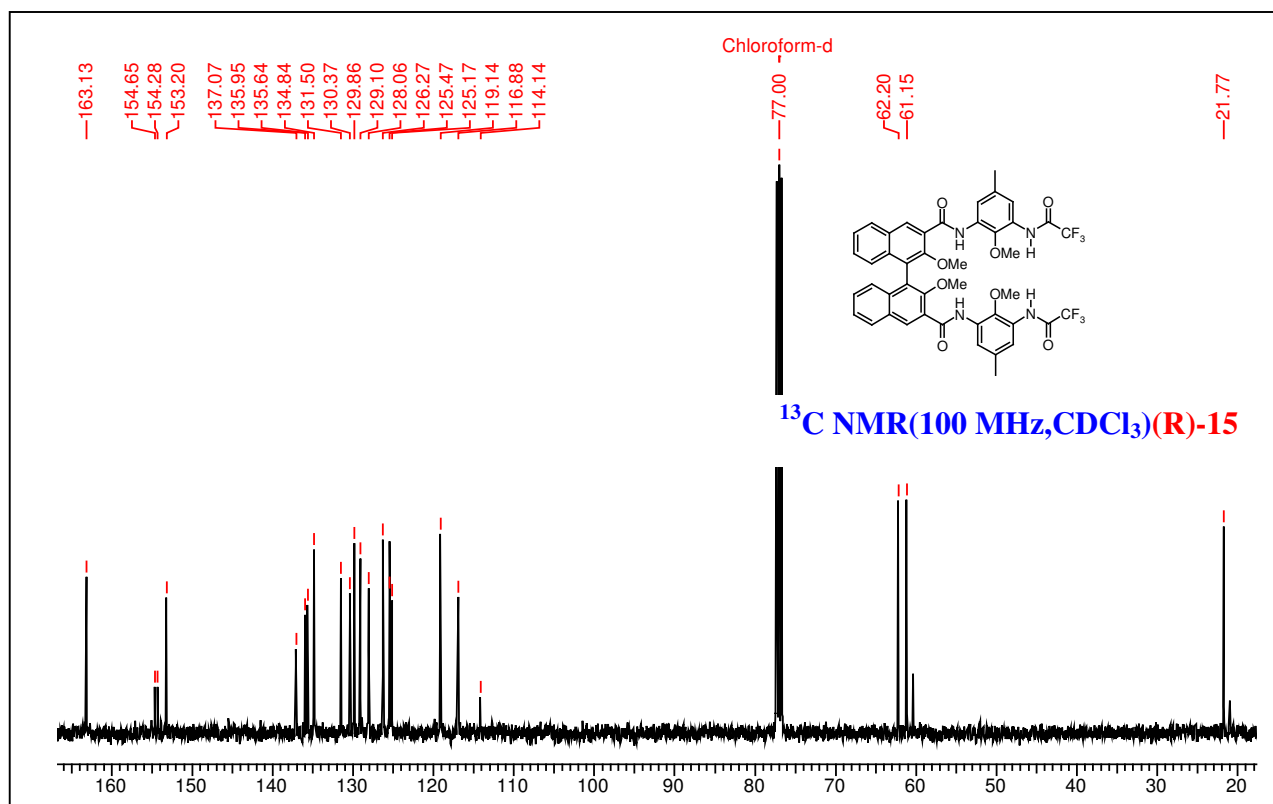












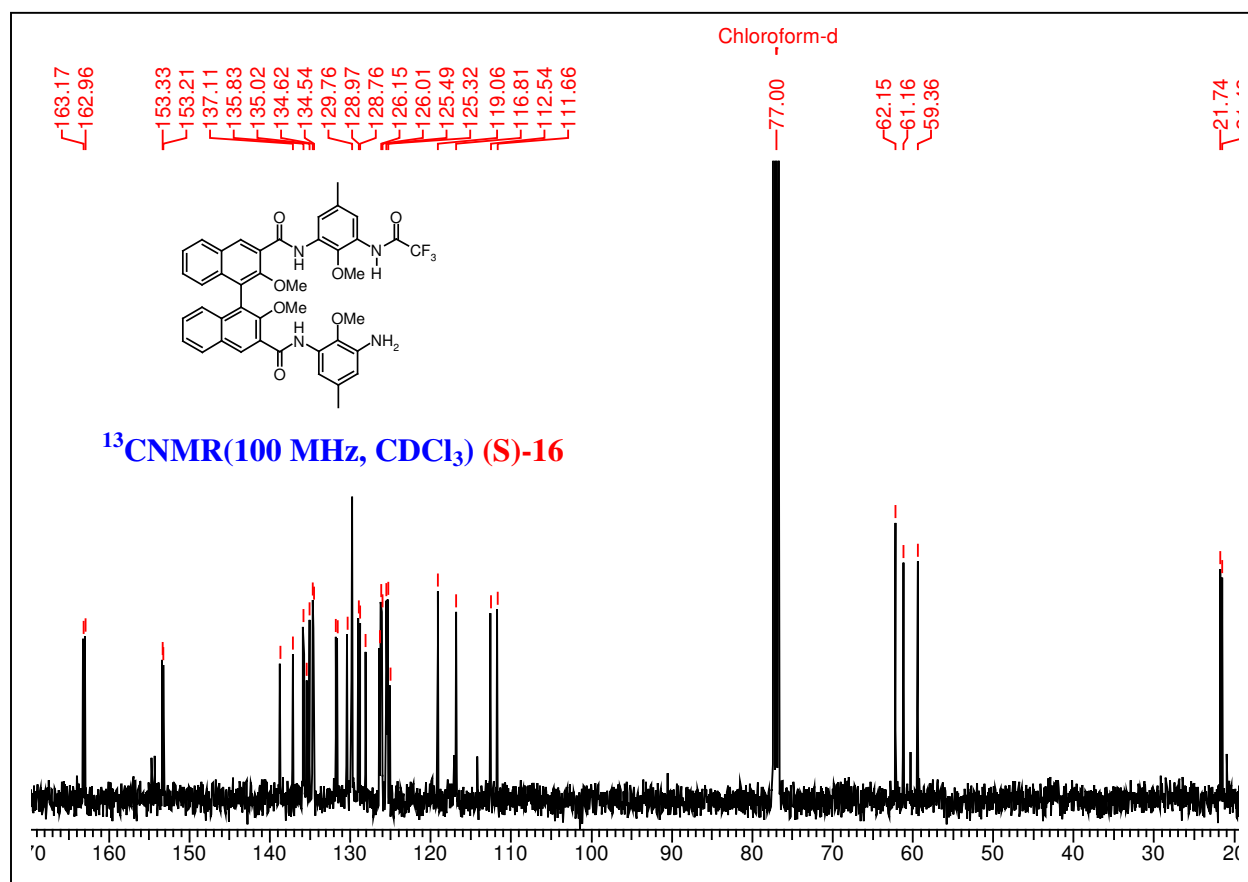
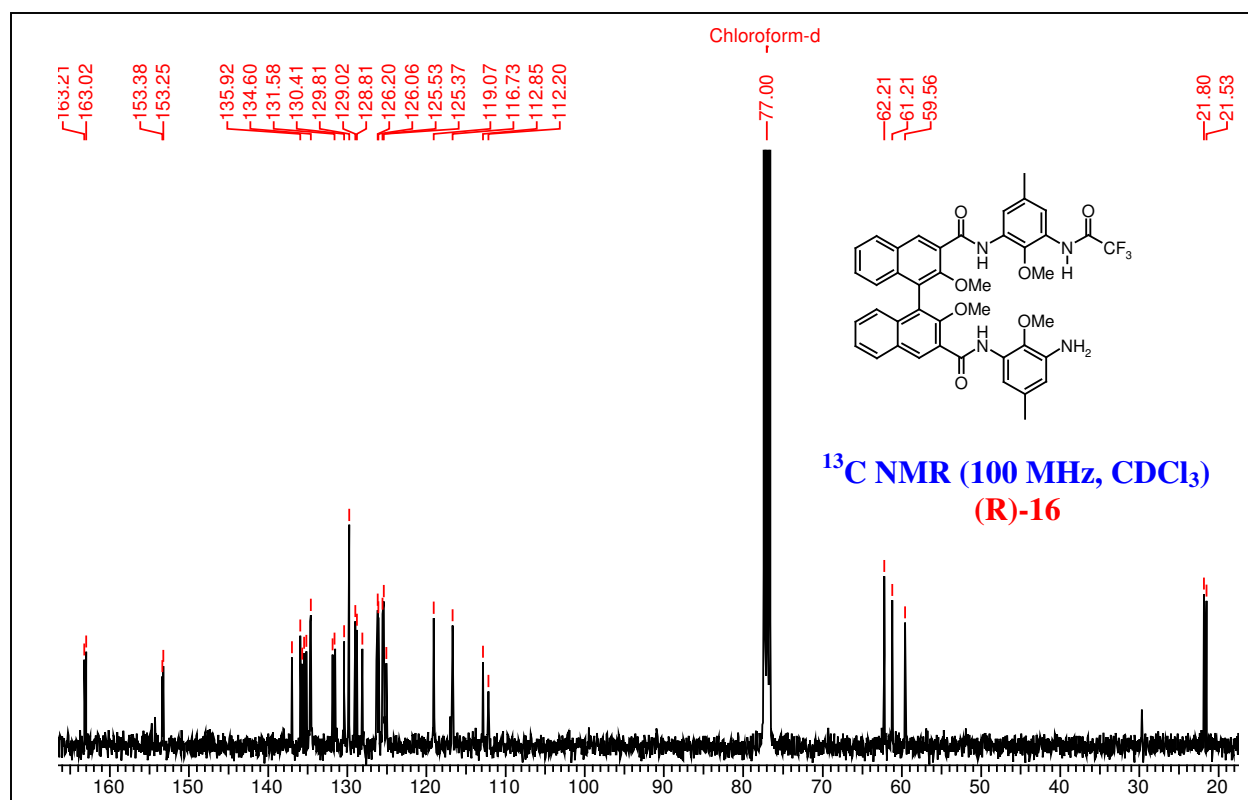


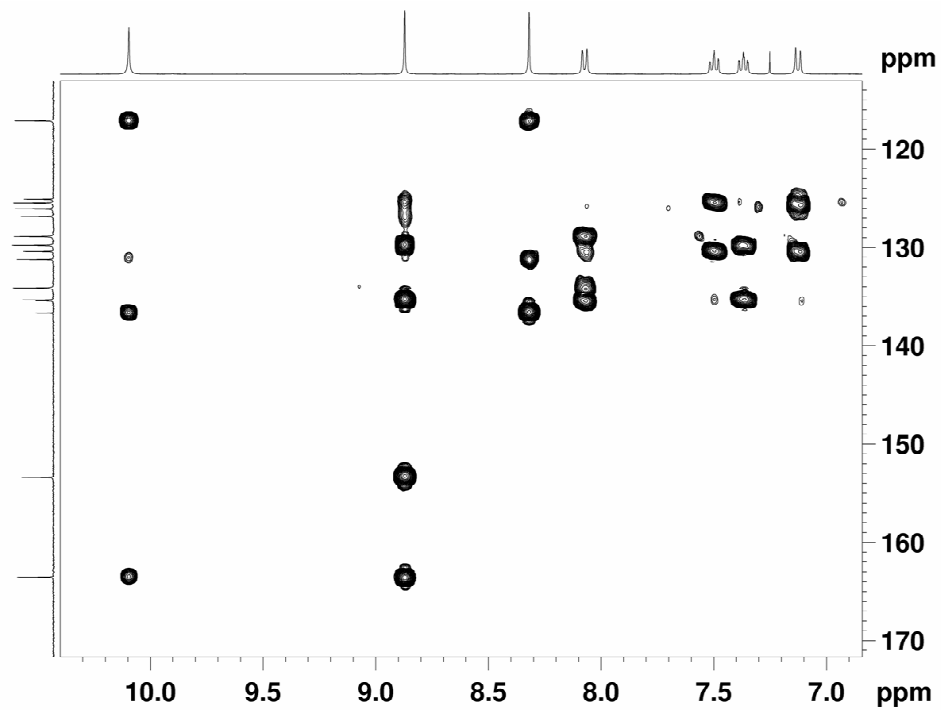
Table 1: ^1H NMR DMSO-*d*₆ Titration Experiments of the Macrocycle (S, S)-13

S.No	DMSO (μL)	NH
1	0	10.1
2	10	10.1
3	20	10.11
4	30	10.11
5	40	10.11
6	50	10.11
7	60	10.11
8	70	10.11
9	80	10.11
10	90	10.11
11	100	10.11

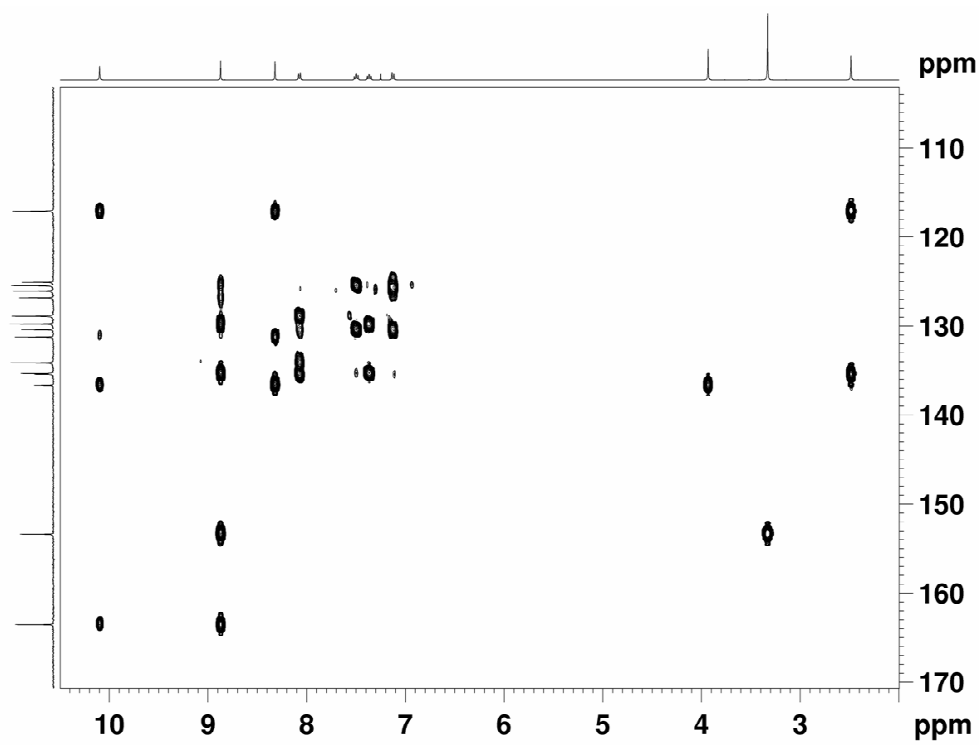
^1H NMR DMSO-*d*₆ Titration Experiments of the Macrocycle (S, S)-13: Amide proton chemical shifts as a function of the amount of DMSO-*d*₆ added in a 16.0 mM solution of the macrocycle (S, S)-13 (0.6 mL in CDCl_3).

Table 2: ^1H , ^{13}C HMBC assignments for (S, S)-13

^1H (/ppm)	^{13}C (/ppm)
10.1	163.7, 136.6, 131.19, 117.12
8.88	163.7, 153.6, 135.5, 129.76, 126.87, 125.47
8.32	136.65, 131.3, 117.1
8.07	135.36, 134.16, 130.42, 128.9
7.50	130.39, 125.38, 135.32
7.37	135.37, 129.85,
7.13	135.4, 130.44, 125.5
3.93	136.64
3.32	153.7
2.49	135.34, 117.1



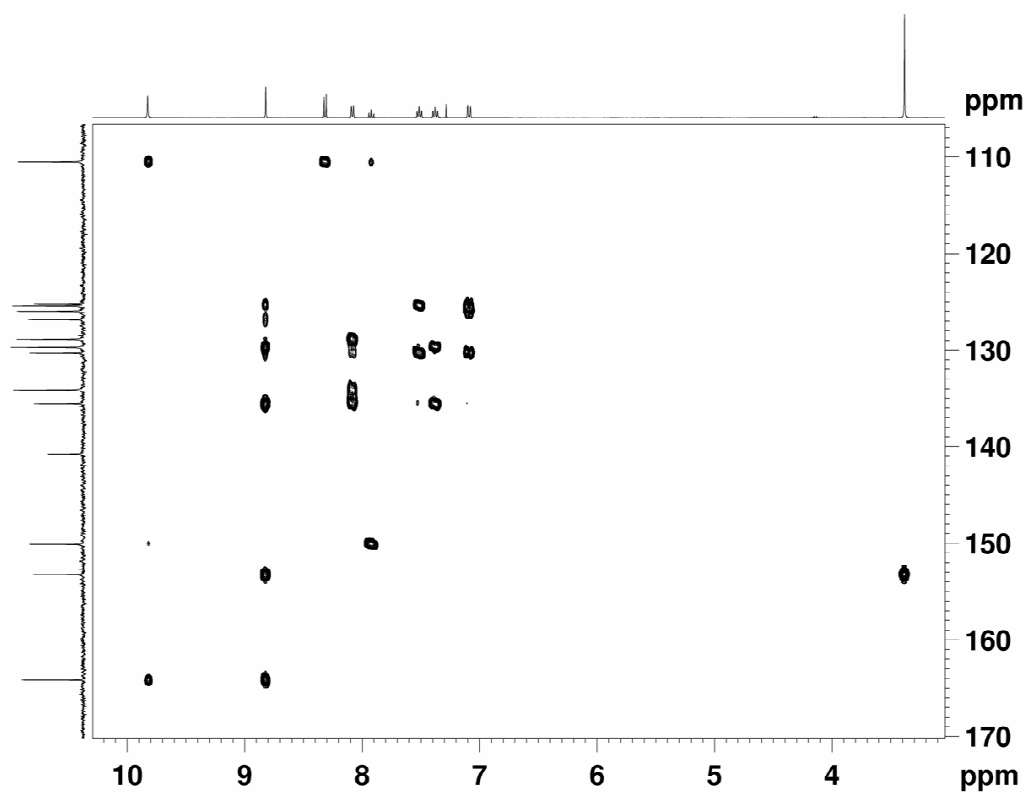
2D HMBC (^1H - ^{13}C) spectrum of (S, S)-13 (400 MHz, CDCl_3)



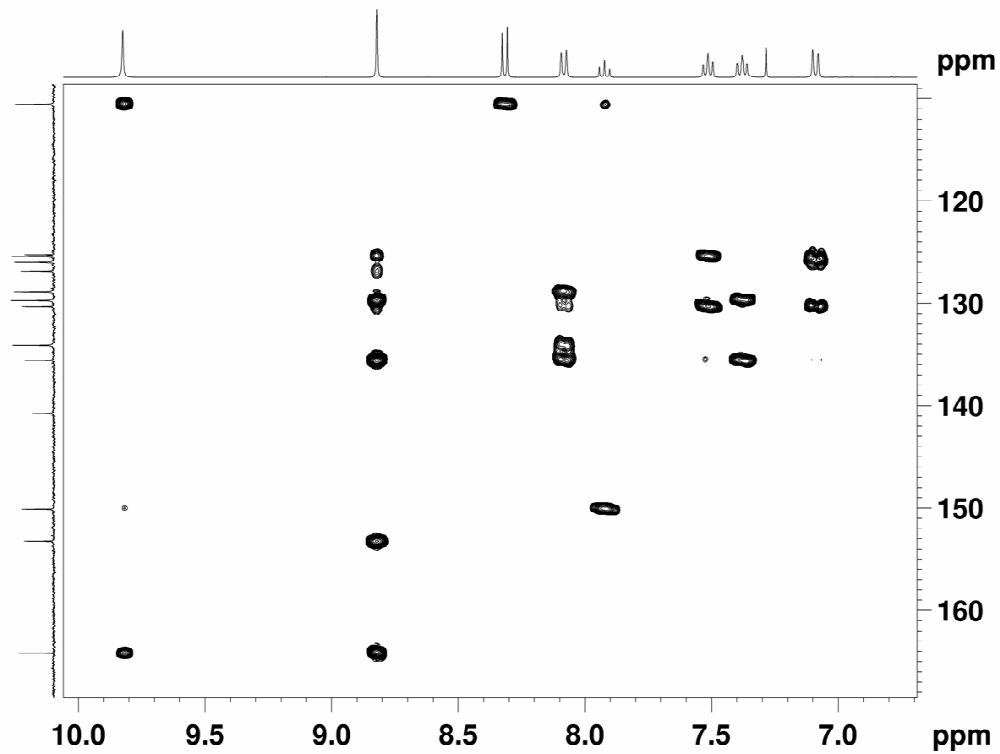
2D HMBC (^1H - ^{13}C) spectrum of (S, S)-13 (400 MHz, CDCl_3)

Table 3: ^1H , ^{13}C HMBC assignments for **(R, R)-14**

^1H (/ppm)	^{13}C (/ppm)
9.8	164.3, 150.2, 141.0, 110.6
8.82	164.3, 153.5, 135.69, 129.9, 126.84, 125.28
8.31	150.2, 140.9, 110.6
8.07	135.69, 134.5, 130.3, 125.28
7.51	130.3, 125.6
7.39	135.69, 129.9
7.10	130.33, 126.1, 125.28
3.38	153.29



2D HMBC (^1H - ^{13}C) spectrum of **(R, R)-14** (400 MHz, CDCl_3)



2D HMBC (^1H - ^{13}C) spectrum of **(R, R)-14** (400 MHz, CDCl_3)

3.6 References and notes

- (1) Gellman, S. H. *Acc. Chem. Res.* **1998**, *31*, 173.
- (2) Hill, D. J.; Mio, M. J.; Prince, R. B.; Hughes, T. S.; Moore, J. S. *Chem. Rev.* **2001**, *101*, 3893.
- (3) Huc, I. *Eur. J. Org. Chem.* **2004**, 17-19.
- (4) (a) Gong, B. *Chem. Eur. J.* **2001**, *7*, 4336; (b) Sanford, A. R.; Yamato, K.; Yuan, L.; Han, Y.; Gong, B. *Eur. J. Biochem.* **2004**, *271*, 1416.
- (5) Seebach, D.; Overhand, M.; Kuhnle, F. N. M.; Martinoni, B.; Oberer, L.; Hommel, U.; Widmer, H. *Helv. Chim. Acta* **1996**, *79*, 913.
- (6) Seebach, D.; Matthews, J. L. *Chem. Commun.* **1997**, 2015.
- (7) (a) Hamuro, Y.; Geib, S. J.; Hamilton, A. D. *J. Am. Chem. Soc.* **1997**, *119*, 10587; (b) Berl, V.; Khoury, R. G.; Huc, I.; Krische, M. J.; Lehn, J.-M. *Nature* **2000**, *407*, 720; (c) Huc, I.; Maurizot, V.; Gornitzka, H.; Leger, J. M. *Chem. Commun.* **2002**, 578; (d) Jiang, H.; Leger, J. M.; Huc, I. *J. Am. Chem. Soc.* **2003**, *125*, 3448. (e) Jiang, H.; Dolain, C.; Leger, J. M.; Gornitzka, H.; Huc, I. *J. Am. Chem. Soc.* **2004**, *126*, 1034; (f) Yi, H. P.; Shao, X. B.; Hou, J. L.; Li, C.; Jiang, X. K.; Li, Z. T. *New J. Chem.* **2005**, *29*, 1213; (g) Ernst, J. T.; Becerril, J.; Park, H. S.; Yin, H.; Hamilton, A. D. *Angew. Chem. Int. Ed.* **2003**, *42*, 535.
- (8) (a) Garrett, T. M.; Koert, U.; Lehn, J.-M.; Rigault, A.; Meyer, D.; Fischer, J. *J. Chem. Soc., Chem. Commun.* **1990**, 557; (b) Lehn, J. M. *Supramolecular Chemistry*; VCH: Weinheim, Germany, 1995, and references therein. (c) Lehn, J.-M.; Rigault, A. *Angew. Chem., Int. Ed. Engl.* **1988**, *27*, 1095.

- (9) (a) Heemstra, J. M.; Moore, J. S. *J. Am. Chem. Soc.* **2004**, *126*, 1648; (b) Oh, K.; Jeong, K. S.; Moore, J. S. *J. Org. Chem.* **2003**, *68*, 8397; (c) Matsuda, K.; Stone, M. T.; Moore, J. S. *J. Am. Chem. Soc.* **2002**, *124*, 11836; (d) Brunsveld, L.; Meijer, E. W.; Prince, R. B.; Moore, J. S. *J. Am. Chem. Soc.* **2001**, *123*, 7978; (e) Lahiri, S.; Thompson, J. L.; Moore, J. S. *J. Am. Chem. Soc.* **2000**, *122*, 11315; (f) Prest, P. J.; Prince, R. B.; Moore, J. S. *J. Am. Chem. Soc.* **1999**, *121*, 5933.
- (10) Hill, D. J.; Mio, M. J.; Prince, R. B.; Hughes, T. S.; Moore, J. S. *Chem. Rev.* **2001**, *101*, 3893-4011.
- (11) (a) Hamuro, Y.; Geib, S. J.; Hamilton, A. D. *J. Am. Chem. Soc.* **1996**, *118*, 7529; (b) Jiang, H.; Le'ger, J.-M.; Dolain, C.; Guionneau, P.; Huc, I. *Tetrahedron* **2003**, *59*, 8365.
- (12) (a) Huc, I.; Maurizot, V.; Gornitzka, H.; Le'ger, J.-M. *Chem. Commun.* **2002**, 578; (b) Berl, V.; Huc, I.; Khoury, R. G.; Lehn, J.-M. *Chem. Eur. J.* **2001**, *7*, 2798.
- (13) Delnoye, D. A. P.; Sijbesma, R. P.; Vekemans, J. A. J. M.; Meijer, E. W. *J. Am. Chem. Soc.* **1996**, *118*, 8717.
- (14) Corbin, P. S.; Zimmerman, S. C. *J. Am. Chem. Soc.* **2000**, *122*, 3779.
- (15) Garric, J.; Le'ger, J.-M.; Grelard, A.; Ohkita, M.; Huc, I. *Tetrahedron Lett.* **2003**, *44*, 1421.
- (16) (a) Nowick, J. S.; Cary, J. M.; Tsai, J. H. *J. Am. Chem. Soc.* **2001**, *123*, 5176; (b) Zeng, H.; Yang, X.; Flowers, R. A.; Gong, B. *J. Am. Chem. Soc.* **2002**, *124*, 2903.
- (17) (a) Gong, B.; Yan, Y.; Zeng, H.; Skrzypczak, J.; Kim, Y. W.; Zhu, J.; Ickes, H. *J. Am. Chem. Soc.* **1999**, *121*, 5607; (b) Zeng, H.; Miller, R. S.; Flowers, R. A.; Gong, B. *J. Am. Chem. Soc.* **2000**, *122*, 2635; (c) Zhu, J.; Parra, R. D.; Zeng, H.; Skrzypczak-Jankun, E.; Zeng, X. C.; Gong, B. *J. Am. Chem. Soc.* **2000**, *122*, 4219.

- (18) Malone, J. F.; Murray, C. M.; Dolan, G. M.; Docherty, R.; Lavery, A. J.; *Chem. Mater.* **1997**, *9*, 2983-2989.
- (19) Kanamori, D.; Okamura, T.; Yamamoto, H.; Ueyama, N. *Angew. Chem. Int. Ed.* **2005**, *44*, 969.
- (20) Howard, H. A. K.; Hoy, V. J.; O'Hagan, D.; Smith, G. T. *Tetrahedron* **1996**, *52*, 12613.
- (21) (a) Zhao, X.; Wang, X.-Z.; Jiang, X.-K.; Chen, Y.-Q.; Li, Z.-T.; Chen, G.-J. *J. Am. Chem. Soc.* **2003**, *125*, 15128; (b) Li, C.; Ren, S.-F.; Hou, J.-L.; Yi, H.-P.; Zhu, S.-Z.; Jiang, X.-K.; Li, Z.-T. *Angew. Chem. Int. Ed.* **2005**, *44*, 5725.
- (22) Wurtz, N. R.; Turner, J. M.; Baird, E. E.; Dervan, P. B. *Org. Lett.* **2001**, *3*, 1201-1203.
- (23) Wender, P. A.; Jessop, T. C.; Pattabiraman, K.; Pelkey, E. T.; VanDeuse, C. L.; *Org. Lett.* **2001**, *3*, 3229-3232.
- (24) Dietrich, B.; Viout, P.; Lehn, J.-M. *Macrocyclic Chemistry: Aspects of Organic and Inorganic Supramolecular Chemistry*, VCH, Weinheim, 1993.
- (25) Knops, P.; Sendhoff, N.; Mekelburger, H. B.; Vo'gtle, F.; *Top. Curr. Chem.*, **1992**, *161*, 1-36.
- (26) Busch, D. H.; *J. Inclusion Phenom. Macrocyclic Chem.*, **1992**, *12*, 389-395.
- (27) Rowan, S. J.; Cantrill, S. J.; Cousins, G. R. L.; Sanders, J. K. M.; Stoddart, J. F. *Angew. Chem., Int. Ed.*, **2002**, *41*, 898-952.
- (28) Zhang, W.; Moore, J. S. *J. Am. Chem. Soc.*, **2004**, *126*, 12796.
- (29) Blankenstein, J.; Zhu, J. *Eur. J. Org. Chem.*, **2005**, 1949-1964.
- (30) Hunter, C. A.; *Chem. Soc. Rev.*, **1994**, *23*, 101-109.

- (31) Yuan, L.; Feng, W.; Yamato, K.; Sanford, A. R.; Xu, D.; Guo, H.; Gong, B. *J. Am. Chem. Soc.* **2004**, *126*, 11120-11121.
- (32) Jiang, H.; Leger, J-M.; Guionneau, P.; Huc, I. *Org. Lett.* **2004**, *6*, 2985-2988.
- (33) (a) Rose, G. D.; Gierasch, L. M.; Smith, J. A. *Adv. Protein Chem.* **1985**, *38*, 1-109;
(b) Kahn, M. *Synlett* **1993**, 821-826.
- (34) (a) Milburn, P. J.; Konishi, Y.; Meinwald, Y. C.; Scheraga, H. A. *J. Am. Chem. Soc.* **1987**, *109*, 4486-4496.
- (35) (a) Meng, Q. C.; Hesse, M. *Top. Curr. Chem.* **1992**, *161*, 107; (b) Sessler, J. L.; Burrell, A. K. *Top. Curr. Chem.* **1992**, *161*, 177.
- (36) For reviews, see: (a) Baldwin, J. E. *J. Chem. Soc., Chem. Commun.* **1976**, 734; (b) Knops, P.; Sendhoff, N.; Mekelburger, H. B.; Vogtle, F. *Top. Curr. Chem.* **1992**, *161*, 3;
(c) Anderson, S.; Anderson, H. L.; Sanders, J. K. M. *Acc. Chem. Res.* **1993**, *26*, 469.
- (37) For recent examples, see: (a) Lee, C. W.; Choi, T. L.; Grubbs, R. H. *J. Am. Chem. Soc.* **2002**, *124*, 3224; (b) Li, X. H.; Upton, T. G.; Gibb, C. L. D.; Gibb, B. C. *J. Am. Chem. Soc.* **2003**, *125*, 650.
- (38) Zhang, A.; Han, Y.; Yamato, K.; Zeng, X. C.; Gong, B. *Org. Lett.* **2006**, *8*, 803-806.
- (39) Xing, L.; Ziener, U.; Sutherland, T. C.; Cuccia, L. A. *Chem. Commun.* **2005**, 5751-5753.
- (40) Baruah, P. K.; Gonnade, R.; Rajamohanam, P. R.; Hofmann, H.-J.; Sanjayan, G. J. *J. Org. Chem.*; **2007**; *72*, 5077-5084.
- (41) (a) S. Hecht, S.; Huc, I.; *Foldamers: Structure, Properties, and Applications*, **2007** WILEY-VCH; (b) Gellman, S. H. *Acc. Chem. Res.* **1998**, *31*, 173-180; (c) Smith, M. D.; Fleet, G. W. J. *J. Peptide Sci.* **1999**, *5*, 425-441; (d) Stigers, K. D.; Soth, M. J.; Nowick, J.

- S. Curr. Opin. Chem. Biol.* **1999**, *3*, 714-723; (e) Davis, J. M.; Tsou, L. K.; Hamilton, A. D. *Chem. Soc. Rev.* **2007**, *36*, 326-334.
- (42) Jiang, H.; Leger, J-M.; Guionneau, P.; Huc, I. *Org. Lett.* **2004**, *6*, 2985-2988.
- (43) Kodama, H; Ito, J.; Hori, K.; Ohta, T, Furukawa, I. *J. Org. Chem.* **2000**, *603*, 6.
- (44) Li, X.; Hewgley, J. B.; Mulrooney, C. A.; Yang, J.; Kozlowski, M. C. *J. Org. Chem.* **2003**, *68*, 5500.
- (45) Cram, D. J.; Helgeson, R. C.; Peacock, S. C.; Kaplan, L. J.; Domeier, L. A.; Moreau, P.; Koga, K.; Mayer, J. M.; Chao, Y.; Siegel, M. G.; Hoffman, D. H.; Dotsevi, G.; Sogah, Y. *J. Org. Chem.* **1978**, *43*, 1930.
- (46) During the course of this work, Takashi's group reported a very closely resembling macrocycle derived from BINOL and diamino pyridine building blocks see: (a) Ema, T.; Tanida, D.; Sakai, T. *J. Am. Chem. Soc.* **2007**, *129*, 10591-10596.
- (47) For selected reviews see (a) Blankenstein, J.; Zhu, J. *Eur. J. Org. Chem.* **2005**, 1949–1964; (b) Pu, L. *Chem. Rev.* **1998**, *98*, 2405-2494; (c) Gibson, S. E.; Lecci, C. *Angew. Chem. Int. Ed.* **2006**, *45*, 1364-1377; (d) Bong, D. T.; Clark, T. D.; Granja, J. R.; Ghadiri, M. R. *Angew. Chem., Int. Ed.* **2001**, *40*, 988-1011.
- (48) (a) Yuan, L.; Feng, W.; Yamato, K.; Sanford, A. R.; Xu, D.; Guo, H.; Gong, B. *J. Am. Chem. Soc.* **2004**, *126*, 11120-11121; (b) He, L.; An, Y.; Yuan, L.; Yamato, K.; Feng, W.; Gerlitz, O.; Zheng, C.; Gong, B. *Chem. Commun.* **2005**, 3788-3790; (c) Xing, L.; Ziener, U.; Sutherland, T. C.; Cuccia, L. A. *Chem. Commun.* **2005**, 5751-5753.
- (49) (a) Heo, J.; Jeon, Y-M.; Mirkin, C. A. *J. Am. Chem. Soc.* **2007**, *129*, 7712-7713; (b) Li, Z-B.; Lin, J.; Sabat, M.; Hyacinth, M.; Pu, L. *J. Org. Chem.* **2007**, *72*, 4905-4916.

- (50) For an excellent account on H-bonding graph set analysis, see: Etter, M. C. *Acc. Chem. Res.* **1990**, *23*, 120-126.
- (51) Li, X.; Hewgley, J. B.; Mulrooney, C. A.; Yang, J.; Kozlowski, M. C. *J. Org. Chem.* **2003**, *68*, 5500-5511.
- (52) For the use of hydrogen bonds to control molecular aggregation, see also: Simard, M.; Su, D.; Wuest, J. D. *J. Am. Chem. Soc.* **1991**, *113*, 4696-4698.
- (53) Separate sets of NMR signals become evident if more than one protamers exist in solution, see: Corbin, P. S.; Zimmerman, S. C. *J. Am. Chem. Soc.* **1998**, *120*, 9710-9711.
- (54) Formation of hydrogen-bonded aggregates causes the solubility profile to drop sharply, see: Kendhale, A.; Gonnade, R.; Rajamohanan, P. R.; Sanjayan. G. J. *Chem. Commun.* **2006**, 2756-2758.
- (55) Sanford, A. R.; Yamato, K.; Yang, X.; Yuan, L.; Han, Y.; Gong, B. *Eur. J. Biochem.* **2004**, *271*, 1416-1425.